

# **Functional analysis of clusterin and its wide spread enhancer element, rs2279590 in the pathogenesis of pseudoexfoliation**

*By*

**BISWAJIT PADHY**

**Enrolment No. LIFE11201104005**

**NATIONAL INSTITUTE OF SCIENCE EDUCATION AND RESEARCH,  
BHUBANESWAR**

*A thesis submitted to the*

*Board of Studies in Life Sciences*

*In partial fulfillment of requirements*

*for the Degree of*

**DOCTOR OF PHILOSOPHY**

*of*

**HOMI BHABHA NATIONAL INSTITUTE**

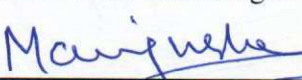
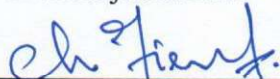
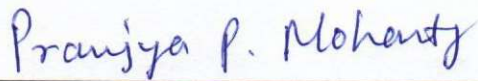


**May, 2018**

# HOMI BHABHA NATIONAL INSTITUTE

## RECOMMENDATIONS OF THE VIVA VOCE COMMITTEE

As members of the Viva Voce Committee, we certify that we have read the dissertation prepared by Mr. Biswajit Padhy entitled "Functional analysis of clusterin and its wide spread enhancer element, rs2279590 in the pathogenesis of pseudoexfoliation" and recommend that it may be accepted as fulfilling the thesis requirement for the award of Degree of Doctor of Philosophy.

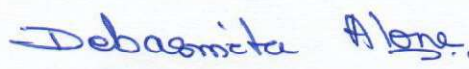
	7/5/18
Chairman – Dr. Chandan Goswami	Date:
	7/5/2018
Guide / Convener – Dr. Debasmita P. Alone	Date:
	7/5/2018
Examiner- Dr. Parimal Das	Date:
	7.5.2018
Member 1- Dr. Praful Singru	Date:
	7/5/2018
Member 2- Dr. Manjusha Dixit	Date:
	7/5/2018
Member 3- Dr. Tirumala K. Chowdary	Date:
Member 4- Dr. Pranjya P. Mohanty	Date:
	7/5/2018

Final approval and acceptance of this thesis is contingent upon the candidate's submission of the final copies of the thesis to HBNI.

I/We hereby certify that I/we have read this thesis prepared under my/our direction and recommend that it may be accepted as fulfilling the thesis requirement.

Date: 07/05/2018

Place: NISER, Jatni

  
Dr. Debasmita P. Alone  
(Thesis Supervisor)

## ACKNOWLEDGEMENTS

I owe my deepest gratitude to my supervisor **Dr. Debasmita P. Alone**, whose invaluable support and contribution helped me in completing my doctoral work. Her optimism concerning my work, enthusiasm, friendly behaviour, motivation and freedom of conscience made me what I am today. I would also like to thank **Prof. V. Chandrasekhar**, Director NISER, and **Prof. T. K. Chandrashekar**, Founder Director, NISER for providing the necessary laboratory amenities and instrumentation facilities to carry out this work. I thank **NISER** for granting the fellowship during the PhD tenure.

My sincere gratitude towards my Thesis Monitoring Committee members, **Dr. Chandan Goswami**, Chairperson SBS, **Dr. Praful Singru**, **Dr. Manjusha Dixit**, **Dr. Tirumala K. Chowdhary** and **Dr. Pranjya P. Mohanty**, Sri Sri Borda hospital, for providing critical and useful suggestions that immensely improved my thesis. I also owe my deepest gratitude to my collaborator **Dr. Pranjya P. Mohanty** and the study participants for providing the necessary samples. For imbibing the knowledge and excitement to pursue a career in science, I am forever indebted to all my teachers from school, graduation and post-graduation. It is unimaginable to have completed this thesis without the motivation, love and the friendship of my lab mates **Gargi di, Bushra, Maynak, Ramani**; and **my friends** who always made a dull day bright.

It is my greatest honour to have such motivating **Mom** and **Daddy** who never ceased to believe in me and are more than **God** to me. It is their belief, dedication, hardship and endurance that has brought me this opportunity and I wish to thank them. I am also blessed to have a cute and lovely **Sister** as my confidante and best friend for life, who has encouraged and supported me in every frontier of life.

## **DEDICATION**

*This thesis is dedicated to my mom, **Mrs. Sanjukta Padhy** and my father, **Mr. Satya Narayan Padhy** for their genes, love and continuous motivation and also to my sweet sister, **Bidyut Prabha Padhy** for her love and support.*

## List of Publications arising from the thesis

### Publications in refereed journals:

#### a) Published:

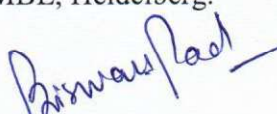
1. Role of an extracellular chaperone, Clusterin in the pathogenesis of Pseudoexfoliation Syndrome and Pseudoexfoliation Glaucoma. **Biswajit Padhy**, Gargi G. Nanda, Mahasweta Chowdhury, Debanand Padhi, Aparna Rao, Debasmita P. Alone. *Experimental Eye Research*, Oct 2014, Vol.127, Pages 69–76.
2. Pseudoexfoliation and Alzheimer's associated risk variant, rs2279590 lies within an enhancer element and regulates CLU and PTK2B gene expression. **Biswajit Padhy**, Bushra Hayat, Gargi G. Nanda, Pragnya P. Mohanty, Debasmita P. Alone. *Human Molecular Genetics*, 2017, 26(22), Pages 4519-4529.

#### b) Under Preparation:

1. Regulation of PTK2B and EPHX2 gene expression through a distal clusterin intronic enhancer element. **Biswajit Padhy**, K. Ramani Shyam, Bushra Hayat, Debasmita P. Alone.
2. Role of Fibulin-5, a scaffold protein in the progression of pseudoexfoliation syndrome. **Biswajit Padhy**, K. Ramani Shyam, Bushra Hayat, Gargi G. Nanda, Pranjya P. Mohanty, Debasmita P. Alone.

### Conference Proceedings:

1. Genetic association of a chaperone, Clusterin with pseudoexfoliation glaucoma in Indian population. **Biswajit Padhy**, Gargi G. Nanda, Mahasweta Chowdhury, Debanand Padhi, Aparna Rao Debasmita P. Alone. Page-210, **ASIA-ARVO**, New-Delhi, India, 2014.
2. Binding of heat shock factors to an intronic variant rs2279590 within clusterin gene and their role in progression of pseudoexfoliation syndrome. **Biswajit Padhy**, Bushra Hayat, Gargi G. Nanda, Rohit K. Mendke, Pranjya P. Mohanty, Debasmita P. Alone. Page-311, **EMBL Conference: Transcription and Chromatin**, Heidelberg, Germany 2016.
3. Pseudoexfoliation and Alzheimer's associated CLU risk variant, rs2279590 lies within an enhancer element and regulates CLU, EPHX2 and PTK2B gene expression. **Biswajit Padhy**, Bushra Hayat, Gargi G. Nanda, Pranjya P. Mohanty, Debasmita P. Alone. **NextGen Genomics, Biology, Bioinformatics and Technologies** (NGBT) 2nd-4th October 2017, Page 116, Bhubaneswar, India.
4. Pseudoexfoliation and Alzheimer's associated CLU risk variant, rs2279590 lies within an enhancer element and regulates CLU, EPHX2 and PTK2B gene expression. **Biswajit Padhy**, Bushra Hayat, Gargi G. Nanda, Pranjya P. Mohanty, Debasmita P. Alone. **EMBL Conference "Mammalian Genetics and Genomics: From Molecular Mechanisms to Translational Applications"** 24th-27th October 2017, Page 201, EMBL, Heidelberg.

  
**Biswajit Padhy**

## DECLARATION

I, hereby declare that the investigation presented in the thesis has been carried out by me.  
The work is original and has not been submitted earlier as a whole or in part for a degree /  
diploma at this or any other Institution / University.

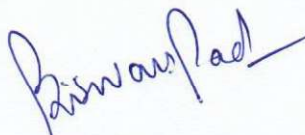
A handwritten signature in blue ink, appearing to read 'Biswajit Padhy', with a stylized flourish at the end.

**Biswajit Padhy**

## STATEMENT BY AUTHOR

This dissertation has been submitted in partial fulfillment of requirements for an advanced degree at Homi Bhabha National Institute (HBNI) and is deposited in the Library to be made available to borrowers under rules of the HBNI.

Brief quotations from this dissertation are allowable without special permission, provided that accurate acknowledgement of source is made. Requests for permission for extended quotation from or reproduction of this manuscript in whole or in part may be granted by the Competent Authority of HBNI when in his or her judgment the proposed use of the material is in the interests of scholarship. In all other instances, however, permission must be obtained from the author.



**Biswajit Padhy**

6.5 Methods standardized during the course of this project in the laboratory.....	131
6.6 Future prospective.....	132
<b>7.0 References.....</b>	<b>133</b>

4.4 Discussion.....	105
4.4.1 Gene expression of <i>PTK2B</i> is modulated by rs2279590 through a wide-spread enhancer effect.....	105
4.4.2 Regulation of <i>EPHX2</i> by rs2279590, a PEX risk variant implies a probable role of <i>EPHX2</i> in the progression of PEX.....	106
4.5 Conclusion.....	107
<b>5.0 Fibulin-5; an extracellular scaffold protein in the development of PEX.....</b>	<b>108</b>
5.1 Introduction.....	109
5.1.1 Fibulin-5 is a crucial scaffold protein in the extracellular matrix.....	109
5.1.2 Fibulin-5 and ECM disorders.....	110
5.1.3 Potential role of F5 as a risk factor in PEX progression.....	112
5.2 Materials and Methods.....	112
5.2.1 Study subjects.....	112
5.2.2 DNA extraction, PCR, elution and sequencing.....	114
5.2.3 RNA extraction and cDNA synthesis.....	114
5.2.3 Western blotting.....	114
5.2.4 Genetic and statistical analysis.....	114
5.3 Results.....	115
5.3.1 Association of genetic variants in the Fibulin-5 gene with PEX.....	115
5.3.2 Downregulation of Fibulin-5 gene expression in PEXS affected tissues.....	120
5.4 Discussion.....	122
5.4.1 Polymorphisms in F5 gene can be a risk factor for PEX pathogenesis.....	122
5.4.2 Decreased F5 expression may lead to abnormal maintenance of ECM.....	123
5.5 Conclusion.....	124
<b>6.0 Discussion.....</b>	<b>125</b>
6.1 Clusterin, in the pathogenesis of pseudoexfoliation.....	126
6.1.1 Genetic variants in clusterin as a risk factor for PEX.....	126
6.1.2 Dysregulated expression of <i>CLU</i> can be pathogenic for PEX progression.....	127
6.2 Fibulin-5 as a novel candidate gene in development of PEX.....	128
6.2.1 Genetic association of polymorphisms in F5 gene with PEX.....	128
6.2.2 Downregulated F5 expression may lead to impaired maintenance of ECM.....	129
6.3 Conclusion.....	130
6.4 Key findings from the study.....	131

3.3 Results.....	69
3.3.1 <i>In silico</i> analysis reveals the presence of enhancer marks around genomic region of rs2279590.....	69
3.3.2 Genomic region containing rs2279590 acts as an enhancer for clusterin gene expression in vitro.....	71
3.3.3 Transition from G→A at rs2279590 creates a binding site for HSF1.....	75
3.3.4 HSF1 binding to allele “A” at rs2279590 abrogates the enhancer effect of the locus.....	81
3.3.5 Chromosome conformation capture (3C) assay revealed a promoter-enhancer interaction between clusterin promoter and rs2279590 loci.....	83
3.3.6 Upregulation of HSF1 suggests proteotoxic stress in anterior eye tissues of PEX affected subjects.....	85
3.4.0 Discussion.....	86
3.4.1 rs2279590 is a functional intronic variant and regulates clusterin gene expression.....	87
3.4.2 HSF1 is a critical regulator in clusterin gene expression.....	89
3.5 Conclusion.....	91
<b>4.0 Wide-spread enhancer effect of rs2279590 on regulating PTK2B and EPHX2 gene expression.....</b>	<b>92</b>
4.1 Introduction.....	93
4.1.1 Genomic locus encompassing <i>CLU</i> gene harbors many risk variants for ageing disorders.....	93
4.1.2 Aberrant expression of genes surrounding <i>CLU</i> gene is related with various pathological disorders.....	94
4.2 Materials and methods.....	95
4.2.1 Study subjects recruitment.....	95
4.2.2 Cell culture.....	96
4.2.3 CRISPR/Cas9 construct preparation and genome editing.....	96
4.2.4 Chromosome conformation capture assay.....	96
4.2.5 RNA extraction, cDNA synthesis and Quantitative real-time PCR (qRT-PCR)...	96
4.2.6 Statistical analysis.....	96
4.3 Results.....	99
4.3.1 Regulatory effect of rs2279590 region on <i>PTK2B</i> and <i>EPHX2</i> expression.....	99
4.3.2 rs2279590 modulates <i>PTK2B</i> and <i>EPHX2</i> gene expression through promoter-enhancer interaction.....	101
4.3.3 Dysregulated expression of <i>EPHX2</i> in PEX affected tissues.....	103

2.2.10 Immunohistochemistry.....	40
2.2.11 Statistical analysis.....	40
2.3 Results.....	41
2.3.1 Genetic association of clusterin variants in the pathogenesis of PEX.....	41
2.3.2 Clusterin expression in anterior eye tissues of pseudoexfoliation.....	45
2.3.3 Regulatory role of clusterin intronic variants.....	49
2.3.4 Expression of <i>Dickopff-1</i> in the anterior eye tissues of PEX affected individuals..	50
2.4 Discussion.....	53
2.4.1 Both rs308754 and rs2279590 are risk factors for development of PEX in Indian population.....	53
2.4.2 Over-accumulation of CLU in the anterior eye tissues of PEXG affected individuals.....	54
2.5 Conclusion.....	56
<b>3.0 Functional significance of clusterin intronic variant, rs2279590 in PEX progression.....</b>	<b>57</b>
3.1 Introduction.....	58
3.1.1 Pseudoexfoliation and Alzheimer’s disease shares similar pathological alterations.....	58
3.1.2 Paradoxical role of clusterin as an inducer of cytotoxicity.....	59
3.2 Materials and Methods.....	60
3.2.1 Study subjects recruitment.....	60
3.2.2 Cell culture.....	61
3.2.3 Luciferase reporter assays.....	61
3.2.4 CRISPR/Cas9 construct preparation and genome editing.....	63
3.2.5 Chromosome conformation capture (3C) assay.....	64
3.2.6 Bioinformatic analysis.....	66
3.2.7 Electrophoretic mobility shift assay (EMSA).....	66
3.2.8 Chromatin immunoprecipitation (ChIP).....	67
3.2.9 Knockdown assays.....	67
3.2.10 Quantitative real-time PCR (qRT-PCR).....	68
3.2.11 Western blotting.....	68
3.2.12 DNA sequencing.....	69
3.2.13 Statistical analysis.....	69

# Contents

<b>Synopsis</b> .....	I
<b>List of Tables</b> .....	XV
<b>List of Figures</b> .....	XVI
<b>List of Abbreviations</b> .....	XVIII
<b>1.0 Introduction &amp; Review of Literature</b> .....	1
1.1 Introduction.....	2
1.2 Ocular manifestation of pseudoexfoliation.....	3
1.3 Pseudoexfoliation: A Systemic Disorder.....	4
1.4 PEX demographics.....	6
1.5 PEX material composition and pathology.....	7
1.6 Environmental factors in PEX pathogenesis.....	12
1.7 Genetic factors as a risk factor in the predisposition of PEX.....	13
1.8 Cellular pathways involved in the pathomechanism of pseudoexfoliation.....	19
1.9 Possible models explaining the pathogenesis of PEX based on current literature.....	23
1.10 Lacunae in the field of pseudoexfoliation.....	25
<b>2.0 Role of Clusterin, an extracellular protein in the pathogenesis of PEX</b> .....	28
2.1 Introduction.....	29
2.1.1 Clusterin, a multifunctional protein.....	29
2.1.2 Clusterin isoforms have discrete roles in cells.....	30
2.1.3 Clusterin and pseudoexfoliation.....	32
2.2 Materials and Methods.....	33
2.2.1 Study subject recruitment.....	33
2.2.2 DNA extraction.....	35
2.2.3 Polymerase chain reaction.....	36
2.2.4 Elution and Sanger's sequencing.....	37
2.2.5 RNA extraction.....	38
2.2.6 cDNA synthesis.....	38
2.2.7 Quantitative real-time PCR.....	39
2.2.8 Protein estimation.....	39
2.2.9 Western blotting.....	39

117  
01A

*Biswan Pady*

Signature of Student:

Date: 22/6/17

Doctoral Committee:

S. No.	Name	Designation	Signature	Date
1.	Dr. Chandan Goswami	Chairman	<i>Chandan Goswami</i>	22/6/17
2.	Dr. Debasmita P. Alone	Guide (Convener)	<i>Debasmita Alone</i>	22/6/17
3.	Dr. Manjusha Dixit	Member	<i>Manjusha Dixit</i>	22/06/2017
4.	Dr. Praful Singru	Member	<i>Praful Singru</i>	22/6/2017
5.	Dr. Tirumala Ku. Chowdary	Member	<i>Ch. Tirumala</i>	22.06.17
6.	Dr. Pranjya P. Mohanty	Member (External)	<i>Pranjya P. Mohanty</i>	22.06.17

Version approved during the meeting of Standing Committee of Deans held during 29-30 Nov 2013

### **Conference proceedings:**

1. **Biswajit Padhy**, Gargi G. Nanda, Mahasweta Chowdhury, Debanand Padhi, Aparna Rao, Debasmita P. Alone. Genetic association of a chaperone, Clusterin with pseudoexfoliation glaucoma in Indian population. Page-210, ASIA-ARVO, New-Delhi, India, 2014.
2. **Biswajit Padhy**, Bushra Hayat, Gargi G. Nanda, Rohit K. Mendke, Pranjya P. Mohanty, Debasmita P. Alone. Binding of heat shock factors to an intronic variant rs2279590 within clusterin gene and their role in progression of pseudoexfoliation syndrome. Page-311, EMBL Conference: Transcription and Chromatin, Heidelberg, Germany, 2016.

### **List of publications pertaining to thesis:**

a. Published:

**Biswajit Padhy**, Gargi G. Nanda, Mahasweta Chowdhury, Debanand Padhi, Aparna Rao, Debasmita P. Alone. Role of an extracellular chaperone, Clusterin in the pathogenesis of Pseudoexfoliation Syndrome and Pseudoexfoliation Glaucoma. *Experimental Eye Research*, Oct 2014, Vol.127, Pages 69–76.

b. Communicated:

**Biswajit Padhy**, Bushra Hayat, Gargi G. Nanda, Pragnya P. Mohanty, Debasmita P. Alone. Pseudoexfoliation and Alzheimer's associated risk variant, rs2279590 lies within an enhancer element and regulates *CLU* and *PTK2B* gene expression.

c. Under Preparation:

**Biswajit Padhy**, K. Ramani Shyam, Bushra Hayat, Gargi G. Nanda, Pragnya P. Mohanty, Debasmita P. Alone. Role of Fibulin-5, a scaffold protein in the progression of pseudoexfoliation syndrome.

### **Other Publications not pertaining to thesis:**

Gargi G. Nanda, **Biswajit Padhy**, Sujata Samal, Sujata Das, Debasmita P. Alone. Genetic Association of *TCF4* Intronic Polymorphisms, CTG18.1 and rs17089887, with Fuchs' Endothelial Corneal Dystrophy in an Indian Population. *Investigative Ophthalmology & Visual Science*, Nov 2014, Vol.55, Pages 7674-7680.

22. Chen, L.H. *et al.* Polymorphisms of CR1, CLU and PICALM confer susceptibility of Alzheimer's disease in a southern Chinese population. *Neurobiol Aging* **33**, 210 e1-7 (2012).
23. Yerbury, J.J. *et al.* The extracellular chaperone clusterin influences amyloid formation and toxicity by interacting with prefibrillar structures. *FASEB J* **21**, 2312-22 (2007).
24. Padhy, B. *et al.* Role of an extracellular chaperone, Clusterin in the pathogenesis of Pseudoexfoliation Syndrome and Pseudoexfoliation Glaucoma. *Exp Eye Res* **127**, 69-76 (2014).
25. Yang, H.C. *et al.* The DAO gene is associated with schizophrenia and interacts with other genes in the Taiwan Han Chinese population. *PLoS One* **8**, e60099 (2013).
26. Guadagno, N.A. *et al.* Neuroserpin polymers cause oxidative stress in a neuronal model of the dementia FENIB. *Neurobiol Dis* **103**, 32-44 (2017).
27. Guerreiro, R.J. *et al.* Genetic variability in CLU and its association with Alzheimer's disease. *PLoS One* **5**, e9510 (2010).
28. Mendes-Jorge, L. *et al.* L-ferritin binding to scara5: a new iron traffic pathway potentially implicated in retinopathy. *PLoS One* **9**, e106974 (2014).
29. Lambert, J.C. *et al.* Meta-analysis of 74,046 individuals identifies 11 new susceptibility loci for Alzheimer's disease. *Nat Genet* **45**, 1452-8 (2013).
30. Scofield, M.D., Tapper, A.R. & Gardner, P.D. A transcriptional regulatory element critical for CHRN4 promoter activity in vivo. *Neuroscience* **170**, 1056-64 (2010).
31. Chapuis, J. *et al.* Genome-wide, high-content siRNA screening identifies the Alzheimer's genetic risk factor FERMT2 as a major modulator of APP metabolism. *Acta Neuropathol* (2016).
32. Kohler, C., Dinekov, M. & Gotz, J. Active glycogen synthase kinase-3 and tau pathology-related tyrosine phosphorylation in pR5 human tau transgenic mice. *Neurobiol Aging* **34**, 1369-79 (2013).
33. Dourlen, P. *et al.* Functional screening of Alzheimer risk loci identifies PTK2B as an in vivo modulator and early marker of Tau pathology. *Mol Psychiatry* (2016).
34. Koerner, I.P. *et al.* Polymorphisms in the human soluble epoxide hydrolase gene EPHX2 linked to neuronal survival after ischemic injury. *J Neurosci* **27**, 4642-9 (2007).
35. Liu, X. *et al.* Elastic fiber homeostasis requires lysyl oxidase-like 1 protein. *Nat Genet* **36**, 178-82 (2004).
36. Chin, K. *et al.* Pelvic Organ Support in Animals with Partial Loss of Fibulin-5 in the Vaginal Wall. *PLoS One* **11**, e0152793 (2016).
37. Lotery, A.J. *et al.* Reduced secretion of fibulin 5 in age-related macular degeneration and cutis laxa. *Hum Mutat* **27**, 568-74 (2006).

## Chapter 7. References

1. Schlotzer-Schrehardt, U. *et al.* LOXL1 deficiency in the lamina cribrosa as candidate susceptibility factor for a pseudoexfoliation-specific risk of glaucoma. *Ophthalmology* **119**, 1832-43 (2012).
2. Schlotzer-Schrehardt, U. & Naumann, G.O. Ocular and systemic pseudoexfoliation syndrome. *Am J Ophthalmol* **141**, 921-937 (2006).
3. Mitchell, P., Wang, J.J. & Smith, W. Association of pseudoexfoliation syndrome with increased vascular risk. *Am J Ophthalmol* **124**, 685-7 (1997).
4. Naumann, G.O., Schlotzer-Schrehardt, U. & Kuchle, M. Pseudoexfoliation syndrome for the comprehensive ophthalmologist. Intraocular and systemic manifestations. *Ophthalmology* **105**, 951-68 (1998).
5. Schumacher, S., Schlotzer-Schrehardt, U., Martus, P., Lang, W. & Naumann, G.O. Pseudoexfoliation syndrome and aneurysms of the abdominal aorta. *Lancet* **357**, 359-60 (2001).
6. Roedl, J.B. *et al.* Homocysteine in tear fluid of patients with pseudoexfoliation glaucoma. *J Glaucoma* **16**, 234-9 (2007).
7. Arvind, H. *et al.* Pseudoexfoliation in South India. *Br J Ophthalmol* **87**, 1321-3 (2003).
8. Thomas, R., Nirmalan, P.K. & Krishnaiah, S. Pseudoexfoliation in southern India: the Andhra Pradesh Eye Disease Study. *Invest Ophthalmol Vis Sci* **46**, 1170-6 (2005).
9. Jonas, J.B. *et al.* Pseudoexfoliation: normative data and associations. The Central India Eye and Medical Study. *PLoS One* **8**, e76770 (2013).
10. Thorleifsson, G. *et al.* Common sequence variants in the LOXL1 gene confer susceptibility to exfoliation glaucoma. *Science* **317**, 1397-400 (2007).
11. Krumbiegel, M. *et al.* Exploring functional candidate genes for genetic association in german patients with pseudoexfoliation syndrome and pseudoexfoliation glaucoma. *Invest Ophthalmol Vis Sci* **50**, 2796-801 (2009).
12. Rosenberg, M.E. & Silkenen, J. Clusterin: physiologic and pathophysiologic considerations. *Int J Biochem Cell Biol* **27**, 633-45 (1995).
13. Jones, S.E. & Jomary, C. Clusterin. *Int J Biochem Cell Biol* **34**, 427-31 (2002).
14. Burdon, K.P. *et al.* Genetic analysis of the clusterin gene in pseudoexfoliation syndrome. *Mol Vis* **14**, 1727-36 (2008).
15. Lambert, J.C. *et al.* Genome-wide association study identifies variants at CLU and CR1 associated with Alzheimer's disease. *Nat Genet* **41**, 1094-9 (2009).
16. Daimon, M. *et al.* Association of the clusterin gene polymorphisms with type 2 diabetes mellitus. *Metabolism* **60**, 815-22 (2011).
17. Zhou, Y. *et al.* Intracellular clusterin interacts with brain isoforms of the bridging integrator 1 and with the microtubule-associated protein Tau in Alzheimer's disease. *PLoS One* **9**, e103187 (2014).
18. Giri, M., Zhang, M. & Lu, Y. Genes associated with Alzheimer's disease: an overview and current status. *Clin Interv Aging* **11**, 665-81 (2016).
19. Schrijvers, E.M., Koudstaal, P.J., Hofman, A. & Breteler, M.M. Plasma clusterin and the risk of Alzheimer disease. *JAMA* **305**, 1322-6 (2011).
20. Karch, C.M. *et al.* Expression of novel Alzheimer's disease risk genes in control and Alzheimer's disease brains. *PLoS One* **7**, e50976 (2012).
21. DeMattos, R.B. *et al.* Clusterin promotes amyloid plaque formation and is critical for neuritic toxicity in a mouse model of Alzheimer's disease. *Proc Natl Acad Sci U S A* **99**, 10843-8 (2002).

risk factors for PEX pathogenesis in Indian population. Further, despite being a chaperone, CLU over-accumulation in PEXG but not in PEXS individuals implicates a cytotoxic role of CLU. Detailed analysis of rs2279590 locus suggests its regulatory role on *CLU* gene expression. It harbours a TFBS for HSF1 which plays a protective role by abolishing the enhancer effect of the locus. Surprisingly, our work suggests a widespread enhancer effect of rs2279590 on *PTK2B* and *EPHX2* expression which opens up new avenues to study the role of these genes in PEX pathogenesis. Decreased expression of *F5* in affected tissues provide a novel insight in the disease progression. Further studies are warranted to investigate the role of *PTK2B*, *EPHX2* and *F5* genes which will illuminate more into the existing knowledge of PEX aetiology.

We found a significantly decreased expression of *F5* in PEXS but not in PEXG individuals in comparison with controls. Further, an increase in expression of *LoxL1* is seen in PEXS compared to control but was not significant. With a designed case-control study we scanned eleven exon including exon-intron boundaries of *F5* gene. In the discovery set, three control and thirty PEX affected individuals were sequenced to search for single nucleotide polymorphism (SNP) with a risk factor for PEX. We found two intronic variations residing in the 1<sup>st</sup> and 10<sup>th</sup> intron (rs7149187 and rs929608 respectively) and one nonsynonymous coding SNP in the 9<sup>th</sup> exon (rs2430347) of *F5* gene. Further analysis of these variations were done by increasing the sample size in a replicate set comprising of 130 control and 110 PEX (PEXS=57, PEXG=53) affected subjects. With the sample size used in the study the statistical p-value was found to be 0.48, 0.24 and 0.19 for rs7149187, rs929608 and rs2430347 respectively. Haplotype analysis of these polymorphisms resulted in a p-value of 0.06 with C-A-C as the risk haplotype.

#### 5.4. Discussion

Role of polymorphisms in *F5* gene as a risk factor for PEX need to be analyzed in a larger sample size. Additionally, genetic variations in the uncovered intronic region of *F5* gene need to be checked further to exclude any probable role of *F5* variants in PEX progression. Surprisingly, we found a decreased mRNA expression of *F5* in PEX affected tissues which suggests *F5* may play a crucial role in PEX progression. Consistent to our report, earlier studies also have reported decreased expression of *F5* in diseases involving elastinopathy.<sup>36,37</sup> However, the adverse effects of decreased *F5* expression during the onset of PEX remains to be studied.

### **Chapter 6. Discussion**

This work highlights the mechanistic role of *CLU* gene and its intronic variant, rs2279590 in the progression of PEX. Our result suggest that both variants; rs3087554 and rs2279590 are

induced regulation of ion channels and MAPK pathway activation and is reported to promote Tau fibrillar pathology in AD patients.<sup>32,33</sup> In this study, we found decreased levels of *PTK2B* mRNA in cells with the deleted enhancer element containing rs2279590 with risk allele “G”; suggesting a distal enhancer effect of the locus over *PTK2B* expression. Deletion of rs2279590 locus also leads to downregulation of *EPHX2* that metabolises neuroprotective epoxyeicosatrienoic acids and pose as risk factor for AD.<sup>34</sup> Our study implicates a combined regulatory role of PEX/AD risk variant, rs2279590 on *CLU*, *EPHX2* and *PTK2B* gene expression thereby modulating a common pathway in PEX/AD progression.

## **Chapter 5. Fibulin-5; an extracellular scaffold protein in the development of PEX.**

### 5.1. Introduction

Fibulin-5 (F5) is an extracellular scaffold protein in the ECM. It plays a vital role in the ECM as it lays foundation for deposition of elastin and Lysyl-oxidase like-1 (LoxL1) and decides the tissue integrity.<sup>35</sup> Earlier studies in elastinopathic diseases like cutis laxa and pelvic organ prolapse and in age related macular degeneration, have shown that decreased expression of F5 leads to abnormal deposition of elastin and LoxL1 in the ECM.<sup>36,37</sup> Evidence of irregular deposition of elastin and LoxL1 also has been reported in the posterior tissues of PEX affected eyes.<sup>1</sup> Both abnormal deposition of elastin and LoxL1 in PEX tissues and crucial role of F5 in maintaining the ECM led us to hypothesize that F5 might play a role in the progression of PEX. The aim of this chapter was set to check the involvement of F5 in PEX pathogenesis.

### 5.2. Materials and methods

The materials and methods employed to accomplish the designed specific aims will be described in detail.

### 5.3. Results

gene like *PTK2B* (protein tyrosine kinase 2 beta) and *EPHX2* (Epoxide hydrolase 2) contains risk variants associated with Alzheimer's disease.<sup>29,31</sup> Similarly, studies have shown association of other nearby genes (5' to that of *CLU* gene) such as SCARA3 (Scavenger Receptor Class A Member 3) with Parkinson's, SCARA5 (Scavenger Receptor Class A Member 5) with glaucoma and CCDC25 (Coiled-Coil Domain Containing 25) with AD progression.<sup>26-28</sup> In this chapter, we have studied the broad enhancer effect of rs2279590 on regulating other nearby genes to that of *CLU* gene.

#### 4.2. Materials and methods

The materials and methods employed to accomplish the designed specific aims will be described in detail.

#### 4.3. Results

We checked mRNA expression of nine crucial genes clustered around 5' and 3' ends of *CLU* gene, within a stretch of around 558 kb in knockout HEK293 cells with deleted rs2279590 region than that of control non-deleted cells. A significantly downregulation of two upstream genes, *PTK2B* and *EPHX2* was observed in rs2279590 deleted HEK293 cells in comparison with control HEK293 cells. This indicates genomic region around rs2279590 possess a distant regulatory role on *PTK2B* and *EPHX2*. We also checked the enhancer-promoter interaction between rs2279590 locus and promoter of both *EPHX2* and *PTK2B* genes through 3C assay. 3C analysis of the ligated product through qRT-PCR suggest a strong interaction between rs2279590 loci with the promoter region of both *PTK2B* and *EPHX2*. This confirms the regulatory effect of rs2279590 element on *EPHX2* and *PTK2B* gene expression through promoter-enhancer interaction apart from *CLU*.

#### 4.4. Discussion

Previous studies have shown a genetic association between *PTK2B-CLU* locus and other ageing disorders.<sup>25-30</sup> *PTK2B* is a non-receptor protein kinase and is involved in calcium

element might be necessary for regulating *CLU* expression. Through bioinformatic analysis and molecular assays, we found allele “A” at rs2279590 creates a transcription factor binding site (TFBS) for Heat shock factor 1 (HSF1). After binding to allele “A” at rs2279590, HSF1 abrogates enhancer effect of the locus and decreases *CLU* gene expression as shown through reporter assays. Moreover, knockdown of HSF1 through siRNA restored the enhancer effect of rs2279590 locus. We also have checked the expression of HSF1 in the anterior eye tissues of PEX affected individuals and found to be significantly upregulated only in PEXS than that of PEXG or control individuals.

### 3.4. Discussion

In this chapter, we aimed to characterize the functional significance of *CLU* risk variant, rs2279590. We found rs2279590 with risk allele “G” has an enhancer effect, on both *sCLU* and *nCLU* and suggests their accumulation may have cytotoxic effect. Studies have shown that elevated level of *CLU* is linked to disease severity in both PEXG and AD affected patients.<sup>18-20,24</sup> HSF1 binds to rs2279590 and plays a protective role by regulating *CLU* and thus implying a lowered risk of developing PEX or AD. Upregulated HSF1 expression in the anterior eye tissues of PEXS subjects but not in PEXG suggests a protective role of HSF1 which is diminished in the later stage; thus increasing the severity of the disease. Collectively, this chapter uncovers the mechanistic role of the risk variant rs2279590 that can affect a variety of ageing disorders including PEX by regulating the expression of a specific set of genes.

## **Chapter 4. Widespread enhancer effect of rs2279590 on regulating *PTK2B* and *EPHX2* gene expression.**

### 4.1. Introduction:

Genetic studies have previously shown that various genes surrounding the *CLU* locus (8p21.1) are associated with many age related disorders.<sup>25-30</sup> Genes situated in the 3’ region of *CLU*

## **Chapter 3. Functional significance of clusterin intronic variant, rs2279590 in PEX progression.**

### 3.1. Introduction

In this chapter, we have addressed the functional significance of rs2279590 intronic variant in PEX progression. Previously, rs2279590 has been reported as a risk factor for AD and type-2 diabetes.<sup>15,16,22</sup> Studies suggest that PEX and AD share similar pathological alterations including abnormal deposition of proteinaceous material in the extracellular space and gradual deterioration of optic and brain nerves respectively. Similar to PEX, CLU accumulation in AD is linked with disease severity and brain nerves in AD affected individual degenerates faster with deposition of CLU similar to that in PEXG.<sup>18-20</sup> Although CLU plays a chaperonic role in the extracellular space, it can be cytotoxic at a higher substrate to CLU ratio and deposits along with abnormal protein aggregates.<sup>23</sup> We have used genetic and molecular techniques to reveal the mechanistic role of rs2279590 locus in the pathogenesis of PEX.

### 3.2. Materials and methods

The materials and methods employed to accomplish the designed specific aims will be described in detail.

### 3.3. Results

Both bioinformatics analysis and luciferase reporter assays revealed the presence of rs2279590 locus within an active regulatory region. Further knockout of HEK293 cells with a homozygous deletion for rs2279590 was created to understand the *in vivo* effect of the locus on *CLU* gene expression by using CRISPR/Cas9 genome editing method. *CLU* expression was checked by qRT-PCR, western blot and immunofluorescence in rs2279590 knockout cells and was found to be significantly downregulated than that of control cells. Chromosome conformation capture (3C) assays revealed chromatin interaction between rs2279590 locus and *CLU* promoter suggesting a promoter-enhancer interaction mediated by rs2279590

The materials and methods employed to accomplish the designed specific aims will be described in detail.

### 2.3. Results:

After genotyping 136 PEX patients (81 PEXS and 55 PEXG) and 89 controls from Indian ethnic group, we found genetic association of both rs3087554 and rs2279590 with PEX with “A” and “G” as risk allele, respectively. qRT-PCR assays revealed no difference in the *CLU* mRNA expression in lens capsule of PEX individuals than control. However, after grouping of fold expression change based on the genotype at rs2279590, we found a significant increase of *CLU* mRNA level per “G” risk allele. Through western blot analysis, we found a two-fold upregulation of *CLU* protein in aqueous humour of PEXG ( $p = 0.009$ ) individuals in comparison to PEXS and control group. Similarly, immunofluorescence staining of lens capsule tissues from PEXG individuals also showed a higher deposition of *CLU* in dense punctuate pattern than PEXS or control individuals.

### 2.4. Discussion

Our study reported both rs3087554 and rs2279590 as risk factors in the development of PEX in Indian population. Further, rs2279590 was found to be a functional variant in progression of PEX with a significant increase in *CLU* expression per “G” risk allele, which suggest its regulatory role on *CLU* expression. As for the functional mechanism, it remained to be seen how the risk allele at rs2279590 regulates *CLU* and has been subsequently addressed in the next chapter. Previously, *CLU* was also found to be upregulated in affected brain tissues of AD patients which implies a shared pathological alterations in such age related disorders.<sup>18</sup> In summary, we found that *CLU* variants are risk factor towards developing PEX. Further, over-accumulated *CLU* in affected tissues might intensify severity of PEX pathogenesis similar to that in other neurodegenerative disorders.

3. Functional significance of clusterin intronic variant, rs2279590 in PEX progression.
4. Wide spread enhancer effect of rs2279590 on *PTK2B* and *EPHX2* gene.
5. Fibulin-5; an extracellular scaffold protein in the development of PEX.
6. Discussion.
7. References.

## **Chapter 1. Introduction.**

- 1.1. Ocular manifestation of pseudoexfoliation
- 1.2. PEX as a systemic disorder
- 1.3. Epidemiology of pseudoexfoliation syndrome and -glaucoma
- 1.4. PEX fibril composition and pathology
- 1.5. Environmental factors in PEX progression
- 1.6. Genetic components as a risk factors in the aetiology of PEX
- 1.7. Possible theories known for development of PEX

## **Chapter 2. Role of an extracellular chaperone, Clusterin in PEX pathogenesis.**

### 2.1. Introduction:

Clusterin plays a pivotal role in preventing protein aggregation in the extracellular matrix.<sup>12,13</sup> Being a protein with chaperonic function in the extracellular space it has been associated with diverse human disorders like Alzheimer's, diabetes and cancer.<sup>12,15,16</sup> Previously two SNPs, rs3087554 and rs2279590 within the *CLU* gene were found to be risk factors in the development of PEX in Australian and German ethnic groups, respectively.<sup>11,14</sup> In absence of any information in Indian ethnicity, the following study was designed to test the genetic association of two SNPs, rs3087554 and rs2279590 of *CLU* as risk factors towards development of PEX in Indian population as well as to find their role in its pathogenesis.

### 2.2. Materials methods:

The following work was pursued to understand the mechanistic role of an extracellular protein, Clusterin (CLU) and its genetic variants in the pathogenesis of PEX. CLU is a multi-functional protein with diverse role in cellular metabolism.<sup>12,13</sup> Previously, case-control studies in both German and Australian population has shown genetic variants in *CLU* gene as risk factors in PEX pathogenesis.<sup>11,14</sup> Role of CLU in the affected tissues of individuals suffering from various ageing disorders is well documented.<sup>11,15,16</sup> Especially, in Alzheimer's disease (AD) which involves extracellular deposition of beta-amyloid plaques, CLU was found to be over accumulated in brain tissues.<sup>17</sup> CLU accumulation leads to faster deterioration of brain function in AD affected individuals and knockout of *CLU* in AD model of mice shows reduced fibrillar plaque and neuritic dystrophy.<sup>18-21</sup>

We have investigated the role of *CLU* variants in PEX pathogenesis by conducting a case-control study in Indian ethnic background. Through molecular assays, we have checked the differential expression of *CLU* in PEX patients in comparison to that of controls. Detailed functional analysis of a *CLU* intronic risk variant, rs2279590 in PEX progression is carried out by utilizing various genetic, molecular and biochemical assays. We have proposed a mechanism through which this risk variant imparts its role in modulating *CLU* and nearby gene expression. Apart from *CLU*, we hypothesized that Fibulin-5, an extracellular scaffold protein might be involved in PEX progression. Along with the differential expression studies, we also carried out a genetic association study with Fibulin-5 to uncover novel genetic variants that might be risk factors in the progression of PEX. The above-mentioned work is divided into following chapters to carry out the respective objectives. Slight modifications might be incorporated if needed during thesis writing.

## Chapters

1. Introduction.
2. Role of an extracellular chaperone, Clusterin in PEX pathogenesis.



## Homi Bhabha National Institute

### SYNOPSIS OF Ph. D. THESIS

- 1. Name of the Student:** BISWAJIT PADHY
- 2. Name of the Constituent Institution:** National Institute of Science Education and Research
- 3. Enrolment No. :** LIFE11201104005
- 4. Title of the Thesis:** Functional analysis of clusterin and its wide spread enhancer element, rs2279590 in the pathogenesis of pseudoexfoliation.
- 5. Board of Studies:** Life Sciences

### SYNOPSIS

Pseudoexfoliation (PEX; OMIM: 177650) is an age related systemic disorder diagnosed by deposition of fibrillar proteinaceous material in the surface of anterior and posterior eye tissues. Deposition of these fibrils gradually leads to death of optic nerve head cells (ONH) and deteriorates normal vision.<sup>1</sup> This later advanced stage is known as pseudoexfoliation glaucoma (PEXG) in contrast to the initial stage called as pseudoexfoliation syndrome (PEXS). PEXG has been reported as the leading cause of secondary glaucoma worldwide.<sup>2</sup> PEX has also been associated with other pathological alterations such as zonular weakness, cataract formation and systemic vascular complications.<sup>3-6</sup> Incidence of PEX varies widely based on their ethnicity. In India, the incidence of PEX is 6.28% in individuals over sixty years.<sup>7-9</sup> Studies suggest a prominent genetic contributor underlying the pathogenesis of PEX. Both genetic and proteomic studies indicates the involvement of proteins that maintain the extracellular matrix (ECM).<sup>10,11</sup>

sCLU	Secretory clusterin
siRNA	Small interfering RNA
SNP	Single nucleotide polymorphism
TEM	Transmission electron microscopy
TFsearch	Transcription factor search
TGF $\beta$	Transforming growth factor beta
TIMP	Tissue inhibitor of metalloproteinase
TRIM35	Tripartite motif-containing 35
TSS	Transcription start site
UCSC	University of California, Santa Cruz

GWAS	Genome wide association study
HEK293	Human embryonic kidney 293 cell
HG	Human genome
HS	Heat shock
HSE	Heat shock element
HSFs	Heat shock factors
HSF1	Heat shock factor-1
HSF2	Heat shock factor-2
HSF4	Heat shock factor-4
HSFs	Heat shock factors
IHC	Immunohistochemistry
IOP	Intra ocular pressure
IP	Immunoprecipitation
KO	Knockout
LC	Lens capsule
LOXL1	Lysyl oxidase like-1
LTBP2	Latent transforming growth factor beta binding protein 2
MAGP1	Microfibrillar associated protein 1
MMP	Matri metalloproteinase
mRNA	Messenger RNA
MTHFR	Methylene tetrahydrofolate reductase
nCLU	Nuclear clusterin
ONH	Optic nerve head
PBK	PDZ binding kinase
PEX	Pseudoexfoliation
PEXG	Pseudoexfoliation glaucoma
PEXS	Pseudoexfoliation syndorme
POP	Pelvic organ prolapse
PTK2B	Protein tyrosine kinase 2-beta
QRT-PCR	Quantitative real time PCR
RNA	Ribose nucleic acid
SCARA3	Scavenger Receptor Class A Member 3
SCARA5	Scavenger Receptor Class A Member 5

## **List of Abbreviations**

3C	Chromosome conformation capture
AD	Alzheimer's disease
AH	Aqueous humour
APOJ	Apolipoprotein J
ARMED	Age related macular degeneration
BIRC6	Baculoviral IAP Repeat Containing 6
CACNA1A	Calcium Voltage-Gated Channel Subunit Alpha 1 A
CCDC25	Coiled-Coil Domain Containing 25
CDKN2B-AS	Cyclin dependent kinase 2-beta- Antisense RNA
CDS	Coding DNA sequence
ChIP	Chromatin immunoprecipitation
CHRNA2	Cholinergic Receptor Nicotinic Alpha 2
CL	Cutis laxa
CLU	Clusterin
CNTNAP2	Contactin Associated Protein-Like 2
CONJ	Conjunctiva
CRISPR-Cas9	Clustered regularly interspaced short palindromic repeat- associated protein-9 nuclease
DANCE	Developing arteries and neural crest EGF-like
DAPI	4',6-diamidino-2-phenylindole
DKK1	Dickopff-1
DNA	Deoxy ribose nucleic acid
DNaseI	Deoxyribonuclease I
ECM	Extracellular matrix
EMSA	Electrophoretic mobility shift assay
ENCODE	Encyclopedia of DNA elements
EPHX2	Epoxide hydrolase-2
ESCO2	Establishment Of Sister Chromatid Cohesion N-Acetyltransferase 2
F5	Fibulin-5
GAPDH	Glyceraldehyde phosphate dehydrogenase
GFAP	Glial fibrillar acidic protein

Figure 5.1 Diagrammatic presentation showing the deposition of ECM proteins in the outer extracellular space.....112

Figure 5.2 Diagrammatic presentation of Fibulin-5 gene present in the long arm of chromosome 14 (q32.12).....116

Figure 5.3 qRT-PCR to check mRNA expression of F5 in lens capsule of cases and controls.....121

Figure 5.4 Differential expression of Fibulin-5 in the lens capsule of PEXS subjects through western blotting.....122

Figure 3.11 EMSA for binding of HSF1 to labelled oligo “A” but not to labelled oligo “G”....	76
Figure 3.12 EMSA for comparison of specific shift between allele “A” at rs2279590 and HSE.....	77
Figure 3.13 Specific competitive assays with unlabelled HSE and unlabelled rs2279590 oligo.....	78
Figure 3.14 Supershift assay with HSFs (HSF1, HSF2, HSF4) and GAPDH.....	79
Figure 3.15 EMSA supershift assay with HSF1 and unlabelled rs2279590 (A) oligo.....	79
Figure 3.16 Chromatin immunoprecipitated samples were used for qRT-PCR assay.....	80
Figure 3.17 Fold enrichment of rs2279590 region through qRT-PCR.....	80
Figure 3.18 Allele specific ChIP was done by sequencing of rs2279590 genomic region from the input or IP sample done with anti-HSF1.....	81
Figure 3.19 Allelic effect on luciferase activity in control HEK293 cells.....	82
Figure 3.20 Normalized luciferase activity is shown in heat shocked, MG132 (5 $\mu$ M) treated and siRNA (HSF1) treated HEK293 cells to differentiate the allelic effect on reporter activity.....	82
Figure 3.21 Knockdown of HSF1 by siRNA pool.....	83
Figure 3.22 Schematic location of EcoRI restriction sites (E1-E10) across CLU gene.....	84
Figure 3.23 Chromosome conformation capture assays for CLU promoter and rs2279590 enhancer interaction.....	85
Figure 3.24 HSF1 upregulation indicates a proteotoxic stress in anterior eye tissues of PEXS affected study subjects.....	86
Figure 3.25 Proposed model explaining the effect of SNP-dependent HSF1 binding at rs2279590, target gene expression and AD/PEXG risk.....	90
Figure 4.1 Locus containing rs2279590 also regulates PTK2B and EPHX2 gene expression..	93
Figure 4.2 qRT-PCR assays were done for genes located in the PTK2B-CLU locus in rs2279590 region deleted cells than that of control non-deleted cells.....	100
Figure 4.3 Chromosome conformation capture assays for PTK2B promoter and rs2279590 enhancer interaction.....	102
Figure 4.4 Chromosome conformation capture assays for EPHX2 promoter and rs2279590 enhancer interaction.....	103
Figure 4.5 qRT-PCR assays to check EPHX2 and PTK2B expression in anterior eye tissues	104
Figure 4.6 Proposed model explaining the effect of SNP-dependent HSF1 binding at rs2279590, EPHX2 and PTK2B gene expression and AD/PEX risk.....	106

## **List of Figures**

Figure 1.1 Anatomy of human eye showing internal anterior and posterior chamber and a detailed tissue structure.....	2
Figure 1.2 A clinical picture of a pseudoexfoliation affected eye showing a classical pattern of PEX fibril deposition on the surface of lens capsule taken by slit-lamp microscopy..	3
Figure 1.3 A diagrammatic presentation of known pathomechanism in progression of pseudoexfoliation.....	23
Figure 2.1 The gene structure of clusterin.....	29
Figure 2.2 Involvement of sCLU and nCLU isoforms in different physiological pathways of the cell.....	31
Figure 2.3 Clusterin mRNA expression change in PEX affected subjects compared to control	45
Figure 2.4 Total protein estimation in in PEX affected subjects compared to control.....	46
Figure 2.5 Differential Clusterin accumulation in PEX affected subjects compared to control.	48
Figure 2.6 Immunostaining of Clusterin protein on the lens capsule in control.....	49
Figure 2.7 rs3087554 genotype wise comparison of CLU mRNA expression.....	50
Figure 2.8 rs2279590 genotype wise comparison of CLU mRNA expression.....	51
Figure 2.9 qRT-PCR assays for DKK1 expression in the lens capsule of study subjects.....	52
Figure 2.10 HapMap data was used to find out the linkage disequilibrium.....	54
Figure 2.11 A model showing decreased degradation of total proteins in PEX individuals which with increasing age leads to accumulation of ECM protein.....	55
Figure 3.1 rs2279590 is located within an enhancer element as indicated by active regulatory marks.....	70
Figure 3.2 Expression.eQTL data for rs2279590 from GTEx portal.....	70
Figure 3.3 Regulatory effect of rs2279590 locus on luciferase reporter activity.....	71
Figure 3.4 A representative figure showing deletion of 115 bp region around rs2279590.....	72
Figure 3.5 Gel picture depicting confirmed deletion of a 115bp region around rs2279590 generating homozygous knockout HEK293 cell.....	72
Figure 3.6 qRT-PCR assays for checking sCLU expression in control and knockout cells.....	73
Figure 3.7 Western blotting for checking sCLU expression in control and knockout cells.....	73
Figure 3.8 Immunostaining for checking sCLU expression in control and knockout cells.....	74
Figure 3.9 qRT-PCR assays for checking nCLU expression in control and knockout cells.....	75
Figure 3.10 EMSA shows shift specific to allele “A” but not to allele “G” at rs2279590.....	76

## **List of Tables**

Table 1.1 A detailed list of proteins studied so far in the development of pseudoexfoliation and their functions are described.....	9
Table 2.1 Demographic and clinical features of study subjects included for genotyping of clusterin variants.....	34
Table 2.2 List of oligos used in the study.....	36
Table 2.3 Distribution of clusterin variants in PEX and control subjects.....	42
Table 2.4 Distribution of rs3087554 and rs2279590 genotypes in PEX and control subjects.....	43
Table 2.5 Haplotype association of the two variants rs3087554 and rs2279590, respectively with pseudoexfoliation.....	44
Table 2.6 Odds ratio (OR) and Confidence interval (CI) of two clusterin variants.....	45
Table 3.1 List of Oligos used in the study.....	62
Table 3.2 eQTL effect of SNPs within clusterin gene were analysed in GTEx portal on 07/11/17.....	88
Table 4.1 List of crucial genes and their functions surrounding rs2279590.....	94
Table 4.2 List of oligos used in the study.....	97
Table 5.1 List of oligos used in the study.....	113
Table 5.2 Demographic and clinical features of study subjects included for genotyping of Fibulin-5 variants.....	115
Table 5.3 Distribution of F5 variants in PEX and control subjects.....	117
Table 5.4 Distribution of genotypes of variants within F5 in PEX and control subjects.....	119
Table 5.5 Haplotype association of the F5 variants with pseudoexfoliation.....	120
Table 5.6 Odds ratio (OR) and Confidence interval (CI) of F5 variants.....	120

work is focused on finding the functional role of these two genes; Clusterin, an extracellular chaperone protein and Fibulin-5, a scaffold protein in the ECM. Very little is known about the functional role of clusterin in relation to PEX from earlier reports. Moreover, the role of Clusterin in preventing extracellular aggregates and its dual role as either cytoprotective or cytotoxic in stress conditions, makes it a highly probable risk factor in PEX development. Similarly, Fibulin-5 can also play a crucial role in the formation of elastic fibers and in regulating matrix proteases in the ECM. Following key questions were addressed in the current work:

1. Finding the association of clusterin polymorphisms with PEX in Indian population.
2. Functional role of clusterin common risk variants in the progression of PEX.
3. Fibulin-5 gene as a novel genetic factor in PEX pathogenesis.

that there could be more undiscovered genetic factors acting as risk factors for PEX aetiology.

**a. Absence of genetic association of previously reported variants in replicate studies**

Krumbiegel *et al.* have shown association of genetic variants, rs2107856 and rs2141388 in the *CNTNAP2* gene in German population.<sup>65</sup> However, an analogous case-control study carried out in Polish cohort could not find any genetic association of the reported variants.<sup>95</sup> Further, rs1048661 SNP in *LoxL1* which is a risk variant in Caucasian.<sup>67</sup> and Indian<sup>91</sup> population was not found to be associated with PEX in Chinese<sup>89</sup> and Polish population.<sup>95</sup>

**b. Association of reverse alleles in population of different ethnic backgrounds**

Previous case-control studies have shown that flipping of risk alleles occurs for genetic variants associated with PEX in population with different ethnic background. For instance, case-control study conducted in Caucasian and Indian population found allele “G” as the risk allele at rs1048661 in *LoxL1* gene as risk factor for PEX while a similar study in Japanese population found allele “A” as the risk allele.<sup>67,90,91</sup> Likewise, at rs3825942 another variant within *LoxL1* gene, allele “A” was found to be the risk allele in Black South African populations while “G” in Caucasian population.<sup>67,102</sup>

**c. Higher frequency of risk allele in normal population**

Challa *et al.* have shown that the normal control population also have a higher frequency of risk alleles in *LoxL1* gene variants. Low penetrance of these common genetic variants implies a low specificity in predicting the affected status in individuals carrying the risk allele.<sup>97,103</sup>

Altogether, based on above facts we hypothesized probable role of two genetic factors in the formation of abnormal fibrillar PEX aggregates in affected individuals. My doctoral

PEX origin.<sup>83</sup> Moreover, development of PEX in younger individuals with a history of early intraocular surgery or after a penetrating keratoplasty from elderly donor also supports an infectious origin of PEX.<sup>87,152</sup> However, more studies need to be done to support the theory of infectious agents leading to PEX.

**e. Protein-sink theory:**

Lee *et al.* proposed a protein-sink model to explain the aberrant deposition of PEX material in the anterior eye tissues.<sup>153</sup> According to this model, in the preliminary stage a deformed protein complex in the aqueous humour gradually binds to other proteins and forms a large complex protein aggregate. This large aggregate ultimately settles down from the aqueous humour and deposits on the surface of eye tissues. Formation of abnormal aggregate in the initial stage can originate from a single mutant protein like LoxL1 which then acts as a core of the large protein aggregate.<sup>67</sup> Subsequently, it binds to other extracellular scaffold proteins like Fibrillin-1, Fibulin-5, Clusterin, LTBP-1 and LTBP-2 that leads to the formation of a supra-molecular protein assembly.<sup>113,154</sup>

**1.10 Lacunae in the field of pseudoexfoliation:**

Despite numerous earlier studies, precise cause of the pathogenesis of PEX is not clear. The following are the three key unresolved questions that need to be studied extensively-

1. What is the exact molecular mechanism leading to the onset of PEX in aged individuals?
2. What is the possible site of origin of PEX fibril formation?
3. What are the factors that are responsible for progression of pseudoexfoliation syndrome (PEXS) to more severe form of pseudoexfoliation glaucoma (PEXG)?

Various genetic and molecular studies have shown various genes as risk factors in the development of PEX. However, inconsistent outcomes of previous studies indicate the presence of other genetic factors in the aetiology of PEX. Following facts strongly suggest

**b. Amyloid theory:**

Amyloid theory suggests an involvement of amyloid like protein in the pathogenesis of PEX. Aberrant deposition of amyloid- $\beta$ -peptide and phosphorylated tau protein in the brain tissues leads to gradual deterioration of brain neurons in Alzheimer's disease (AD) affected individuals. Proteomic studies have shown the presence of AD related proteins like amyloid- $\beta$ -peptide, serine proteinase inhibitor, alpha-1-antichymotrypsin in PEX aggregates.<sup>32</sup> Similarly, Linner *et al.* showed an increased risk of PEX in AD patients than in normal age-matched individuals in Norwegian population.<sup>33</sup> Also, PEXG individuals have more number of closely arranged myelinated fibers with decreased glial fibrillary acidic protein (GFAP) staining which is also seen in AD affected brains. Together, this suggests an involvement of amyloid like proteins in the production of PEX aggregates similar to that in AD patients.

**c. Basement membrane theory:**

Presence of basement membrane proteins in the PEX material advocates a distorted basement membrane as the root cause in the origin of PEX material. IHC assays have shown the presence of protein epitopes for laminin, nidogen and heparan sulphate proteoglycan in the PEX aggregates.<sup>54,151</sup> Eagle *et al.* have shown that PEX fibrils are also present in the anterior iridic stroma near the endothelial basement membrane and may be locally produced by iris. Such fibrils with a unique 500-A periodicity are also present in the basement membrane in the artery of non-ocular tissues.<sup>39</sup> Also, localised deposition of PEX material along the surface of affected anterior eye also suggests that they might have originated from basement membrane protein components.<sup>4</sup>

**d. Infectious theory:**

Studies also suggest an infectious origin of PEX pathogenesis. Ringvold *et al.* have shown an increased prevalence of PEX in both partners of married couple than the control population and this implicates an involvement of a contaminating particle responsible for

## 1.9 Possible models explaining the pathogenesis of PEX based on current literature

Though extensive studies have been done to find the cause of PEX material formation, its origin is still unclear. Following prospective models have been proposed as the possible causes of PEX pathogenesis (**Figure 1.3**).

### a. Ageing theory:

PEX is an age related ocular disorder with an increase in incidence among aged individuals. For instance, Arnarsson *et al.* have shown that PEX incidence rate is found to be 17.7% in individuals in the age group 70-79 years and later increased to 40.6% in the study subjects aged above 80.<sup>38</sup> Also, in individuals aged above 50, the chance of getting affected by PEX becomes two-fold with each decade.<sup>38-40</sup> This might be due to reduced ability of the aged cell in maintaining proteostasis and the rate of abnormal protein formation elevates in aged individuals. Proteomic analysis of PEX material shows the presence of many extracellular proteins which suggests a decrease in the clearance of abnormal proteins in the extracellular space.<sup>4,52,53</sup> Further, presence of PEX aggregates in non-ocular tissues suggests a systemic manifestation and supports the idea of age related abnormal deposition.<sup>14</sup>

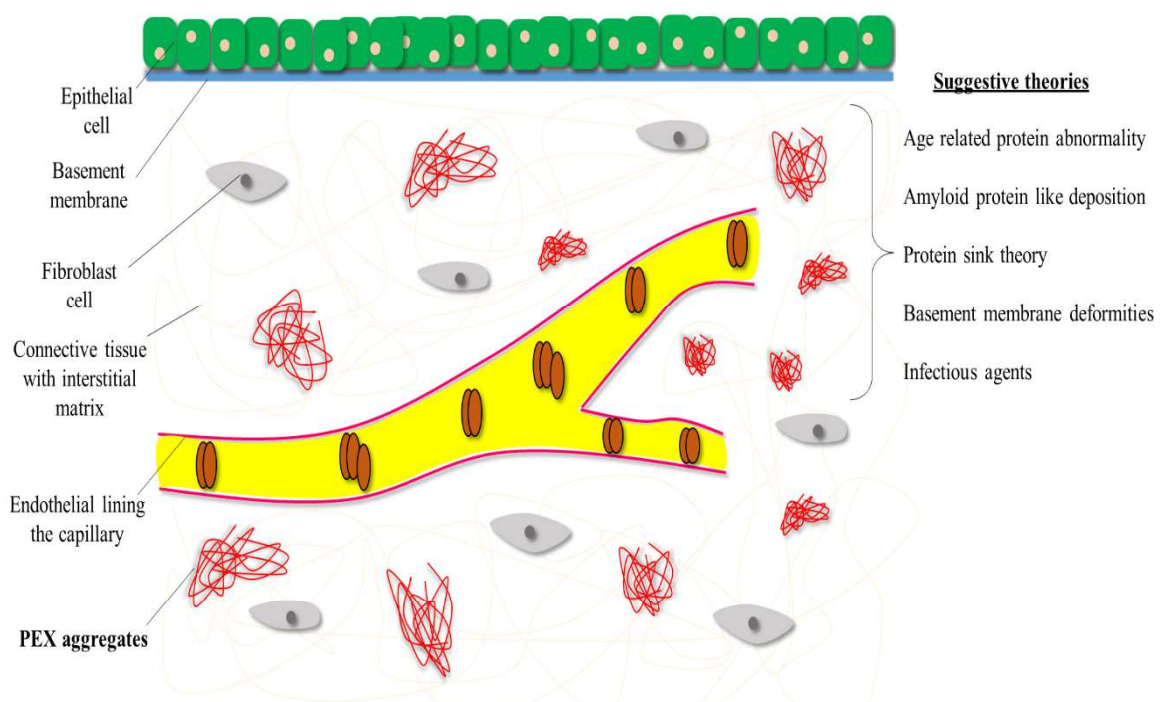


**Figure 1.3.** A diagrammatic presentation of known pathomechanism in progression of pseudoexfoliation.

cell. Khaled *et al.* have shown that total antioxidant status (TAS) which is a measure of antioxidative defence capacity in the cell of diseased tissues was found to be decreased in the plasma of PEXG individuals. However, they have not studied the status of TAS in PEXS affected individuals.<sup>146</sup> Additionally, systemic antioxidant capacity measured by ferric-reducing activity is lower in of the peripheral blood of patients from a Japanese population.<sup>147</sup> Levels of antioxidant enzymes like Paraoxonase (PON) and Arylesterase (ARE) were found to be significantly downregulated in AH and serum in PEXG individuals from Turkish population than in control.<sup>148</sup> Proteomic study of serum collected from PEXG individuals has shown 17 differentially altered proteins (also mentioned in **Table 1.1**) and they are part of a network related to regulating immune and inflammatory-related processes.<sup>59</sup>

Dysregulation in the level of ascorbic acid, nitric oxide (NO) and TNF $\alpha$ , an inflammatory cytokine in the AH was also found in both PEXS and PEXG individuals implicating a local oxidative stress led inflammation.<sup>149</sup> Further, deletion genotypes in the isoforms of the gene, glutathione s- transferase (GST; GST $\theta$ 1 and GST $\mu$ 1) were significantly associated with PEX in Arab population.<sup>146</sup> Increased levels of GSH (Glutathione, an antioxidant measure), malondialdehyde (MDA, lipid peroxidation product), mitogen activated protein kinase (MAPKp38), heat shock proteins (HSP40 and HSP60) and superoxide dismutase 2 (SOD2) were also seen in PEX.<sup>71,150</sup> Other cytoprotective genes like microsomal glutathione transferase 1 (mGST1) and glutathione transferase  $\theta$ 1 (GSTT1), ubiquitin conjugating enzymes (UBE2A and UBE2B), DNA repair protein mutL homolog 1 (MLH1) and stress inducible transcription factor (GADD153) were found to be decreased in PEX.<sup>71</sup>

to methionine. Thus, MTHFR regulates the level of homocysteine and deficiency of MTHFR ultimately leads to homocystinemia. However, case control studies conducted in the Greek and Iranian populations did not find genetic variants, rs1801131 and rs1801133 within MTHFR to be causative risk factors in the pathogenesis of PEX.<sup>37,138</sup> Expression of another homocysteine metabolism gene, tumor necrosis factor alpha (TNF $\alpha$ ; Gene ID: 7124) was also found to be upregulated in PEXG in comparison to control.<sup>131</sup> However, unlike *MTHFR*, a genetic polymorphism tested in TNF $\alpha$ , rs1800629 was found to be strongly associated with PEXG in a Pakistani cohort.<sup>139</sup> Further, an increased level of TNF $\alpha$  was found in the serum of PEX affected individuals.<sup>140</sup>

### **c. Oxidative stress:**

Aberrant deposition of protein aggregates also might be a result of increased oxidative stress and a decrease in antioxidant defence capacity in the tissues of PEX affected eye tissues. This is evident from the elevated protein oxidation in the AH and serum from PEX patients. The amount of carbonyl groups on proteins which is a marker for oxidative stress and protein oxidation was found to be increased in PEX than in control and thus oxidative stress may play a role in the physiopathology of PEX.<sup>141</sup> Further, oxidative selenium that acts as an antioxidant and helps in preventing oxidative stress was shown to be decreased in AH, conjunctiva and serum of PEX individuals thereby, supporting a decreased antioxidative capacity in the disease progression.<sup>142</sup> Also, components of antioxidative defence system like Superoxide dismutase 2 (SOD2), aldehyde dehydrogenase I (ALDH1) and microsomal glutathione-s-transferase I (MGST1) are also found to be elevated in the lens capsule of PEXS cases than those of control subjects and indicate an increased oxidative stress in diseased tissues.<sup>143,144</sup> However, genetic variants in the SOD enzyme, rs10432782 and rs2070424 were not found to be associated with PEXS.<sup>145</sup> This implicates an epigenetic factor playing a role in regulating SOD gene expression during an oxidative insult in the

kinase) and MAPK (Mitogen activated protein-kinase) pathways.<sup>136</sup> TGFβ1 also has a role in stabilizing PEX fibrillar aggregates.<sup>129</sup> Thus, increase in TGFβ1 may enhance local synthesis and activation of extracellular proteins in the ECM. Studies also have shown an increase in the level of latent TGFβ1 binding protein (LTBP1; Gene ID: 4052 and LTBP2; Gene ID: 4053) in the aqueous humour of PEX patients. LTBPs are a group of secreted glycoproteins and are important regulators of TGFβ1 metabolism.<sup>73</sup> Elevated expression of LTBPs thus, may lead to enhanced metabolism of ECM formation. However, earlier reports did not find any SNP polymorphisms within LTBP as risk factors for PEX pathogenesis.<sup>74</sup>

**b. Homocysteine metabolism:**

Homocysteine (Hcy) is a highly reactive amino acid and is synthesized during the metabolism of methionine. Level of homocysteine is a crucial hallmark for oxidative stress in the cells and genes involved in homocysteine metabolism have been studied in the past with relation to PEX, both at genomic and proteomic level. Both PEXS and PEXG patients were found to have elevated levels of homocysteine and vitamin B12 in blood plasma and in the aqueous humour.<sup>80</sup> It is well known that homocysteine can induce vascular injury thereby, altering extracellular matrix proteins and high concentration of homocysteine thus, may trigger abnormal matrix accumulation in the anterior eye surface. Impairment of blood-aqueous barrier may also lead to increase in hcy level in the anterior segment of the eye.<sup>137</sup> Elevated homocysteine is also known to be a risk factor for various vascular diseases and plays a major role in ischemic changes and oxidative stress. Abnormal level of vitamin B12 and folic acid which are required as cofactors in the homocysteine metabolism can elevate Hcy plasma levels.<sup>80</sup>

Methylene tetrahydrofolate reductase (*MTHFR*; Gene ID: 4524) is another gene involved in homocysteine metabolism that produces 5-methyltetrahydrofolate from 5, 10-methylenetetrahydrofolate and is an important cofactor for the conversion of homocysteine

of PEX while alpha-1-antitrypsin and arylsulphatase are found to be increased.<sup>132</sup> Dysregulation in the level of genes involved in autophagy may lead to decreased clearance of protein aggregates and ultimately lead to PEX material deposition with age. Adenosine-3 receptor, a G-protein coupled receptor was shown to be upregulated in non-pigmented ciliary epithelium of PEX affected eyes than in that of control. It plays a role in hypoxia or ischemia and regulates many physiologic processes such as AH secretion and IOP through regulation by adenosine.<sup>133</sup> Turkyilmaz *et al.* found an increased level of a proinflammatory protein, YKL-40 in the serum of PEX cases. It plays a role in the pathogenesis of endothelial dysfunction and atherosclerosis. Increased serum YKL-40 concentration has been associated with cardiovascular morbidity and can be used as a biomarker for atherosclerosis or coronary artery diseases.<sup>134</sup>

## **1.8 Cellular pathways involved in the pathomechanism of pseudoexfoliation**

Previous studies have shown that development of PEX depends on a cumulative effect of various genes and their association with various pathways. Following metabolic pathways suggest the involvement of various proteins and their dysregulation in PEX affected individuals.

### **a. TGF- $\beta$ and ECM metabolism:**

Transforming growth factor beta 1 (TGF- $\beta$ 1; Gene ID: 7040) belongs to transforming growth factor beta superfamily and is a secreted protein with multifunctional role including cellular proliferation, differentiation and apoptosis. Elevated levels of tissue growth factor were reported in the AH of PEX patients than in that of control.<sup>131,135,136</sup> It is well known that an increase in tissue growth factor increases the rate of ECM formation while production of anti-connective tissue growth factor antibody reduces ECM production by inhibiting TGF $\beta$  in trabecular meshwork and lamina cribrosa cells.<sup>135</sup> Increase in TGF also induces expression of fibrillin-1, an ECM scaffold protein through JNK (c-Jun N-terminal

in the development of various forms of cancer and arthritis.<sup>127,128</sup> Past studies also implicate a possible role of MMPs and TIMPs in the progression of PEX. Fountoulakis *et al.* found a significant upregulation of TIMP4 in the aqueous humour (AH) of PEXG affected individuals than that of control. An increase in TIMP4 activity in the AH may lead to a downregulated activity of MMPs and a subsequent disruption of ECM homeostasis in the PEXG individuals.<sup>69</sup> Selecuk *et al.* however, showed that there is no difference in the protein level of both MMP2 and TIMP2 in both AH and serum samples of PEX individuals in comparison to control.<sup>70</sup> Studies also suggest an imbalance in the protein level of other family members of MMPs and TIMPs in the PEX affected anterior eye tissues such as TIMP1, MMP9<sup>72</sup> and TIMP2.<sup>71</sup> Altogether, dysregulation of MMPs and TIMPs may aid in decreased proteolytic activity and eventually lead to accumulation of aberrant proteins in the extracellular space.

#### **f. Cytokines:**

Cytokines play a major role in mediating inflammation and immunity. Certain proinflammatory cytokines such as interleukin-6 (IL-6) and interleukin-8 (IL-8) are found to be elevated in the AH and anterior eye tissues of PEXS affected individuals but not in PEXG cases.<sup>129,130</sup> While another study also found elevated level of IL-8 in PEXG than that of control.<sup>131</sup> Both IL-6 and IL-8 were also found to be upregulated in ciliary processes in response to hypoxia or oxidative stress *in vitro*. IL-6 in turn induces the expression of transforming growth factors and elastic fiber proteins in the extracellular matrix. This implicates a role of stress induced cytokines in the onset of excessive production of ECM proteins which is a characteristic feature of PEX.<sup>129</sup>

#### **g. Other genetic factors:**

Impaired function of autophagy was also shown to be a risk factor in the progression of PEX. Acid phosphatase, a lysosomal enzyme, is found to be decreased in the blood plasma

*CNTNAP2* gene were found to be risk factors for PEX pathogenesis through a GWAS approach. Although, mRNA expression of *CNTNAP2* was not found to be different between control and PEX affected tissues, immunohistochemistry showed a decreased expression of *CNTNAP2* in the cell membranes of anterior eye tissues. However, in a replicate group from an Italian cohort, both of these SNPs were not found to be associated with PEX. Later, an independent case-control study conducted in the Polish population also did not find a genetic association with PEX for the two reported SNPs.<sup>95</sup> Though the exact role of *CNTNAP2* in the pathogenesis of PEX is not clear; it is suggested that it may be involved in membrane stabilization and an imbalance in maintaining the ion channel function may lead to cell deformities.

**d. Clusterin:**

Clusterin (*CLU*; Gene ID: 1191) is an extracellular secreted glycoprotein with multifunctional role in the cell. It plays a crucial role in lipid transport, cell-matrix interaction and in preventing deposition of aggregates in the outer space of the cell. Cell under stress also produces a rare shorter isoform of clusterin that tends to localize inside the nucleus and mediates apoptosis. Variants in *CLU* have been associated with PEX as risk factors in German and Australian population, independently.<sup>62,124</sup> Clusterin variants also have been picked up as risk factors for many other age- related disorders like AD and diabetes.<sup>125,126</sup>

**e. Matrix Metalloproteinases and Tissue inhibitor of matrix metalloproteinases:**

Matrix metalloproteinases (MMP) are a group of enzymes which are involved in degrading extracellular matrix proteins while tissue inhibitors of metalloproteinases (TIMP1-4) include four protease inhibitors that inhibit the activity of MMPs in the ECM. Together the ratio of MMPs and TIMPs controls the rate of protein degradation and turnover of ECM proteins in the extracellular space.<sup>127</sup> Impairment in the MMPs/TIMPs ratio has been studied

groups and presence of risk allele in a higher frequency in control population indicates other genetic factors as risk factors in the pathogenesis of PEX.<sup>97</sup>

**b. Calcium voltage-gated channel subunit- $\alpha$ 1A:**

Recently, Aung *et al.* discovered a genetic association between an intronic variant, rs4926244 in the gene, Calcium voltage-gated channel subunit- $\alpha$ 1A (*CACNA1A*; Gene ID: 773) and PEX.<sup>61</sup> Bioinformatic analysis suggests that the risk allele at rs4926244 may decrease mRNA expression of *CACNA1A*. Immunostaining of *CACNA1A* shows that it is present in both anterior and posterior eye tissues.<sup>61</sup>

*CACNA1A* (calcium channel, voltage dependent, P/Q type, alpha 1A) is a protein coding gene and a prominent member in the family of calcium channels (CACN). It codes for alpha-1A subunit for the multi-subunit complexes of a calcium channel called CaV2.1 and is primarily expressed in neuronal tissue. It is involved in a variety of calcium dependent processes including neurotransmitter release and gene expression.<sup>115</sup> Previously, mutations in *CACNA1A* have been associated with autism, episodic ataxia type-2 and eye related disorders.<sup>116-118</sup> Earlier studies have also shown the presence of calcium in aggregates of PEX fibrils.<sup>73</sup> Calcium is also known to play a role in stabilizing fibrillin-1 to form stable aggregates.<sup>119</sup> Collectively, this insinuates a role of *CACNA1A* in forming PEX fibrils by altering calcium concentration.

**c. Contactin-associated protein-like 2:**

Contactin-associated protein-like 2 (*CNTNAP2*; Gene ID: 26047, 7q35-q36.1) is a membrane protein in the neurons and is a member of neurexin family. It helps in neuron-glia cell interactions and is involved in potassium channel trafficking.<sup>120,121</sup> Previously, it has been associated with neuropsychiatric disorders like schizophrenia, epilepsy and autism.<sup>122,123</sup> Krumbiegel *et al.* showed a genetic association between *CNTNAP2* and PEX in a German cohort.<sup>65</sup> Two SNPs, rs2107856 and rs2141388 within the 11<sup>th</sup> intron of

phenylalanine at 407 has a protective role by upregulating ECM proteins like elastin and fibrillin-1 and also by increasing cell-cell adhesion in human lens epithelial cell line. Jian Fan *et al.* reported yet another polymorphism, rs16958477 located upstream to *LoxLI* gene as a risk factor for PEX in a Caucasian population.<sup>107</sup> Lately, another report revealed a significant association between a *LoxLI* intronic variant, rs11638944 (C>G) and PEX. Risk allele “G” at rs11638944 disrupts the binding site for the transcription factor retinoid X receptor alpha and upregulates *LoxLI* expression with enhanced alternative splicing and through nonsense-mediated decay decreases *LoxLI* expression.<sup>99</sup>

LoxL1 plays a crucial role in polymerizing monomeric tropoelastin molecules into elastin fibrils and in crosslinking collagen fibrils through a highly conserved C-terminus region with copper-dependent amino-oxidase activity. LoxL1 does so by oxidatively deaminating the lysine residues present in tropoelastin monomers. LoxL1 not only helps in crosslinking elastin and collagen fibrils but also helps in maintaining and remodelling ECM. Immunohistochemical (IHC) studies on PEX affected tissues suggest the presence of both LoxL1 and elastin in PEX fibrils.<sup>104</sup> Earlier studies have checked the mRNA expression of LoxL1 in lens capsules and ciliary body from PEX affected subjects and found a higher expression of LoxL1 in PEXS but a decreased expression in PEXG.<sup>68,104</sup> In the PEX affected eye tissues from posterior chamber like lamina cribrosa and peripapillary sclera, LoxL1 protein is severely depleted and abnormally deposited along with aberrant deposition of elastin fibrils.<sup>66</sup> LoxL1 protein expression is altered in several vascular anomalies such as pelvic organ prolapse, aortic aneurysm and myocardial infarction all of which previously have been associated with PEX.<sup>17,108-112</sup> Mice knockout for LoxL1 resulted in loosening of skin and vascular abnormalities showing impaired elastin maintenance confirming its substantial role in the ECM maintenance.<sup>113,114</sup> Although, both at genomic and proteomic level, LoxL1 has been associated with PEX; reverse allelic association in different ethnic

contributing factors for PEX in Icelandic and Swedish population.<sup>67</sup> Both rs1048661 and rs3825942 are missense variants with a change in amino-acid at 141 (Arg→Leu, R141L) and 153 (Gly→Asp, G153D), respectively. Later, case-control studies consistently found association of variants in *LoxL1* with PEX in populations from Australia,<sup>88</sup> China,<sup>89</sup> Japan,<sup>90</sup> India,<sup>91</sup> Korea,<sup>92</sup> Mexico,<sup>93</sup> Pakistan,<sup>94</sup> Poland,<sup>95</sup> Saudi Arabia,<sup>96</sup> and the USA.<sup>97,98</sup>

Studies have shown that the “G” allele at both rs1048661 and rs3825942 are risk factors in PEX development in Caucasian and Indian populations.<sup>67,88,91,97,99</sup> However, a case-control study conducted in Japanese and Chinese population found “T” as the risk allele at rs1048661 while “A” at rs3825942 in Black South African population opposite to that reported in Caucasian population.<sup>90,100-102</sup> Few reports also indicate the absence of genetic association between rs1048661 with PEX in Greek population<sup>37</sup> and also in Polish population.<sup>95</sup> Further, risk alleles at *LoxL1* variants have higher frequency in the normal population and very low specificity in predicting the affected status.<sup>97,103</sup>

The variant rs1048661 was found to affect *LoxL1* gene expression unlike rs3825942. Transition from allele “A” to “G” at rs1048661 leads to a decrease in *LoxL1* expression by 7.7% in adipose tissue and by 20% in eye tissues.<sup>67,104</sup> Bioinformatic analysis indicates that both coding variants, rs1048661 and rs3825942 are surface residues and amino-acid substitutions at these variants can change the electrostatic potential on the protein surface and thereby, may affect protein-protein interactions. These two variants possibly alter the processing and enzymatic activation of *LoxL1*. However, ectopic expression of *LoxL1* in RFL6 (Rat fetal lung fibroblast) cells with these two variants does not show any significant difference in the elastin deposition in ECM.<sup>105</sup> Recently, Aung *et al.* also did not find a role of these two variants in *LoxL1* secretion or in ECM formation.<sup>106</sup> Instead they have found a novel rare nonsynonymous variant rs201011613 (A>T, Tyr→Phe) within *LoxL1* coding region as a risk factor for PEX. Minor “T” allele at rs201011613 which codes for

contributes to ischemic changes and oxidative stress.<sup>79,80</sup> Similarly, study subjects with lower daily intake of caffeine have a reduced risk of developing PEX.<sup>81</sup> Caffeine is known to induce the expression of extracellular matrix genes including *LoxL1*.<sup>82</sup> Thus, a large intake of caffeine and subsequent increase in ECM protein production can contribute to the pathogenesis of PEX.

Few studies support the theory of infectious agents being a cause for PEX pathogenesis.<sup>83</sup> A structural similarity between PEX fibrils and fibrillar material deposited in individuals with scrapie disorder implies the role of an infectious agent in the onset of PEX.<sup>84</sup> Development of PEX following intraocular surgery (keratoplasty) in individuals of younger age also hints that an infectious agent might be the cause of PEX pathogenesis.<sup>85</sup> Konstas *et al.* and Horven *et al.* independently showed deposition of PEX fibrils in the eyes of two patients after cataract surgery aged 17 and 35, respectively.<sup>86,87</sup> However, onset of PEX in these cases could be a result of trauma during intraocular surgeries. In a study conducted among married couples from Norwegian population, researchers have found that the prevalence of PEX is significantly higher in both partners of married couples compared to control population which also implicates that environmental factors play a role in PEX pathogenesis.<sup>83</sup>

## **1.7 Genetic factors as a risk factor in the predisposition of PEX**

### **a. Lysyl oxidase like-1:**

First genetic association study done through GWAS found variants in *Lysyl oxidase like-1* (*LoxL1*; Gene ID: 4016) situated in the chromosome 15 (q24.1) as a risk factor in the pathogenesis of PEX. *LoxL1* is a member of Lysyl oxidase gene family that codes for a group of enzymes responsible for maintenance of elastic fibers in the ECM. Two coding sequence variants, rs1048661 and rs3825942 located in the first exon and one intronic variant, rs2165241 residing in the first intron within *LoxL1* gene have been discovered as

## 1.6 Environmental factors in PEX pathogenesis

Studies in the past suggest that environmental factors play a role in the etiogenesis of PEX. Epidemiologic studies indicate a profound role of geographic location and work occupation of an individual in developing pseudoexfoliation. A report suggests that study subjects residing in the higher latitude are at higher risk for PEX.<sup>75</sup> This could be due to different amount of UV exposure at various geographic locations. It is well known that absorption of high energetic UV radiation by proteins can alter their native structure and abnormal protein may thus precipitate in the form of protein aggregates as in the case of PEX. Higher the UV exposure, greater is the risk of developing PEX.<sup>76</sup> Studies also suggest that individuals who spend more time outdoors have higher chance of developing PEX probably due to increased exposure to UV radiation.<sup>77</sup>

Environmental factors like extreme temperatures and work occupation in colder temperatures also increases the risk of PEX.<sup>77,78</sup> Both higher and colder temperature destabilise the normal structure of proteins in the extracellular matrix and basement membrane and with age deposition of such abnormal proteins may cause PEX aggregates. Higher prevalence of PEX in cold countries like Finland supports the idea of cold precipitation hypothesis.<sup>77,78</sup> Other factors such as increased number of sunny days that the person is exposed to and individuals having regular work with water and/or snow were also found to have increased risk of developing PEX.<sup>77,78</sup> Evidence from a population based epidemiologic study carried out in a south Indian population also suggests that people whose occupation involves outdoor activities have higher risk of PEX.<sup>50</sup>

Kang *et al.* studied the role of dietary supplements like vitamin-B6, vitamin-B12 and folate in the pathogenesis of PEX. Individuals having a diet with higher amount of folate are less likely to have PEX.<sup>79</sup> Although, the link between folate metabolism and risk of PEX is not clear, it probably involves homocysteine, a metabolic product of methionine that

metalloproteinases (TIMP2 and 4)		
Nidogen (Gene ID: 4811)	A basement membrane protein that plays a role in organogenesis.	A significant part of PEX material deposits is shown to have components of Nidogen. <sup>52</sup>
Syndecan-3 (Gene ID: 9672)	A type of heparan sulphate proteoglycan in the outer cellular space that mediates cell signalling and cytoskeletal organization.	Syndecan-3 also forms an integral part of PEX aggregates. <sup>52</sup>
Vitronectin (Gene ID: 7448)	An extracellular glycoprotein, promotes cell-adhesion by interacting with membrane protein integrin.	Proteomic study revealed the presence of vitronectin protein in PEX aggregates. <sup>52</sup>
<b>Proteins derived from blood serum</b>		
Complement factors (C1q, C3c and C4c)	Complement system is a part of immune system.	Proteomic studies also found deposition of complement factors in fibrillar deposits in affected tissues. <sup>52</sup>
Hemoglobin A2 (Gene ID: 3040)	A variant of hemoglobin.	Fibrillar deposits of PEX were shown to contain increased amount of Hemoglobin A2. <sup>53,54</sup>
LTBP1 and -2 (Gene ID: 4051 and 4053)	Latent Transforming Growth Factor Beta Binding Protein 1 regulates transforming growth factor beta in the ECM.	Deposition of LTBP variants in PEX aggregates and its dysregulated expression was shown in PEX tissues. <sup>73</sup>  However, genetic polymorphisms in LTBP variants were not found to be associated with PEX. <sup>74</sup>
Serum amyloid protein (Gene ID: 6288)	A group of apolipoproteins that transport cholesterol and responds to inflammation.	Different variants of serum amyloid protein are the components of PEX aggregates. <sup>52</sup>

Fibronectin (Gene ID: 2335)	Another glycoprotein, also promotes cell-adhesion by binding to integrin and ECM proteins like collagen and fibrin.	Fibronectin is also involved in the stabilization of fibrillar aggregates found in PEX individuals. <sup>52</sup>
Fibulin-2 (Gene ID: 2199)	Adapter protein in the extracellular matrix and interlinks elastin and fibrillin-1	A significant part of PEX aggregates consists of Fibulin-2 protein. <sup>52</sup>
Heparan sulphate (Gene ID: 3339)	A type of polysaccharide, remains attached to protein in form of proteoglycan in the extracellular space with various physiologic roles in the ECM.	Electron microscopic studies have shown that PEX fibrils are made up of proteins largely coated with heparan sulphate. <sup>56</sup>
Laminin (Gene ID: 284217)	A part of basal lamina that mediates cell differentiation and cell migration.	Laminin epitopes have been shown to be present in the PEX fibrils. <sup>52</sup>
LoxL1 (Gene ID: 4016)	A secretory amino-oxidase enzyme that crosslinks monomeric tropoelastin to polymeric elastin.	Genetic variants in LoxL1 gene were found to be risk factors for PEX pathogenesis. <sup>67</sup> Dysregulated expression and deposition of LoxL1 also has been seen in PEX affected tissues. <sup>66,68</sup>
MAGP-1 (Gene ID: 4237)	Microfibril associated glycoprotein-1 along with fibrillin-1 maintains microfibril function.	MAGP-1 also was shown to be a part of PEX deposits. <sup>53,54</sup>
Matrix metalloproteinases (MMP2,7 and 9) Tissue inhibitor of matrix	Matrix metalloproteinases and tissue inhibitor of matrix metalloproteinases maintain the proteostasis in the extracellular space by degrading abnormal proteins.	Deregulated expression of MMPs and TIMPs was shown in the anterior eye tissues and aqueous humour of PEX individuals. <sup>69-72</sup>

**Table 1.1.** A comprehensive list of proteins known so far in development of pseudoexfoliation and their functions are described. Proteins were divided into two categories according to their involvement and origin.

<u>Protein</u>	<u>Functional pathway</u> <u>involved</u>	<u>Relevance to PEX</u>
<b>Proteins involved in extracellular matrix maintenance</b>		
CACNA1A (Gene ID: 773)	Calcium voltage-gated channel subunit alpha1 A is a membrane channel for calcium.	Previously, impaired regulation of CACNA1A and association of its common genetic variants with PEX was shown. <sup>61</sup>
Clusterin (Gene ID: 1191)	A secretory glycosylated protein with divergent roles in the ECM including prevention of protein aggregate formation.	Variants in clusterin gene were found to be associated with PEX. <sup>62,63</sup> Expression studies also suggest an impaired regulation of clusterin expression and its deposition in diseased tissues. <sup>63,64</sup>
CNTNAP2 (Gene ID: 26047)	Contactin Associated Protein-Like 2 is a member of neurexin family and mediates interactions between neurons.	Variants in the CNTNAP2 gene have been associated with PEX as risk factors. <sup>65</sup> Dysregulated expression of CNTNAP2 was shown in PEX affected tissues. <sup>65</sup>
Desmocolin-2 (Gene ID: 1824)	A cadherin-type protein that helps in forming desmosomes.	Desmocolin type proteins were seen in the proteomic analysis of PEX aggregates. <sup>52</sup>
Elastin (and Tropoelastin) (Gene ID: 2006)	Elastin fibers are polymerized forms of monomeric tropoelastin secreted by the fibroblast cells into outer cellular space.	Elastin deposition was found to be impaired in affected tissues in cases. <sup>66</sup> Also, elastin forms an integral part of PEX deposits. <sup>52</sup>
Emilin (Gene ID: 11117)	It is a matrix glycoprotein which helps in anchoring smooth muscle cells to elastic fibers.	It is also found to be a part of PEX materials. <sup>54</sup>
Fibrillin-1 (Gene ID: 2200)	Extracellular scaffold protein which polymerizes to insoluble microfibrils in the ECM.	Proteomic study has shown the presence of fibrillin-1 in PEX deposits. <sup>52</sup>

the surface of lens capsule, zonules, ciliary body and iris, and has an electron-dense amorphous appearance under electron microscopy.<sup>4,14,56</sup>

Proteins that are reported to be a part of PEX aggregates and the functional pathway that they are involved in are listed in **Table 1.1**. Broadly, these proteins can be grouped into two categories depending on their localization and function: Extracellular matrix (ECM) proteins and Blood derived proteins. Proteins in the basement membrane and those that form the extracellular scaffold are predominantly present in the PEX aggregates. Evidently, ECM related proteins like fibrillin-1, fibulin-2, tropoelastin, elastin, desmocollin-2, emilin, heparan sulphate, syndecan-3, microfibril associated glycoprotein (MAGP-1), Lysyl oxidase like-1 (LoxL1), vitronectin, fibronectin, laminin, nidogen, matrix metalloproteinases (MMPs), tissue inhibitor of matrix metalloproteinases (TIMPs) and the extracellular chaperone Clusterin (CLU) are predominantly found in the PEX deposits.<sup>52-54</sup> Presence of such proteins in the PEX aggregates suggests that an elastotic process which involves improper maintenance of ECM proteins underlies the pathogenesis of PEX. However, it is unknown whether age-related deposition of PEX fibrils is due to excess production or decreased degradation of ECM proteins.

PEX aggregates are also known to contain blood derived proteins such as LTBP1 and -2 (latent transforming growth factor  $\beta$  binding proteins), Hemoglobin A2, Complement factors (C1q, C3c and C4c) and serum amyloid protein.<sup>52-54</sup> Finding of such proteins in the deposits indicates a breakdown in the blood-aqueous barrier which allows leakage of these proteins into the aqueous humour and their subsequent deposition on the surface of eye tissues. Presence of PEX fibril like materials on the extra-ocular tissues provides further evidence towards impairment of the blood-aqueous barrier in PEX subjects.<sup>54,57-60</sup>

second eye was found to be 6.8% after 5 years and 16.8% after 10 years from the date of diagnosis.<sup>46</sup>

Thomas *et al.* reported for the first time, the prevalence of PEX in an Indian population from southern region.<sup>50</sup> Accordingly, the overall prevalence was found to be 0.69% among the population which increases with age. While in individuals aged 40 or older, PEX incidence was found to be 3.01%, it increased to 6.28% in subjects aged above 60. PEX was also found to be associated with loss of vision or PEXG with an odds ratio of 4.25 after age correction. Increased intraocular pressure is significantly high in PEXG group than that of individuals only with glaucoma. Around 20.5% of PEXS affected individuals are found to be visually impaired.<sup>45,50</sup> Another demographic study conducted in a population from central India also found that PEX prevalence is age dependent and is associated with lower body-mass index and higher diastolic blood pressure, but PEX was not associated with retinal nerve fiber layer cross section area (a parameter used to determine the healthy state of ocular vision) and open-angle glaucoma.<sup>51</sup>

### **1.5 PEX material composition and pathology**

Previous studies have done proteomic, immunostaining and electron microscopic analysis of PEX aggregates which shows that they are made up of extracellular protein aggregates arranged in a microfibrillar form.<sup>4,52-54</sup> As seen through transmission electron microscopy (TEM) these microfibrils fall into two categories depending on their diameter: type-A fibrils with a diameter of 18-25 nm and type-B fibrils with a diameter of 30-45 nm. Each of these fibrils is made up of microfibrils of 8-10 nm in diameter and are deposited side by side to form large PEX aggregates. Mature PEX fibrils also show characteristic bands at a periodicity of 50 nm.<sup>55</sup> Previous studies have reported the presence of a core consisting of glycoproteins covered by heavily glycosylated glycoconjugates like hyaluronan, heparan sulphate proteoglycan, chondroitin sulphate, dermatan and keratin sulphate proteoglycan on

## 1.4 PEX demographics

PEX is an age-related disorder, the incidence of which increases with age in the population. Prevalence of PEX varies widely among population. Demographic studies on PEX prevalence suggest that it is highest in the population of Greece (15.2%) and lowest in the South African population (2.8%).<sup>37</sup> However, segregation of study subjects into different age group showed an increased incident rate in relatively aged individuals. Around 33% of recruited study subjects were found to be affected by PEX in the age group of 80-89 years. Similarly, in an Icelandic population, PEX incidence rate is found to be 17.7% in individuals in the age group of 70-79 years which increased to 40.6% in the study subjects aged more than 80.<sup>38</sup> Accordingly, with individuals aged above 50 the chance of getting affected by PEX becomes two-fold with each decade.<sup>38-40</sup>

Studies conducted on PEX incidence by segregating recruited study subjects based on gender suggests more prevalence of PEX in men than in women.<sup>41</sup> This is, however, inconsistent as some studies suggest PEX frequency to be higher in women.<sup>42,43</sup> Some report also disapprove of sex bias in PEX incidence.<sup>38,42,44</sup>

Reports suggest PEXG to be the most significant risk factor towards developing secondary glaucoma worldwide. Around 50% of PEXS affected individuals over age 70 develop PEXG with deteriorated ONH cells resulting in decreased vision at a later stage.<sup>45</sup> Henry *et al.* showed that PEX patients have a ten-fold higher chance of developing ocular hypertension or glaucoma within ten years than the normal population.<sup>46</sup> Development of PEX can involve one (unilateral) or both (bilateral) of the eyes. Previous studies have indicated a higher occurrence of bilateral cases in PEX individuals than unilateral cases.<sup>47,48</sup> Further, individuals affected bilaterally have higher progression rate towards glaucoma compared to unilateral cases.<sup>49</sup> According to a report, chance of developing PEX in the

Despite being associated with various non-ocular diseases, the mechanism through which PEX underlies the pathogenesis of such vascular complications is unknown. Deposition of fibrillar aggregates in the vessel walls and increased oxidative stress might be attributed to PEX related vascular complications.<sup>31</sup>

Earlier reports have studied the interrelation between PEX and the age related neurodegenerative disorder, Alzheimer's disease (AD; OMIM: 104300). Accumulation of abnormal protein aggregates made up of amyloid- $\beta$ -peptide and phosphorylated tau protein in the brain tissues results in the degeneration of brain neurons which are required for daily activity and leads to onset of AD. Thus, both PEX and AD share similar pathological alterations like characteristic deposition of fibrillar protein aggregates and gradual deterioration of optic and brain nerves, respectively. AD related proteins such as amyloid beta-peptide, serine proteinase inhibitor and alpha-1-antichymotrypsin were found in both PEXS and PEXG cases suggesting a common aetiology between AD and PEX pathogenesis.<sup>32</sup> An epidemiological survey on Norwegian population suggests an increased risk of PEX in AD patients suffering from dementia and cognitive impairments compared to an age matched population.<sup>33</sup> PEXG is also associated with a reduction in the blood flow velocity and elevation in the resistance of the middle cerebral arteries.<sup>34</sup> Albricht *et al.* showed that PEXG individuals have increased number of dense pattern of closely arranged myelinated fibers with lost staining for glial fibrillary acidic protein (GFAP) within the nerve fibre bundles of the retrolaminar optic nerve compared to non-glaucomatous control eyes. GFAP is a general marker for astrocytes and loss of GFAP staining indicates death of astroglial cells in such densified regions. Decreased GFAP was also found in chronic swelling and vacuolation of white matter astroglia in AD.<sup>35</sup> However, an epidemiological study on Swedish cohort didn't find a correlation between PEX and AD.<sup>36</sup>

Progression of PEX leads to other ocular complications like zonular weakness, cataract formation, iris depigmentation, xerophthalmia, retinal-vein occlusion, lens subluxation and lens dislocation.<sup>5,6</sup> PEX also has been found to be associated with age-related macular degeneration.<sup>6</sup> Studies on tissue structure from PEX affected eyes suggest cell loss in different forms in comparison to control unaffected eye tissues. Thinner cornea and decreased endothelial cell densities were reported in eyes affected with PEX.<sup>7-9</sup> Further, cells in the anterior lens capsule from PEX show more affinity to trypan blue suggesting increased number of dead cells than in control subjects. Also, in the posterior segment of affected eyes both circumpapillary and macular retinal nerve fibre layer thickness was found to be decreased.<sup>10</sup> The mean value of choroidal thickness in such regions is further lowered in more severe stage of PEXG than in PEXS.<sup>11</sup> Lamina cribrosa that forms an integral structural element of optic nerve head is also found to be thinned in PEX and a marked decrease in the stiffness of ONH cells is reported.<sup>12,13</sup>

### **1.3 Pseudoexfoliation: A Systemic Disorder**

Presence of PEX material in tissues other than the eye and its association with non-ocular disorders suggests its systemic manifestation. PEX fibrils in both intra-ocular and extra-ocular tissues are found to contain the same sugar residues of glyco-conjugates which implicates, PEX is a systemic disorder.<sup>14</sup> Previous studies have shown that individuals with PEX have higher incidences of various non-ocular disorders including renovascular disease, abdominal aorta aneurysm, coronary artery disease, peripheral vascular diseases, cardiovascular and cerebrovascular complications, sensorineural hearing impairment, erectile dysfunction, systemic endothelial dysfunction and pelvic organ prolapse.<sup>15-26</sup> However, few reports also negate the association between cardiovascular complications and PEX.<sup>27-29</sup> Regardless of being a systemic disorder, PEX was not found to be a life-threatening condition.<sup>30</sup>

## 1.2 Ocular manifestation of pseudoexfoliation

Clinically, PEX is diagnosed by using a slit-lamp to check the presence of PEX fibrils in the iris-pupillary margin and on the anterior surface of lens capsule (**Figure 1.2**). PEX fibrils on the lens capsule surface can be seen deposited in two different patterns; classical concentric ring form or radial pigmentary form. It is reported that radial pigment form of deposits represents an early or less severe form of PEX.<sup>2</sup> Such characteristic deposition of PEX fibrils on the pupillary surface of lens capsule may be due to iris-capsular rubbing during iris movement. PEX fibrils were also found to be deposited on the tissue surface of posterior eye segment such as lamina cribrosa, peripapillary sclera and vitreous.<sup>3</sup>

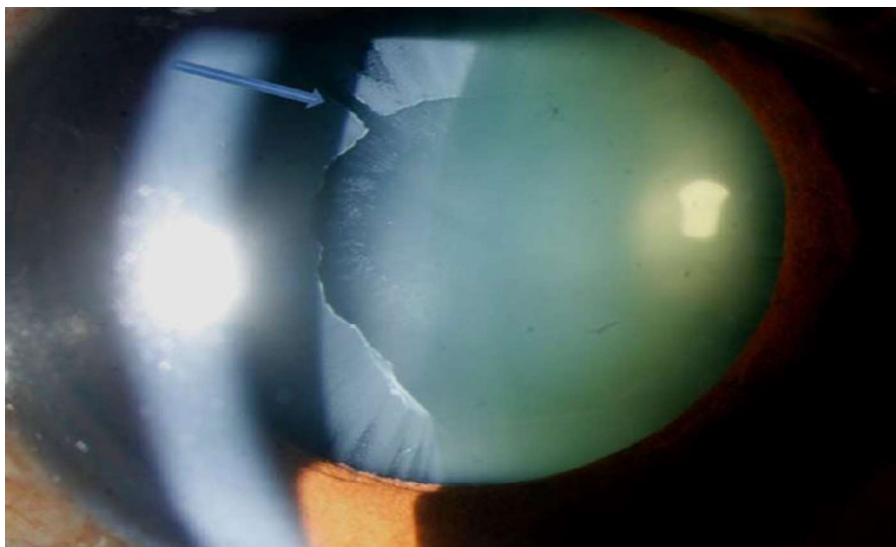


**Figure 1.2.** A clinical picture of a pseudoexfoliation affected eye showing a classical pattern of PEX fibril deposition on the surface of lens capsule taken by slit-lamp microscopy (Adopted from International glaucoma association).

In PEXG individuals, optic nerve damage can result from pathology in the ganglion cell and inner plexiform layers of the retina. Death of these cells gradually lead to loss of vision or blindness. The severity of ONH damage corresponds to the amount of PEX material deposited. PEXG affected individuals also show more advanced visual field loss, greater mean intraocular pressure (IOP) and poorer response to treatment.<sup>4</sup>

## 1.1 Introduction:

Pseudoexfoliation (PEX; OMIM: 177650) is an age-related systemic disorder which is diagnosed by deposition of proteinaceous aggregates called PEX fibrils on the tissue surface of anterior eye segment which includes lens capsule, iris pupillary border, zonules, ciliary body, corneal endothelial surface, irido corneal angle, trabecular meshwork and also in the juxtacanalicular tissue area adjacent to the inner and outer wall of Schlemm's canal (Anatomy of human eye; **Figure 1.1**).<sup>1</sup> This initial stage of PEX is called as pseudoexfoliation syndrome (PEXS) which is characterized by fibrillar aggregates with no damage to optic nerve head (ONH) cells. In the later more severe form of PEX, degeneration of retinal ganglion cell axons in the optic nerve head (ONH) region located in the posterior segment of the eye is seen and is known as pseudoexfoliation glaucoma (PEXG). PEXG is a leading cause of secondary glaucoma worldwide. Around half of the PEX affected individuals develop into such severe form, PEXG in comparison to the less severe or early form, PEXS.

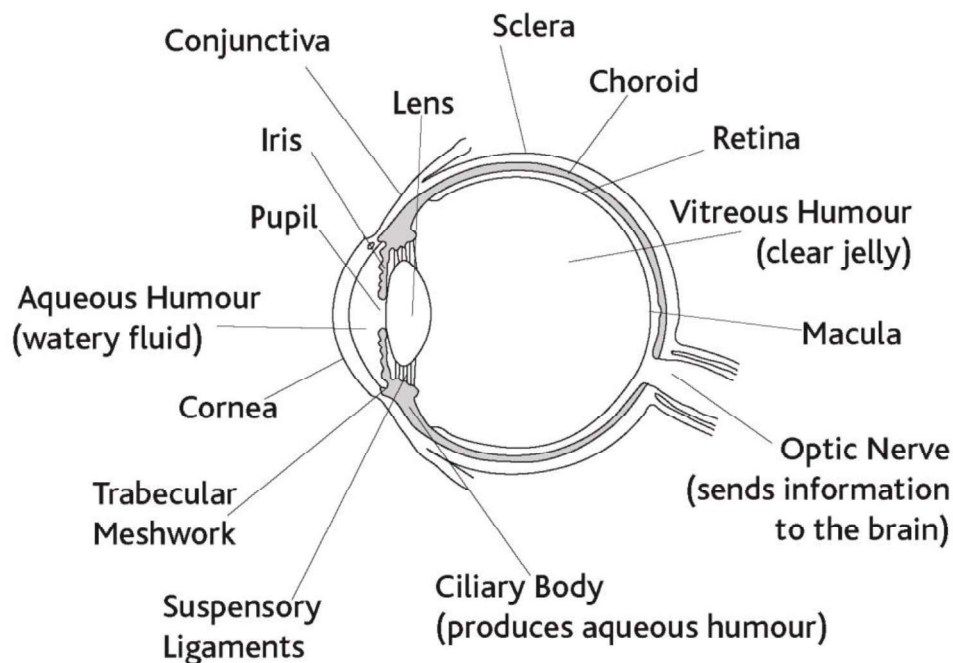


**Figure 1.1.** Anatomy of human eye showing internal anterior and posterior chamber and a detailed tissue structure (Adopted from International glaucoma association <https://www.glaucoma-association.com/>).

# **CHAPTER 1**

**Introduction**

**&**

**Review of Literature**

likely consists of individuals for all of these genotypes. Consistent with the previous reports, upregulation of clusterin mRNA in PEXG individuals is also observed in this study.<sup>64</sup> Although, rs2279590 resides in the seventh intronic region of clusterin gene, the mechanism through which it affects *CLU* gene transcription still remains to be seen.

## **2.5 Conclusion**

It can be inferred that the risk allele “G” at rs2279590 confers an allele specific upregulation of clusterin mRNA either by itself or through a nearby locus with strong LD and is a strong risk factor towards developing PEXS. Accumulation of Clusterin in aqueous humor as well as on the surface of lens capsules in PEXG individuals augments further protein deposition and might enhance the severity of PEX similar to that of Alzheimer’s disease.

related disorder. Also, upregulated expression of CLU has been reported as a pathological manifestation in tissues undergoing apoptosis in an ocular disorder, retinitis pigmentosa.<sup>180</sup> CLU might be doing so by inducing the expression of DKK1, a cytotoxic protein as shown by Killinck *et al.*<sup>176</sup>

There was also a significant increase of Clusterin protein in the aqueous humor of PEXG individuals. As previously reported, Clusterin protein is upregulated in individuals suffering from Alzheimer’s disease; yet it remains to be proven whether it’s an effect after the development of these disorders or the cause.<sup>181</sup> As for the functional significance of the associated risk allele, it needs to be seen whether the risk allele, either by itself or because of a nearby SNP in linkage, affects the synthesis process or proper secretion of the protein.

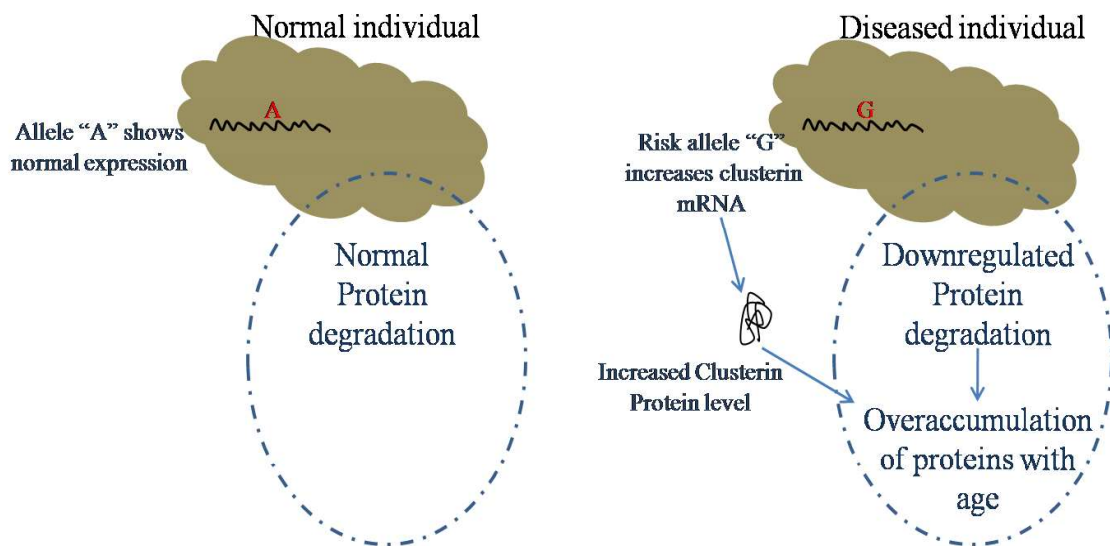


**Figure 2.11.** A model showing decreased degradation of total proteins in PEX individuals which with increasing age leads to accumulation of ECM proteins. The risk allele “G” in rs2279590 further enhances the severity by increasing the expression level of clusterin mRNA.

The present study showed that there is no difference in the mRNA level of clusterin between cases and controls. However, a significant increase in mRNA per “G” risk allele with a half-fold difference was found. Accordingly, the high risk “GG” genotype showed a two-fold increased expression compared to “AA” genotype. This difference in genotypic expression can explain why there is no difference between PEXS and PEXG groups, since each group most

GIH (represents Gujarati Indians in Houston, Texas) the tagged SNPs surrounding rs2279590 are found to be in strong LD (**Figure 2.10**).

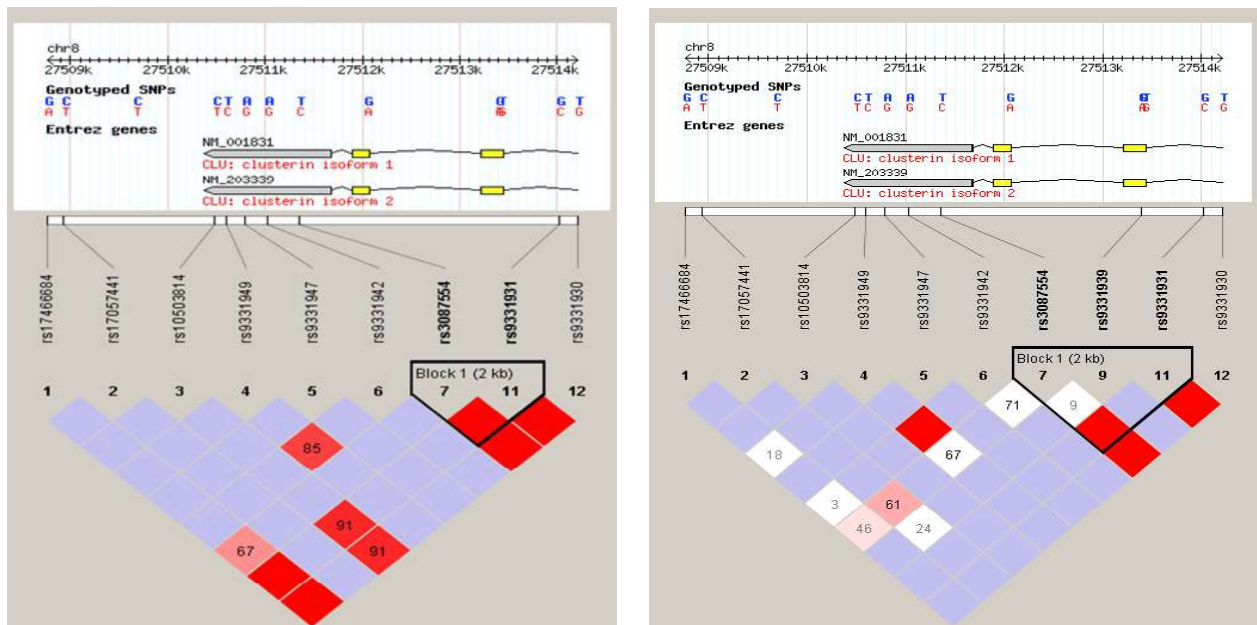


**Figure 2.10.** HapMap data was used to find out the linkage disequilibrium differences between Caucasian (CEU: Utah residents from North and West Europe ancestry from the CEPH collection) and Indian (GIH: Gujarati Indians from Houston, Texas) population. Tagged SNPs surrounding rs2279590 (rs1746684, rs17057441, rs10503814, rs9331949, rs9331947, rs9331942, rs3087554, rs9331931 and rs9331930) were selected by Haploview 4.2 and their corresponding LD was compared between CEU and GIH group. There is a strong LD between the tagged SNPs surrounding rs2279590 in both CEU and GIH.

## 2.4.2 Over-accumulation of CLU in the anterior eye tissues of PEXG affected individuals

Consistent with western blot analysis there was significantly higher deposition of Clusterin in the lens capsules of PEXG individuals but not in the control or PEXS individuals as seen by immunohistochemistry. All these results showing higher level of clusterin mRNA in the associated genotype “GG” as well as upregulated protein in later stages of PEXG can be explained by a proposed model as shown in **Figure 2.11**. The risk allele “G” enhances protein deposition by increasing the synthesis of mRNA. Since, we also found accumulation of total protein in more advanced stages of PEX, we proposed that decrease in maintenance of extracellular proteins is responsible for the pathogenesis of later stages of PEXG in this age-

## 2.4 Discussion

Clusterin plays a prominent role in the progression of PEX. A fine balance between secretory CLU and nuclear form of CLU is essential for cell survivability. Our work is focused on the role of *CLU* genetic variants in PEX as well as its dysregulated expression in inducing a regulator of apoptosis, DKK1 in affected tissues.

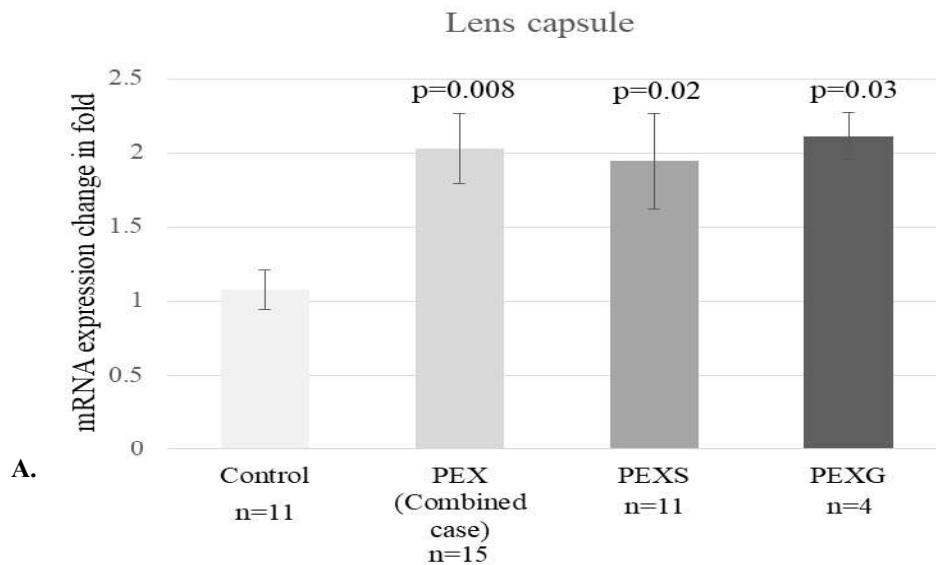
### 2.4.1 Both rs3088754 and rs2279590 are risk factors for development of PEX in Indian population

In our study population, rs2279590 was found to be significantly associated with PEX individuals. Although rs3087554 was not found to be initially associated with PEX, after age and sex correction it was found to be strongly associated. rs2279590 located in the seventh intronic region of clusterin gene has also been genetically associated with Alzheimer's disease (characterized by deposition of amyloid fibers) and type-2 diabetes mellitus.<sup>125,126</sup> However, between Alzheimer's and diabetes the associated risk allele was found to be different. The high- risk allele is "A" for developing type-2 diabetes mellitus, while for Alzheimer's disease it is allele "G". Similarly, as reported earlier for LoxL1, a strong candidate for PEX development, the risk allele was found to be opposite in different populations. In a similar context, we found allele "G" of rs2279590 as the high- risk allele but not the opposite allele "A" as found in German population.<sup>62</sup> Allele "A" of rs3087554 remains the high- risk allele as reported earlier in Australian population but only for PEXS and not PEXG individuals in our population.<sup>124</sup> In order to find out any differences in linkage disequilibrium, tagged SNPs surrounding rs2279590 between the two populations were compared. In both CEU (represents Utah residents with Northern and Western European ancestry from the CEPH collection) and

that of control. This suggests that CLU accumulation might lead to induction of DKK1 and subsequent pathological alterations seen in the anterior eye tissues of PEX affected subjects.

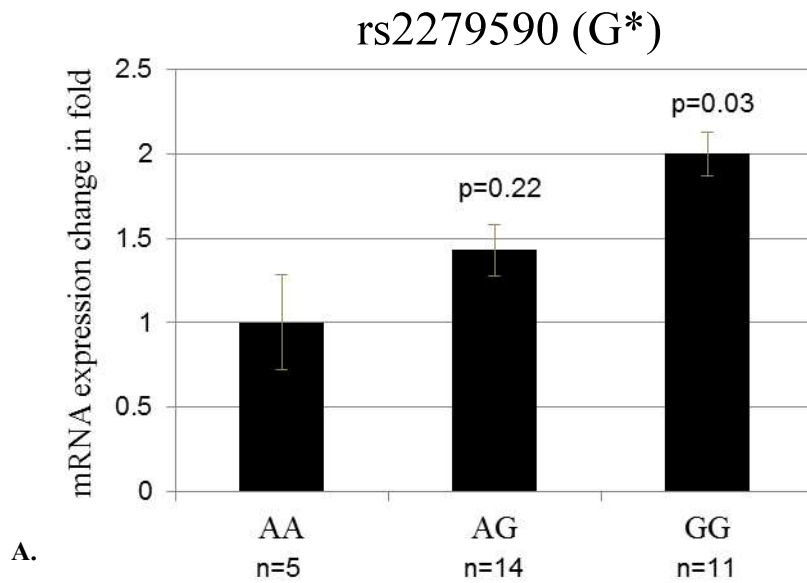
Demographics of study subjects involved for collection of samples were presented in the

**Figure 2.9B.**



Groups	n=	Age (in years)		Sex		Manifestation	
		Mean±SD	Range	Male	Female	Unilateral	Bilateral
Control	11	61±11.4	40-78	5	6	NA	NA
PEX Combined	15	65.9±9.7	40-90	10	5	6	9
PEXS	11	65.1±7.6	40-83	8	3	4	7
PEXG	4	66.33±5.8	40-90	2	2	2	2

**Figure 2.9.** qRT-PCR assays for DKK1 expression in the lens capsule of study subjects. mRNA expression of DKK1 was checked in the lens capsule of control and PEX affected tissues through qRT-PCR assays. **(A)** Compared to that of control (1.07±0.13) there is a significant upregulation of DKK1 in PEX (2.02±0.23, p=0.008), PEXS (1.94±0.32, p=0.02) and PEXG (2.11±0.15, p=0.03) affected individuals. **(B)** Demographic and clinical features of study subjects included for q-RT PCR for group wise comparison. \*p<0.05, n=sample size



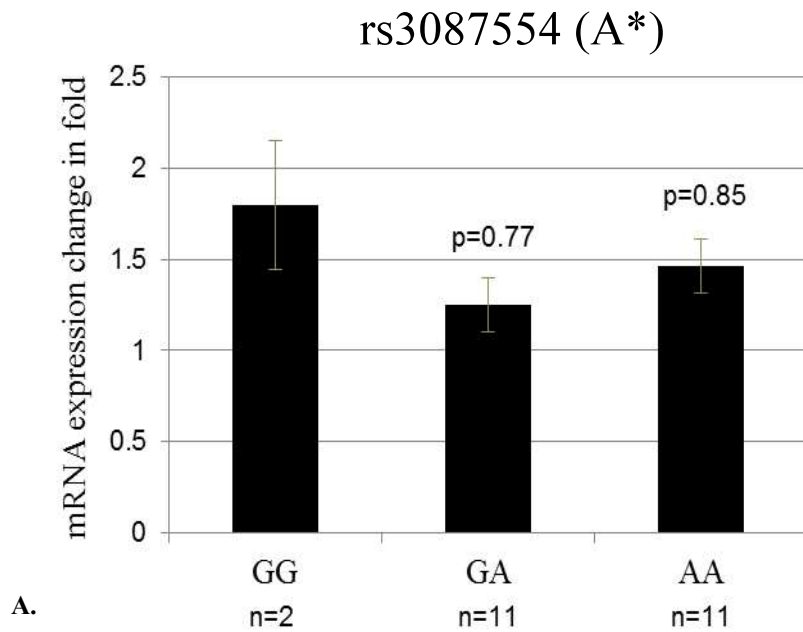
**B.**

rs2279590 Genotype	n=	Age (in years)		Sex		Manifestation in cases	
		Mean±SD	Range	Male	Female	Unilateral	Bilateral
AA	5	64.2±21.6	40-92	2	3	1	3
AG	14	66.07±8.7	40-83	8	6	10	4
GG	11	64.27±13.2	40-80	8	3	7	4

**Figure 2.8.** rs2279590 genotype wise comparison of *CLU* mRNA expression. **(A)** *CLU* mRNA expression is grouped according to genotype of rs2279590 by taking protective genotype “AA” as the reference genotype. Compared to genotype “AA” ( $1 \pm 0.28$ ) and “AG” ( $1.43 \pm 0.15$ ,  $p=0.22$ ) *CLU* expression was found to be significantly upregulated in the risk genotype “GG” ( $2 \pm 0.13$ ,  $p=0.03$ ) in the lens capsule. **(B)** Demographic and clinical features of study subjects included for q-RT PCR for genotype wise comparison. n=sample size.

### 2.3.4 Expression of Dickopff-1 in the anterior eye tissues of PEX affected individuals

We have also checked the expression of dickopff-1 (*DKK1*), an antagonist of canonical signaling pathway. DKK1 regulates the expression of toxic proteins leading to cell death and expression of DKK1 is induced by CLU accumulation.<sup>176</sup> As shown in **Figure 2.9A**, we found a significantly increased mRNA expression of DKK1 gene in the lens capsule of PEX (2.02 fold,  $p=0.008$ ), PEXS (1.94 fold,  $p=0.02$ ) and PEXG (2.11 fold,  $p=0.03$ ) subjects compared to



B.

rs3087554 Genotype	N=	Age (in years)		Sex		Manifestation in cases	
		Mean±SD	Range	Male	Female	Unilateral	Bilateral
GG	2	61.2±19.8	40-81	2	0	1	1
AG	11	63.49±9.6	40-84	8	3	5	6
AA	11	62.38±8.76	40-86	7	4	4	7

**Figure 2.7.** rs3087554 genotype wise comparison of *CLU* mRNA expression. **(A)** *CLU* mRNA expression is grouped according to genotype of rs3087554 by taking protective genotype “GG” as the reference genotype. There is no significant difference of *CLU* expression between genotype “GG” ( $1.8 \pm 0.35$ ) versus “AG” ( $1.2 \pm 0.15$ ,  $p=0.77$ ) or “AA” ( $1.46 \pm 0.14$ ,  $p=0.85$ ). **(B)** Demographic and clinical features of study subjects included for q-RT PCR for genotype wise comparison. n=sample size. Asterisk confers to risk allele.

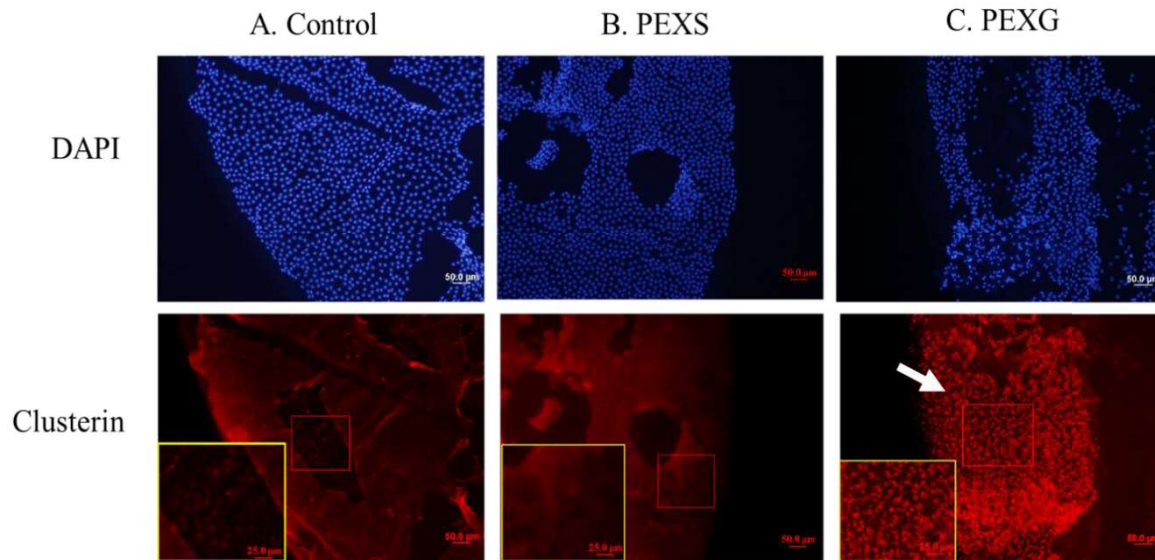
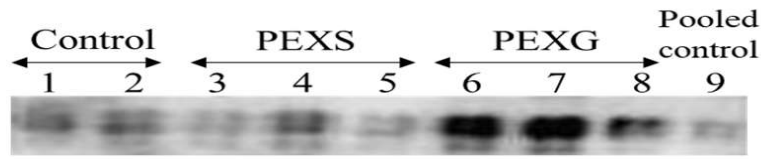


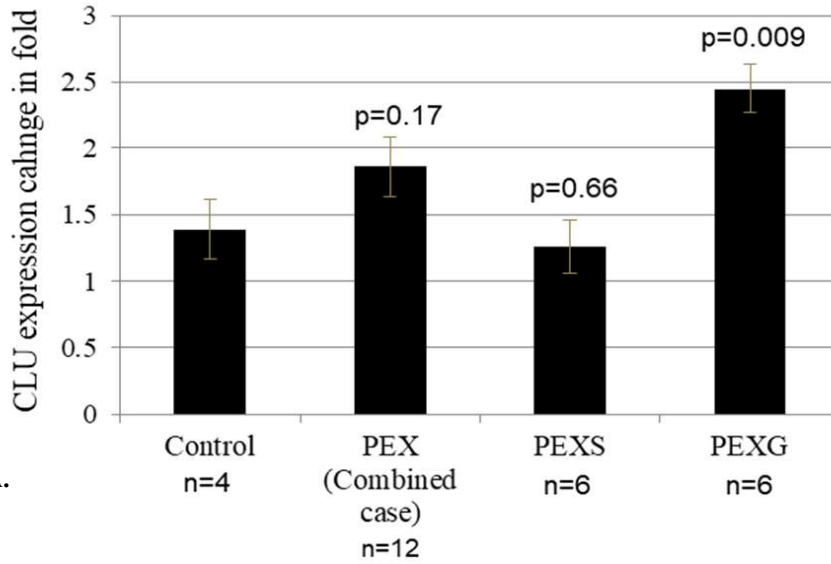
**Figure 2.6.** Immunostaining of Clusterin protein on the lens capsule in control (A), PEXS (B) and PEXG (C). Upper panel represents DAPI stained nuclear pattern while lower panel represents immunopositive Clusterin deposits on the periphery of lens capsule surface in PEXG group only. Comparison of Square insets within the zoomed images shows significant deposition of CLU in PEXG than that of control and PEXS individuals.

### 2.3.3 Regulatory role of clusterin intronic variants

We then checked the regulatory effect of both non-coding variants, rs3087554 and rs2279590.  $\Delta\Delta Ct$  values were grouped for each variant according to the genotype of individuals. There is no significant effect of rs3087554 genotype on *CLU* mRNA expression as shown in **Figure 2.7A**. Demographic and clinical features of study subjects included for q-RT PCR for genotype wise comparison of rs3087554 is shown in **Table 2.7B**. However, after grouping of  $\Delta\Delta Ct$  values according to the genotype of rs2279590, we found a significant increase of clusterin mRNA level per “G” risk allele (**Figure 2.8A**). Demographic and clinical features of study subjects included for q-RT PCR for genotype wise comparison of rs2279590 is shown in **Table 2.8B**. There was a half-fold increase in clusterin mRNA expression in individuals with genotype “AG” (n=14, p=0.22) compared to “AA” (n=5) genotype and this increases to two-fold in “GG” individuals (n=11, p=0.039).



Aqueous humor



A.

Group	n=	Age (in years)		Sex		Manifestation in cases	
		Mean±SD	Range	Male	Female	Unilateral	Bilateral
Control	4	64.34±16.74	40-87	2	2	1	3
PEX Combined	12	68.31±11.86	40-92	8	4	5	7
PEXS	6	66.77±8.93	40-88	4	2	2	4
PEXG	6	69.91±14.7	40-92	4	2	3	3

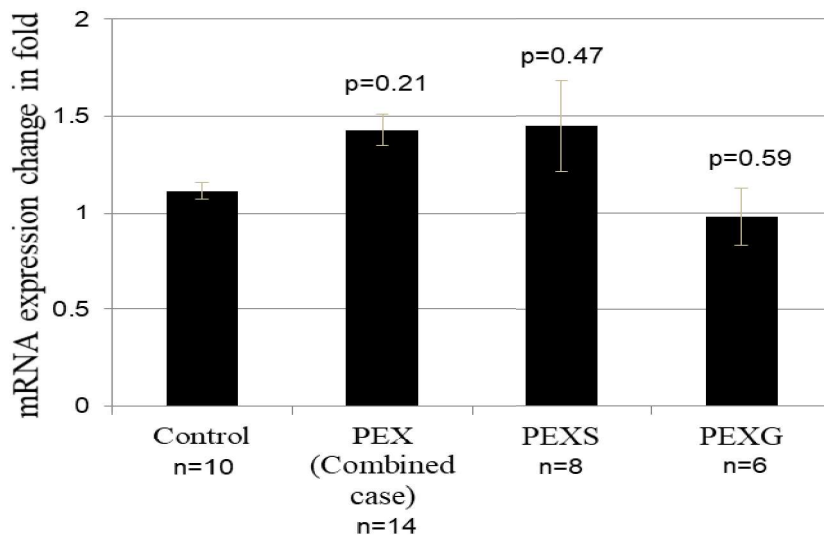
B.

**Figure 2.5.** Differential Clusterin accumulation in PEX affected subjects compared to control. **(A)** Western blot showing fold change of Clusterin in aqueous humour of control (lane 1 and 2), PEXS (lane 3, 4 and 5), PEXG (lane 6, 7 and 8) and pooled sample from fifteen controls (lane 9). Clusterin level averaged from two blots among the groups. Compared to that of control (1.39±0.22) Clusterin was found to be significantly upregulated (p=0.009) in PEXG with a fold difference of 2.45±0.18 but not so in case of PEX (1.86±0.22, p=0.17) and PEXS (1.26±0.18, p=0.66). **(B)** Demographic and clinical features of study subjects included for comparison. n=sample size.

Group	n=	Age (in years)		Sex		Manifestation in cases	
		Mean±SD	Range	Male	Female	Unilateral	Bilateral
Control	17	60.08±16.3	40-91	11	6	8	9
PEX Combined	22	65±11.39	40-92	13	9	9	13
PEXS	10	64.57±7.83	40-88	6	4	5	5
PEXG	12	66.37±13.2	40-92	7	5	4	8

**Figure 2.4.** Total protein estimation in in PEX affected subjects compared to control. **(A)** Total protein level in the aqueous humor of control, combined cases, PEXS and PEXG. There is a significant two-fold upregulation of total protein level in the aqueous humor of PEX (133.4±20.5) and PEXG (162.51±31.04) individuals with a p-value of 0.01 and 0.02 respectively than that of control (76.54±11.64) but not so in case of PEXS (98.46±19.43, p=0.34). **(B)** Demographic and clinical features of study subjects included for protein estimation for group wise comparison. n=sample size.

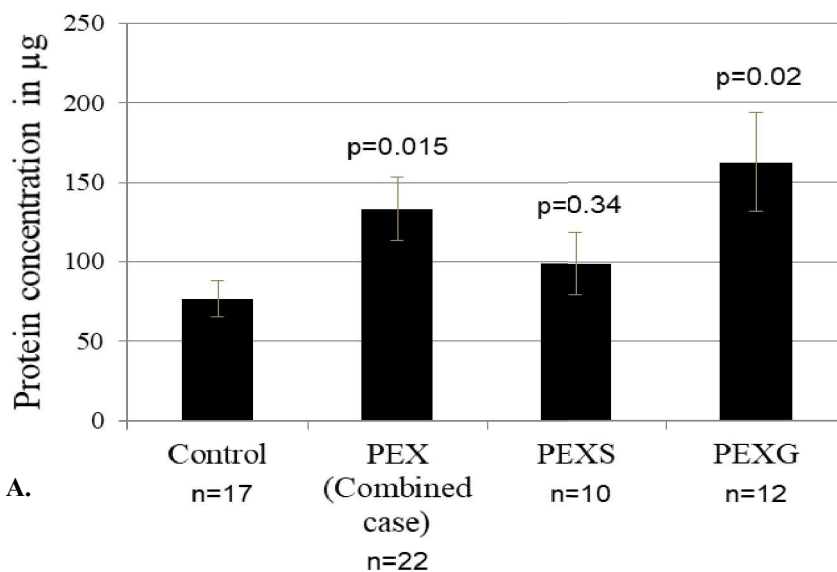
Western blot showed presence of Clusterin in aqueous humor (**Figure 2.5A**). A prominent band at 40kDa was detected which corresponds to secreted Clusterin monomers from cleavage of  $\alpha$  and  $\beta$  chains from *CLU* transcripts in the aqueous humor. Two other light bands of higher (110 and 210 kDa) molecular weight was also seen which may correspond to multimers of *CLU* protein. There was a two-fold upregulation of Clusterin protein in PEXG group (n=6, p=0.009, **Figure 2.5A**) in comparison to control (n=4). There is a little down regulation of Clusterin level in PEXS individuals compared to control but was not found to be statistically significant (n=6, p=0.66). Demographics of the study subjects involved for collection of samples for checking *CLU* amount were presented in the **Table 2.5B**. Immunofluorescence staining in the periphery of the lens capsule surface (site of PEX material deposition) shows a higher deposition of *CLU* in dense punctuate pattern in PEXG individuals. However, there was not much difference observed between PEXS and control (**Figure 2.6**).



**B.**

Groups	n=	Age (in years)		Sex		Manifestation	
		Mean±SD	Range	Male	Female	Unilateral	Bilateral
Control	10	59±14.9	40-74	3	7	NA	NA
PEX Combined	14	67.7±10.4	40-92	9	5	2	12
PEXS	8	67.25±8.2	40-83	6	2	1	7
PEXG	6	68.33±13.7	40-92	3	3	1	5

**Figure 2.3.** Clusterin mRNA expression change in PEX affected subjects compared to control. **(A)** Real-time quantitative PCR showing the fold change of clusterin mRNA in the lens capsules of control, PEX (combined cases), PEXS and PEXG. There was no significant change in expression in lens capsule tissues from control ( $1.11 \pm 0.04$ ), PEX ( $1.43 \pm 0.08$ ,  $p=0.21$ ), PEXS ( $1.45 \pm 0.23$ ,  $p=0.47$ ) and PEXG ( $0.98 \pm 0.14$ ,  $p=0.59$ ) individuals. **(B)** Demographic and clinical features of study subjects included for q-RT PCR for group wise comparison. n=sample size.



In PEXG the association is only nominally significant ( $p=0.04$ ). rs2279590 confers a risk of 1.76 (CI 1.21-2.53) in combined cases while for PEXS and PEXG it is found to be 1.78 (CI 1.15-2.71) and 1.73 (CI 1.07-2.79), respectively (**Table 2.6**). The current study has 87% power at  $\alpha = 0.05$  level significance with risk allele frequency as well as marker allele frequency set to 0.66, with prevalence 3.8%<sup>179</sup> while linkage disequilibrium or  $D'$  was set to 1.

**Table 2.6.** Odds ratio (OR) and Confidence interval (CI) of two clusterin variants. OR of each allelic variant was calculated and presented. Individuals with risk allele at rs2279590 show high risk of developing PEX with a OR of 1.759 (CI: 1.21-2.53) than that with risk allele at rs3087554 (OR: 1.439, CI: 1-2.05).

Group	rs3087554			rs2279590		
	Risk Allele Freq.	OR	95% CI	Risk Allele Freq.	OR	95% CI
<b>Control</b>	0.46			0.52		
<b>PEX Combined</b>	0.55	1.439	1.0-2.05	0.66	1.759	1.21-2.53
<b>PEXS</b>	0.58	1.659	1.08-2.5	0.66	1.778	1.15-2.71
<b>PEXG</b>	0.50	1.17	0.73-1.87	0.65	1.73	1.07-2.79

### 2.3.2 Clusterin expression in anterior eye tissues of pseudoexfoliation

Real-time quantitative PCR showed no significant fold change in the mRNA level of clusterin in the lens capsule of cases ( $n=14$ ,  $p=0.21$ ) compared to control ( $n=10$ ). Even after separation of cases into PEXS ( $n=8$ ,  $p=0.47$ ) and PEXG ( $n=6$ ,  $p=0.59$ ), there was no difference between case and control subjects (**Figure 2.3A**). Demographic data of the study subjects included for the study is presented in the **Figure 2.3B**. The total protein concentration in PEXS ( $n=10$ ) was found to be  $98.46 \pm 61.43$   $\mu\text{g/ml}$  which is slightly but not significantly different (1.3- fold,  $p=0.34$ ) than control ( $n=17$ ) having  $76.54 \pm 48.03$   $\mu\text{g/ml}$ , though each group showed a very high inter-individual variability (**Figure 2.4A**). However, there was a two-fold increase in the total protein level in PEXG individuals having  $162.51 \pm 112.21$   $\mu\text{g/ml}$  ( $n=12$ ,  $p=0.02$ ) compared to control which was statistically significant. Demographics of study subjects involved for collection of samples were presented in **Figure 2.4B**.

Haplotype analysis as shown in **Table 2.5**, revealed “AG” (rs3087554 and rs2279590, respectively) as the high risk haplotype with a significant association both in combined and in PEXS cases (p=0.001 and P=0.0008, respectively) even after permutation correction (p=0.006 and p=0.003, respectively).

**Table 2.5.** Haplotype association of the two variants rs3087554 and rs2279590, respectively with pseudoexfoliation. Frequency of haplotype combinations from alleles at rs3087554 and rs2279590, respectively were compared between cases and controls. Frequency of risk haplotype “A-G” (rs3087554-rs2279590) in control (0.163) is lower in comparison to PEX (0.296, p=0.001), PEXS (0.32, p=0.0008) and PEXG (0.26, p=0.04) individuals. Similarly, frequency of protective haplotype G-A (rs3087554-rs2279590) is higher in control (0.18) than that of PEX (0.08, p=0.003), PEXS (0.07, p=0.003) and PEXG (0.1, p=0.09) individuals. \*p-value after permutation correction where n=10,000.

Haplotype (rs3087554-rs2279590)	Freq. in PEX (Combined Cases)	Freq. in Control	$\chi^2$ value	p-value	p*-value
G-G	0.362	0.359	0.005	0.943	1
A-A	0.256	0.297	0.938	0.332	0.738
A-G	0.296	0.163	10.234	0.001	0.006
G-A	0.086	0.180	8.799	0.003	0.013

Haplotype (rs3087554-rs2279590)	Freq. in PEXS Cases	Freq. in Control	$\chi^2$ value	p-value	p*-value
G-G	0.341	0.359	0.118	0.730	0.982
A-A	0.267	0.297	0.379	0.538	0.910
A-G	0.32	0.164	11.353	0.0008	0.003
G-A	0.073	0.181	8.772	0.0031	0.012

Haplotype (rs3087554-rs2279590)	Freq. in PEXG Cases	Freq. in Control	$\chi^2$ value	p-value	p*-value
G-G	0.394	0.360	0.331	0.564	0.941
A-A	0.239	0.298	1.185	0.276	0.679
A-G	0.261	0.162	4.107	0.042	0.171
G-A	0.106	0.179	2.827	0.092	0.318

was found to be higher in PEX (0.48, p=0.005), PEXS (0.45, p=0.0008) and PEXG (0.52, p=0.004) subjects than that of control individuals.

**Table 2.4.** Distribution of rs3087554 and rs2279590 genotypes in PEX and control subjects. Frequency of risk genotype “AA” at rs3087554 in control (0.25) is lower in comparison to PEX (0.35, p=0.01), PEXS (0.37, p=0.009) and PEXG (0.32, p=0.03) individuals. Similarly, frequency of risk genotype “GG” at rs2279590 is also found to be lower in control (0.27) than that of PEX (0.48, p=0.005), PEXS (0.45, p=0.0008) and PEXG (0.52, p=0.004) individuals. \*Risk genotype. † p- value after permutation correction where n=10,000.

SNP	Genotype	Genotype Count (Freq.) in PEX (combined cases)	Allele Count (Freq.) in control subjects	Model	$\chi^2$ value	p-value	p <sup>†</sup> value
rs3087554	GG	34 (0.25)	30 (0.33)	Dominant	6.83	0.019	0.03
	AG	54 (0.39)	36 (0.4)				
	AA*	48 (0.35)	23 (0.25)				
rs2279590	AA	23 (0.17)	20 (0.22)	Dominant	8.21	0.005	0.01
	AG	47 (0.34)	45 (0.5)				
	GG*	66 (0.48)	24 (0.27)				

SNP	Genotype	Genotype Count (Freq.) in PEXS	Allele Count (Freq.) in control subjects	Model	$\chi^2$ value	p-value	p <sup>†</sup> value
rs3087554	GG	16 (0.19)	30 (0.33)	Dominant	7.31	0.009	0.01
	AG	35 (0.43)	36 (0.4)				
	AA*	30 (0.37)	23 (0.25)				
rs2279590	AA	11 (0.13)	20 (0.22)	Dominant	11.21	0.0008	0.004
	AG	33 (0.4)	45 (0.5)				
	GG*	37 (0.45)	24 (0.27)				

SNP	Genotype	Genotype Count (Freq.) in PEXG	Allele Count (Freq.) in control subjects	Model	$\chi^2$ value	p-value	p <sup>†</sup> value
rs3087554	GG	18 (0.32)	30 (0.33)	Dominant	4.83	0.03	0.04
	AG	19 (0.34)	36 (0.4)				
	AA*	18 (0.32)	23 (0.25)				
rs2279590	AA	12 (0.21)	20 (0.22)	Dominant	10.46	0.004	0.01
	AG	14 (0.25)	45 (0.5)				
	GG*	29 (0.52)	24 (0.27)				

binary logistic regression in SPSS v.20. Interestingly, after correction for confounding factors both rs3087554 and rs2279590 were found to be associated with PEX in Indian population with a p-value of 0.001 and 0.002, respectively.

**Table 2.3.** Distribution of clusterin variants in PEX and control subjects. Frequency of risk allele “A” at rs3087554 in control (0.46) is lower in comparison to PEX (0.55, p=0.059), PEXS (0.58, p=0.034) and PEXG (0.5, p=0.65) individuals. Similarly, frequency of risk allele “G” at rs2279590 is also found to be lower in control (0.52) than that of PEX (0.66, p=0.004), PEXS (0.66, p=0.01) and PEXG (0.65, p=0.03) individuals. \*Risk Allele. † p- value after permutation correction where n=10,000.

SNP	Allele	Allele Count (Freq.) in PEX (combined cases)	Allele Count (Freq.) in control subjects	$\chi^2$ value	p-value	p <sup>†</sup> value
rs3087554	G	122(0.45)	96(0.54)	3.55	0.059	0.16
	A*	150(0.55)	82(0.46)			
rs2279590	G*	179(0.66)	93(0.52)	8.27	0.004	0.015
	A	93(0.34)	85(0.48)			

SNP	Allele	Allele Count (Freq.) in PEXS	Allele count (Freq.) in control subjects	$\chi^2$ value	p-value	p <sup>†</sup> value
rs3087554	G	67(0.42)	96(0.54)	4.458	0.034	0.09
	A*	95(0.58)	82(0.46)			
rs2279590	G*	107(0.66)	93(0.52)	6.386	0.011	0.04
	A	55(0.34)	85(0.48)			

SNP	Allele	Allele Count (Freq.) in PEXG	Allele count (Freq.) in control subjects	$\chi^2$ value	p-value	p <sup>†</sup> value
rs3087554	G	55(0.50)	96(0.54)	0.2	0.65	0.91
	A*	55(0.50)	82(0.46)			
rs2279590	G*	72(0.65)	93(0.52)	4.608	0.031	0.1
	A	38(0.35)	85(0.48)			

Distribution of rs3087554 and rs2279590 genotypes in PEX and control subjects were shown in **Table 2.4**. At genotypic level, “AA” genotype was also found to be risk genotype with lower frequency in control subjects than that of PEX (0.35, p=0.01), PEXS (0.37, p=0.009) and PEXG (0.32, p=0.03) affected individuals. In a similar way risk genotype frequency of “GG”

for multiple testing with permutation analysis (n=10,000) were done in SPSS and Haploview V4.2 with default set of parameters following chi-square statistics. Confounding factors like age and sex were corrected through binary logistic regression in SPSS V20. Group wise results from qRT PCR, Bradford's assay and western blot were analyzed for statistical significance by Student's t-test; for pairwise comparison with  $p < 0.05$  considered as statistically significant. Multiple comparisons were also corrected by the Bonferroni method. Power calculation has been done using online Genetic Power Calculator ([zzz.bwh.harvard.edu/gpc/](http://zzz.bwh.harvard.edu/gpc/)).

## 2.3 Results

### 2.3.1 Genetic association of clusterin variants in the pathogenesis of PEX

A total of 136 PEX patients (81 PEXS and 55 PEXG) and 89 controls were genotyped for the SNPs of interest, rs3087554 and rs2279590 (**Figure 2.1**). Demographic characteristics of the study population are shown in **Table 2.1**. Allele frequencies of both the SNPs are in Hardy Weinberg equilibrium. The distributions of allele, genotype and haplotype frequencies are shown in **Tables 2.3, 2.4** and **2.5** respectively. As evident from the linkage disequilibrium (LD) value ( $D'=0.35$ , LOD score=4.85) there is a nominal linkage between the two markers. Out of these two SNPs, rs2279590 was found to be significantly associated with PEX (p-value = 0.004, nominal  $p < 0.025$  after Bonferroni correction) with "G" as the high risk allele (**Table 2.3**). Even after correction for multiple testing with permutation analysis (n=10,000), the association still remains significant ( $p = 0.01$ ). When cases were segregated into PEXS and PEXG the association remained significant ( $p=0.01$  and 0.03, respectively) with both groups.

Further, rs3087554 was also found to be associated with only PEXS group ( $p = 0.03$ ) but the association doesn't hold after Bonferroni or permutation correction. To eliminate any influence of confounding factors, age and sex of the study subjects were corrected through

secondary antibody at dilution 1:5000 in PBST and skim milk. For detection of bands, a chemiluminescence kit was used (Super Signal Femto Maximum Sensitivity Substrate, Thermo scientific) and signals were detected in a Chemi-Doc (Bio-Rad) and subsequently band intensity was quantified in Quantity One 4.6.9 software (Bio-Rad). Band intensity from each sample was normalized according to a pooled sample from fifteen controls loaded into a single lane in each of the blot.

### **2.2.10 Immunohistochemistry**

For immunofluorescence labeling, lens capsules were obtained from subjects at the time of cataract surgery and immediately frozen in liquid nitrogen and stored at -80°C until further use. In total, three lens capsules from PEXS, three from PEXG and two from control were collected for Clusterin immunofluorescence labeling. Tissues were fixed in 4% paraformaldehyde for 20 minutes, washed in PBS and then permeabilized with 1% Triton X-100 in PBS (PBST) for 5 minutes. Blocking was done in 10% normal horse serum in PBST for 30 minutes and incubated overnight at 4°C in the same primary polyclonal antibody as was used for western blot against human Clusterin at 1:500 dilution in blocking solution. Clusterin peptide along with Clusterin antibody was used as a negative control. After subsequent washing in PBST, the tissue was treated with Alexa-Fluor 594 Chicken anti-goat IgG (Invitrogen) secondary antibody for two hours in dark at room temperature. Nuclear staining was done with DAPI and lens capsule was flat mounted on the slide along with ProLong Gold antifade Reagent (Invitrogen). Immunofluorescence recording was done in Olympus BX51 and processed in Zeiss LSM Image Browser Version 4.2.0.121.

### **2.2.11 Statistical analysis**

Descriptive data are presented as mean  $\pm$  SE. Genetic analysis such as allelic association tests, Hardy-Weinberg equilibrium, haplotype analysis, linkage disequilibrium (LD) and correction

### **2.2.7 Quantitative real time PCR**

Beta-actin or GAPDH was taken as an endogenous control gene for normalizing the expression of each target gene. Gene specific primers designed using primer-BLAST were used for both clusterin and beta-actin (**Table 2.2**). Comparative ( $\Delta\Delta\text{Ct}$ ) real time PCR was performed using 7500 Real time PCR Systems from Applied Biosystems. Total 5ng of cDNA was used in a 20 $\mu\text{l}$  reaction in triplicate for each sample. 0.4  $\mu\text{M}$  each of forward and reverse primers was used for each test and endogenous control genes. Amplification specificity of the PCR product was checked via melting curve analysis and sequencing.  $\Delta\Delta\text{Ct}$  method was used for normalization of target gene and change in expression was represented as fold difference.

### **2.2.8 Protein estimation**

Approximately 100 $\mu\text{l}$  of aqueous humor was collected from subjects at the time of cataract surgery and immediately frozen in liquid nitrogen which was subsequently stored at  $-80^{\circ}\text{C}$ . Proteins from each of these samples were concentrated through acetone precipitation and total protein was measured spectrophotometrically using Bradford's assay by taking BSA as a standard. For Bradford's assay, four BSA protein standard points were used (2.5  $\mu\text{g}/\mu\text{l}$ , 5  $\mu\text{g}/\mu\text{l}$ , 10  $\mu\text{g}/\mu\text{l}$ , 20  $\mu\text{g}/\mu\text{l}$ ) to prepare the standard curve.

### **2.2.9 Western blotting**

10 $\mu\text{l}$  of each aqueous humor sample was loaded in a 12% SDS-polyacrylamide gel (PAGE) and subsequently transferred onto a PVDF membrane (Immobilion-P PVDF from Millipore). Transfer was done in semidry transfer cell (BioRad) at 17V for one hour in 1X transfer buffer (48mM Tris-Base, 39mM Glycine, 0.1% SDS and 20% Methanol). Membranes were then blocked with 5% skim milk for one hour and subsequently incubated overnight at  $4^{\circ}\text{C}$  with goat polyclonal antibody against human Clusterin (Santa Cruz Biotechnology) diluted 1:200 in PBST and skim milk. HRP-conjugated Rabbit anti-goat IgG (Imgenex, India) was used as

Applied Biosystems was used for sequencing and analysis was done using Sequencing analysis software v5.3 (Applied Biosystem) and BioEdit v7.1 (Freely available online at <http://www.mbio.ncsu.edu/bioedit/bioedit.html>).

### **2.2.5 RNA extraction**

Lens capsules were collected from both cases and controls during cataract surgery and immediately kept in RNA later (Invitrogen, USA) and stored at  $-80^{\circ}\text{C}$  until further use. Total RNA was isolated from individual lens capsules by using RNA extraction kit (RNeasy Mini Kit, QIAGEN GmbH, Hilden). Briefly, each tissue was washed in NFW and then the tissue was lysed gently with  $350\mu\text{l}$  RLT buffer and mixed with an equal volume of 75% ethanol (in NFW). This solution was then passed through the RNeasy mini column at 13000 rpm ( $4^{\circ}\text{C}$ ) for one minute. The column was then washed once with  $750\mu\text{l}$  RW1 buffer and twice with  $500\mu\text{l}$  RPE buffer at 13000 rpm for one minute each to remove contaminants from the column. Then the column was centrifuged for a dry spin at 13000 rpm for one minute at  $4^{\circ}\text{C}$ . The column was air dried for 5 minutes at RT. RNA was then eluted from the column with  $20\mu\text{l}$  NFW and quantified. RNA quantification was done spectrophotometrically and quality was checked by A260/A280 and A260/A230 ratios in Nanodrop 2000 (ThermoFisher Scientific, USA).

### **2.2.6 cDNA synthesis**

$1\mu\text{g}$  of eluted RNA was converted into cDNA using Verso cDNA Synthesis Kit (ThermoFisher Scientific, USA) and stored at  $-80^{\circ}\text{C}$  until further use.  $1\mu\text{l}$  of Random hexamers,  $1\mu\text{l}$  of RT enhancer as genome wipeout buffer and  $1\mu\text{l}$  of reverse transcriptase were used as provided in the kit to convert whole RNA into cDNA library in a total  $20\mu\text{l}$  reaction volume. The cDNA synthesis was done at  $45^{\circ}\text{C}$  for 30 minutes in a C100 Touch Thermal Cycler (BioRad, USA) followed by enzyme inactivation at  $95^{\circ}\text{C}$  for 2 minutes.

#### 2.2.4 Elution and Sanger's sequencing

The PCR products were subsequently electrophoresed on 1% agarose gel at 150V and 200mA and further eluted by gel elution kit (QIAquick Gel Extraction Kit, QIAGEN, Hilden) and sequenced unidirectionally using one of the previously mentioned primers (**Table 2.2**) with the help of BigDye Terminator v.3.1 cycle sequencing kit (Applied Biosystems, Austin, TX78744, USA). Briefly, eluted PCR products were quantified before setting up each sequencing PCR. For each PCR, 0.25 $\mu$ l of 2.5X ready reaction mix, 2 $\mu$ l of dilution buffer (5X), 80ng of eluted DNA template, 2 $\mu$ l of primer (2pmol) and nuclease free water (NFW) (MP Biomedicals, USA) were added for a 10 $\mu$ l total reaction volume. The thermal cycling sequencing PCR reaction was carried out for 25 cycles with each cycle having a denaturation step at 96<sup>0</sup>C for 10 seconds, annealing at 50<sup>0</sup>C for 5 seconds, extension at 60<sup>0</sup>C for 4 minutes and kept at -20<sup>0</sup>C until further use.

After sequencing PCR, each reaction product was cleaned by using Master Mix-I (10 $\mu$ l NFW and 2 $\mu$ l of 125mM EDTA per reaction) and Master Mix-II (2 $\mu$ l of 3M NaOAc pH 4.6 and 50 $\mu$ l of ethanol per reaction). 12 $\mu$ l of master mix I was added to each sequencing reaction containing 10 $\mu$ l of PCR product and thoroughly mixed. Then 52 $\mu$ l of master Mix-II was added to each reaction, mixed and incubated at RT for 20 minutes. After incubation, the sample was centrifuged at 12000g for 20 minutes at RT. The pellet was then washed by adding 250 $\mu$ l of 70% ethanol and centrifuged at 12000g for 10 minutes at RT. After removing the supernatant, the pellet was air dried at room temperature for 1 hour and resuspended in 15 $\mu$ l of Hi-Di formamide. Final product was then transferred to a 96 well sequencing plate (ABI 1400, Applied Biosystems, USA), covered with septa, denatured at 95<sup>0</sup>C for 5 minutes and snap chilled on ice for 10 minutes and finally sequenced on 3130xl Genetic Analyzer. The sequencing read-out were obtained in .abi format and were analyzed using BioEdit v7.1 (Tom Hall, Ibis Biosciences, USA) software. The automated sequencer 3130xl genetic analyzer from

### 2.2.3 Polymerase chain reaction

For genotyping, the region containing the two SNPs (rs3087554 and rs2279590; **Figure 2.1**) were amplified by polymerase chain reaction using two sets of primers (PCR; model Mastercycler® pro; Eppendorf AG, Hamburg) and subsequently sequenced. The primers were designed by Primer-BLAST. Both sequence details and annealing temperature of primers are listed in **Table 2.2**. PCR reactions were performed in 25µl volumes containing Taq Buffer A (GeNei, Bangalore, India), 1.5 mM MgCl<sub>2</sub>, 0.5 µM of each primer (IDT, USA), 100mM dNTP mixture (GeNei, Bangalore, India), 100ng of genomic DNA, 0.5 unit of Taq DNA polymerase (GeNei, Bangalore, India) and 2.5µl of DMSO. These reactions were incubated at 94<sup>0</sup>C for 5 minutes followed by 35 cycles of 45 seconds of denaturation at 95<sup>0</sup>C, 45 seconds at annealing temperatures (**Table 2.2**) and extended for 45 seconds at 72<sup>0</sup>C and finally incubated at 72<sup>0</sup>C for 10 minutes for final extension. The amplicons were stored at -20<sup>0</sup>C until further use.

**Table 2.2.** List of oligos used in the study.

Sl. No.	ID	Purpose	Sequence (5'→3')	Melting temperature (T <sub>m</sub> <sup>0</sup> C)
1	rs3087554	Genotyping	For: CCCTATACCATCTTAGCCACTGCT Rev: TGC ACTCTAACACTCGACTCTGCT	58
2	rs2279590	Genotyping	F: ACTCTGACCAAGGGCTGCTTCTAA R: CGGTGCTTTTTGCGGTATTCCTG	52.5
3	Clusterin (NM_001831.3)	qRT-PCR	F: TTCATACGAGAAGGCGACGAT R: CTGGTCAACCTCTCAGCGAC	60
4	β-Actin (NM_001101.3)	qRT-PCR	F: GCACAGAGCCTCGCCTT R: GTTGTCGACGACGAGCG	60
5	DKK1 (NM_012242.3)	qRT-PCR	F: AGCACCTTGGATGGGTATTC R: CTGATGACCGGAGACAAACA	60
5	GAPDH (NM_001101.3)	qRT-PCR	F: GGTGTGAACCATGAGAAGTATGA R: GAGTCCTCCACGATACCAAAG	60

### 2.2.2 DNA extraction

4 ml peripheral blood was collected in EDTA (ethylene diamine tetraacetic acid) vials from both case and control subjects and stored at  $-80^{\circ}\text{C}$  until further use. Subsequently, genomic DNA was extracted using phenol-chloroform extraction method. Briefly, 0.5 ml of blood sample was centrifuged at 11000 rpm (rotation per minute) for 10 minutes at  $25^{\circ}\text{C}$ . After centrifugation, supernatant was discarded and 1ml of RBC (red blood cell) lysis buffer (0.32M Sucrose, 1mM  $\text{MgCl}_2$ , 1% Triton X-100, 12mM Tris-HCl, pH adjusted to 7.6) was added to the cell pellet. The cell pellet was disrupted by rapid pipetting and the sample was subsequently centrifuged at 11000 rpm for 5 minutes. Then the supernatant was removed and to the pellet another 200 $\mu\text{l}$  of RBC lysis buffer was added and the pellet was dissolved by pipetting. Then it was centrifuged for 5 minutes at 11000 rpm and to the pellet 200 $\mu\text{l}$  of Milli-Q (MQ) water was added to the pellet and the previous step was repeated. After centrifugation, 10 $\mu\text{l}$  of 10% SDS (sodium dodecyl sulphate) and 80  $\mu\text{l}$  of proteinase K buffer (20mM Tris-HCl, 4mM  $\text{Na}_2\text{EDTA}$ , 100mM NaCl, pH 7.4) was added and pipetted till frothing was observed. Then, 100 $\mu\text{l}$  of chilled NaCl (sodium chloride) was added and mixed by tapping. After adding another 200 $\mu\text{l}$  of MQ and mixing, 400 $\mu\text{l}$  of phenol: chloroform (Tris saturated Phenol: Chloroform: Isoamyl Alcohol 25:24:1, Sigma-Aldrich, USA) was added and mixed vigorously by inverting the tube. Subsequently, the sample was centrifuged at 12000 rpm for 10 minutes. Then upper transparent aqueous phase was collected carefully and 1ml of absolute ethanol was added and mixed to precipitate the DNA pellet. After centrifugation at 13000 rpm for 10 minutes, 200 $\mu\text{l}$  of 70% ethanol was added to the DNA pellet and centrifuged again at 13000 rpm for 5 minutes. Then the supernatant was discarded and the pellet was air dried overnight at room temperature. Later, the dried DNA pellet was dissolved in 30 $\mu\text{l}$  of TE-buffer (Tris-EDTA 0.5M, pH 7) and quantitated in NanoDrop 2000 (ThermoFisher Scientific, USA).

like material over lens, pupillary ruff with or without poor dilatation; open or closed angles on gonioscopy, normal IOP<21mm Hg without any prior anti-glaucoma treatment and no evidence of glaucomatous optic nerve damage or visual field defects.

PEXG affected participants comprised of adults >40 years with or without visually significant cataract, having clinically evident pseudoexfoliation like material over lens, pupillary ruff, raised IOP>21mm Hg without prior anti-glaucoma treatment and evidence of glaucomatous optic nerve head damage (defined as vertical cup-to-disc ratio of 0.8 or more, cup-to-disc asymmetry of more than 0.2, focal notching, or a combination thereof) with repeatable field defects corresponding to disc damage. Patients with corneal or retinal pathology precluding reliable visual field and disc examination were excluded.

Controls were selected on the basis of adults >40 years with or without visually significant cataract, without clinically evident pseudoexfoliation like material over lens, pupillary ruff, untreated IOP<21mm Hg and normal discs and visual field. Demographics as well as clinical features of the study group are shown in **Table 2.1**.

**Table 2.1.** Demographic and clinical features of study subjects included for genotyping of clusterin variants. \* IOP = Intraocular pressure; #VCDR = vertical cup disc ratio, n=sample size.

Subjects	n=	Age (in years)		Sex		IOP* Mean± SD mm Hg	VCDR# Mean ± SD	Manifestation (Unilateral/ Bilateral)	
		Mean±SD	Range	Male	Female			U	B
PEX Combined	136	67.1±9.1	40-92	101	35	16±18	0.3±0.5	43	93
PEXS	81	68.9±9.1	40-86	55	26	14±4.2	0.20±0.1	20	61
PEXG	55	65.2±8.7	47-92	46	9	23±10	0.7±0.2	23	32
Control	89	57.9±8.9	40-82	52	37	12±3.2	0.1±0.2	NA	NA

which involves patho-physiological processes similar to those seen in PEX, it is logical to explore the role of Clusterin in PEX development.

The following study has been conducted to check the role of clusterin in the progression of PEX. Following specific aims were addressed in this chapter.

1. Genetic association of two *CLU* variants, rs3087554 and rs2279590 in the pathogenesis of PEX in Indian population.
2. Status of *CLU* mRNA expression in the anterior eye tissues of individuals affected with PEX.
3. Differential expression of CLU protein, if any in the PEX affected ocular tissues.
4. Possible mechanism through which CLU imparts its role in the disease progression.

## **2.2. Materials and Methods**

### **2.2.1 Study subject recruitment**

This study was approved by the ethics review boards of National Institute of Science Education and Research (NISER) and LV Prasad Eye Institute (LVPEI), Bhubaneswar. All patients underwent detailed ocular examination, including slit lamp examination, ocular biometry, Goldman applanation tonometry, +90D biomicroscopic fundus evaluation and 4 mirror gonioscopy. All procedures were followed according to the tenets of the Declaration of Helsinki and an informed consent was taken from all subjects included in this study. Humphrey visual field 24-2 program was done in all cases.

Inclusion criteria for PEXS involved adults >40 years with or without visually significant cataract, best corrected visual acuity >20/100. Clinically evident pseudoexfoliation

chronic stress, deposition of extracellular aggregates leads to intracellular accumulation of CLU. This leads to induced expression of dickkopf-1 (DKK1), an antagonist of canonical signaling pathway which ultimately produces toxic proteins detrimental to the cell survivability.<sup>176</sup> In addition, nCLU also acts as a prodeath protein in cells with chronic stress.<sup>174</sup>

### **2.1.3 Clusterin and pseudoexfoliation**

Through atomic force microscopy, Creasey *et al.* have shown that CLU is localized as large deposits on the surface of lens capsules from PEX individuals compared to small spots in normal individuals.<sup>177</sup> Mass spectrometric analysis of PEX fibrillar material also showed clusterin as a major component of PEX deposits.<sup>52,178</sup> Furthermore, the expression level of Clusterin was found to be decreased in the anterior eye tissues of PEXS individuals.<sup>64</sup> On the contrary, CLU was found to be accumulated in the aqueous humor of PEXG individuals than in that of PEXS or control subjects.<sup>64</sup> Altered expression of CLU between the initial and advanced stages of PEX suggests its role in disease progression which needs to be studied further.

Additionally, genetic association studies conducted in an Australian population found a non-coding polymorphism, rs3087554 in the 3' UTR (untranslated region) of *CLU* gene as a risk factor in the PEX pathogenesis.<sup>124</sup> A case-control study done in a German cohort found rs2279590 but not rs3087554, within *CLU* gene as a risk factor in the pathogenesis of PEX.<sup>62</sup> However, the same study did not find an association of this common variant, rs2279590 with PEX in an Italian cohort. Inconsistency in the genetic association of these variants in cohorts with different ethnic groups warrants further investigation in other populations. Further, rs2279590 which resides in the 7<sup>th</sup> intron of *CLU* gene has been associated with Alzheimer's disease.<sup>125</sup> Since Clusterin is also implicated for protein aggregation in Alzheimer's disease

(Figure 2.2). Compared to sCLU, nCLU is short (lacks exon-II) and localizes to the nucleus with the help of a nuclear localization signal.<sup>174</sup> Unlike sCLU, nCLU does not undergo  $\alpha/\beta$  cleavage.

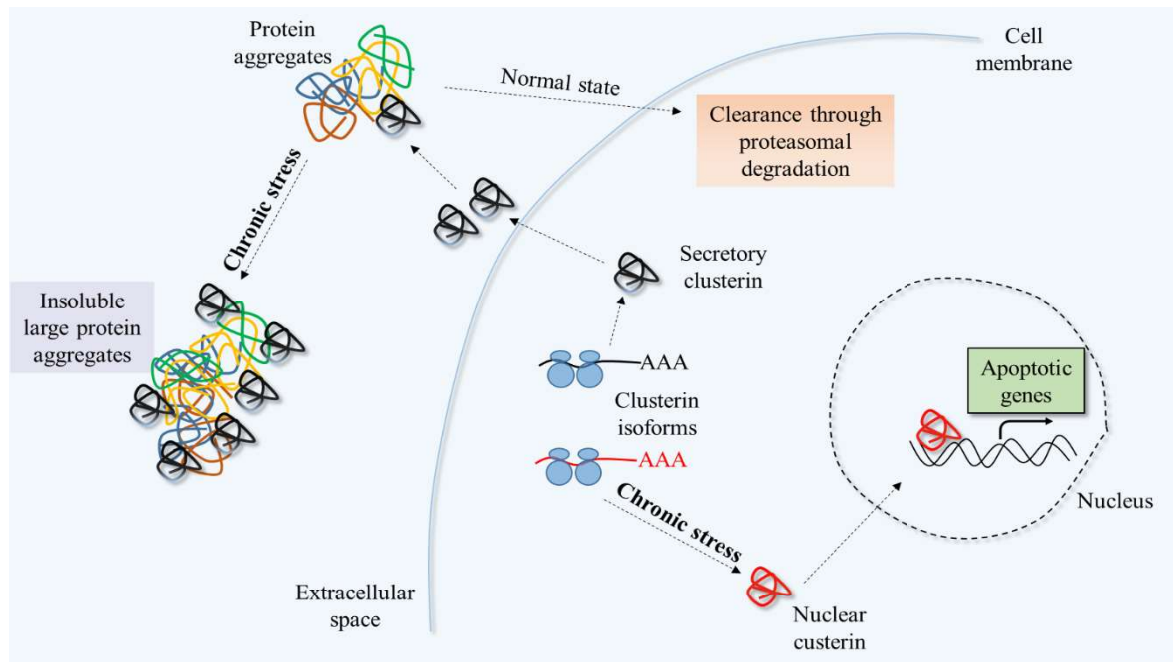


**Figure 2.2.** Involvement of sCLU and nCLU isoforms in different physiological pathways of the cell. While sCLU is secreted outside of the cell to prevent formation of protein aggregates, nCLU induces apoptotic genes under chronic stress.

These two different forms of CLU have diverse roles in the cells. While sCLU primarily plays a cytoprotective role by preventing protein aggregation in ECM, nCLU induces apoptosis.<sup>172</sup> Further, the fate of sCLU as cytoprotective also changes depending on its substrate concentration in the extracellular space. *In vivo* studies have shown that in the initial stages, sCLU binds to and prevents the aggregation of A $\beta$  peptides and subsequent formation of senile plaques.<sup>175</sup> When the ratio of clusterin to substrate is high while within the sub-stoichiometric ratio/concentrations, clusterin has a preventive role on aggregate formation. However, at a later stage when the ratio of sCLU protein to its substrate decreases clusterin is proamyloidogenic and in a failed attempt deposits along with its substrate and becomes cytotoxic by increasing oxidative stress.<sup>173</sup> Past studies have also shown that during clearance, sCLU produces soluble oligomeric A $\beta$  peptides which are also cytotoxic.<sup>172</sup> Further, during

It has been found to play a major role in formation of neurofibrillary tangles in Alzheimer's disease. Studies have shown that CLU regulates a subgroup of matrix metalloproteinases (MMP3 and MMP9) that degrade ECM proteins and also positively regulates morphological modulation of smooth muscle cells from monolayer to a nodular cell culture and thus, is involved in cell matrix formation and cell membrane remodeling.<sup>163-165</sup> It also plays a crucial role in DNA repair by binding to ku70 (a dimeric protein complex with DNA repair function) and is involved in nonhomologous DNA DSB (double strand break) repair.<sup>166</sup>

CLU expression is shown to be dysregulated in various cancerous tissue samples thus is used as a diagnostic marker.<sup>167,168</sup> Invariably CLU upregulation has been found as a marker of apoptotic response as well as a cell cycle regulator.<sup>169</sup> It also acts as a complement inhibitor by binding to common structural motif of complement proteins like C7, C8- $\alpha$  and C9b.<sup>170</sup> As a predominant serum protein, it forms a part of HDL (high density lipoprotein) complex and acts as a regulator of lipid transport which helps in local lipid redistribution.<sup>171</sup> One of the key function of CLU in extracellular space is to prevent deposition of abnormal protein aggregates and to aid in their effective clearance. Due to its chaperone role in ECM maintenance it has been implicated as a key player in the development of amyloid- $\beta$  peptide deposits in Alzheimer's patients.<sup>172</sup> Though, exact role of CLU in the formation of amyloid- $\beta$  deposits is not resolved, its primary function is to prevent the aggregation of A $\beta$ -peptides.<sup>173</sup>

### **2.1.2 Clusterin isoforms have discrete roles in cells**

*CLU* gene codes for two types of transcripts: secretory *CLU* (*sCLU*) and nuclear *CLU* (*nCLU*) depending on the physiologic state of the cell. Under normal conditions, *CLU* gene codes for the predominant secreted form, sCLU (80 kDa) which consists of  $\alpha$  and  $\beta$  peptides linked by five disulfide bonds.<sup>168</sup> Cells under chronic stress or after low doses of ionizing radiation produce a shorter alternative form, nCLU (55 kDa) from a second in-frame AUG codon

## 2.0 Role of Clusterin, an extracellular protein in the pathogenesis of PEX.

### 2.1 Introduction

Clusterin (CLU) is also known as Apolipoprotein-J (APOJ), serum protein-40 (SP-40), sulfated glycoprotein 2 (SGP-2) or complement lysis inhibitor.<sup>155-157</sup> It is located in the short arm of chromosome 8 (p21.1) between *EPHX2* (epoxide hydrolase 2) and *SCARA3* (scavenger receptor class A member 3). *CLU* gene is organized into 9 exons and 8 introns (**Figure 2.1**) and codes for a secretory glycosylated protein under normal condition. Upon maturation, it consists of two 40-kDa chains, alpha and beta, covalently joined by disulfide bonds.<sup>156</sup> Clusterin is ubiquitously expressed in all human tissues and body fluids including ocular tissues like conjunctival epithelium, cornea, ciliary body and retina.<sup>155,158-161</sup> Clusterin plays a crucial role in a number of cellular pathways and has been associated with a number of disorders such as diabetes, cancer and neurodegenerative disorders like Alzheimer's disease.<sup>125,126,162</sup> Part from these, we got interested as *CLU* was genetically associated with PEX.<sup>62</sup>

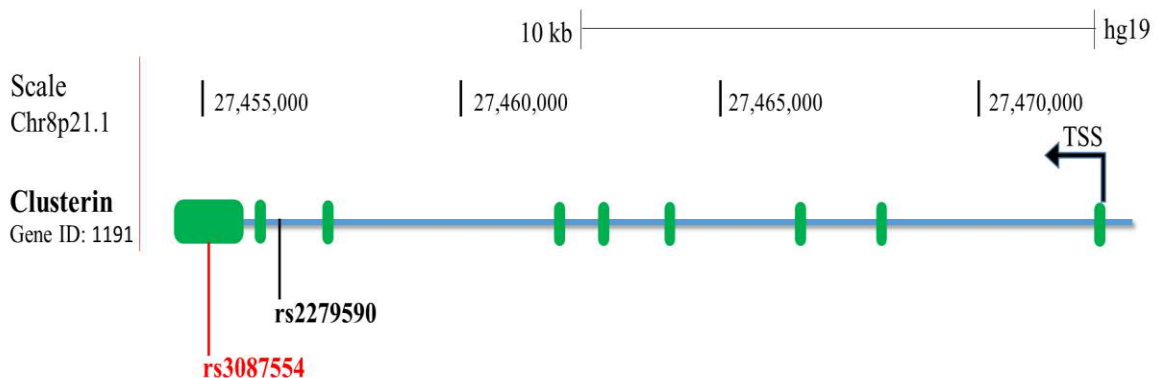


**Figure 2.1.** The gene structure of clusterin. rs3087554 lies in the 3' untranslated region while rs2279590 in the seventh intronic region of the clusterin gene.

#### 2.1.1 Clusterin, a multifunctional protein

Clusterin is a heterodimeric multi-functional protein playing important roles in a variety of extracellular processes such as lipid transport, apoptosis, stabilization of cell-cell and cell-matrix interactions and inhibition of complement activation and preventing protein misfolding.

# **CHAPTER 2**

## **Role of Clusterin, an extracellular protein in the pathogenesis of PEX**

**Conclusion:**

With this study, we report that a PEX/AD associated risk variant, rs2279590, resides within an enhancer element and regulates the expression of *CLU* which was previously known to be a modulator in the progression of AD. Increase in *CLU* expression by the risk allele at rs2279590 provides a mechanistic insight into the cytotoxic role of *CLU* in PEXG individuals.

endogenous protein aggregation.<sup>196</sup> Similarly, in AD animal models, HSF1 expression was remarkably decreased in the cerebellum; whereas, overexpression of HSF1 reduces brain  $\beta$ -amyloid levels and improves memory function.<sup>197,198</sup> These studies suggest a protective role of HSF1 in such aging disorders. This was in-sync with the recent reports where the Alzheimer's patients showed significantly lower levels of HSF1 than control individuals.<sup>199</sup> In this study we identified an upregulated HSF1 mRNA levels in the anterior eye tissues of PEXS subjects but not in the later more severe form of disease, i.e., PEXG; suggesting the protective role of HSF1 is diminished in the later stages of the disease condition and may augment the severity.

After considering all results, an enhancer-promoter model is being proposed as shown in **Figure 3.25** that rs2279590 resides within a regulatory genomic region and with risk allele "G" shows a regulatory enhancer effect on PEX/AD risk associated candidate gene, *CLU*. However, binding of HSF1 to the protective allele "A" abolishes the enhancer effect of the locus, which is consequent to decreased expression of the target gene; thereby implying a lowered risk of developing PEX or AD.

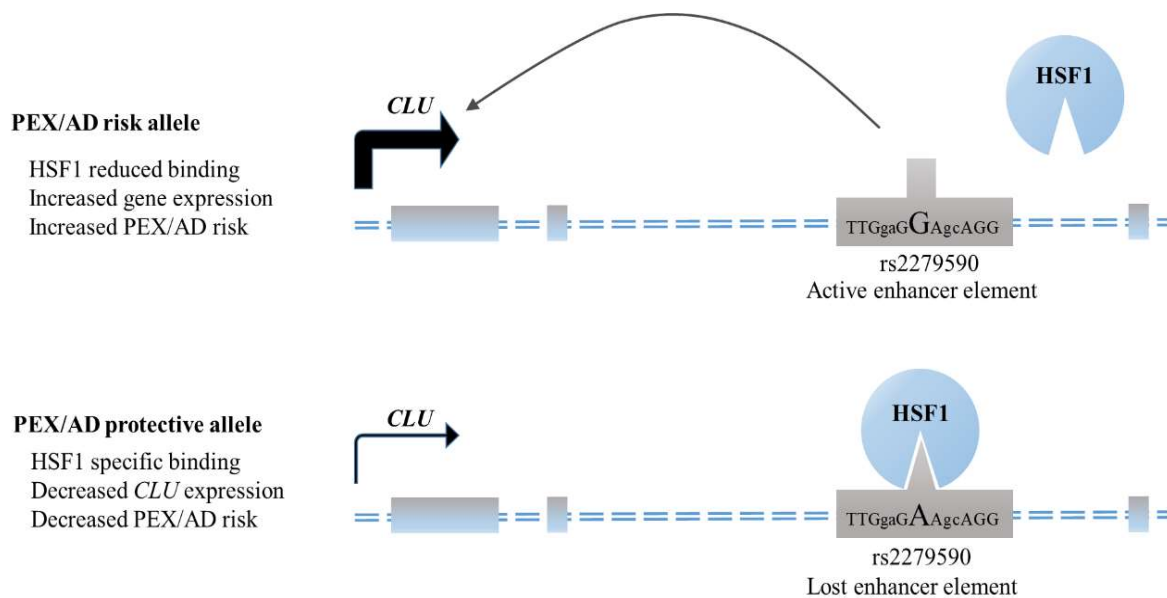


**Figure 3.25.** Proposed model explaining the effect of SNP-dependent HSF1 binding at rs2279590, *CLU* gene expression and AD/PEXG risk. Genomic region containing rs2279590/G resides within an active enhancer element and increases gene expression of *CLU*. However, binding of HSF1 to protective allele "A" at rs2279590 diminishes the enhancer effect of the locus; which leads to decrease in *CLU* gene expression with a lowered risk of developing PEX/AD.

controls.<sup>63,64,192</sup> Although CLU was upregulated whether it's the cause or an effect is still speculative. Clusterin knockout in PDAPP mice has shown to be beneficial due to reduced fibrillar plaque formation and neuritic dystrophy.<sup>183</sup> Nonetheless, being an extracellular chaperone, the protective role of CLU cannot be undermined. A study suggests that it is the extracellular CLU: substrate ratio that decides the fate of CLU to be pathogenic or protective. When substrate is in large molar excess, CLU coincorporates itself within the complex in a failed attempt to prevent aggregation; leading to large insoluble aggregates.<sup>173</sup> Further, in chronic stress a nuclear form of Clusterin (nCLU) tends to increase which initiates caspase-3 dependent apoptosis.<sup>186</sup> Enhancer effect associated with risk allele "G" at rs2279590 locus, on both secretory and nuclear forms of Clusterin suggests a cytotoxic effect of both sCLU and nCLU can augment neurodegeneration.

### **3.4.2 HSF1 is a critical regulator in clusterin gene expression**

Through bioinformatic and molecular analysis we identified HSF1 to bind preferentially to protective allele "A" at rs2279590 and consequently regulate clusterin gene expression. HSF1 is a prominent member of a family of transcription factors called heat shock factors known to be activated upon heat shock, stress or inflammatory triggering agents. Upon activation, it differentially regulates either by upregulating or downregulating a cascade of genes. It is a complex regulator and affect gene expression differently under similar conditions in different tissues.<sup>193</sup> Here, binding of HSF1 to the protective allele "A" negatively regulates *CLU* gene expression; suggesting a suppressor effect. By negatively regulating, HSF1 might help in reducing the cytotoxicity associated with CLU overaccumulation.

Earlier studies have related HSF1 to various types of neurodegenerative proteinopathies. Downregulation of HSF1 accelerated the formation of protein aggregates in Huntington's disease;<sup>194</sup> whereas, activated HSF1 in R6/2 Huntington disease mice prevents polyglutamine aggregate formation.<sup>195</sup> Thus, HSF1 could be regarded as a key controller of

Analysis of eQTL data for entire *CLU* gene (GTEx Portal on 07/11/17) also indicates that there are dozens of SNPs acting as eQTL for *CLU* expression each with an effect size around 0.2 (**Table 3.2**). Altogether, the combined effect of nearby SNPs including rs9331896 and rs11136000 may supersede the moderate effect shown by rs2279590 in different ethnic background. Further, ongoing functional studies of these eQTL SNPs in relation to rs2279590 will define the role of *CLU* in PEXG and AD progression. This substantiates the fact that certain risk alleles in *CLU* gene enhance clusterin expression and thereby contribute towards PEX/AD pathogenesis.

**Table 3.2.** eQTL effect of SNPs within clusterin gene were analysed in GTEx portal on 07/11/17. Effect of listed SNPs on clusterin gene expression were checked in muscle skeletal and skin-sun exposed tissues.

Sl No.	ID	Muscle Skeletal	Effect size	Skin - Sun Exposed (Lower leg)	Effect size
1	rs7982	0.0000055	0.19	0.0000092	0.2
2	rs4236673	0.0000032	0.21	0.000019	0.2
3	rs11136000	0.0000021	0.2	NA	NA
4	rs11787077	0.0000022	0.2	0.000055	0.18
5	rs4236673	0.0000032	0.21	0.000019	0.2
6	rs1532278	0.0000043	0.2	NA	NA
7	rs1532277	0.0000024	0.21	0.00003	0.2
8	rs1532276	0.0000015	0.2	NA	NA
9	rs2070926	0.000017	0.19	0.00004	0.19
10	rs9331896	0.0000065	0.19	NA	NA

Studies have shown that elevated level of *CLU* is linked to disease severity in both PEXG and AD affected patients.<sup>63,184,192</sup> Both in the anterior eye tissues of PEXG and in the brain of AD affected individuals *CLU* was found to be upregulated compared to their respective

### 3.4.1 rs2279590 is a functional intronic variant and regulates clusterin gene expression

Recent studies have reported the involvement of genetic variants in *CLU* gene with the risk of developing PEX and AD. Since then, attempts have been made to identify the significance of these risk variants in regulating *CLU* expression. One such study reported that the AD-risk allele at *CLU*, rs9331888, increased the clusterin expression as compared to its counter allele.<sup>190</sup> Similarly, two other GWAS-associated risk variants; rs9331896 and rs11136000 which are located in the second and third intron of *CLU* gene,<sup>125,191</sup> respectively, have regulatory role over *CLU* expression as evident through eQTL data from GTEx project. Accordingly, examined tissue samples with risk allele of both these SNPs, rs9331896 (T) and rs11136000 (C) reportedly have elevated *CLU* expression than their respective reference alleles (GTEx Portal on 07/11/17). This suggests a cumulative effect of these risk variants in *CLU* upregulation during pathogenesis of AD. However, same wasn't true for another AD-risk variant, rs7982; suggesting that not all associated variants in clusterin gene have functional implications in disease causation.<sup>185</sup>

Similar to the above studies, as reported in the previous chapter, individuals homozygous for risk allele "G" at rs2279590 (another risk variant for PEX/AD) within *CLU* showed two-fold increased clusterin gene expression compared to "AA" carriers in lens capsules.<sup>63</sup> In this chapter, we found an enhancer effect of the genomic region surrounding rs2279590 with the risk allele "G" on *CLU* expression. Further, we showed regulatory effect of rs2279590 on *CLU* expression was mediated by a promoter-enhancer interaction between *CLU* promoter and the enhancer element. This is also supported by the eQTL data from GTEx that indicates tissue samples with genotype "GG" (alternative allele- G) at rs2279590 have elevated *CLU* expression than samples with that of "AA" (reference allele- A) with an effect size of 0.2. However, reverse allelic association (allele "A") in German cohort suggests a profound effect of other nearby SNPs compared to moderate effect shown by rs2279590.<sup>62</sup>

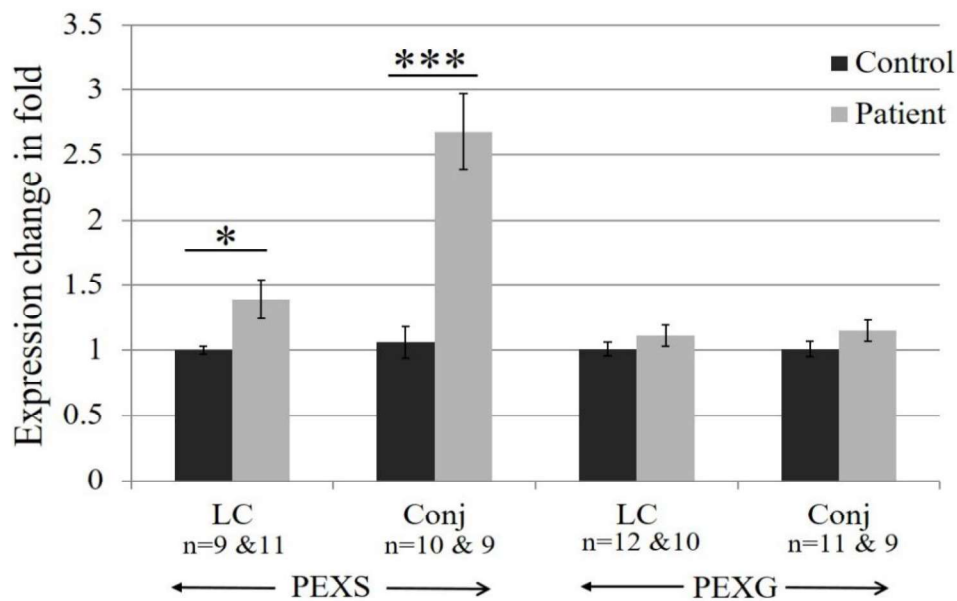


**Figure 3.24.** *HSF1* upregulation indicates a proteotoxic stress in anterior eye tissues of PEXS affected study subjects. qRT-PCR assays were done to check the expression of *HSF1* in anterior eye tissues of PEX (including both PEXS and PEXG) and control subjects. *HSF1* is found to be upregulated in both lens capsule ( $1.39 \pm 0.15$ ,  $P=0.02$ ) and conjunctiva ( $2.68 \pm 0.29$ ,  $P=0.0003$ ) in PEXS individuals compared to that of control ( $1 \pm 0.03$  and  $1.06 \pm 0.12$ , respectively). However, no difference was observed between control and PEXG in lens capsule ( $1.01 \pm 0.05$  versus  $1.11 \pm 0.08$ ) and conjunctiva ( $1.01 \pm 0.06$  versus  $1.15 \pm 0.08$ ), respectively). This implicates a proteotoxic stress in the anterior eye tissues of PEXS subjects and a failed stimulation to upregulate *HSF1* in PEXG individuals might be responsible for the death of optic nerve head (ONH) cells. LC and Conj correspond to lens capsule and conjunctiva, respectively. Sample size is denoted by “n” and expression change in fold is represented as mean  $\pm$  SEM. Student’s t-test was used to calculate statistical significance between groups, \* $P < 0.05$ , \*\*\* $P < 0.0005$ .

### 3.4 Discussion

Clusterin, a multifunctional protein has divergent roles from being cytoprotective to cytotoxic. Extensive studies have reported the association of *CLU* variants with the risk of developing various diseases like PEX, diabetes and AD.<sup>62,63,125,189</sup> This indicates that a complex mechanism employed by *CLU* is responsible for the progression of these diseases. Understanding the role of risk variants within *CLU* can help in better diagnosis and treatment of such disorders. In this chapter, we aimed at characterizing the functional significance of the risk variant, rs2279590, housed in the 7<sup>th</sup> intron of *CLU* gene. This particular variant has been reported to be a risk factor for both PEX and AD.<sup>62,63,125</sup> We therefore intended to understand the functional role of this SNP.

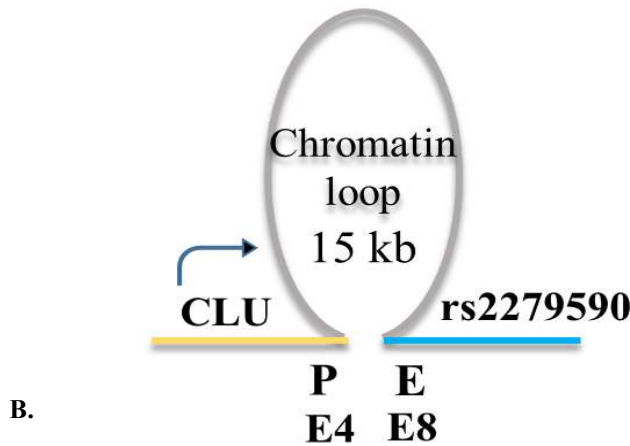


**Figure 3. 23.** Chromosome conformation capture assays for *CLU* promoter and rs2279590 enhancer interaction (A) Relative cross-linking frequency was calculated by quantifying ligated products by using a combinations of primers (E1-E7, E9 and E10) with reference primer (E8) through qRT-PCR. Data was normalized to frequency from two distal segments from beta-tubulin and an internal loading control from GAPDH without restriction sites. Experiments were performed three times and values are represented as mean $\pm$ SEM. (B) A model suggesting the formation of a chromatin loop of 15 kb between the promoter of *CLU* gene and rs2279590 loci. P and E corresponds to promoter and enhancer, respectively.

### 3.3.6 Upregulation of HSF1 suggests proteotoxic stress in anterior eye tissues of PEX affected subjects.

In response to proteotoxic stress, cell activates HSF1, which in turn upregulates the heat shock proteins (HSPs) to prevent protein misfolding. Earlier studies have reported that HSF1 overexpression has a protective role in a variety of neurodegenerative disorders caused due to accumulation of misfolded proteins (Verma et al. 2014, Fujimoto et al. 2005, Neef et al. 2011). Further, aberrant expression of HSF1 has also been implicated in neurodegeneration (Kim et al. 2016). Assuming an involvement of proteotoxic stress in anterior eye tissues of PEX affected subjects, we checked the expression of HSF1. Interestingly, HSF1 level was found to be significantly upregulated in both lens capsule and conjunctiva of PEXS affected individuals (Figure 3.24). However, we didn't find any upregulation of HSF1 in PEXG affected individuals; a later stage of PEX with degenerated optic nerve head (ONH) cells.

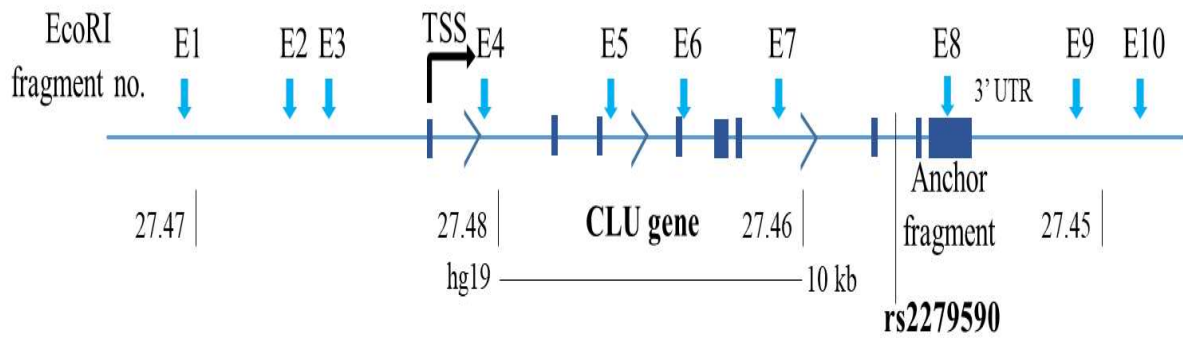
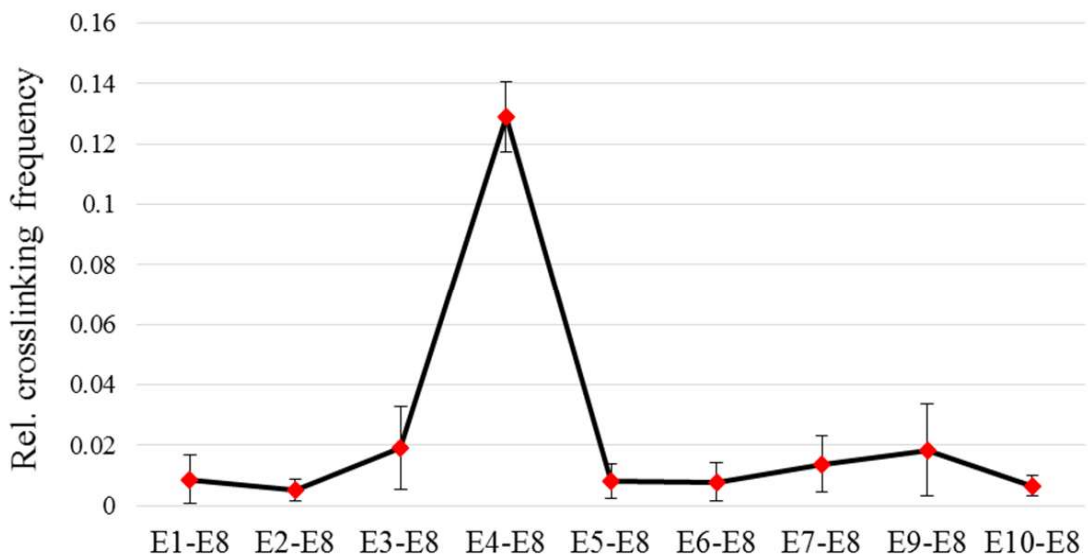


**Figure 3.22.** Schematic location of EcoRI restriction sites (E1-E10) across *CLU* gene. E8 restriction site is closest to rs2279590 and the E8 restriction fragment is used as anchor fragment to represent rs2279590. TSS represents transcription start site of *CLU* gene and 3'UTR represents the 3' untranslated region

3C ligation products were measured through qRT-PCR and normalized to loading control and ligation control. Normalized data is presented as relative crosslinking or relative ligation frequency for each combination of primer set with E8 and presented in the **Figure 3.23A**. We found a significantly higher relative crosslinking frequency for the E4-E8 ligation product compared to that of any other ligation products. This implies an interaction between rs2279590 loci and *CLU* promoter and suggests a promoter-enhancer interaction is required for rs2279590 to regulate *CLU* expression. Accordingly, we proposed a chromatin loop model suggesting a chromatin-chromatin interaction between *CLU* promoter and rs2279590 loci in the **Figure 3.23B**.



A.

As expected no significant difference ( $P=0.31$ ) was observed in the reporter activity between constructs containing either allele “G” or “A” in HSF1 knocked down cells (**Figure 3.20**). This suggests binding of HSF1 to allele “A” abrogates the enhancer effect of the locus.

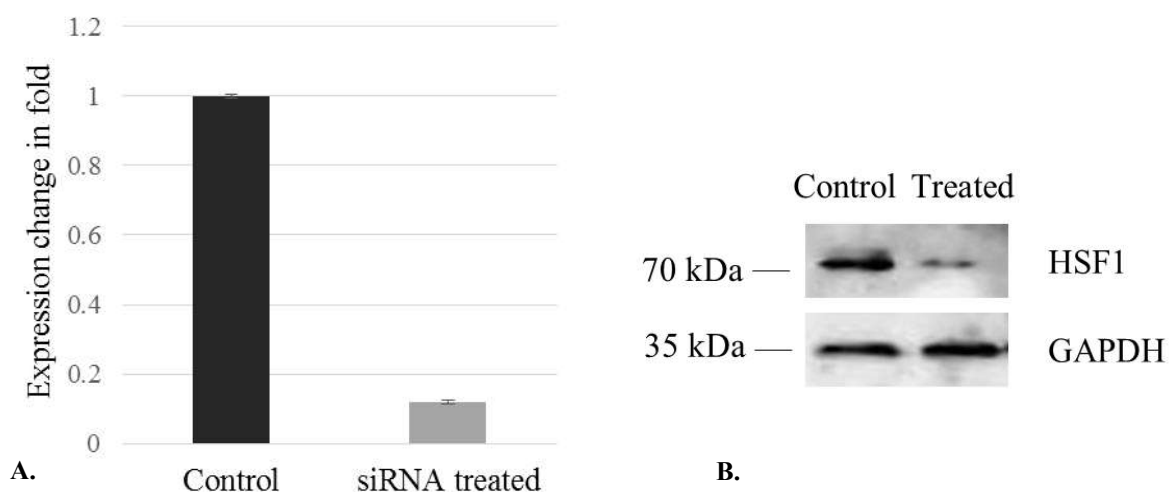


**Figure 3.21.** Knockdown of HSF1 by siRNA pool. **(A)** Shows qRT-PCR assay show an effective knockdown of HSF1 expression in HEK293 cells after treating with HSF1 specific siRNA ( $0.12\pm 0.01$ ) than that of control cells ( $1\pm 0.01$ ). **(B)** Shows protein level of HSF1 in control and HSF1 specific siRNA treated HEK293 cells was checked through western blot. Experiments were performed at least three times and values are represented as mean $\pm$ SEM. Student’s t-test was used to calculate statistical significance between groups,  $*P<0.05$ .

### 3.3.5 Chromosome conformation capture (3C) assay revealed a promoter-enhancer interaction between clusterin promoter and rs2279590 loci.

Assuming a chromatin interaction between genomic region containing rs2279590 and clusterin promoter which can play a crucial role in regulating *CLU* expression, we performed 3C assay. As depicted in the **Figure 3.22** we have selected ten EcoRI restriction sites across clusterin gene, where E1-E3 is present upstream to the *CLU* promoter while E4-E8 within the *CLU* gene and E9-E10 downstream to the 3’ UTR of the *CLU* gene. E8 restriction fragment is taken as anchor fragment as the reference restriction site and is nearby to rs2279590 loci. Similarly, E4 restriction fragment represents *CLU* promoter.

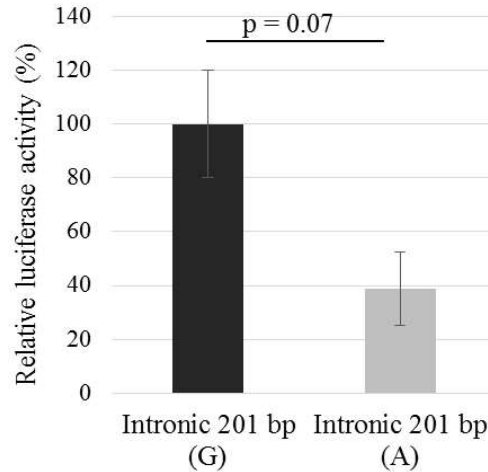


**Figure 3.19.** Allelic effect on luciferase activity in control HEK293 cells. Although, substitution from allele “G” to allele “A” decreased the reporter activity from 100±19.94 to 38.86±13.59, it was not statistically significant with a p-value of 0.07. Experiments were performed at least three times and values are represented as mean±SEM. Student’s t-test was used to calculate statistical significance between groups, \* $P < 0.05$ .

However, heat shock or MG-132 treatment significantly reduced the reporter activity; suggesting a loss of enhancer effect with rs2279590/A allele (**Figure 3.20**). To understand allele specific enhancer activity in absence of HSF1, luciferase activity in HEK293 transfected cells was checked after knocking down HSF1 expression by 0.12 (±0.01) fold compared to control cells (1±0.01) using a pool of HSF1 specific siRNA to (**Figure 3.21**).

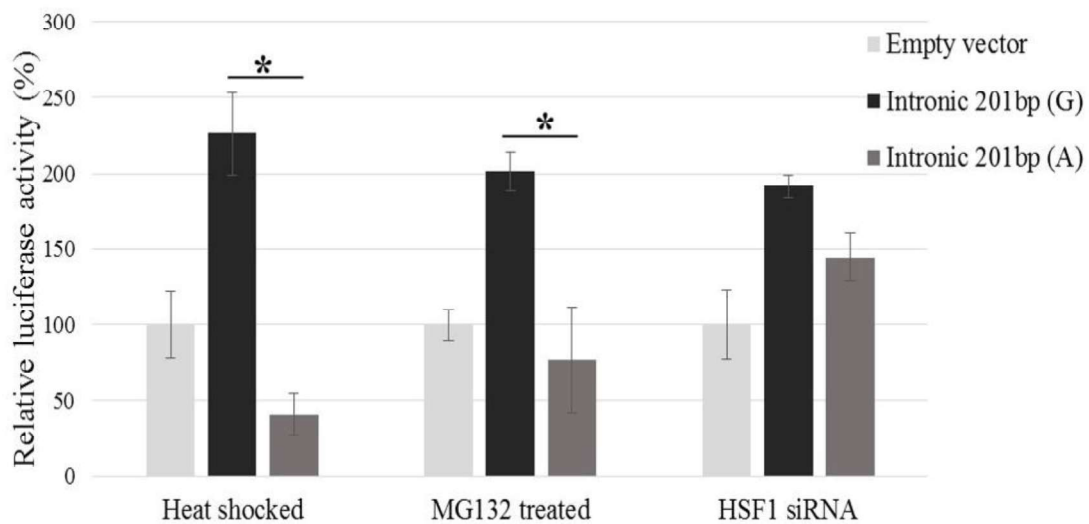


**Figure 3.20.** Normalized luciferase activity is shown in heat shocked, MG132 (5  $\mu$ M) treated and siRNA (HSF1) treated HEK293 cells to differentiate the allelic effect on reporter activity. Cells transfected with constructs containing allele “A” show reduced reporter activity in both heat shocked (41.23±13.61,  $P=0.01$ ) and MG132 (76.72±34.73,  $P=0.03$ ) treated cells than cells with allele “G” (226.11±27.43 and 201.39±12.84, respectively); while it was found to be similar with P value of 0.31 between constructs with allele “G” (191.6±7.43) and “A” (144.46±16.05) after knockdown of HSF1 with a pool of HSF1 specific siRNA. All experiments were performed at least three times and values are represented as mean±SEM. Student’s t-test was used to calculate statistical significance between groups, \* $P < 0.05$ , \*\* $P < 0.005$ .

**Figure 3.18** shows the electrophoregram for input template and from IP sample. Although, input template from HEK293 cells were heterozygous for rs2279590 as visualized from two peaks at rs2279590 for both allele “A” and “G”, IP samples were enriched with template containing allele “A” compared to allele “G”. This indicates a preferential binding of HSF1 to allele “A” *in vivo*.

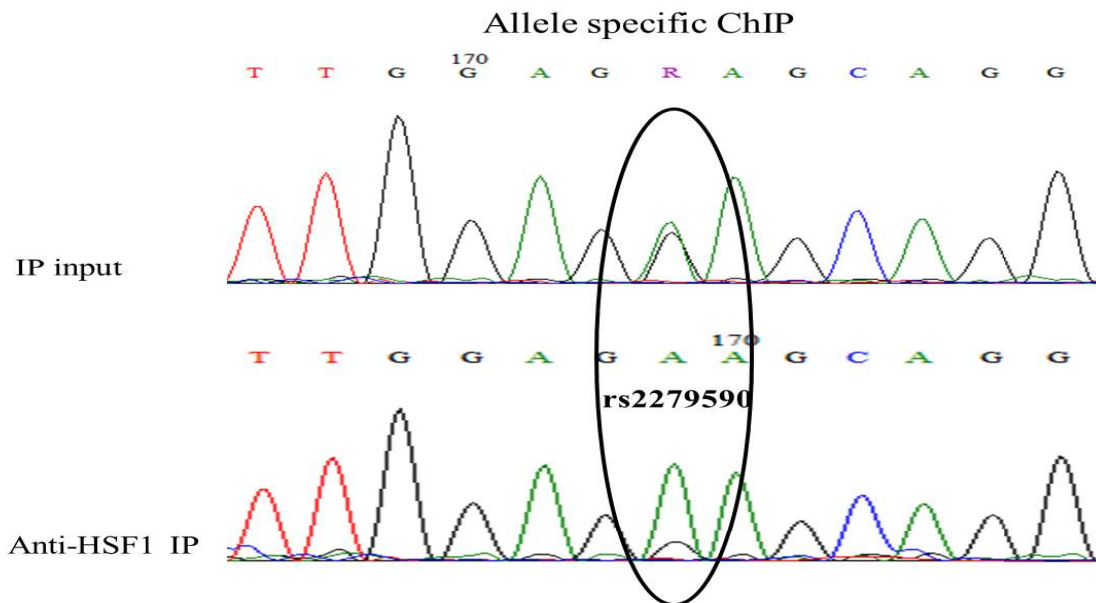


**Figure 3.18.** Allele specific ChIP was done by sequencing of rs2279590 genomic region from the input or IP sample done with anti-HSF1. HEK293 cells were found to be heterozygote for rs2279590 (A/G) and makes it suitable for allele-specific ChIP. Unlike that of input genomic fragment containing the allele “A” at rs2279590 is highly enriched in anti-HSF1 IP sample than that with allele “G”. Location of rs2279590 is represented by the oval. Experiments were replicated three times.

### 3.3.4 HSF1 binding to allele “A” at rs2279590 abrogates the enhancer effect of the locus.

In order to check the allele specific effect on the reporter activity, a 201 bp intronic region harbouring rs2279590 (with either “A” or “G” allele) was cloned into pGL4.23 luciferase vector and transfected into HEK293 cells and the reporter activity was checked. As represented in **Figure 3.19**, changing the allele from “G” to “A” reduced the reporter activity in non-treated HEK293 cells growing at normal conditions but was not found to be significant.

Additionally, to validate the binding of HSF1 to rs2279590 *in vitro*, ChIP assays were performed in HEK293 cells. As shown in **Figures 3.16** and **3.17** the genomic region surrounding rs2279590 was enriched by qRT-PCR after immunoprecipitation with anti-HSF1 antibody but not by rabbit IgG (negative control). This confirms *in vivo* binding of HSF1 to the sequences comprising of rs2279590. Allele-specific ChIP is also done to differentiate the binding of HSF1 to alleles at rs2279590.

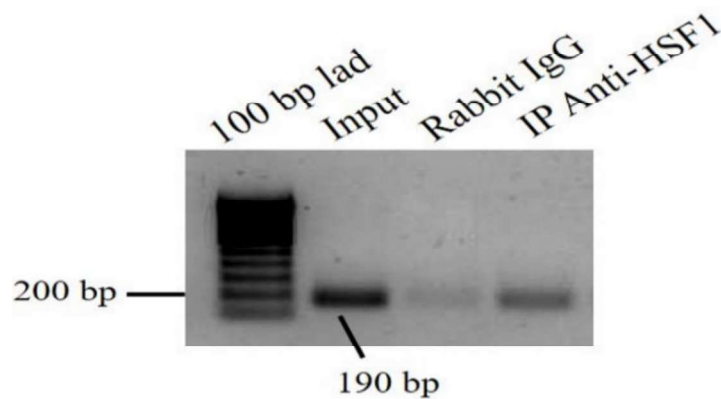


**Figure 3.16.** Chromatin immunoprecipitated samples were used for qRT-PCR assay. Fixed and digested but unprocessed genomic DNA was used as input which is 5% of the total sample used for test experiments. Enrichment of rs2279590 flanking region with HSF1 antibody was found to be higher than that with rabbit IgG in HEK293 cells. Experiments were replicated three times.

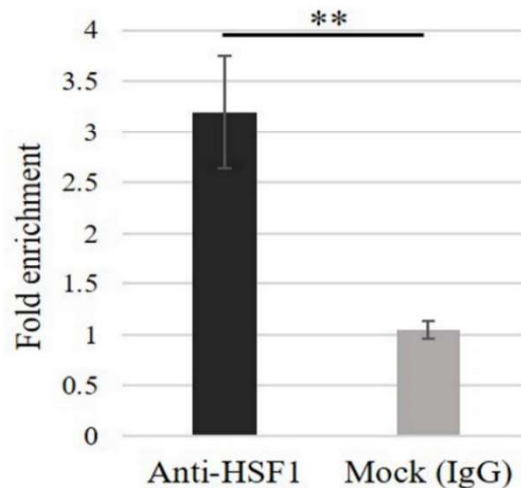


**Figure 3.17.** Fold enrichment of rs2279590 region through qRT-PCR. Fold enrichment of genomic region around rs2279590 is significantly higher ( $P=0.004$ ) in IP samples with HSF1 ( $3.19 \pm 0.55$ ) antibody than that of rabbit IgG ( $1.04 \pm 0.08$ ). Experiments were replicated three times and values are represented as mean  $\pm$  SEM. Student's t-test was used to calculate statistical significance between groups,  $**P < 0.005$ .

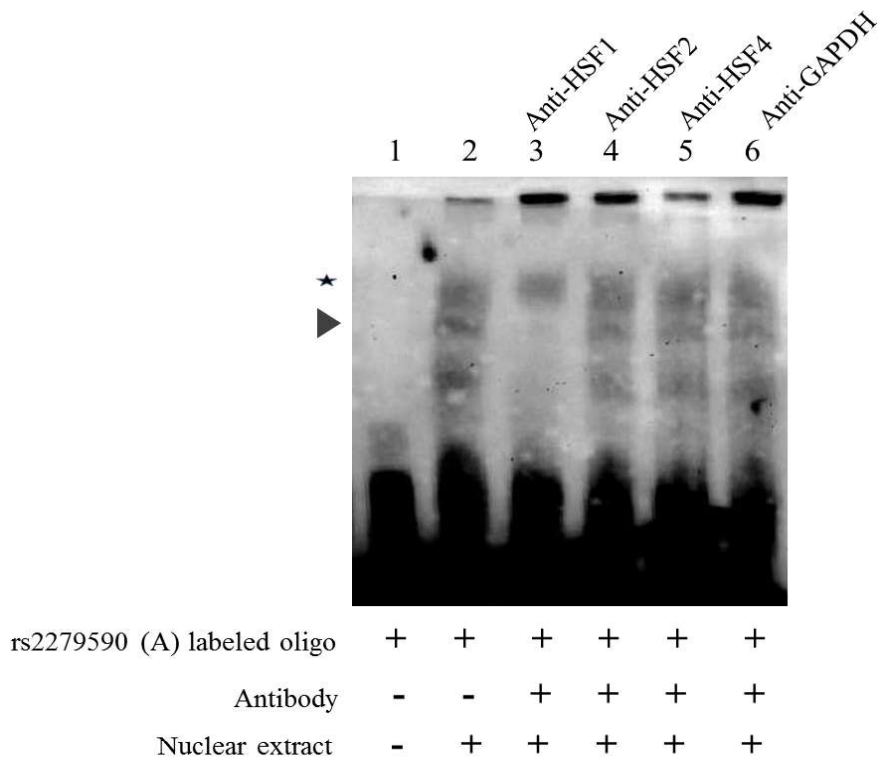


**Figure 3.14.** Supershift assay with HSFs (HSF1, HSF2, HSF4) and GAPDH. Addition of anti-HSF1 antibody in the lane 3 completely dissolves the shift made by DNA-protein complex in lane 2, unlike to that for HSF2 and HSF4 antibodies (lane 4 and 5 respectively). Anti-GAPDH antibody was used as a negative control (lane 6). Experiments were replicated at least three times. Arrowhead and Starmark represent the specific shift and nonspecific shift, respectively.

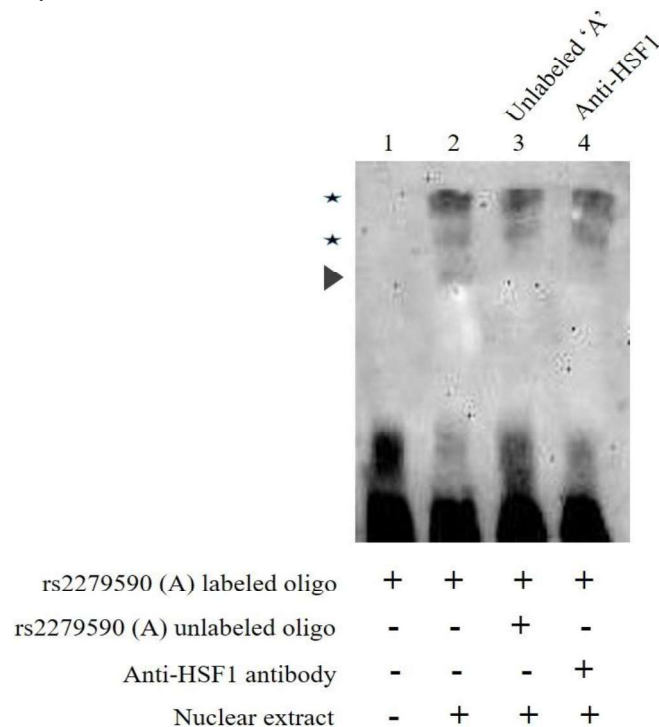


**Figure 3.15.** EMSA supershift assay with HSF1 and unlabelled rs2279590(A) oligo. Supershift assay with EMSA validated HSF1 antibody (Lane 4) shows elimination of the shift which signifies the binding of HSF1 to allele "A" at rs2279590. Experiments were replicated three times. Arrowhead and Starmark represent the specific and nonspecific shift, respectively.

(lane 3 and 5 respectively) oligos were sufficient to compete for the binding complex, thereby drastically reducing the intensity of the shift.

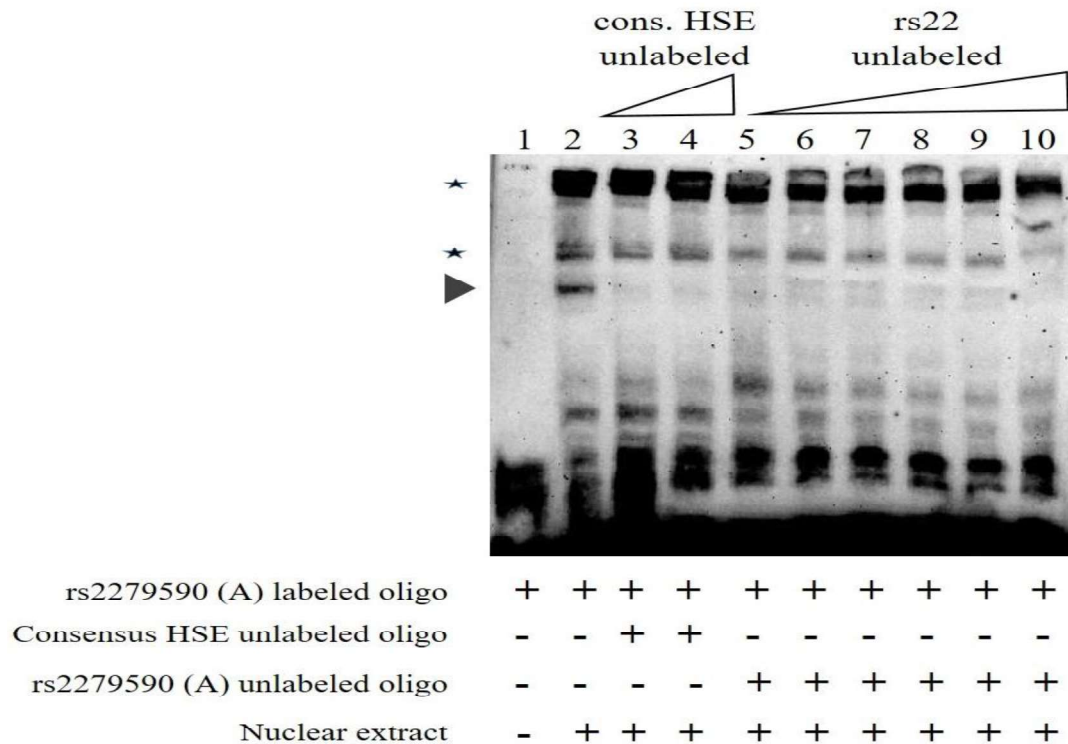


**Figure 3.13.** Specific competitive assays with unlabelled HSE and unlabelled rs2279590 oligo. Specific competitive assays were done with increasing concentrations of unlabeled HSE (1x-50fmol and 100x-5pmol fold excess) or unlabeled rs2279590 probe with allele “A” (1x-50fmol, 10x-500fmol, 50x-2.5pmol, 100x-5pmol, 200x-10pmol and 400x-20pmol fold excess). The shift abolished in the lanes 3-10 indicates that the same protein complex binds to HSE and rs2279590 region. Experiments were replicated three times. Arrowhead and Starmark represent the specific and nonspecific shift, respectively.

Super-shift assays with HSFs (HSF1, HSF2 and HSF4) made the shift disappear completely only with antibody for HSF1 (Lane 3, **Figure 3.14**) but not for, HSF2 and HSF4 (Lane 4 and 5). Also, disappearance of the specific shift with antibody for HSF1 (Lane 4, **Figure 3.15**) is similar to that for competition with unlabelled oligo with allele “A” (Lane 5) indicating that the protein binding complex bound to allele “A” at rs2279590 comprises of HSF1 protein. However, absence of any super-shift could be because the antibodies are bound to the epitope of proteins necessary for DNA-protein complex formation.

A three-tier experimental validation was further carried out to validate the binding of HSFs at rs2279590. **Figure 3.12** shows a comparative shift in lanes 2 and 5 when a labeled consensus heat shock element (HSE) and labeled rs2279590 oligo with allele “A” were used, respectively.

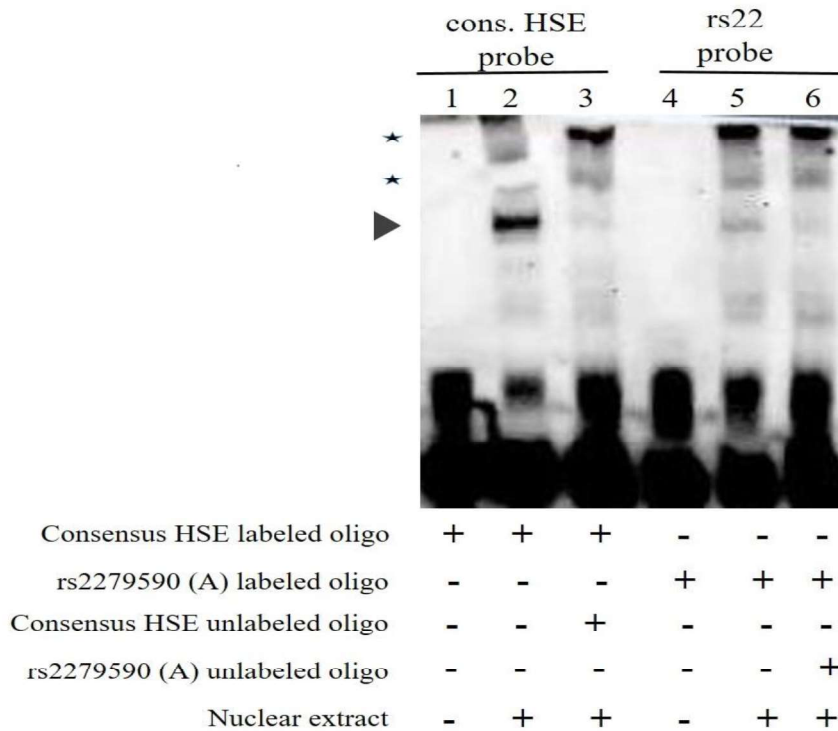


**Figure 3.12.** EMSA for comparison of specific shift between allele “A” at rs2279590 and HSE . Two biotin labeled probe: a 28 bp reported heat shock element (HSE) (Lane 1-3) and one identical to 29 bp flanking region of rs2279590 with allele “A” (Lane 4-6) was used. The presence of a shift in lane 2 and 5 (arrowhead) implies binding of a protein complex from HEK293 nuclear extract to both HSE and to the genomic region surrounding rs2279590. However, addition of their identical but unlabeled oligos in excess (lane 3 and 6) dissolves the shift suggesting specificity of the binding complex. Experiments were replicated three times. Arrowhead and Starmark represent the specific and nonspecific shift, respectively.

A competitive EMSA on labeled oligo containing rs2279590/A allele, when challenged with increased concentrations (1- and 100-fold excess) of consensus unlabeled HSE oligo (lanes 3 and 4, **Figure 3.13**) or unlabeled rs2279590/A oligo (1-, 10-, 50-, 100-, 200- and 400-fold excess) (Lanes 5-10, **Figure 3.13**) the shift disappears; indicating that the 29bp rs2279590/A sequence binds to protein complexes similar to those binding to a heat shock element. As shown in **Figure 3.13**, one fold addition of either unlabeled HSE or rs2279590/A

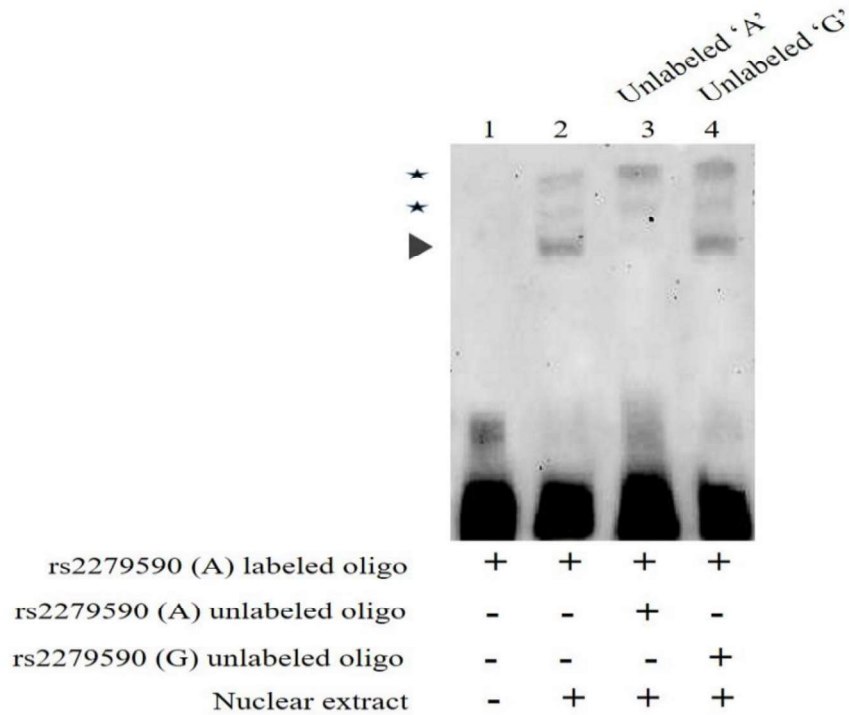


**Figure 3.10.** EMSA shows shift specific to allele “A” but not to allele “G” at rs2279590. HSF1 binds to allele “A” but not to allele “G” at rs2279590. Mobility shift assays were done by using heat shocked nuclear extract from HEK293 cells. Unlike unlabeled oligo with allele “A” (lane 3) addition of unlabeled oligo with allele “G” (lane 4) at rs2279590 couldn’t abolish the shift suggesting the specificity of binding complex to allele “A”. All experiments were replicated at least three times. Arrowhead and Starmark represent the specific and nonspecific shift, respectively.

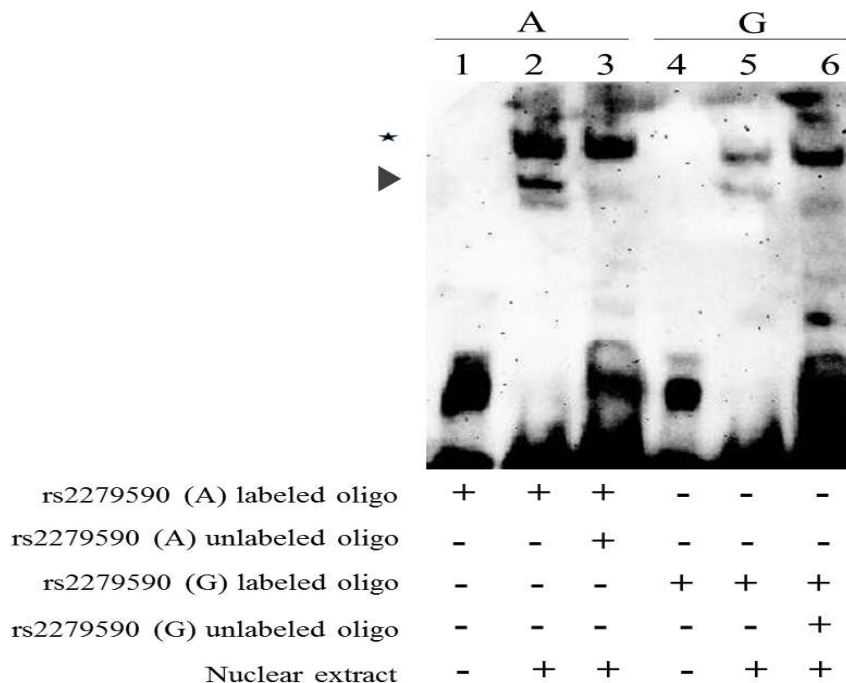


**Figure 3.11.** EMSA for binding of HSF1 to labelled oligo “A” but not to labelled oligo “G”. EMSA was also performed with labelled oligo with allele “G” (lane 4-6) compared to that of with allele “A” (lane 1-3) by using heat shocked nuclear extract from HEK293 cells. Unlike that of allele “A” (lane 2), with allele “G” does not show a prominent shift (lane 5). Experiments were replicated three times. Arrowhead and Starmark represent the specific and nonspecific shift, respectively.

( $p=0.02$ ) (**Figure 3.9**) by 0.47 fold in rs2279590 locus deleted cells (HEK293<sup>115-/-</sup>) in comparison to 1 fold in control cells similar to its secretory isoform, suggesting a regulatory effect of the said locus on both s*CLU* and n*CLU* expression.

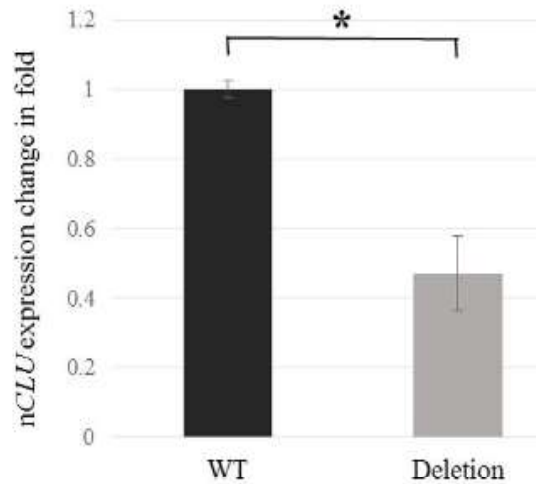


**Figure 3.9.** qRT-PCR assays for checking n*CLU* expression in control and knockout cells. An alternate transcript form of clusterin called as nuclear clusterin (n*CLU*) is also found to be significantly downregulated ( $P=0.02$ ) in cells with deletion ( $0.47\pm 0.12$ ) compared to that of non deleted cells ( $1\pm 0.05$ ) is shown through qRT-PCR assay. WT corresponds to wild type. Experiments were performed three times and values are represented as mean $\pm$ SEM. Student's t-test was used to calculate statistical significance between groups, \* $P<0.05$ .

### 3.3.3 Transition from G→A at rs2279590 creates a binding site for HSF1.

Suspecting the presence of a transcription factor binding site (TFBS) at rs2279590, we analysed its surrounding region by online TFSEARCH program. *In silico* results showed that heat shock factors (HSFs) specifically bound to the flanking region of rs2279590 with allele “A” but not with allele “G”. To validate the same, electromobility shift assays (EMSAs) were performed using nuclear extracts from HEK293 cells and a 29bp labeled oligo identical to surrounding genomic region at rs2279590 with allele “A”. It was observed that a specific protein complex bound to the labeled oligos (Lane 2, **Figure 3.10**) marked by a shift (arrowhead). With addition of unlabeled oligos comprising allele “A” (Lane 3) the shift disappears but not with unlabeled oligos with allele “G” (Lane 4); suggesting the binding complex is specific for allele “A”. Similar binding assays with labeled oligos comprising “G” allele does not show a prominent shift as shown with allele “A” (**Figure 3.11**).

Similarly, through immunofluorescence we also found a decreased localization of CLU protein in deleted cells ( $0.45\pm 0.02$ ,  $p=0.03$ ) than that of control wild cells ( $1\pm 0.1$ ) (**Figure 3.8**).

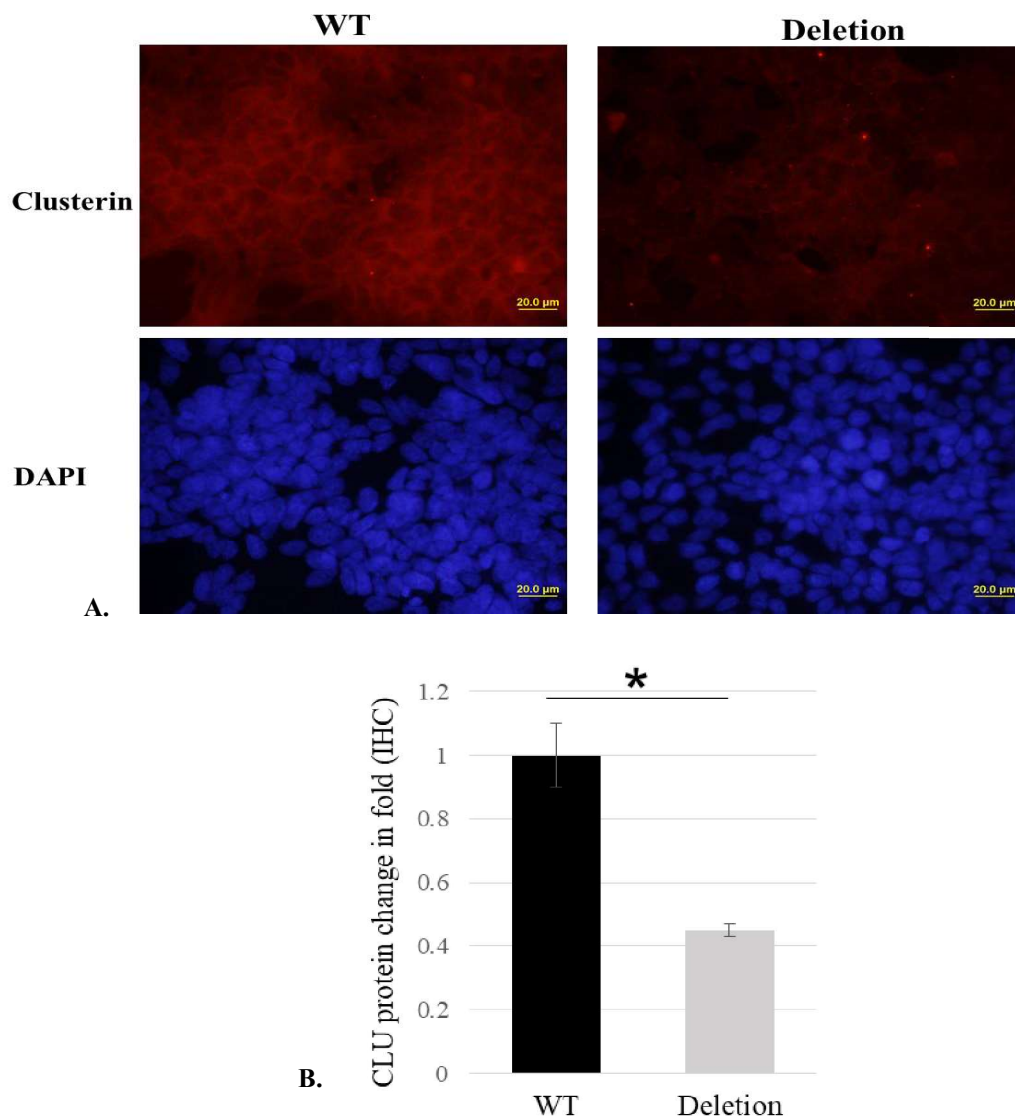


**Figure 3.8.** Immunostaining for checking sCLU expression in control and knockout cells (**A**) Shows differential expression of CLU protein in HEK293 wild control cells versus HEK293<sup>115-/-</sup> deleted cells through IHC. CLU was found to be downregulated in deleted cells in comparison to non-deleted control cells. (**B**) Fold change of CLU protein was analysed and shown in wild cells ( $1\pm 0.1$ ) compared to that of deleted cells ( $0.45\pm 0.02$ ,  $p=0.03$ ). WT corresponds to wild type. Experiments were replicated three times and values are represented as mean $\pm$ SEM. Student's t-test was used to calculate statistical significance between groups, \* $P<0.05$ .

Furthermore, we have also checked the effect of this locus on another transcript variant of clusterin coding for a proapoptotic nuclear form of clusterin or nCLU which only expresses during high level of cytotoxic stress (e.g. ionic radiation) including lethal heat shock (Trogakos et al. 2009). nCLU expression was also found to be significantly downregulated

Two independent single-cell derived homozygous clones were subsequently used to check for *CLU* gene expression compared to that of control non-deleted cells. qRT-PCR assays (**Figure 3.6**) confirmed a significant downregulation ( $p=0.01$ ) of transcripts for secretory form of clusterin (sCLU) in HEK293<sup>115/-</sup> cells versus non-deleted cells. Further, we also have checked the expression of CLU protein in wild cells and deleted cells through western and immunofluorescence. CLU protein was found to be downregulated by ( $0.38\pm 0.1$ ,  $p=0.04$ ) in rs2279590 deleted cells than that of control cells ( $0.97\pm 0.26$ ) as shown through western (**Figure 3.7**).

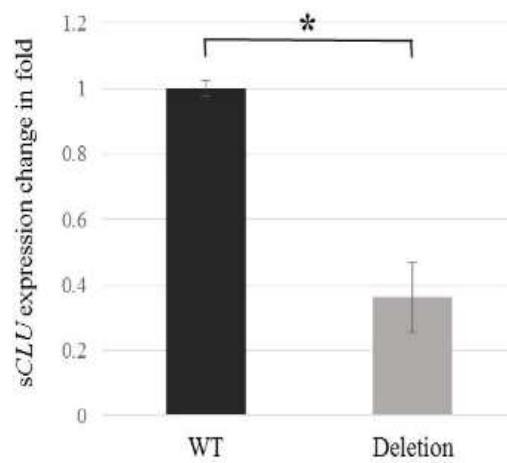


**Figure 3.6.** qRT-PCR assay for checking sCLU expression in control and knockout cells. There is a significant downregulation with a  $P$  value of 0.01 for secretory form of clusterin (sCLU) in cells with deletion ( $0.36\pm 0.1$ ) compared to that of non deleted cells ( $1\pm 0.02$ ). WT corresponds to wild type. Experiments were performed three times and values are represented as mean $\pm$ SEM. Student's t-test was used to calculate statistical significance between groups,  $*P<0.05$

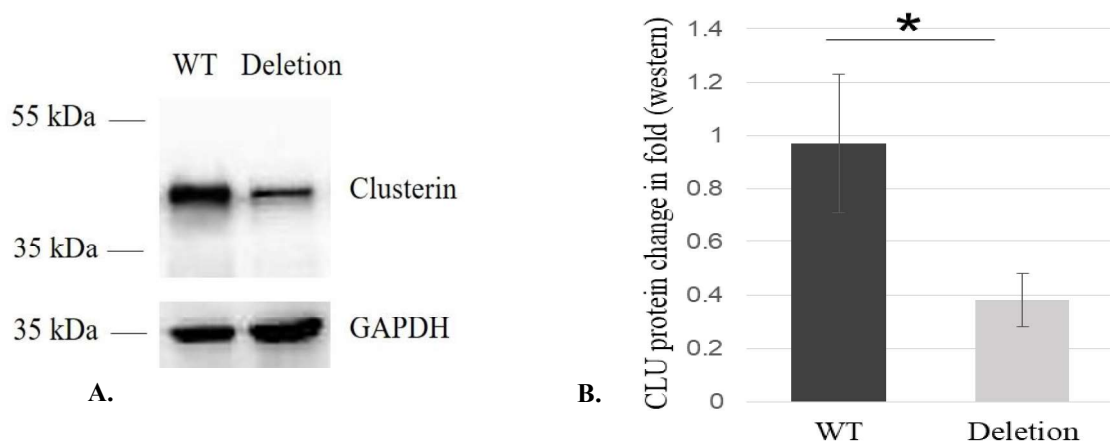


**Figure 3.7.** (A) Western blotting for checking sCLU expression in control and knockout cells. There is a significant downregulation of CLU protein in cells with deletion than that of control non deleted cells. (B) Fold change of CLU protein was analysed and shown in wild cells ( $0.97\pm 0.26$ ) compared to that of deleted cells ( $0.38\pm 0.1$ ,  $p=0.04$ ). Experiments were replicated three times and values are represented as mean $\pm$ SEM. Student's t-test was used to calculate statistical significance between groups,  $*P<0.05$ . WT corresponds to wild type. GAPDH is used as endogenous control.

In addition, to check the *in vitro* effect of the locus on clusterin gene expression, we generated HEK293<sup>115-/-</sup> cells in which 115 bp genomic region around rs2279590 was deleted using CRISPR/Cas9 system. As shown in the **Figure 3.4**, two sgRNA targeting sites were selected for genomic deletion. Clonal selection was done by amplifying a PCR product of 481 bp for wild cells, while cells with homozygous deletion showed a band with 366 bp and cells with heterozygous deletion showed both at 481 and 366 bp (**Figure 3.5**).

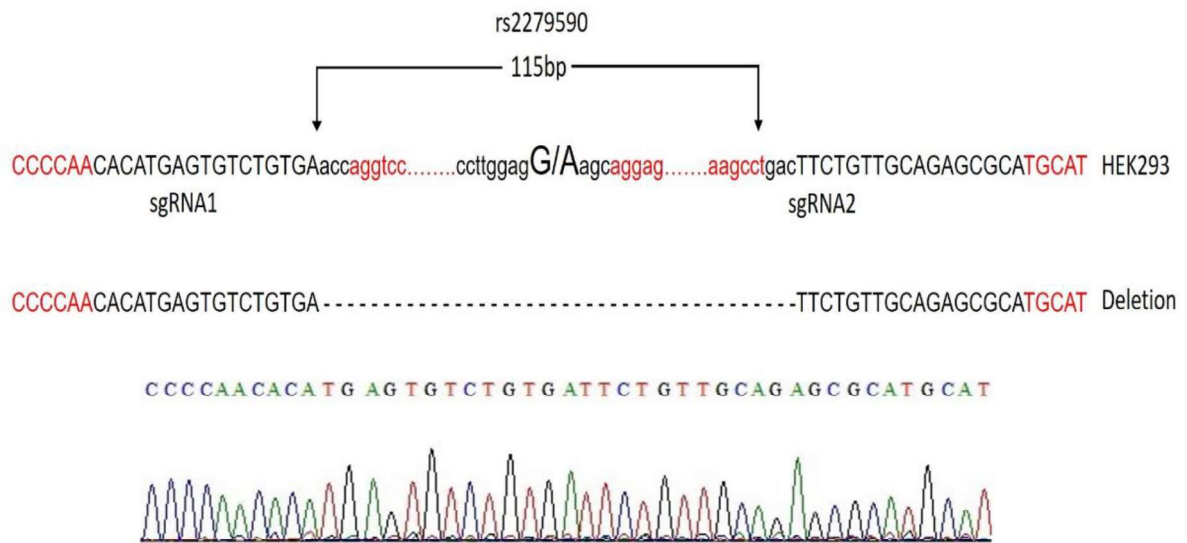


**Figure 3.4.** A representative figure showing deletion of 115 bp region around rs2279590. This is done by using a pair of sgRNA through CRISPR/Cas9 genome editing method in HEK293 cells which are heterozygote (A/G) for rs2279590.

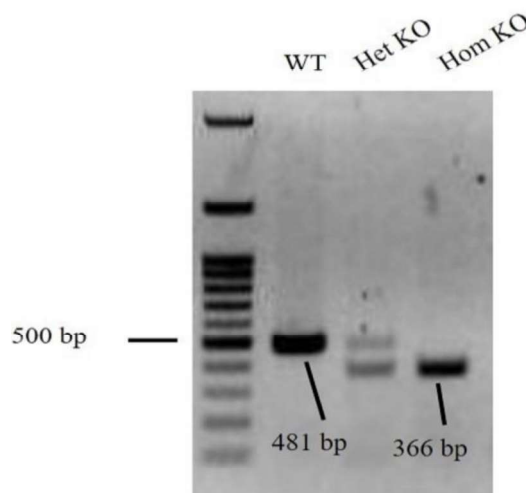


**Figure 3.5.** Gel picture depicting confirmed deletion of a 115bp region around rs2279590 generating homozygous knockout HEK293 cells. WT corresponds to wild type and corresponds to a PCR product size of 481 bp. Het KO corresponds to heterozygous deletions comprising two PCR bands of 481 and 366 bp. Homo KO corresponds to homozygous knockout deletions with a PCR product size of 366 bp.

Altogether, it indicates the role of rs2279590 as an eQTL SNP with regulatory effect over *CLU* expression.

### 3.3.2 Genomic region containing rs2279590 acts as an enhancer for clusterin gene expression *in vitro*.

To validate the *in silico* analysis we performed luciferase reporter assay to check the regulatory effect of rs2279590 loci. We cloned a 201bp genomic region surrounding rs2279590 into a luciferase reporter vector and checked its regulatory effect in HEK293 cells. As shown in **Figure 3.3**, the luciferase activity was significantly higher (~2 fold,  $p= 0.03$ ) in constructs containing the rs2279590 locus as compared to the cells with empty luciferase vector; implying a regulatory effect of this locus.

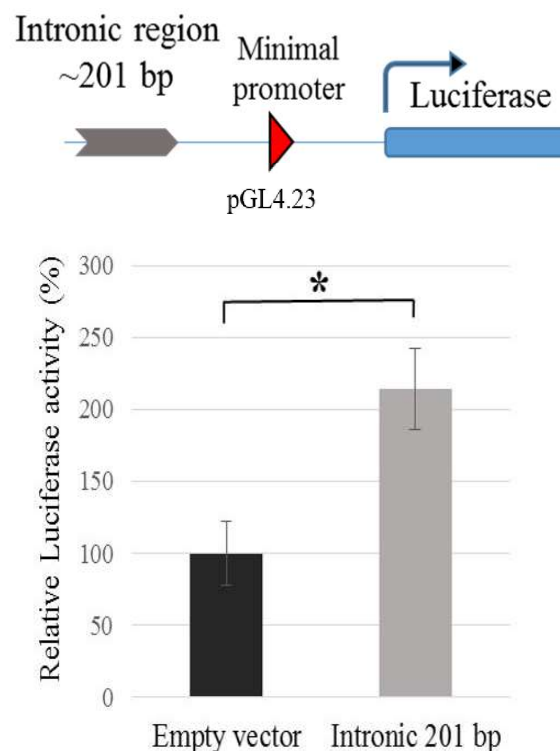


**Figure 3.3.** Regulatory effect of rs2279590 locus on luciferase reporter activity.(A) Diagrammatic presentation, showing cloning of the 201 bp intronic region around rs2279590 into the upstream region of minimal promoter of pGL4.23 reporter vector. (B) Normalized luciferase activity (214.4±28.2) is shown for reporter construct containing the region surrounding rs2279590 (201 bp with major allele “G”) compared to that of empty vector (100±21.9) ( $P=0.03$ ). Experiments were performed three times and values are represented as mean±SEM. Student’s t-test was used to calculate statistical significance between groups, \* $P<0.05$ .

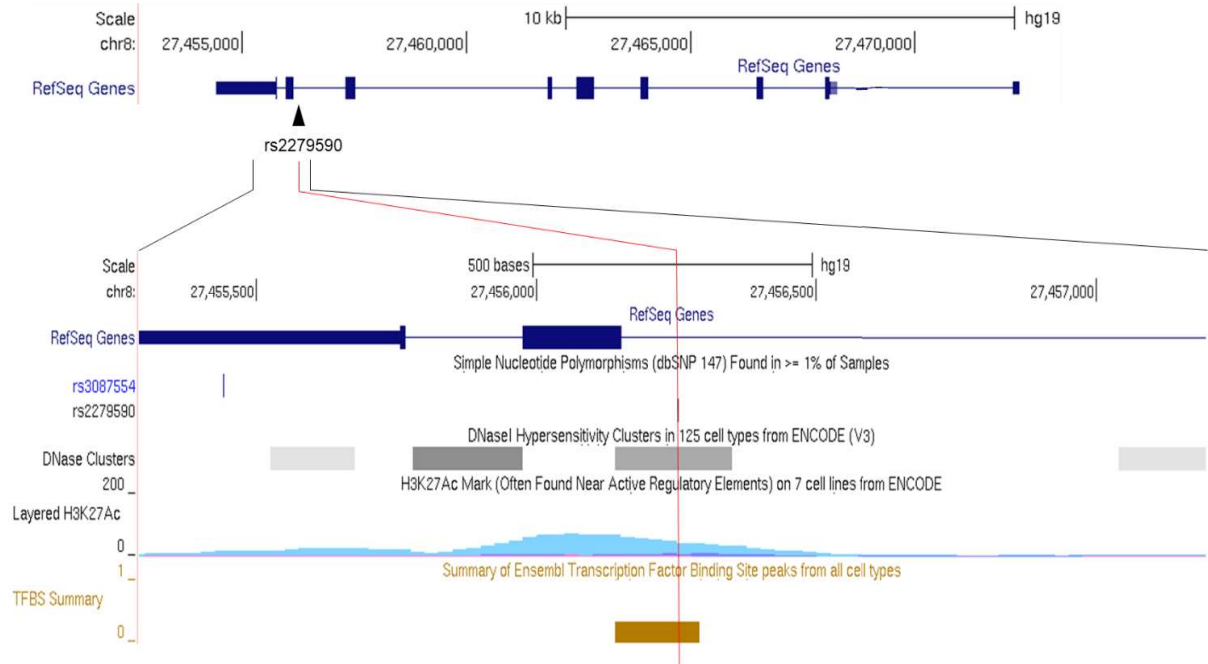


**Figure 3.1.** rs2279590 is located within an enhancer element as indicated by active regulatory marks. Region around rs2279590 viewed in UCSC genome browser using ENCODE data. Three selected tracks: DNase hypersensitivity site, H3K27Ac (Histone H3 acetylated at lysine 27) and TFBS (Transcription factor binding site) are shown. Location of rs2279590 is indicated by a vertical red line.

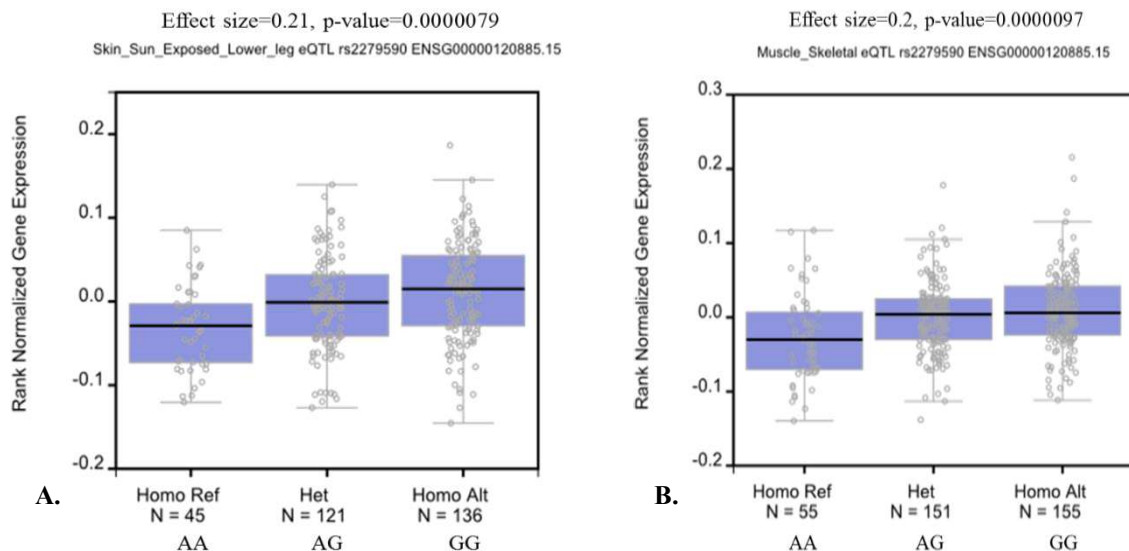


**Figure 3.2.** Expression of eQTL data for rs2279590 from Gtex portal. rs2279590 is an expression quantitative trait loci (eQTL) for *CLU* expression. eQTL data for rs2279590 were obtained from GTEx portal (Genotype tissue expression project: <https://www.gtexportal.org/home/>) on 07/11/17. (A) and (B) represents the eQTL effect of rs2279590 on *CLU* expression in both mouse-skeletal and skin-sun exposed tissue samples, respectively.

clusterin gene compared to individuals homozygous for reference allele (A). This is consistent to our finding in the previous chapter that the individuals with risk allele “G” have elevated expression of clusterin than individuals with protective allele “A” in lens capsule tissues.

### 3.2.12 DNA sequencing:

Bidirectional Sanger's sequencing of all the constructs was done using BigDye Terminator v.3.1 cycle sequencing kit (Applied Biosystem), with their respective primers (**Table 3.1**) on 3130xl Genetic Analyser (Applied Biosystem) platform. For sequencing analysis, BioEdit v7.1 (<http://www.mbio.ncsu.edu/bioedit/bioedit.html>) and sequence analysis software v5.3 (Applied Biosystem) were used.

### 3.2.13 Statistical analysis:

All experiments were repeated at least three times. Descriptive data were presented as mean  $\pm$  SE. Group wise results for statistical significance was compared by Student's t-test and  $p < 0.05$  was considered as statistically significant.

## 3.3 Results

### 3.3.1 *In silico* analysis reveals the presence of enhancer marks around genomic region of rs2279590.

Suspecting a functional role of rs2279590 we have analysed the surrounding region of rs2279590 for regulatory marks by using publicly available data from ENCODE (Encyclopedia of DNA Elements) and GTEx (Genotype-Tissue Expression) project. Using the data from ENCODE project in UCSC genome browser, we observed that the region surrounding polymorphic site, rs2279590 located in the 7<sup>th</sup> intron of clusterin gene, is within a DNase I hypersensitive site and has modified H3K27Ac mark, suggesting the presence of an active regulatory region (**Figure 3.1**). In addition, we used eQTL (Expression quantitative trait loci) data from GTEx project to check the role of rs2279590 on *CLU*.

As shown in the **Figure 3.2**, rs2279590 is shown to be regulating *CLU* expression with an effect size of 0.2 in both muscle-skeletal and skin-sun exposed tissue samples. Accordingly, individuals homozygous for alternate allele (G) show a significantly increased expression of

with a total volume of 1 ml diluted with siRNA transfected medium were transfected together, cell lysates were prepared after 36 hours and subsequently checked for reporter activity.

### **3.2.10 Quantitative real-time PCR (qRT-PCR):**

Total RNA was isolated from individual lens capsules or HEK293 cells by using a RNA extraction kit (RNeasy Mini Kit, QIAGEN). cDNA was synthesized with 1 $\mu$ g of total RNA using a Reverse Transcription Kit (Verso cDNA Synthesis Kit - AB1453A; Thermo Fisher Scientific). Gene specific primers overlapping exon-exon junction were designed by using PrimerQuest Tool (IDT) (**Table 3.1**). qRT-PCR was performed using 7500 Real time PCR Systems (Applied Biosystems, Foster city, California). Total 5 ng of cDNA and 0.8 $\mu$ M each of forward and reverse primers were used per 20  $\mu$ l reaction volume in triplicate for each sample. Amplification specificity of the PCR product was checked via melt curve analysis and sequencing.  $\Delta\Delta$ Ct method was used to calculate expression change in fold for each target gene. For normalization, GAPDH expression was taken as an endogenous control.

### **3.2.11 Western blotting:**

Cytosolic extract from HEK293 cells was prepared using NE-PER kit (Thermo Fisher Scientific). Denatured cytosolic extract (10 $\mu$ g) was then loaded on a 12% SDS-PAGE and subsequently transferred onto a PVDF membrane (Immobilion-P PVDF from Merck Millipore, Billerica, Massachusetts). Subsequent steps were followed as previously described <sup>63</sup>. A polyclonal antibody for Clusterin (sc-6419; Santa Cruz Biotechnology) was used as primary antibody and HRP-conjugated rabbit anti-goat IgG (480011730; Imgenex, India) was used as secondary antibody. GAPDH antibody (6665A; Imgenex, India) was used for endogenous control experiments. Detection was done using chemiluminescence kit (Super Signal FEMTO Maximum Sensitivity Substrate, Thermo Fisher Scientific) in a Chemi-Doc (Bio-Rad, Hercules, California).

incubated with the final reaction mixture for an additional 30 minutes on ice. Protein-DNA complexes were separated on 6% native polyacrylamide gels in 0.5X TBE, transferred to nylon membranes (Thermo Fisher Scientific, USA) and observed by chemiluminescent detection methods post-UV crosslinking.

### **3.2.8 Chromatin immunoprecipitation (ChIP):**

Pierce Agarose ChIP kit (Thermo Fisher Scientific, USA) was used for *in vivo* ChIP assays and the protocol suggested by the manufacturer was followed. Briefly,  $2 \times 10^6$  HEK293 cells were seeded and used for each experiment. Micrococcal nuclease (20 U) was used for efficient digestion of formaldehyde fixed chromatin. Digested chromatin with an average length of 500bp was subsequently used for immunoprecipitation (IP). For each IP, 25 $\mu$ g of digested chromatin was incubated overnight at 4<sup>0</sup>C with 5 $\mu$ g of ChIP validated HSF1 antibody (Santa Cruz Biotechnology, sc-9144X). As negative control, normal Rabbit IgG (1 $\mu$ l) provided in the ChIP kit was used. Later, 20 $\mu$ l of ChIP grade protein A/G plus agarose beads was added to each IP and incubated for 2 hour at 4<sup>0</sup>C with continuous rocking. IP complexes were then washed twice with each wash buffer supplied in the kit. Elution of the IP complex was done by incubating in IP elution buffer at 65<sup>0</sup>C for 1 hour. Reverse crosslinking and protein digestion were done by NaCl and Proteinase K, respectively. Subsequently, DNA was purified by using DNA Clean-Up column supplied in the kit. Fold enrichment of the target region in IP compared to that of input was assayed by a specific primer set (**Table 3.1**) through quantitative real time PCR (qRT-PCR).

### **3.2.9 Knockdown assays:**

siRNA pool for targeting HSF1 was procured from Santa Cruz Biotechnology, USA (sc-35611) and transfection was done as per manufacturer's protocol. For luciferase assays, luciferase reporter vector (1  $\mu$ g), renilla reporter vector (10 ng) and 8 $\mu$ l of siRNA pool duplex (80 pmol)

which were then individually digested and religated together and this was used as control template to normalize against primer efficiency across each primer set and to avoid experimental variations. 200 ng of 3C template or control template was used per reaction in the qRT in triplicate and a combination of the reference primer (E8) denoting the restriction fragment containing rs2279590 loci is used with every other primer for quantifying the ligation frequency across the clusterin gene. Normalized relative ligation frequencies were plotted in reference to the position of respective restriction sites.

### **3.2.6 Bioinformatic analysis:**

Online program, TFSEARCH (<http://www.cbrc.jp/research/db/TFSEARCH.html>) was used for candidate search with a default threshold score set to 85.

### **3.2.7 Electrophoretic mobility shift assay (EMSA):**

Two pairs of complementary 29-mer oligonucleotides, centered around rs2279590 with allele “A” or “G” and a previously reported heat shock element (HSE) were ordered<sup>188</sup>; both with and without biotin 5'-end labelling [Integrated DNA Technologies (IDT), Iowa]. Sequences of the oligomers are listed in **Table 3.1**. Annealing of complementary oligos was done by incubating them at 95°C for 5 minutes, followed by step-cooling to room temperature.

Nuclear extract from heat shocked (1 hour at 42°C) HEK293 was prepared by using NE-PER kit (Thermo Fisher Scientific, USA) and protein concentrations were estimated by Bradford's assay. EMSA was performed using LightShift Chemiluminescent EMSA Kit (Thermo Fisher Scientific, USA) following the manufacturer's instructions. DNA-protein binding assays were carried out using 3µg of total nuclear extract and 100 fmol of biotinylated annealed oligonucleotides for each 20µl total reaction volume. Competitive EMSA was done using 400 fold excess (40 pmol) of unlabeled double-stranded oligonucleotides. For supershift assays, 2µg of EMSA validated HSF1, HSF2 and HSF4 antibody (sc-9144X, sc-13056 and sc-366983; respectively) were procured from Santa Cruz Biotechnology, Dallas, Texas and were

37<sup>0</sup>C overnight with continuous shaking. After overnight incubation, 40 µl of 20% SDS (final 1.6%) was added to the sample to denature the enzyme and incubated at 65<sup>0</sup>C for 25 minute with shaking. Then the sample was transferred into a 50 ml falcon tube and 6.125 ml of 1.15 fold ligation buffer (10 fold ligation buffer 660 mM Tris-HCl, pH 7.5; 50 mM DTT; 50 mM MgCl<sub>2</sub>; 10 mM ATP) was added for ligation of digested products. After incubating this mixture for 1 hour at 37<sup>0</sup>C with 375 µl of 20% Triton X-100 (final 1%), 5 µl of T4 DNA ligase (100U total, NEB) was added for ligation and incubated further for 4 hour at 16<sup>0</sup>C followed by 30 minute at RT. To de-crosslink the chromatin, 30 µl of 10 mg/ml Proteinase K (300 µg total, ThermoScientific) was added and incubated at 65<sup>0</sup>C overnight. Then 30 µl of 10 mg/ml RNase was added for 45 minute at 37<sup>0</sup>C to remove RNA contamination. After incubation 7 ml of phenol-chloroform was added and mixed thoroughly for separation of genomic DNA into the aqueous phase. It was then centrifuged for 15 minute at 2,200 rcf at RT. To the collected aqueous phase, 7 ml of nuclease free water, 1.5 ml of 2M sodium acetate (pH 5.6) and 35 ml of ethanol was added for precipitation of genomic DNA. Above mixture was then kept at -80<sup>0</sup>C for 1 hour and then centrifuged for 45 minute at 2,200 rcf at 4<sup>0</sup>C. The supernatant is discarded and 10 ml of 70% ethanol was added for removing salts or phenolic impurities and again centrifuged for 15 minute at 2,200 rcf at 4<sup>0</sup>C. Then after discarding the supernatant, pellet was dried at RT. Subsequently the DNA pellet was dissolved in 150 µl of 10mM Tris pH 7.5.

Prepared 3C template was then used to quantify the ligated product by qRT-PCR using a set of designed primers (**Table 3.1**). In total, 10 restriction sites overlapping clusterin gene were used for 3C analysis where the restriction fragment no.8 (E8) represents rs2279590 loci and E4 represents *CLU* gene promoter. As internal loading control, a genomic region without EcoRI site from human GAPDH gene was used. For normalizing ligation frequency, two restriction fragment located distant from each other in the human Tubulin gene was used. For standard curve, loci containing EcoRI restriction sites were amplified by another set of primers

Carlsbad, California). Transfected cells were selected after 24 hour post-transfection in complete media supplemented with 2.5 µg/µl puromycin. Single cell clones were then isolated and cultured by dilution cloning and subsequently genomic DNA was isolated using DNeasy Blood & Tissue Kit (Qiagen, Hilden, Germany) following manufacturer's instructions. Screening was done to find out homozygous deletion of genomic region containing rs2279590 by using a specific set of primers (**Table 3.1**) outside the targeted sites and subsequently confirmed by sequencing. Positive clones were used for subsequent experiments.

### **3.2.5 Chromosome conformation capture (3C) assay:**

To analyse the chromatin interaction between loci containing rs2279590 and CLU promoter we employed chromatin conformation capture (3C) assay. The protocol carried out for 3C assay was followed according to Halene *et al.*<sup>187</sup> and described here in detail. HEK293 cells were used as *in vivo* cell model to study the chromatin interaction, if any. Cells were grown to 70% confluent and then crosslinked by formaldehyde (2%) (Thermoscientific, USA) for 10 minute at room temperature (RT). Cross-linking was then stopped by quenching with 1.425 ml of 1M glycine (Thermoscientific, USA) for 5 minute. Cells were then washed twice by cold PBS, scraped and collected by centrifugation (8 minute at 500 rcf at 4<sup>0</sup>C). Cells were then lysed by gentle pipetting in cell lysis buffer (10 mM Tris-HCl, pH 7.5; 10 mM NaCl; 5 mM MgCl<sub>2</sub>; 0.1mM EGTA; complete protease inhibitor; 11836145001 Roche) and centrifuged again (5 minute at 500g at 4<sup>0</sup>C). Then to the pelleted nuclei 0.5 ml of 1.2x CutSmart buffer (NEB) was added and pipetted to make a homogenous solution. It was incubated for 1 hour at 37<sup>0</sup>C with 7.5 µl of 20% SDS (final 0.3% SDS) in continuous shaking. After incubation 50 µl of 20% Triton X-100 (final 2%) (MP Biomedicals, USA) was added and incubated further for 1 hour at 37<sup>0</sup>C with shaking.

5 µl of the sample was used as an undigested genomic DNA control to determine the digestion efficiency. To the remaining aliquot 400 U of HF-EcoRI was added and incubated at

22	E10 clu	3C qPCR	F: TTGTTCTCCATTTGTCTTGAT	60
23	Control E1	3C Control	F: AAGTCCCATCTGGTCATTGC R: TCCAAGAAGAAGTGGGCTGT	58
24	Control E2	3C Control	F: CATGCATGGCTCTTGTTTCAT R: TGCCAGCTCAGGTTTCTCTT	58
25	Control E3	3C Control	F: TGCCATGATGATGGAAAAGA R: TTACAGCACCCTGCACTCC	54
26	Control E4	3C Control	F: CCCCTCTCTGAGGTCTGGAT R: CCCCTGAAAGCAACAACCTC	54
27	Control E5	3C Control	F: TAGGGTTAAGGCAGGCACAC R: CCAAGAAAGGCATGAAACT	58
28	Control E6	3C Control	F: TCCAGGACAGGTTCTTCACC R: TCAAACCTCCTGGCCTCAAAT	58
29	Control E7	3C Control	F: TTTTCAAACCTGGCATCTTGTTA R: AACTTGTCTTTTGAGCATGTCTGTA	52
30	Control E8	3C Control	F: GGCGTTTCTCGGCTTTTAGT R: GCAAATACCTCTGACCCATAAT	58
31	Control E9	3C Control	F: GAAAACCAGGGTGGAAACTAA R: TCTTATCCTTAGGTCTGCGGTTAC	54
55	Tub E1	3C qPCR	F: CCCTGTCAATGTACCGCTCTA	60
56	Tub E2	3C qPCR	F: CCCC GGCTAATTGTTTTGTA	60
57	Control Tub E1	3C Control	F: GCTCTCTTTTGTGCGTAACT R: CAGCAGTCTGAGCGCAGTAG	56
58	Control Tub E2	3C Control	F: CCATACTCCAGAGCTGCTACA R: TCAAGGAGGGGATGAACAGTA	56
59	GAPDH 3C	3C Control	F: ACAGTCCATGCCATCACTGCC R: GCCTGCTTCACCACCTTCTTG	54

### 3.2.4 CRISPR/Cas9 construct preparation and genome editing:

Genome editing of HEK293 was done by CRISPR/Cas9 system as described previously. A pair of sgRNA was designed (<http://crispr.mit.edu/>) with a little off-target specificity to delete a 115 bp region around the SNP, rs2279590 (**Table 3.1**). Annealed oligonucleotides were phosphorylated and ligated into BbsI digested PX459 (Plasmid #62988; Addgene, Cambridge, Massachusetts).

At 50% confluency, the HEK293 cells were transfected with 2.5  $\mu$ g of each CRISPR construct (with sgRNA1 and sgRNA2) simultaneously using lipofectamine 2000 (Invitrogen,

**Table 3.1.** List of oligos used in the study.

Sl. No.	ID	Purpose	Sequence (5'→3')	T <sub>m</sub> <sup>0</sup> C
1	rs2279590 intronic region	Luciferase assay	F: CTCCGGTACCCACATGAGTGTCTGTGAACC R: CACCCTCGAGCTAAATGGAACAAGAGAAAAG	58
2	CRISPR sgRNA pair 1	Genome editing	Sense: CACCGCACATGAGTGTCTGTGAACC Antisense: AAACGGTTCACAGACACTCATGTGC	-
3	CRISPR sgRNA pair 2	Genome editing	S: CACCGTGCCTCTGCAACAGAAGTC A: AAACGACTTCTGTTGCAGAGCGCAC	-
4	CRISPR rs22-KO	Genome editing	F: CCTACTCTGACCAAGGGCTG R: CCGGTGCTTTTTGCGGTATT	55
5	EMSA rs22 (A) labeled/unlabeled	EMSA	S: GTTTCCTTGGAGAAGCAGGAGGACTTCCT A: AGGAAGTCCTCCTGCTTCTCCAAGGAAAC	-
6	EMSA rs22 (G) unlabelled	EMSA	S: GTTTCCTTGGAGGAGCAGGAGGACTTCCT A: AGGAAGTCCTCCTGCTCCTCCAAGGAAAC	-
7	EMSA HSE labeled/Unlabeled	EMSA	S: GAGGAAGTTCTAGAACGTTCTTCAGGCC A: GGCCTGAAGAACGTTCTAGAACTTCCTC	-
8	rs2279590 intronic region	ChIP	F: CTCCCTGGGCTGGTCATTTG R: CATGCGCTCTGCAACAGAAG	60
9	Secretory <i>CLU</i> (NM_001831.3)	qRT-PCR	F: AGGCGTGCAAAGACTCCA R: GCCCACTCTCCCAGGTCA	60
10	Nuclear <i>CLU</i> (NM_001831.3)	qRT-PCR	F: GCTGACCGAAATGTCCAATC R: GTTGTGAGCAGTGTCTTGC	60
11	HSF1 (NM_005526.3)	qRT-PCR	F: GCAACAGAAAGTCGTCAACAAG R: CCACTGTGCTTCAGCATCA	60
12	GAPDH (NM_002046.5)	qRT-PCR	F: GGTGTGAACCATGAGAAGTATGA R: GAGTCCTCCACGATACCAAAG	60
13	E1 clu	3C qPCR	F: GAGTTGCTACTGGTCTACAGAAA	60
14	E2 clu	3C qPCR	F: TCCACATGGATAGTATAGCTTTGA	60
15	E3 clu	3C qPCR	F: GAATTGAGGGTAGGAGCTGATATT	60
16	E4 clu	3C qPCR	F: AGAGAGGTTGGGTGAGAGAA	60
17	E5 clu	3C qPCR	F: CATGATCCATCGTGCATGTTAAA	60
18	E6 clu	3C qPCR	F: CCTCACTTCTTCTTTCCCAAGT	60
19	E7 clu	3C qPCR	F: CCCTGACTCACGTTTGATGTA	60
20	E8 clu Anchor	3C qPCR	F: ATCTCAGTCTTAAAGCTCAGGCT	60
21	E9 clu	3C qPCR	F: TTCTGTCTCCAGTCTTCCATTT	60

### **3.2.2 Cell culture:**

The human cell line, HEK293 was cultured in HiGlutaXL Dulbecco's Modified Eagle Medium, High Glucose (AL007G) with 10% fetal bovine serum (RM9952) and 1% penicillin (100U/ml) and streptomycin (0.1mg/ml) (A001), maintained at 37<sup>0</sup>C and 5% CO<sub>2</sub>. All cell culture chemicals were procured from HiMedia, Mumbai, India.

### **3.2.3 Luciferase Reporter assays:**

For reporter assays, pGL4.23 luciferase reporter vector with minimal promoter and pGL4.74 renilla vector were used (Promega, Madison, Wisconsin). Genomic DNA was extracted from peripheral blood leucocytes of the study subjects by phenol-chloroform extraction method. An intronic region of 201 bp surrounding rs2279590 variant (harbouring either "AA" or "GG" genotype at the polymorphic site) was PCR-amplified using a specific primer pair (**Table 3.1**) from the extracted genomic DNA. The amplified products were then cloned into pGL4.23 vector by double digestion at KpnI-XhoI site (KpnI-HF and XhoI-HF, New England Biolabs, Ipswich, MA).

For transfection, HEK293 cells were seeded in a 12-well plate. At 80% confluency, the cells were transiently co-transfected (Lipofectamine 2000, Invitrogen) with luciferase constructs (1µg) and renilla vector (pGL4.74, 10ng). Transfection efficiency was normalized by renilla reporter activity. After 24 hours of post-transfection, cell lysates were prepared following Dual-Luciferase® Reporter Assay System (Promega). Reporter activities were measured with Varioskan® Flash Multimode reader (Thermo Fisher Scientific, Waltham, Massachusetts, USA) following manufacturer's instructions. Values for luciferase activity, post normalisation with renilla reporter activity, were used for further analysis. Each of the experiments was repeated independently with at least three replicates.

which is the common extracellular form, cells with chronic stress also transcribes for an alternative form of CLU protein known as nuclear clusterin or nCLU. This rare isoform of secretory clusterin tends to localize within the nucleus and activates the expression of a group of cytotoxic genes which ultimately lead to death of the cell.<sup>186</sup> Stress induced expression of nCLU in the neurons can lead to apoptosis, a pathogenic feature seen in both PEX and AD. Thus, an increase in the expression of both secretory and nuclear CLU can be detrimental to the neuronal cell. Further, we have shown that individuals homozygous for the risk allele “G” at rs2279590 have a 2- fold higher clusterin expression in lens capsule tissues than those with protective allele “A”.<sup>63</sup> An increase in the *CLU* expression by the risk allele suggests a cytotoxic effect of accumulated CLU. Additionally, it also implicates a functional role of rs2279590 and its regulatory effect on *CLU* gene expression. This chapter is focused on finding the functional mechanism by which rs2279590 variant regulates *CLU* gene expression.

## **3.2 Materials and Methods**

### **3.2.1 Study subjects recruitment:**

This study was approved by the ethics review boards of National Institute of Science Education and Research and JPM Rotary Club of Cuttack Eye Hospital and Research Institute, India and adhered to the tenets of the Declaration of Helsinki. All participants underwent a detailed ocular examination, including slit lamp, ocular biometry, Goldman applanation tonometry, +90D biomicroscopic fundus evaluation and 4 mirror gonioscopy. Inclusion and exclusion criteria for the grouping of control and PEX affected individuals were followed as reported previously in chapter 2. Anterior eye tissues (lens capsules and conjunctiva) from PEX affected study subjects and age matched controls were collected in RNAlater stabilisation solution (Invitrogen, USA) during cataract surgery and stored at -80°C until further use.

individuals with PEXG also have decreased blood flow velocity thereby increasing the resistance of the middle cerebral arteries and linking with brain atrophy.<sup>34</sup> PEXG individuals which share a resemblance for advanced stage of neuron degeneration with AD have shown to possess multiple dense pattern of tightly packed myelinated fibers with diminished staining for glial fibrillary acidic protein (GFAP) within the nerve fibre bundles of the retrolaminar optic nerve than that of control eyes. GFAP is a well-known marker for astrocytes and decreased staining of GFAP indicates dying astroglial cells in such regions. GFAP is also found to be decreased during chronic swelling and vacuolation of white matter astroglia in Alzheimer's patients.<sup>35</sup> Existence of such analogous pathological symptoms between PEX and AD hints at a common aetiology for these age related neurodegenerative disorders.

### **3.1.2 Paradoxical role of clusterin as an inducer of cytotoxicity**

Earlier studies suggest a protective role of CLU in preventing formation of extracellular deposits and its clearance through endocytosis and subsequent degradation.<sup>182</sup> However, recent reports have questioned the protective role of CLU in the ECM. Demattos *et al.* have reported that knock out of clusterin in an Alzheimer's mice model (PDAPP mice) have decreased fibrillar plaque and neuritic dystrophy.<sup>183</sup> Further, individuals affected by AD have shown a faster decline of brain function with overaccumulated CLU than unaffected subjects.<sup>181,184,185</sup> It has been shown that it's the Clusterin: substrate ratio in the extracellular space that decides the fate of the CLU to be cytotoxic or cytoprotective. At a higher substrate to clusterin ratio it deposits along with the extracellular deposits in a failed attempt to clear the fibrillar aggregates.<sup>173</sup>

In the previous chapter, we have shown that CLU accumulation differentiates the severe advanced stage of PEX called pseudoexfoliation glaucoma (PEXG) from the less severe syndrome stage, pseudoexfoliation syndrome (PEXS).<sup>63</sup> However it is unclear, whether accumulation of CLU in PEXG is the cause or a consequence. Unlike that of secretory clusterin

## **Chapter 3. Functional significance of clusterin intronic variant, rs2279590 in PEX progression.**

### **3.1 Introduction**

Clusterin has been associated at both genomic and proteomic level with age-related disorders such as, Alzheimer's disease (AD) and Type 2 Diabetes mellitus including pseudoexfoliation.<sup>62,63,125,126</sup> Genetic polymorphisms within clusterin gene are shown to be risk factors for these disorders. rs2279590 is one of such common variant and has been associated with both PEX, AD and diabetes.<sup>62,63,125,126</sup> This chapter is focused on finding out the functional role of this common risk variant in the progression of PEX.

#### **3.1.1 Pseudoexfoliation and Alzheimer's disease shares similar pathological alterations**

Earlier reports have studied the interrelation between PEX and the age related neurodegenerative disorder, AD. Both PEX and AD share similar pathological alterations like characteristic deposition of fibrillar protein aggregates and gradual deterioration of optic and brain nerves respectively.<sup>35,154</sup> Onset of AD starts from deposition of fibrillar aggregates consisting of amyloid- $\beta$ -peptide in the affected areas of brain tissues of AD individuals. Amyloid- $\beta$ -peptides are short peptide in the extracellular space that leads to the formation of amyloid plaques. This is further aggravated by accumulation of hyperphosphorylated tau protein around brain neurons. Hyperphosphorylation of tau protein loses its capacity to stabilize microtubules and assembles into insoluble aggregates called tau tangles.

Although, detailed studies of PEX aggregates is yet to be carried out like that of AD but there are similar pathological changes seen in PEX. Proteins like amyloid beta-peptide, serine proteinase inhibitor and alpha-1-antichymotrypsin which are predominantly present in amyloid plaques, also has been found in PEX deposits demonstrating a common aetiology in both PEX and AD pathogenesis.<sup>32</sup> Incidence of PEX is also higher in AD patients with dementia and cognitive impairments than normal control population.<sup>33</sup> Additionally,

# **CHAPTER 3**

**Functional significance of  
*clusterin* intronic variant,  
rs2279590 in PEX  
progression**

## 4.5 Conclusion

According to all cumulative data known till date, a model is being proposed as shown in **Figure 4.6** that rs2279590 resides within a regulatory genomic region and with risk allele “G” shows a widespread enhancer effect on three PEX/AD risk associated candidate genes; *CLU*, *PTK2B* and *EPHX2*.

#### 4.4.2 Regulation of *EPHX2* by rs2279590, a PEX risk variant implies a probable role of *EPHX2* in the progression of PEX.

*EPHX2* or epoxide hydrolase-2 metabolises epoxyeicosatrienoic acids which are proven to be neuroprotective. Deletion of rs2279590 locus also leads to downregulation of *EPHX2*, another candidate gene for AD pathogenesis. Upregulation of hydrolase activity of soluble *EPHX2* leads to an increased OGD-induced (oxygen-glucose deprived) neuronal cell death.<sup>206</sup> Recently, *EPHX2* too has been associated with AD as a risk factor through GWAS.<sup>202</sup> Our work also found a decreased expression of *EPHX2* in the lens capsule of

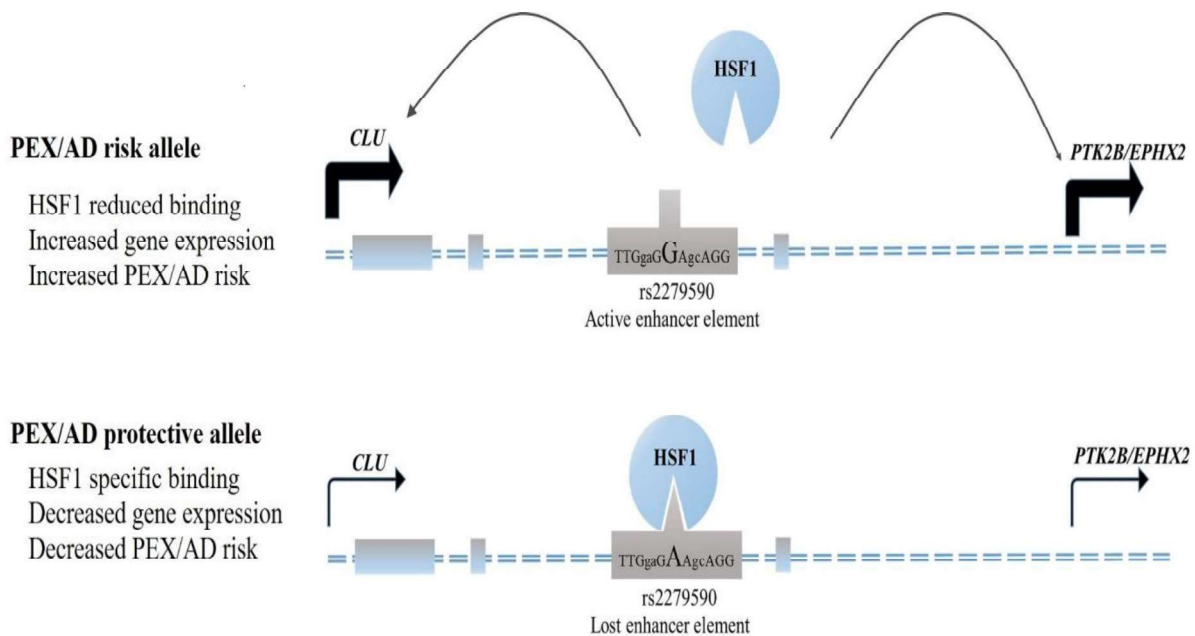


**Figure 4.6.** Proposed model explaining the effect of SNP-dependent HSF1 binding at rs2279590, *EPHX2* and *PTK2B* gene expression and AD/PEX risk. Genomic region containing rs2279590/G resides within an active enhancer element and increases gene expression of *CLU*, *PTK2B* and *EPHX2*. However, binding of HSF1 to protective allele “A” at rs2279590 diminishes the enhancer effect of the locus; which leads to decrease in target gene expression with a lowered risk of developing PEX/AD.

PEXS subjects. However, whether decrease in *EPHX2* expression is a consequence or the cause is unknown. In addition to that, the hydrolase activity of *EPHX2* and also the level of epoxyeicosatrienoic acids needs to be checked in PEX affected eye tissues. Further, future studies need to be done to check the status of both *EPHX2* and *PTK2B* genes in PEXG individuals and their exact role in PEX pathogenesis.

## 4.4 Discussion

Locus containing *CLU* (8p21) is surrounded by various crucial genes that has been associated with various age related disorders. Our finding about distal regulation of both *PTK2B* and *EPHX2* by an eQTL SNP, rs2279590 further provides a novel insight in the role of this locus as a contributing factor in the pathogenesis of PEX and AD.

### 4.4.1 Gene expression of *PTK2B* is modulated by rs2279590 through a wide-spread enhancer effect.

Genetic association studies like case-control and GWAS reports have previously shown an association of genetic variations in *PTK2B-CLU* loci with both PEX and AD.<sup>62,125,191</sup> Protein tyrosine kinase 2 beta or PTK2B, belongs to a non-receptor protein kinase family involved in calcium induced regulation of ion channels and MAPK pathway activation. It plays a role in inducing phosphorylation of GSK3 (Glycogen synthase kinase 3) which then promotes Tau fibrillar pathology. In hippocampus of AD affected individuals, heightened phosphotyrosine immunoreactivity was found in the neuritic plaques, tangle-bearing neurons and microglia, which are characteristic features of increased PTK2B activity.<sup>204</sup> Accumulation of PTK2B was also reported in the early event of AD pathogenesis with progressive Tau pathology.<sup>189</sup> However, it is unclear whether accumulation of PTK2B in aiding the Tau pathology, is a consequence or a cause. In this study, we found decreased levels of *PTK2B* mRNA in cells with the deleted enhancer element containing rs2279590; suggesting a distal enhancer effect of the locus over *PTK2B* expression. Although, regulatory effect of rs2279590 on *PTK2B* was not established in eQTL data from GTEx project, it may depend on various confounding factors including the type of tissue analysed. Further, earlier reports have shown an increased PTK2B expression with AD associated risk alleles at rs28834970 and rs2718058 (a cis-pQTL within *PTK2B* locus and a trans-pQTL within *NME8* locus).<sup>205</sup>

of these two genes in the conjunctiva (**Figure 4.5A**) and lens capsule (**Figure 4.5B**) of PEX affected subjects and compared to that of control individuals. There was no differential expression of *PTK2B* and *EPHX2* ( $p=0.89$  and  $0.83$ , respectively) in the conjunctiva tissue samples of control and PEXS affected individuals. However, we found a significantly decreased expression of *EPHX2* by 0.62 fold ( $p\text{-value}= 0.01$ ) in the lens capsule tissues from PEXS subjects compared to that of control but not in case of *PTK2B* ( $p=0.26$ ). However, because of unavailability of PEXG tissue samples we were unable to check the expression of *PTK2B* and *EPHX2* genes.

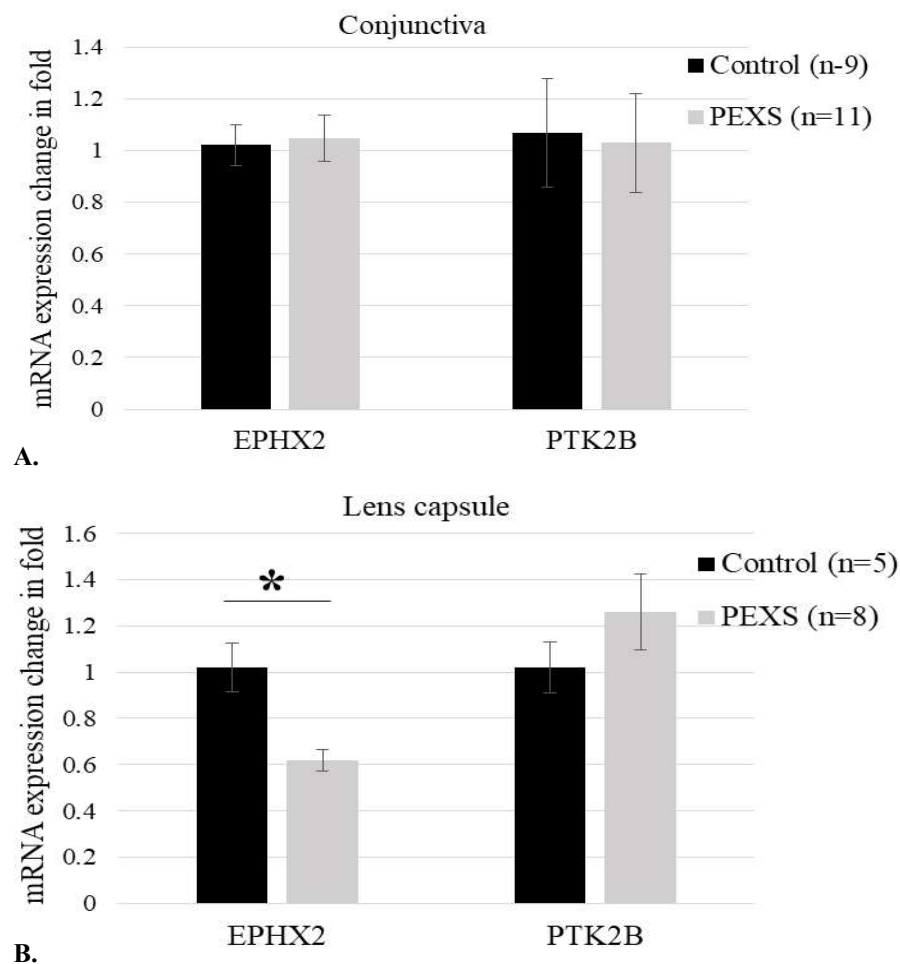


**Figure 4.5.** qRT-PCR assays were done to check the expression of *EPHX2* and *PTK2B* in anterior eye tissues (Conjunctiva and lens capsule) of PEX and control subjects. In conjunctiva, there is no difference ( $p=0.89$ ) in the gene expression of *EPHX2* between control ( $1.02\pm0.07$ ) and PEXS ( $1.04\pm0.16$ ) subjects. Also, there is no difference ( $p=0.83$ ) in the mRNA expression of *PTK2B* between control ( $1.06\pm0.12$ ) and PEXS ( $1.02\pm0.14$ ) individuals. However, in lens capsule mRNA expression of *EPHX2* was found to be significantly ( $p=0.01$ ) downregulated in PEXS subjects ( $0.62\pm0.04$ ) compared to that control ( $1.02\pm0.1$ ) while there is no difference in the expression of *PTK2B* ( $p=0.26$ ) in PEXS ( $1.26\pm0.16$ ) versus control individuals ( $1.02\pm0.11$ ). Sample size is denoted by “n” and expression change in fold is represented as mean $\pm$ SEM. Student’s t-test was used to calculate statistical significance between groups, \* $P<0.05$ .

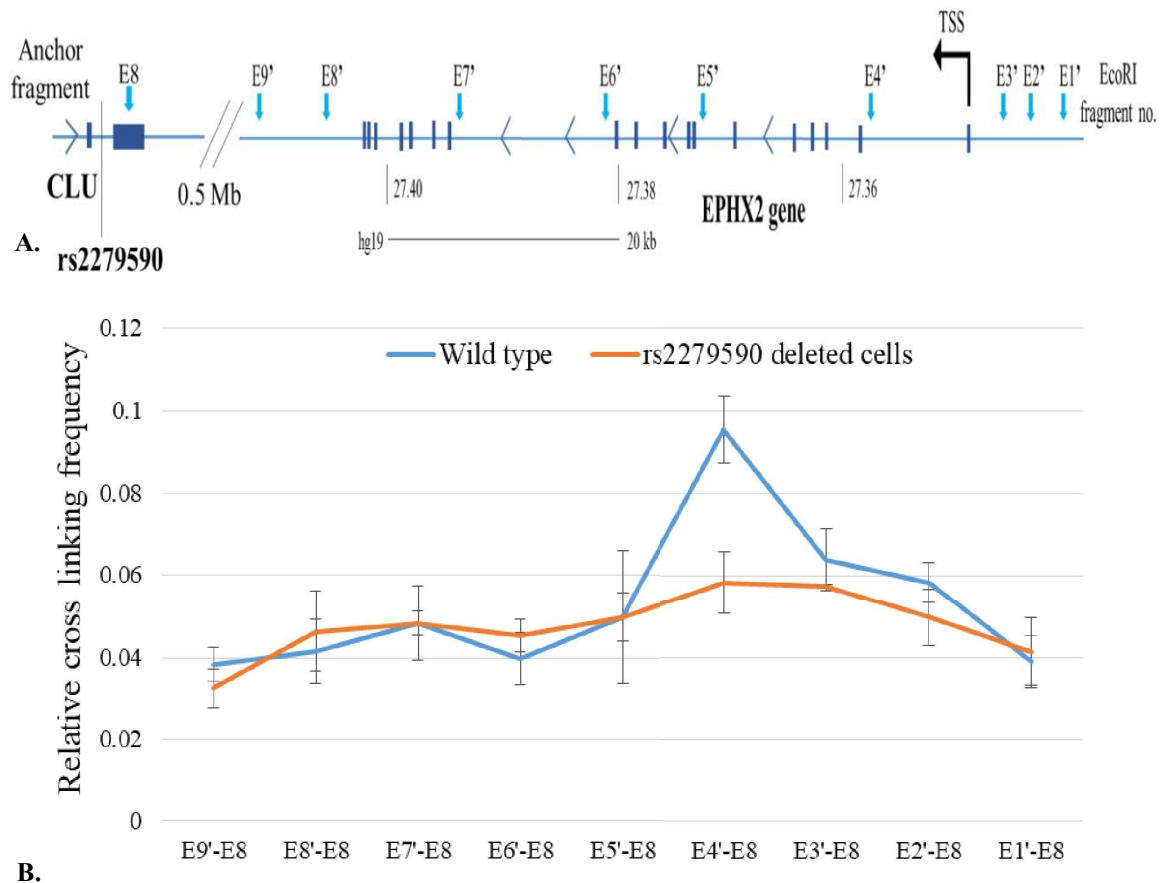


**Figure 4.4.** Chromosome conformation capture assays for *EPHX2* promoter and rs2279590 enhancer interaction (A) Schematic location of EcoRI restriction sites E1'-E9' across *EPHX2* gene in relation to E8 representing rs2279590 at *CLU* locus. E3' restriction site is located near to that of the transcription start site (TSS) of *EPHX2* gene. (B) E8 restriction fragment is used as anchor fragment and used with other fragments within *EPHX2* gene. Relative cross linking frequency of ligated product between E4' and E8 restriction fragment was shown to be higher than that of nearby restriction fragments in non-deleted control wild type cells. However, in cells with rs2279590 deletion the ligation frequency between E4' and E8 is not different as compared to that of other fragments indicating a chromatin-chromatin interaction between E8 and E4' restriction fragments is mediated by rs2279590 element. Also, in comparison to control cells (0.095±0.008) the relative crosslinking frequency between E4' and E8 is lower in deleted cells (0.058±0.007). Data was normalized to frequency from two distal segments from beta-tubulin and an internal loading control from GAPDH without restriction sites. Experiments were performed three times and values are represented as mean±SEM.

#### 4.3.3 Dysregulated expression of *EPHX2* in PEX affected tissues.

Previous studies have shown that dysregulation of PTK2B and *EPHX2* are markers of disease progression. Accumulation of PTK2B was reported in the early event of AD pathogenesis with progressive Tau pathology. Similarly, upregulation in *EPHX2* that metabolizes neuroprotective epoxyeicosatrienoic acids are the cause of increased OGD-induced (oxygen-glucose deprived) neuronal cell death. To find out the status of these two genes we checked the mRNA expression

deletion the ligation frequency between E4' and E8 is not different as compared to that of other fragments indicating a chromatin-chromatin interaction between E8 and E4' restriction fragments is mediated by rs2279590 element. Also, in comparison to control cells ( $0.095\pm 0.008$ ) the relative crosslinking frequency between E4' and E8 is lower in deleted cells ( $0.058\pm 0.007$ ). This further, confirms that a chromatin-chromatin interaction between genomic loci containing rs2279590 and the proximal promoter region of *EPHX2* gene plays a role in regulating *EPHX2* expression.

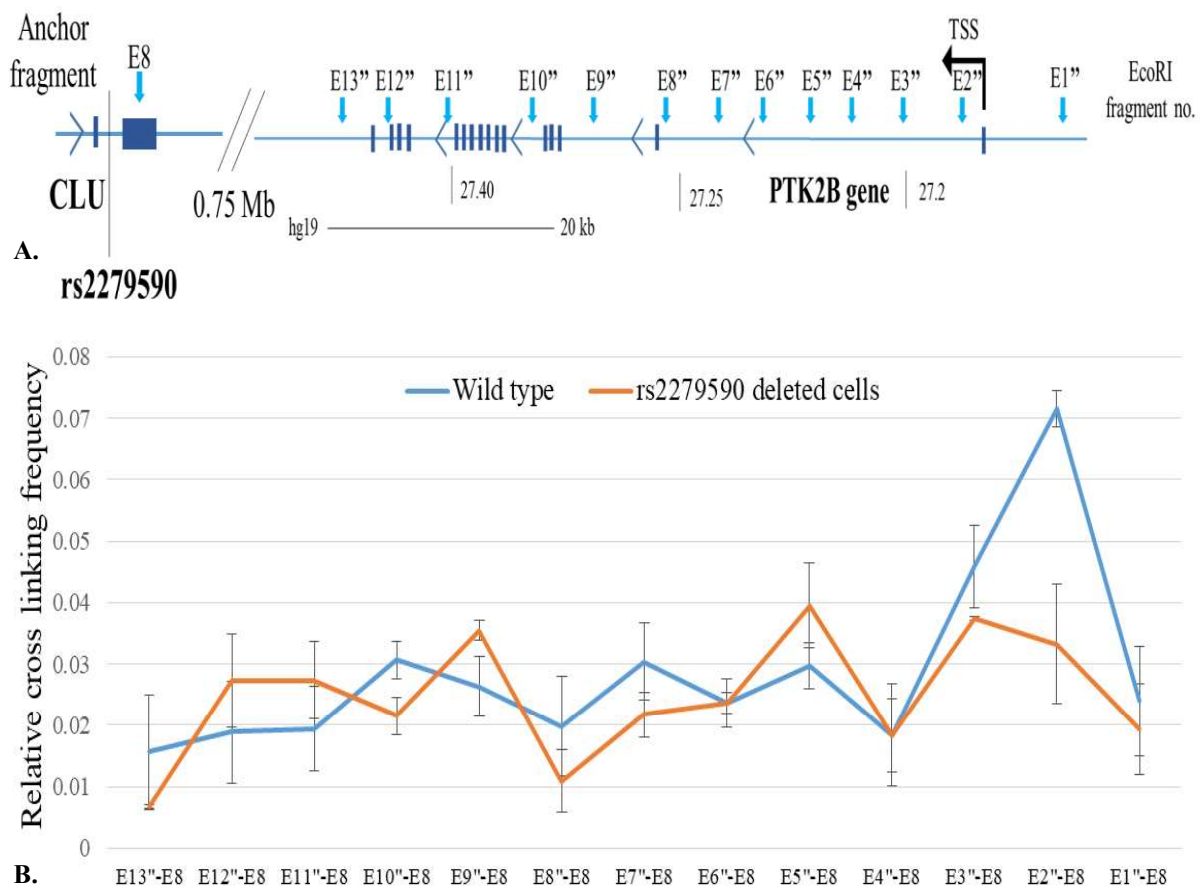


**Figure 4.3.** Chromosome conformation capture assays for *PTK2B* promoter and rs2279590 enhancer interaction (A) Schematic location of EcoRI restriction sites E1"-E13" across *PTK2B* gene in relation to E8 representing rs2279590 at *CLU* locus. (B) E2" restriction site is located near to that of the transcription start site (TSS) of *PTK2B* gene. E8 restriction fragment is used as anchor fragment and used with other fragments within *PTK2B* gene. Relative cross linking frequency of ligated product between E2" and E8 restriction fragment was shown to be higher than that of nearby restriction fragments in non-deleted control wild type cells. However, in cells with rs2279590 deletion the ligation frequency between E2" and E8 was not significantly different as compared to that of other fragments indicating a chromatin-chromatin interaction between E8 and E2" restriction fragments is mediated by rs2279590 element. Also, in comparison to control cells ( $0.071\pm 0.003$ ) the relative crosslinking frequency between E2" and E8 is lower in deleted cells ( $0.033\pm 0.009$ ). Data was normalized to frequency from two distal segments from beta-tubulin and an internal loading control from GAPDH without restriction sites. Experiments were performed three times and values are represented as mean $\pm$ SEM

### 4.3.2 rs2279590 modulates *PTK2B* and *EPHX2* gene expression through promoter-enhancer interaction.

In order to find out the functional mechanism through which rs2279590 element regulates *PTK2B* and *EPHX2*, we have employed chromosome conformation capture (3C) assays. As depicted in **Figure 4.3A**, thirteen EcoRI sites were selected around *PTK2B* gene tagged as E1'' through E13'' for 3C assays. Primers for (E1''-E13'') tagging each of these restriction sites were paired with E8 primer (as mentioned previously in the result section 3.3.3 of chapter 3) representing rs2279590 restriction fragment within the *CLU* gene. Amount of cross-linked and ligated product were quantified through qRT-PCR and presented as relative crosslinking frequency in the Y-axis (**Figure 4.3B**). As shown in the **Figure 4.3B**, relative crosslinking frequency between E2'' restriction fragment representing *PTK2B* promoter and E8 restriction fragment was higher compared to that of other combinations in wild type control HEK293 cells. Further, in cells with genomic deletion for rs2279590, the ligation frequency between E2'' and E8 was not significantly different as compared to that of other fragments which also indicates a chromatin-chromatin interaction between E8 and E2'' restriction fragments is mediated by rs2279590 element. Also, in comparison to control cells ( $0.071 \pm 0.003$ ) the relative crosslinking frequency between E2'' and E8 is lower in deleted cells ( $0.033 \pm 0.009$ ). This confirms a chromatin-chromatin interaction between genomic loci containing rs2279590 and the promoter regions of *PTK2B* gene.

Similarly, we have selected (**Figure 4.4A**) nine EcoRI sites around *EPHX2* gene for 3C assays. Primers tagging each restriction fragment were tagged as E1' through E9'. Each of these tagged primers were paired with E8 primer representing rs2279590 restriction fragment within *CLU* gene. As depicted in **Figure 4.4B** the relative crosslinking frequency between E4' restriction fragment tagging *EPHX2* proximal promoter region combined with E8 was higher than that of nearby ligated products in control wild type cells. Further, in cells with rs2279590

mRNA expression of *PTK2B* was found to be significantly downregulated by 0.58 fold with a p-value of 0.006 while, *EPHX2* is found to be 0.34 fold downregulated with a p-value of 0.008 in comparison to wild type cells. However, expression of other genes were not found to be significantly different from that of control cells. This indicates that the genomic region containing rs2279590 has an extended regulatory role with a widespread enhancer effect on *PTK2B* and *EPHX2*. mRNA expression of *CHRNA2* gene was null in control HEK293 cells, therefore omitted for further analysis.

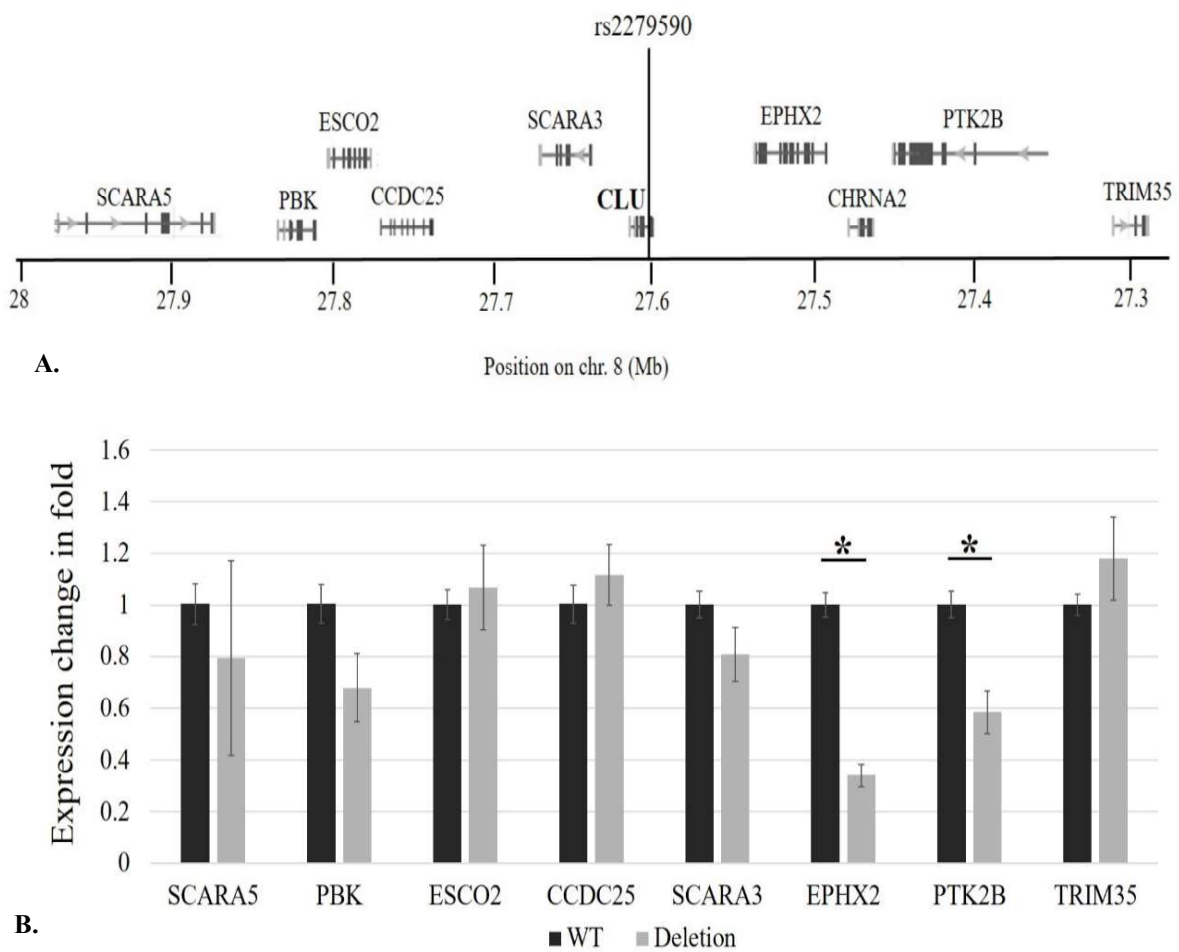


**Figure 4.2.** qRT-PCR assays were done for genes located in the *PTK2B-CLU* locus in rs2279590 region deleted cells than that of control non-deleted cells. Expression of *PTK2B* and *EPHX2* is significantly downregulated with a P value of 0.006 and 0.008 respectively in deleted cells ( $0.58 \pm 0.08$  and  $0.34 \pm 0.04$ , respectively) compared to control non-deleted cells ( $1 \pm 0.05$  and  $1 \pm 0.04$ , respectively). Experiments were performed at least three times and values are represented as mean  $\pm$  SEM. Student's t-test was used to calculate statistical significance between groups, \*P<0.05.

46	Control E1'	3C Control	F: GGTTCCCAAGCTCTTGTACTG R: CAAATGCCTGGGCAAATAG	54
47	Control E2'	3C Control	F: GGAAGCTGGAAAATGACAAATAAG R: CATTCCATCAGCAAATATGTATCA	55
48	Control E3'	3C Control	F: AAAAGGGGGCTTTATGAAATCTA R: CCATTCCGTTCAAAGATTGTGTA	58
49	Control E4'	3C Control	F: AGTTGAGCAAGGCCACAGATA R: CATCCAGTCTCTGTTTGCTGTTA	54
50	Control E5'	3C Control	F: TTCTGCACGTGACCATGAATA F: TCACCTGGTACCTCCAAGAATA	56
51	Control E6'	3C Control	F: GGCTGAAAGGCTGGTGATTA R: TGGAAACGGTCCCTCCTAAG	55
52	Control E7'	3C Control	F: GAACCAGGCTACCCCCACTA R: TTCCAGTTCTTGGGAGCAGTA	57
53	Control E8'	3C Control	F: GGTGGTGGGCACCTGTAAT R: CAGAAAATGGAAACCAGCTATG	54
54	Control E9'	3C Control	F: GATTCTTCTTGGCCTTTCTGTA R: GGTGGTGGGCACCTGTAAT	55
55	Tub E1	3C qPCR	F: CCCTGTCAATGTACCGCTCTA	60
56	Tub E2	3C qPCR	F: CCCC GGCTAATTGTTTTGTA	60
57	Control Tub E1	3C Control	F: GCTCTCTTTTGTGCGGTA R: CAGCAGTCTGAGCGCAGTAG	56
58	Control Tub E2	3C Control	F: CCATACTCCAGAGCTGCTACA R: TCAAGGAGGGGATGAACAGTA	56
59	GAPDH 3C	3C Control	F: ACAGTCCATGCCATCACTGCC R: GCCTGCTTCACCACCTTCTTG	54

## 4.3 Results

### 4.3.1 Regulatory effect of rs2279590 region on *PTK2B* and *EPHX2* expression.

A stretch of around 558 kb genomic region containing nine genes were selected to check the broad regulatory effect of rs2279590 loci. For this, expression of these genes clustered around 5' and 3' ends of *CLU* was analyzed in HEK293<sup>115-/-</sup> knockout cells lacking the regulatory locus (**Figure 4.2A**). We found a significant downregulation in the expression of two genes, *PTK2B* and *EPHX2* in HEK293<sup>115-/-</sup> cells as compared to control HEK293 cells (**Figure 4.2B**).

23	E13'' <i>PTK2B</i>	3C qPCR	F: CCCGGCATGCACATTTATAG	60
24	Control E1''	3C Control	F: AAAGTGGCCCAATGACAATAC R: TCTCTGGAATCGGGCTCTTA	58
25	Control E2''	3C Control	F: TGTCTAGAAGTTCTTCTTGTTCCCTAAC R: CTTGGCTCTGAACCCCTAAC	58
26	Control E3''	3C Control	F: AGAGCATCGCCATGGATAGT R: GGGATGAGGAGGCAGGTAAT	54
27	Control E4''	3C Control	F: GGTGAGTCCCCTGGGTAAG R: CTCCCGCCACTCACACATAC	54
28	Control E5''	3C Control	F: CCCATGGTCTCTTCAATAAATATG R: TTGCTCCAACAAGCATTTAGAA	58
29	Control E6''	3C Control	F: GCAGAGGAGCTGTTTTCCACTA R: CAAGAAGGGCAGGGGTAGAC	58
30	Control E7''	3C Control	F: CAGAGAAACAGAACAGACAAGATGTA R: AAGTGGATCGACCTCCCTAAC	52
31	Control E8''	3C Control	F: TTGATCCTCTGTTAAAGCCATAATC R: TCTCCAGTCTCTGAAAGTTGTTA	58
32	Control E9''	3C Control	F: CTGATCTTGCTGCCCTACT R: AACCATCAGCAACTGTCTATGA	54
33	Control E10''	3C Control	F: CAACGACAGGGACCAAAGTA R: GCCAAACCCATAGAACATACAA	54
34	Control E11''	3C Control	F: TTGCCACGAACACTTGATCTAT R: GAAACCGAACACAGCCTAAATTAT	55
35	Control E12''	3C Control	F: TGCTTTGCTCCTGCTTATGA R: TTTTGATTTTCAGTGATTGTTTCTTA	54
36	Control E13''	3C Control	F: TCGATCTTGGCCTTGTACATA R: AAAAATAGGCAATCAAGCAACATA	55
37	E1' <i>EPHX2</i>	3C qPCR	F: GCAAGTAGCCACCACCACTAT	60
38	E2' <i>EPHX2</i>	3C qPCR	F: TCTGTAGGTATGTCGTTCTCTACA	60
39	E3' <i>EPHX2</i>	3C qPCR	F: CCTGCAAGAGGGTGTCTGATA	60
40	E4' <i>EPHX2</i>	3C qPCR	F: GCAGAAAACAAATTAGGAAAGGTTAG	60
41	E5' <i>EPHX2</i>	3C qPCR	F: GAGTATGGGGCCTTGTAGA	60
42	E6' <i>EPHX2</i>	3C qPCR	F: CCCAGATGTGGCTGATACA	60
43	E7' <i>EPHX2</i>	3C qPCR	F: AGGAAGGTTCTGGAGCCTATT	60
44	E8' <i>EPHX2</i>	3C qPCR	F: AGACCACGTTTTGTTTACCTACTC	60
45	E9' <i>EPHX2</i>	3C qPCR	F: CATTCTTCTCTCCAGGTATAG	60

**Table 4.2.** List of oligos used in the study.

Sl. No.	ID	Purpose	Sequence (5'→3')	T <sub>m</sub> <sup>0</sup> C
1	CCDC25 (NM_018246.2)	qRT-PCR	F: CACCAGCAGCAGCGTTAATTC R: GAGCCGAAGAGAGTTTGTCCA	60
2	CHRNA2 (NM_000742.3)	qRT-PCR	F: ACCACCAACGTCTGGCTAAA R: CTCCCCATCTGCATTGTTGT	60
3	<i>EPHX2</i> (NM_001979.5)	qRT-PCR	F: ACTCCCTTCATACCAGCAAATC R: GACTCAGGTTCTGTTCCAGTTC	60
4	ESCO2 (NM_001017420.2)	qRT-PCR	F: TCTCCTAAGTCCACTGTCTATCC R: GAAGTTGACAGATCCCACAGAA	60
5	PBK (NM_018492.3)	qRT-PCR	F: TTGAAAGCCAGGAGGGTTCG R: CTCAGTCCAGAGTCTCACCGC	60
6	<i>PTK2B</i> (NM_173174.2)	qRT-PCR	F: GGGAGGTCTATGAAGGTGTCTA R: CTTCTCCTTGTTGTCCAGAGTG	60
7	SCARA3 (NM_016240.2)	qRT-PCR	F: CATCTCCTTGACCCAGTCTATTT R: TGGCAGAAAGAGCAGTTGT	60
8	SCARA5 (NM_173833.5)	qRT-PCR	F: CGATTCGGGCAAGGCACT R: CGGCATGTCCACAGTTTGTC	60
9	TRIM35 (NM_171982.4)	qRT-PCR	F: AACACAAGAGCCGAAAACGC R: GCCCAGGTACTIONTGCAGACAT	60
10	GAPDH (NM_002046.5)	qRT-PCR	F: GGTGTGAACCATGAGAAGTATGA R: GAGTCCTTCCACGATACCAAAG	60
11	E1 <sup>''</sup> <i>PTK2B</i>	3C qPCR	F: TGGCATGCAAACCTTGTTAGTG	60
12	E2 <sup>''</sup> <i>PTK2B</i>	3C qPCR	F: TGCAGCAATCTGCTTTCCT	60
13	E3 <sup>''</sup> <i>PTK2B</i>	3C qPCR	F: CTTGTACCTGAGTTGCTTGTA	60
14	E4 <sup>''</sup> <i>PTK2B</i>	3C qPCR	F: AGGCAAGAGCCCAATATAAAC	60
15	E5 <sup>''</sup> <i>PTK2B</i>	3C qPCR	F: CTCCCCATCACCCCATTACT	60
16	E6 <sup>''</sup> <i>PTK2B</i>	3C qPCR	F: GCCCAGGAAGTTACAGAAAAGTA	60
17	E7 <sup>''</sup> <i>PTK2B</i>	3C qPCR	F: GCTCAAGACCCAGGAAGAGTTA	60
18	E8 <sup>''</sup> <i>PTK2B</i>	3C qPCR	F: TTTAATAACCACAAGCTCCTTCATA	60
19	E9 <sup>''</sup> <i>PTK2B</i>	3C qPCR	F: AGCATGTCAAATCTCAGCACTTA	60
20	E10 <sup>''</sup> <i>PTK2B</i>	3C qPCR	F: CACAGCCTCCCCACTATC	60
21	E11 <sup>''</sup> <i>PTK2B</i>	3C qPCR	F: TTTGGAAGATGTAGGCAAGTATG	60
22	E12 <sup>''</sup> <i>PTK2B</i>	3C qPCR	F: GGTGGGTTCTATGTGGCTTAT	60

#### **4.2.2 Cell culture:**

All *in vivo* molecular assays were done using HEK293 cells as a model system. Protocol followed for culturing and harvesting cells are explained in the materials and methods section 3.2.2 of chapter 3 (Page no. 60).

#### **4.2.3 CRISPR/Cas9 construct preparation and genome editing:**

Deletion of genomic region containing rs2279590 in HEK293 cells were done using CRISPR/Cas9 genome editing. Detailed protocol for construct preparation and genomic deletion is outlined in the materials and methods section 3.2.4 of chapter 3 (Page no. 62).

#### **4.2.4 Chromosome conformation capture (3C) assay:**

3C assays were followed as described in the section 3.2.5 of chapter 3 (Page no. 63). For quantifying the chromatin interactions between rs2279590 loci and promoter region of both *EPHX2* and *PTK2B*, oligos were designed and presented in the **Table 4.2**. In total thirteen EcoR1 sites were selected around *PTK2B* gene for 3C and nine EcoR1 sites for *EPHX2*. Control primers for normalizing primer efficiency and tubulin ligation control for normalizing ligation frequency were also designed and are presented in **Table 4.2**.

#### **4.2.5 RNA extraction, cDNA synthesis and Quantitative real-time PCR (qRT-PCR):**

Protocol used for RNA extraction, cDNA library preparation and qRT-PCR is elaborated in the section 2.2.5-2.2.7 of chapter 2 (Page no. 38-39). Designed qRT primers for both *PTK2B* and *EPHX2* targeted genes are mentioned in the **Table 4.2**.

#### **4.2.7 Statistical analysis:**

All experiments were repeated at least three times. Descriptive data were presented as mean  $\pm$  SEM. Group wise results for statistical significance was compared by Student's t-test and  $p < 0.05$  was considered as statistically significant.

		nicotinic alpha 2 subunit	lobe epilepsy type 4	receptors, a neuronal receptor
3	<i>EPHX2</i> (NM_001979.5)	epoxide hydrolase 2	Familial hypercholesterolea	Binds to specific epoxides and converts them to the corresponding dihydrodiols
4	<i>ESCO2</i> (NM_001017420.2)	establishment of sister chromatid cohesion N-acetyltransferase 2	Roberts syndrome	Encodes a protein that may have acetyltransferase activity and may be required for the establishment of sister chromatid cohesion during the S phase of mitosis
5	<i>PBK</i> (NM_018492.3)	PDZ binding kinase	Cancer	Encodes a MAPKK with role in spermatogenesis
6	<i>PTK2B</i> (NM_173174.2)	protein tyrosine kinase 2 beta	Cancer	Encodes a cytoplasmic protein tyrosine kinase which involves in calcium flux & activation map kinase signaling pathway
7	<i>SCARA3</i> (NM_016240.2)	scavenger receptor class A member 3	Cancer	Encodes a macrophage scavenger receptor-like protein which deplete ROS, protects cells from ROS, it is induced by oxidative stress
8	<i>SCARA5</i> (NM_173833.5)	scavenger receptor class A member 5	Retinopathy	Binding and Uptake of Ligands by Scavenger Receptors and Vesicle-mediated transport
9	<i>TRIM35</i> (NM_171982.4)	tripartite motif containing 35	Carcinoma	Encodes a member of tripartite motif family, function unknown

## 4.2 Materials and methods

### 4.2.1 Study subject recruitment:

Anterior eye tissue samples such as lens capsule and conjunctiva required for study purpose were collected from subjects (both control and case) undergoing cataract surgery. Detailed information about study subjects recruitment and inclusion or exclusion criteria followed for sample collection is in the materials and methods section 2.2.1 of chapter 2 (Page no. 33).

contains risk variants for individuals with Alzheimer's.<sup>202</sup> Nelson *et al.* have also shown higher frequency of a missense variant, rs751141 (G860A) with a change in amino acid from arginine to glutamic acid at position 287 in cognitive impairment cases than that of control.<sup>203</sup>

#### 4.1.2 Aberrant expression of genes surrounding *CLU* gene is related with various pathological disorders.

Studies have shown that PTK2B, coded by the gene adjacent to *CLU* localizes with hyperphosphorylated tau and acts as an early marker in AD pathology by modulating tau toxicity.<sup>189</sup> Dysregulation of *EPHX2* was also seen in brain tissues of individuals affected by cognitive impairment.<sup>203</sup> Similarly, studies have shown association of other nearby genes (5' to that of *CLU* gene) such as *SCARA3* (Scavenger Receptor Class A Member 3) with Parkinson's, *SCARA5* (Scavenger Receptor Class A Member 5) with glaucoma and *CCDC25* (Coiled-Coil Domain Containing 25) with AD progression. A list of targeted genes surrounding rs2279590 and their location is presented in the **Table 4.1**.

In this chapter, we have addressed the following key objectives:

1. Does DNA element containing *CLU* variant, rs2279590 have broad enhancer effect on any nearby genes?
2. Does rs2279590 modulates distance genes through chromatin interaction?
3. What is the status of candidate genes in anterior eye tissues of PEX affected individuals?

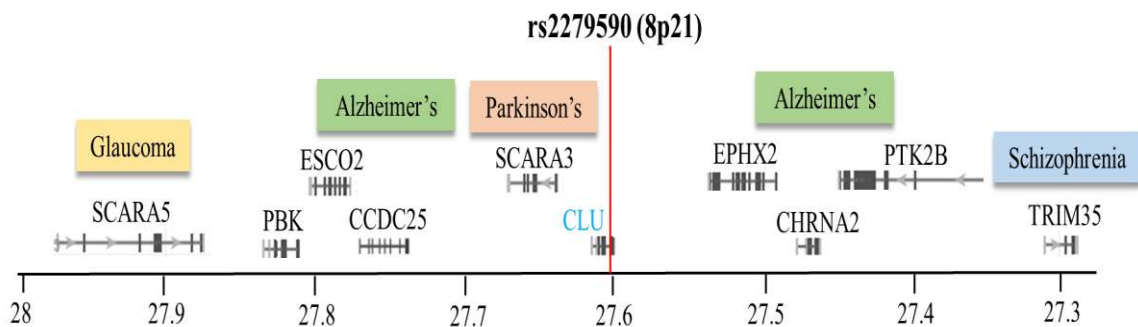
**Table 4.1** List of crucial genes and their functions surrounding rs2279590.

SI No.	GENE	Name	Associated diseases	Function
1	CCDC25 (NM_018246.2)	coiled-coil domain containing 25	NA	NA
2	CHRNA2 (NM_000742.3)	cholinergic receptor	Autosomal dominant nocturnal frontal	Encodes alpha subunit for nicotinic acetylcholine

#### 4.0 Wide-spread enhancer effect of rs2279590 on regulating *PTK2B* and *EPHX2* gene expression.

##### 4.1 Introduction

Evidence from earlier reports indicate that *CLU* is located within a high risk loci (8p21) for various pathophysiological disorders. Both at genomic and proteomic level, genes surrounding *CLU* has been implicated in various neurological disorders like glaucoma, Alzheimer's and Parkinson's. Our preceding results have shown that element containing rs2279590 is a regulatory region and it is also residing in the same high risk loci. In this chapter, we hypothesized that this genomic region may have regulatory effect on the neighbouring genes around *CLU*.



Location of crucial genes relative to rs2279590 on chr. 8 (Mb)

**Figure 4.1.** Locus containing rs2279590 also regulates *PTK2B* and *EPHX2* gene expression. A stretched genomic region of ~700 kb around clusterin gene in chromosome 8 is shown. Position of crucial genes relative to that of clusterin are depicted.

##### 4.1.1 Genomic locus encompassing *CLU* gene harbors many risk variants for ageing disorders

**Figure 4.1** depicts the genes surrounding *CLU* loci with their actual chromosomal distance. Genetic variants within these genes has been associated with various neurological disorders. rs28834970, a common polymorphism within *PTK2B* (protein tyrosine kinase 2 beta) situated in the 3' region of *CLU* gene has been associated as a risk factor in the pathogenesis of Alzheimer's.<sup>191,200,201</sup> Similarly, genetic variants in the gene *EPHX2* (Epoxide hydrolase 2) also

# **Chapter 4**

**Wide-spread enhancer effect of  
rs2279590 on regulating *PTK2B* and  
*EPHX2* gene expression**

researchers have shown aberrant deposition of Fibulin-5.<sup>228</sup> Additionally, increase in truncated form of F5 was found to be increased with age which may also aggravate the disease condition in ageing disorders like PEX.<sup>229</sup>

### **5.5 Conclusion:**

Finding of genetic association between common genetic variants in F5 with PEX suggests, F5 as a contributing factor in the pathogenesis of PEX. Further, decreased expression of F5 in lens capsule of PEX affected tissues implicates an impaired maintenance of extracellular matrix protein might be a contributing factor in PEX. However, the functional role of these genetic variants, if any and the adverse effect of decreased F5 expression during the onset of PEX remains to be studied.

aneurysm. During discovery stage we found three genetic polymorphisms in the F5 gene (rs7149187, rs2430347 and rs929608) in our case-control study. Earlier these polymorphisms have been associated with various disorders. Studies have shown association that SNP, rs2430347 is a risk factor for ARMD which leads to irreversible vision loss similar to that of PEXG.<sup>231</sup> rs2430347 is a coding variation and cause a synonymous change in exon 9 coding isoleucine 315 from ATT to ATC. Similarly, rs929608 which resides in the 10<sup>th</sup> intron of F5 gene also has been associated with ARMD.<sup>216</sup> Likewise, it also has been picked as a risk factor for ARMD in a case-control study conducted in Indian population with “A” as the risk allele.<sup>232</sup> Here, we have found a significant association of the common variant, rs929608 (A>G) with allele “A” as a risk factor for PEX.

#### **5.4.2 Decreased F5 expression may lead to abnormal maintenance of ECM**

F5 or DANCE is a scaffold structure in the ECM that not only supports microfibrillar structure but also modulates proper deposition of elastin in the ECM. On examination of posterior eye tissues (lamina cribrosa and peripappillary sclera) from PEX affected eyes, abnormal deposition of LoxL1 and elastin were seen in distinct dense punctate pattern.<sup>66</sup> Studies have shown that decreased expression or knockdown of F5 leads to inactivation of LoxL1 and irregular deposition of both LoxL1 and elastin in the ECM.<sup>214</sup> We have found a significantly decreased expression of F5 in PEX affected lens capsule tissues which implicates a decreased maintenance of ECM proteins in the absence of F5. Dysregulated expression of F5 also has been seen in other ECM disorders such as AMRD, cutis laxa and pelvic organ prolapse. Diminished level of F5 in the ECM results in impaired elastic fiber development by a reduced interaction with other extracellular proteins like elastin and fibrillin-1 and is the sole factor in the progression of such diseases. Further, in PEX affected tissues it has been shown that LoxL1 does not co-localize with F5 in the site of PEX material formation which leads to deposition of in-active form of LoxL1. In an *in vivo* 3D culture of tenon fibroblasts from PEX donors

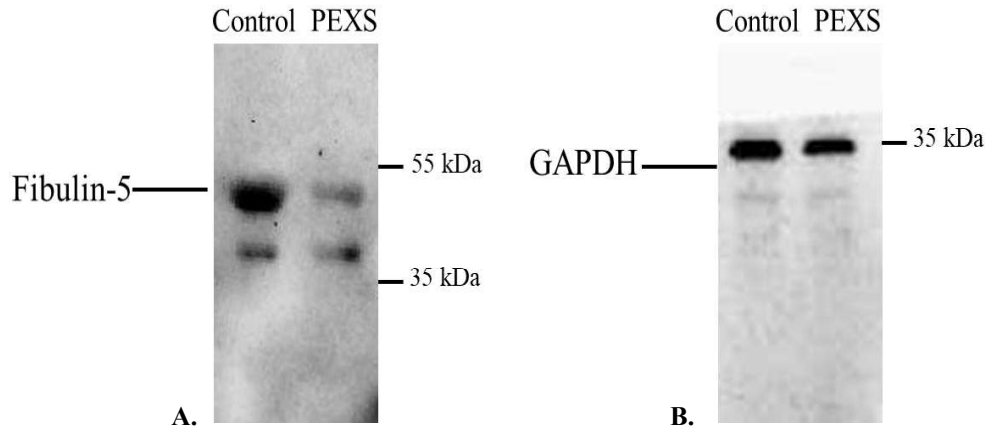


**Figure 5.4.** Differential expression of Fibulin-5 in the lens capsule of PEXS subjects. Western blot showing differential expression of F5 in PEXS subjects compared to that of control (A). GAPDH is used as endogenous control (B).

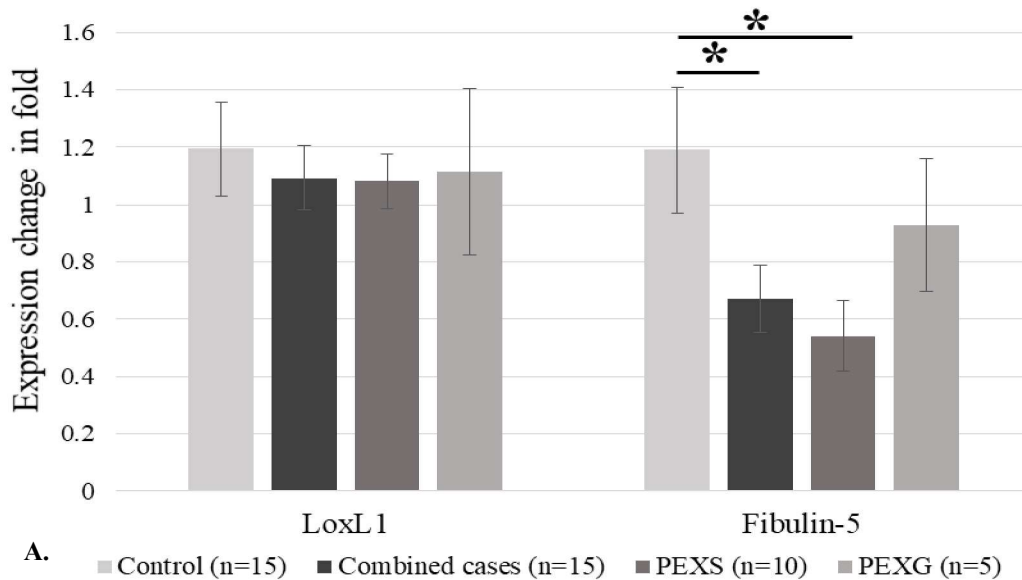
## 5.4 Discussion

Fibulin-5 is an extracellular secreted protein essential for elastogenesis by playing a prominent role in enzymatic activation of LoxL1, polymerization and deposition of tropoelastin monomers into elastin fibrils. Dysregulation in the expression of F5 has been reported in disorders involving impaired maintenance of extracellular matrix. Also, common genomic variations within F5 gene also has been associated with such ECM disorders. Since, PEX involves abnormal deposition and impaired maintenance of ECM proteins there is a likely involvement of F5 in PEX pathogenesis. Additionally, studies have shown that LoxL1 which is regulated by F5 is also a risk factor for PEX pathogenesis. Since F5 modulates LoxL1 function, it further supports our hypothesis of F5 being a candidate gene for development of PEX.

### 5.4.1 Polymorphisms in F5 gene can be a risk factor for PEX pathogenesis

Previous studies have reported many genetic polymorphisms within F5 as risk factor for diseases such as age related macular degeneration (ARMD),<sup>218,225</sup> cutis laxa (CL),<sup>220,225,230</sup> pelvic organ prolapse (POP), Charcot-Marie-Tooth neuropathies<sup>231</sup> and abdominal aortic

in **Figure 5.4** we have found a dense protein band at ~50 kDa corresponding to F5 protein as reported previously.<sup>214</sup> However, we also found an unknown band at around 35 kDa. Compared to control there is a significantly decreased expression of F5 in the lens capsule of PEXS subjects.



**B.**

Group	n=	Age (in years)		Sex		Manifestation in cases	
		Mean±SD	Range	Male	Female	Unilateral	Bilateral
Control	15	63.2±9.8	40-86	9	6	7	8
PEX (Combined)	15	66.8±10.7	40-89	11	4	6	9
PEXS	10	64.5±8.3	40-89	8	2	5	5
PEXG	5	68.4±5.8	40-88	3	2	1	4

**Figure 5.3.** qRT-PCR to check mRNA expression of F5 in lens capsule of cases and controls. mRNA expression of LoxL1 and F5 was checked in the lens capsule of control and PEX (including both PEXS and PEXG) affected subjects through qRT-PCR. (A) F5 downregulation in PEXS affected subjects implicates a dysregulated maintenance of extracellular matrix. There was no difference in the expression of LoxL1 between combined cases (1.09±0.11, p=0.61), PEXS (1.08±0.09, p=0.56), PEXG (1.11±0.28, p=0.81) and control subjects (1.19±0.16). However, F5 expression was found to be significantly downregulated in both PEX (0.67±0.11) and PEXS (0.54±0.12) compared to that of control (1.19±0.21) with a p-value of 0.04 and 0.01, respectively but not in PEXG subjects (0.92±0.23, p=0.42). (B) Demographics of the study subjects used for qRT-PCR was shown. Sample size is denoted by “n” and expression change in fold is represented as mean±SEM. Student’s t-test was used to calculate statistical significance between groups, \*P<0.05.

**Table 5.5.** Haplotype association of the F5 variants with pseudoexfoliation. Frequency of risk haplotype ACC (rs929608-rs2430347-rs7149187) in control (0.2) is lower in comparison to PEX (0.29, p=0.005), PEXS (0.28, p=0.06) and PEXG (0.3, p=0.04) individuals. \*p-value after permutation correction where n=10,000.

Risk haplotype “ACC” (rs929608-rs2430347- rs7149187)	Freq.	$\chi^2$ value	p-value	p*-value
<b>Control</b>	0.20	-	-	-
<b>PEX (combined case)</b>	0.29	7.82	0.005	0.01
<b>PEXS</b>	0.28	5.49	0.02	0.06
<b>PEXG</b>	0.30	6.35	0.01	0.04

**Table 5.6.** Odds ratio (OR) and Confidence interval (CI) of F5 variants. OR of each allelic variant was calculated and presented. Individuals with protective allele at rs7149187 show higher risk ratio of 1.46 (1.19±1.83) for developing PEX, 1.39 (1.08±1.73) for PEXS and 1.63 (1.36±2.11) for PEXG. Similarly, individuals with protective allele at rs929608 show higher risk ratio of 1.86 (1.53±2.39) for developing PEX, 1.73 (1.48±2.13) for PEXS and 1.79 (1.45±1.98) for PEXG individuals.

Group	rs7149187		rs2430347		rs929608	
	Allele freq.	OR (CI)	Allele freq.	OR (CI)	Allele freq.	OR (CI)
<b>Control</b>	0.55	-	0.76	-	0.46	-
<b>PEX combined</b>	0.66	1.46 (1.19±1.83)	0.79	1.03 (0.89±1.23)	0.56	1.86 (1.53±2.39)
<b>PEXS</b>	0.65	1.39 (1.08±1.73)	0.77	1.01 (0.93±1.08)	0.56	1.73 (1.48±2.13)
<b>PEXG</b>	0.68	1.63 (1.36±2.11)	0.83	1.21 (1.13±1.42)	0.56	1.79 (1.45±1.98)

### 5.3.2 Downregulation of Fibulin-5 gene expression in PEXS affected tissues.

We have checked the mRNA expression of LoxL1 and F5 gene in the lens capsule of control and affected subjects through qRT-PCR. As shown in **Figure 5.3**, we did not find any significant difference between control, PEX (p=0.61), PEXS (p=0.56) and PEXG (p=0.81) individuals. However, there is a significant difference in the mRNA expression of F5 in patients. Compared to that of controls, in both combined PEX cases (p=0.01) and PEXS (p=0.01) there is a half fold downregulation of F5 expression but not in case of PEXG (p=0.42) individuals. Demographics of the study subjects used for qRT-PCR was shown in **Table 5.3B**.

We also have checked the expression level of F5 in the PEXS subjects versus control. As shown

**Table 5.4.** Distribution of genotypes of variants within F5 in PEX and control subjects. Frequency of risk genotype “CC” at rs7149187 in control (0.32) is lower in comparison to PEX (0.46, p=0.009), PEXS (0.46, p=0.02) and PEXG (0.42, p=0.03) individuals. Similarly, frequency of risk genotype “AA” at rs929608 is also found to be lower in control (0.23) than that of PEX (0.3, p=0.004), PEXS (0.29, p=0.01) and PEXG (0.33, p=0.007) individuals.\*Risk genotype. † p- value after permutation correction where n=10,000.

SNP	Genotype	Genotype count (freq.) in PEX combined	Genotype count (freq.) in control	Model	$\chi^2$ value	p-value	p <sup>†</sup> value
rs7149187	CC*	53 (0.46)	46 (0.32)	Dominant	7.23	0.009	0.02
	CT	43 (0.37)	66 (0.46)				
	TT	19 (0.16)	32 (0.22)				
rs2430347	CC	154 (0.61)	130 (0.59)	Dominant	1.34	0.67	0.89
	CT	95 (0.37)	75 (0.34)				
	TT	4 (0.01)	14 (0.06)				
rs929608	AA*	84 (0.3)	54 (0.23)	Dominant	7.89	0.004	0.009
	AG	139 (0.5)	112 (0.48)				
	GG	55 (0.2)	68 (0.29)				

SNP	Genotype	Genotype count (freq.) in PEXS	Genotype count (freq.) in control	Model	$\chi^2$ value	p-value	p <sup>†</sup> value
rs7149187	CC*	41 (0.46)	46 (0.32)	Dominant	6.39	0.02	0.04
	CT	30 (0.34)	66 (0.46)				
	TT	17 (0.19)	32 (0.22)				
rs2430347	CC	94 (0.59)	130 (0.59)	Dominant	0.76	0.81	0.97
	CT	63 (0.39)	75 (0.34)				
	TT	3 (0.02)	14 (0.06)				
rs929608	AA*	55 (0.29)	54 (0.23)	Dominant	7.21	0.01	0.03
	AG	96 (0.52)	112 (0.48)				
	GG	33 (0.18)	68 (0.29)				

SNP	Genotype	Genotype count (freq.) in PEXG	Genotype count (freq.) in control	Model	$\chi^2$ value	p-value	p <sup>†</sup> value
rs7149187	CC*	11 (0.42)	46 (0.32)	Dominant	5.66	0.03	0.04
	CT	13 (0.5)	66 (0.46)				
	TT	2 (0.07)	32 (0.22)				
rs2430347	CC	53 (0.64)	130 (0.59)	Dominant	1.47	0.35	0.45
	CT	29 (0.35)	75 (0.34)				
	TT	0	14 (0.06)				
rs929608	AA*	27 (0.33)	54 (0.23)	Dominant	6.39	0.007	0.01
	AG	34 (0.42)	112 (0.48)				
	GG	19 (0.24)	68 (0.29)				

PLINK. After correction both the SNPs, rs7149187 and rs929608 were remained significant with PEX ( $p=0.008$ ), PEXS ( $p=0.02$ ) and PEXG ( $p=0.03$ ). As evident from the linkage disequilibrium (LD) value there is a nominal linkage between the markers rs2430347-rs7149187 ( $D'=0.51$ , LOD score=3.35,  $r\text{-squared}=0.09$ ) and rs2430347-rs929608 ( $D'=0.28$ , LOD score=1.84,  $r\text{-squared}=0.02$ ) but there is no linkage between rs7149187 and rs929608.

Distribution of genotypes for F5 variants for both cases and control subjects were shown in **Table 5.4**. Frequency of risk genotype “CC” at rs7149187 was found to be significantly higher in PEX (0.46,  $p=0.009$ ), PEXS (0.46,  $p=0.02$ ) and PEXG (0.42,  $p=0.03$ ) subjects than that of control (0.32). Similarly, “AA” genotype at rs929608 was also found to be the risk genotype with lower frequency in control subjects (0.23) than that of PEX (0.3,  $p=0.004$ ), PEXS (0.29,  $p=0.01$ ) and PEXG (0.33,  $p=0.007$ ) affected individuals. Permutation analysis with a sample size of 10,000 also resulted in a significant association for cases (**Table 5.4**). Haplotype analysis showed “ACC” (rs929608- rs2430347- rs7149187) as the risk haplotype with higher frequency in PEX (0.29) compared to that of control (0.20) and is significantly associated with PEX with a  $p$ -value of 0.005 and also with PEXS ( $p=0.02$ ) and PEXG ( $p=0.01$ ) (**Table 5.5**). As shown in **Table 5.6** risk analysis showed that risk allele “C” at rs7149187 confers a risk ratio of 1.46 ( $1.19\pm 1.83$ ) for developing PEX, 1.39 ( $1.08\pm 1.73$ ) for PEXS and 1.63 ( $1.36\pm 2.11$ ) for PEXG. Similarly, risk allele “A” at rs929608 confers a risk ratio of 1.86 ( $1.53\pm 2.39$ ) for PEX, 1.73 ( $1.48\pm 2.13$ ) for PEXS and 1.79 ( $1.45\pm 1.98$ ) for PEXG individuals. The current study has 96% power at  $\alpha = 0.05$  level significance with risk allele frequency as well as marker allele frequency set to 0.56, with prevalence 3.8%<sup>179</sup> while linkage disequilibrium or  $D'$  was set to 1.

permutation correction by taking a sample size of 10,000, the association remained significant for PEX

**Table 5.3.** Distribution of F5 variants in PEX and control subjects. Frequency of risk allele “C” at rs7149187 in control (0.55) is significantly lower in comparison to PEX (0.66, p=0.01), PEXS (0.65, p=0.03) and PEXG (0.68, p=0.08) individuals. Similarly, frequency of risk allele “A” at rs929608 is also found to be significantly lower in control (0.46) than that of PEX (0.56, p=0.004), PEXS (0.56, p=0.009) and PEXG (0.56, p=0.04) individuals. n=sample size, \*risk Allele, † p- value after permutation correction where n=10,000.

SNP	PEX combined (n)	Control (n)	Allele	Allele freq. in PEX (combined cases)	Allele freq. in control subjects	$\chi^2$ value	p-value	p <sup>†</sup> value
rs7149187	115	144	C*	0.66	0.55	6.35	0.01	0.04
			T	0.34	0.45			
rs2430347	253	219	C	0.79	0.76	0.67	0.41	0.9
			T	0.21	0.24			
rs929608	278	234	A*	0.56	0.46	7.91	0.004	0.01
			G	0.44	0.54			

SNP	PEXS (n)	Control (n)	Allele	Allele freq. in PEXS	Allele freq. in control subjects	$\chi^2$ value	p-value	p <sup>†</sup> value
rs7149187	89	144	C*	0.65	0.55	4.49	0.03	0.1
			T	0.35	0.45			
rs2430347	171	219	C	0.77	0.76	0.03	0.85	1
			T	0.23	0.24			
rs929608	198	234	A*	0.56	0.46	6.77	0.009	0.03
			G	0.44	0.54			

SNP	PEXG (n)	Control (n)	Allele	Allele freq. in PEXG	Allele freq. in control subjects	$\chi^2$ value	p-value	p <sup>†</sup> value
rs7149187	26	144	C*	0.68	0.55	2.95	0.08	0.3
			T	0.32	0.45			
rs2430347	82	219	C	0.83	0.76	2.58	0.1	0.38
			T	0.17	0.24			
rs929608	80	234	A*	0.56	0.46	4.1	0.04	0.17
			G	0.44	0.54			

(p=0.01) and PEXS (p=0.03) but not with PEXG (p=0.17) as shown in **Table 5.3**. Effect of confounding factors, age and sex were eliminated through linear regression model using

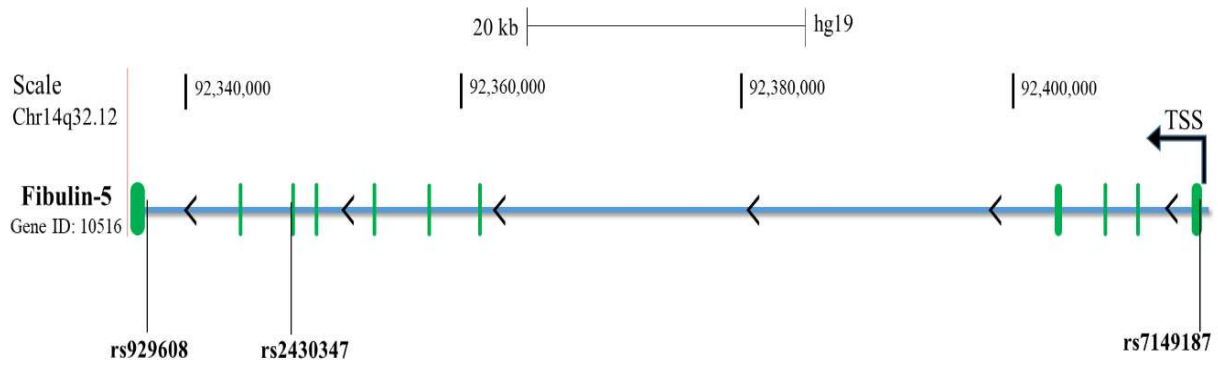


**Figure 5.2.** Diagrammatic presentation of Fibulin-5 gene present in the long arm of chromosome 14 (q32.12). Common genetic variants found in the study subjects are located within the gene; rs7149187 (1<sup>st</sup> exon), rs2430347 (9<sup>th</sup> exon) and rs929608 (11<sup>th</sup> intron).

three variations were further checked in the replicate stage by increasing the sample size as presented in the **Table 5.3** for each variants and groups. Genetic association of allele frequencies for all the SNPs were analyzed after checking for Hardy Weinberg equilibrium. Distribution of allele count, allele frequency, sample size and chi square for each of these SNPs were given in the **Table 5.3**. Genetic analysis has shown that rs7149187 was found to be significantly associated with PEX ( $p=0.01$ ) with allele “C” as the risk allele having higher allele frequency in PEX affected cases (0.66) than that of unaffected controls (0.55). After segregation of PEX combined cases into PEXS and PEXG individuals the association remained significant only for PEXS with a  $p$ -value of 0.03 but not with PEXG (0.08). After correction for multiple testing with permutation analysis ( $n=10,000$ ), genetic association of rs7149187 remained significant for PEX ( $p=0.01$ ) and PEXS ( $p=0.03$ ) but not with PEXG ( $p=0.3$ ) (**Table 5.3**).

Association analysis have also shown another noncoding polymorphism, rs929608 in the 10<sup>th</sup> intron of F5 to be a risk factor with risk allele “A” having lower frequency in control (0.46) as compared to that of PEX (0.56) with a  $p$ -value of 0.004. Further, it also remained significant with PEXS and PEXG with a  $p$ -value of 0.009 and 0.04, respectively. Even after

statistical significance by Student's t-test; for pairwise comparison with  $p < 0.05$  considered as statistically significant. Power calculation has been done using online Genetic Power Calculator ([zzz.bwh.harvard.edu/gpc/](http://zzz.bwh.harvard.edu/gpc/)).

## 5.3 Results

### 5.3.1 Association of genetic variants in the Fibulin-5 gene with PEX

Demographic features of the study subjects included in the work are presented in **Table 5.2**. In the discovery stage, we sequenced 11 exons and their exon-intron boundaries of F5 gene in thirty PEX affected cases and thirty controls. We found a synonymous variation, rs2430347 in the 9<sup>th</sup> exon and two non-coding variations, rs7149187 and rs929608 in the 1<sup>st</sup> exon and 10<sup>th</sup> intron, respectively. Location of these SNPs within F5 gene is depicted in the **Figure 5.2**. These

**Table 5.2.** Demographic and clinical features of study subjects included for genotyping of Fibulin-5 variants. n=sample size, U= unilateral cases, B=bilateral cases.

Subjects	n=	Age (in years)		Sex		Manifestation (Unilateral/Bilateral)	
		Mean±SD	Range	Male	Female	U	B
PEX (combined cases)	278	69.7±8.2	41-88	193	85	143	135
PEXS	198	70.4±8.6	41-87	128	70	103	95
PEXG	80	68.3±8.5	51-88	65	15	40	40
Control	234	64.2±10.8	40-90	119	115	-	-

### **5.2.3 RNA extraction and cDNA synthesis**

Detailed steps followed for tissue sample collection, RNA extraction, cDNA synthesis and qRT-PCR were described in the materials and methods section 2.2.5-2.2.7 of chapter 2 (Page no. 38-39). Gene specific primers for LoxL1, Fibulin-5 and GAPDH for qRT-PCR were designed using Primer-BLAST and IDT primer quest tool. Nucleotide sequence of primers used and their corresponding melting temperature were presented in the **Table 5.1**. Beta-Actin mRNA expression was used as endogenous control for normalizing target gene expression. Amplification specificity of the PCR product was checked via melting curve analysis and sequencing.  $\Delta\Delta C_t$  method was used for normalization of target gene and change in expression was represented as fold difference.

### **5.2.4 Western blotting**

Procedure for western blotting is elaborated in detail in materials and methods section 2.2.9 of chapter 2 (Page no. 39). Primary mouse polyclonal antibody against Fibulin-5 protein (Santacruz Biotech, USA) was used in 1:500 dilution in blocking solution. HRP-conjugated Rabbit anti-mouse IgG (Imgenex, India) was used as secondary antibody at dilution 1:5000 in PBST and skim milk. Bands were detected by using a chemiluminescence kit (Super Signal Femto Maximum Sensitivity Substrate, Thermo scientific) and signals were detected in a Chemi-Doc (Bio-Rad).

### **5.2.5 Genetic and statistical analysis**

Allelic association tests, genotypic association tests, Hardy-Weinberg equilibrium, haplotype analysis, linkage disequilibrium (LD) and correction for multiple testing with permutation analysis (n=10,000) were done using PLINK and Haploview V4.2 with default set of parameters following chi-square statistics. Confounding factors like age and sex were corrected through binary logistic regression in PLINK. Results from qRT PCR were analyzed for

exon boundaries. Primer information and their corresponding melting temperature used for PCR is shown in the **Table 5.1**.

**Table 5.1.** List of oligos used in the study.

Sl. No.	ID	Purpose	Sequence (5'→3')	T <sub>m</sub> <sup>0</sup> C
1	GAPDH (NM_002046.5)	qRT-PCR	F: GGTGTGAACCATGAGAAGTATGA R: GAGTCCTTCCACGATACCAAAG	60
2	Fibulin-5 (NM_006329.3)	qRT-PCR	F: GTTCCCGCTGACATCTTCCA R: CCCGTTTGCCGCATGTAAAA	60
3	LoxL1 (NM_005576.3)	qRT-PCR	F: ACTACGATGTGCGGGTGCTACTG R: TGGCTGAACTCGTCCATGCTGTG	60
4	F5-Exon-1	Sequencing	F: CTGGGTGGGAAGGTCAAGG R: AGAAAGAAAAGTCCAGCGCC	61
5	F5-Exon-2	Sequencing	F: ACTCCCCTAGACCTGAATCTG R: CTCCTCACCCCGGATTTT	56
6	F5-Exon-3	Sequencing	F:TGTGAAATGACCTTGCTGTTT R: GGCATGGCTAATCATTGAACAA	54
7	F5-Exon-4	Sequencing	F: CCACTAATGCTCGCCCTTTC R: CACAGCGGAGAGGAACAAAAG	55
8	F5-Exon-5	Sequencing	F: TGTGAGTGACATTCTTTGGACTA R: CAGCTATGCCCATACCTCAA	54.5
9	F5-Exon-6	Sequencing	F: ACCATCCGTGACACTCAGTAG R: CAGTGGCAAGGAATGGGAATA	55
10	F5-Exon-7	Sequencing	F:GATCATGCTCCCAAAGGTCCT R: CTGTGTGATTCTGACCCCACT	57
11	F5-Exon-8	Sequencing	F: CTCCCATCCCATGTAGACTG R: GCAGCTCCACCTCACACATA	55
12	F5-Exon-9	Sequencing	F: GCCAATAATGCCCTGCCTC R: CTTTCACACCACCTCCAAC	52.5
13	F5-Exon-10	Sequencing	F: GGTGGCCTCATTTTCAGTGTTT R: CCACTCTTACCTGCTTGCATAC	56
14	F5-Exon-11	Sequencing	F: ACAGTTGAGGCACCGAGG R: TAACGTCTGTGTCGCTCTCA	56.5

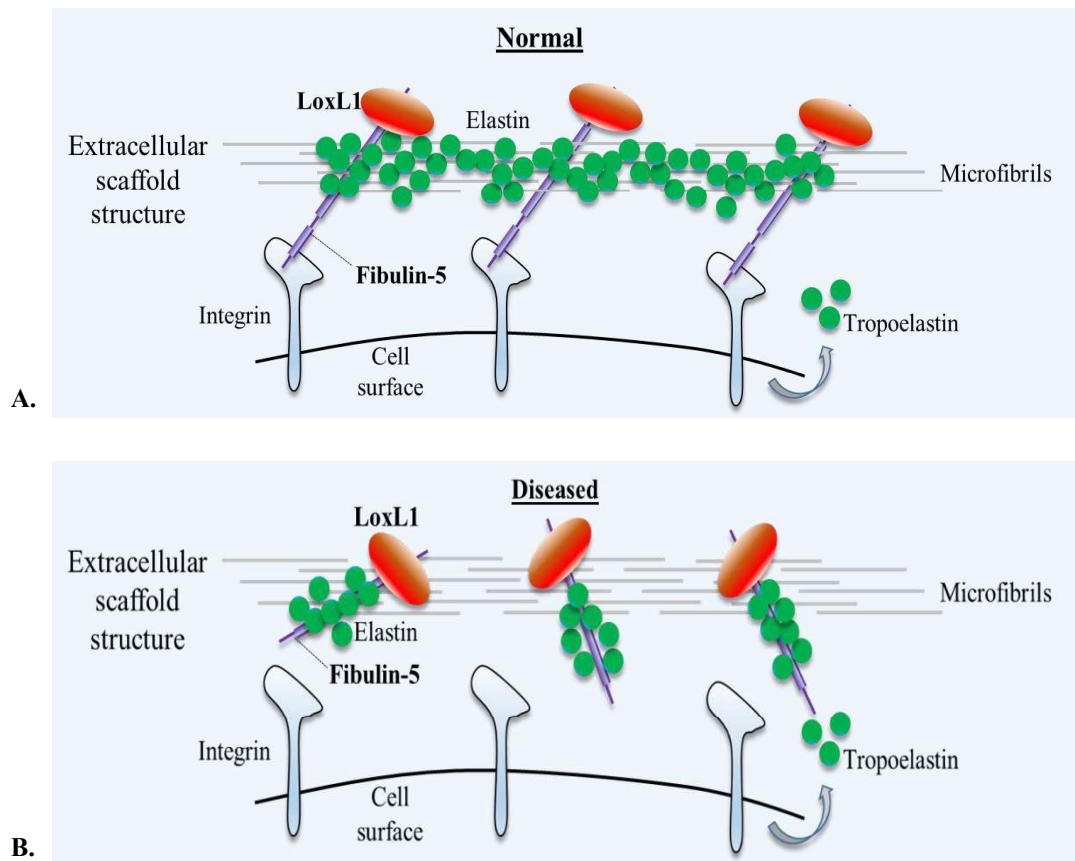


**Figure 5.1.** Diagrammatic presentation showing the deposition of ECM proteins in the outer extracellular space. In comparison to normal state (A), there is an abnormal deposition of ECM proteins in the diseased state (B) due to loss of Fibulin-5, an extracellular scaffold protein.

## 5.2 Materials and Methods

### 5.2.1 Study subjects

Detailed information about study subjects recruitment and inclusion or exclusion criteria followed for sample collection is mentioned in the materials and methods section 2.2.1 of chapter 2 (Page no. 33).

### 5.2.2 DNA extraction, PCR, elution and sequencing

Procedures followed for DNA extraction, PCR, elution and sequencing of targeted product is described in detail in materials and methods section 2.2.2-2.2.4 (Page no. 35-38). Eleven sets of primers were designed to encompass the region of eleven exons and their surrounding intron-

the site of PEX material formation. Choi *et al.* have shown that interaction with F5 is necessary for LoxL1 activation. And decreased expression or Knock-out of F5 leads to irregular deposition of in-active form of LoxL1 in large aggregates along with its substrate elastin.<sup>214</sup> Similar irregular deposition pattern of LoxL1 and elastin aggregates were also seen in PEX affected posterior eye tissues like lamina cribrosa and peripapillary sclera through immunostaining.<sup>66</sup> Recently, a 3D culture of tenon fibroblasts from PEX donors also shown an aberrant deposition of Fibulin-5 *in vivo*.<sup>228</sup> Altogether, these studies indicates a possible involvement of Fibulin-5 in the formation of PEX aggregates.

Hirai *et al.* have shown that the amount of truncated or cleaved form of Fibulin-5 increases with age. Gradual accumulation of this truncated form and its inability to carry out normal elastogenic activity leads to impaired ECM in aged tissues.<sup>229</sup> This implicates a possible role of F5 in PEX affected tissues, severity of which increases with age. Further, studies also have related the pathogenesis of PEX with other ECM disorders like pelvic organ prolapse and abdominal aortic aneurysm.<sup>15,17,109</sup> Studies have shown that female individuals with pelvic organ prolapse (POP), a connective tissue disorder have higher incidence of PEX.<sup>109</sup> Since, Fibulin-5 has been associated with such disorders and both involves altered ECM properties, it is highly likely that F5 may play a decisive role in PEX pathogenesis (**Figure 5.1**). In this chapter, we hypothesized that F5 is a risk factor in the development of PEX. We addressed this by questioning following key objectives:

1. Is there any anomalous change in the Fibulin-5 gene expression in PEX affected tissues versus control?
2. Finding of novel coding and/or non-coding genetic variants in the F5 gene in PEX patients.

coacervation into elastic fibers. Decreased expression or knock-out of F5 gene results in abnormal deposition of LoxL1 and elastic fibers.<sup>214</sup>

### **5.1.2 Fibulin-5 and ECM disorders**

Fibulin-5 has been associated with various elastinopathic disorders like cutis laxa (CL), pelvic organ prolapse (POP), abdominal aorta aneurysm, Charcot-Marie-Tooth neuropathies and age related macular degeneration (AMD).<sup>108,215-218</sup> Aberrant expression and/or abnormal deposition of F5 is seen in patients with such disorders. Individuals affected with such disorders were also shown to have pathogenic variants in the F5 gene.<sup>108,215-224</sup> Past studies have revealed that amino acid substitutions by these pathogenic variants lead to misfolding of F5, decreased secretion and increased protein aggregation.<sup>221,225,226</sup> Diminished level of F5 in the ECM results in impaired elastic fiber development by a reduced interaction with other extracellular proteins like elastin and fibrillin-1 and is the sole factor in the progression of such diseases.

F5 also plays a role in tumor cell progression by modulating metastasis and cell survivability.<sup>210,212</sup> Aberrant expression of F5 is also seen in different cancerous tissues.<sup>227</sup> Chen *et al.* have shown that F5 acts as a metastasis suppressor in lung cancer by inhibiting Wnt/ $\beta$ -catenin pathway thereby reducing MMP-7 (Matrix metalloproteinase-7).<sup>210</sup> Further, it also stimulates integrin-induced production of ROS which then inhibits tumor growth.<sup>213</sup>

### **5.1.3 Potential role of F5 as a risk factor in PEX progression.**

In this chapter, we proposed that Fibulin-5 might play a pivotal role in the pathogenesis of pseudoexfoliation. F5 acts as a scaffold for localization and activation of LoxL1, a key candidate gene for PEX pathogenesis.<sup>113</sup> Mass spec analysis shows the presence of both fibulin and LoxL1 proteins in the PEX aggregates.<sup>52</sup> However, in a normal scenario where LoxL1 co-localizes with F5 in the ECM, in PEX affected tissues it is not found to be co-localized with F5.<sup>133</sup> This suggests a loss of interaction between LoxL1 and its normal binding partner, F5 at

## **Chapter-5. Fibulin-5; an extracellular scaffold protein in the development of PEX.**

### **5.1 Introduction**

The following chapter is focused on finding the potential pathogenic role of Fibulin-5 (F5) (Gene ID: 10516) protein in the progression of pseudoexfoliation. F5 is also known as developmental arteries and neural crest EGF-like protein (DANCE) because of its expression in developmental arteries and contains EGF like domains.<sup>207</sup> It functions as an extracellular matrix protein and is necessary for elastogenesis.

#### **5.1.1 Fibulin-5 is a crucial scaffold protein in the extracellular matrix**

Fibulin-5 belongs to class II fibulin subfamily with shorter repeats of calcium-binding epidermal growth factor like motifs (cbEGF) unlike that of class I subfamily with long repeats. It is secreted as a 66 kDa protein containing 425 amino acids from a wide variety of cells including fibroblast and vascular smooth muscle cells.<sup>208</sup> After secretion, a conserved RGD motif (Arginine-Glycine-Aspartate) present in the N-terminus of F5 binds to integrins on the cell surface and is essential for its cellular function. It plays a prominent role in the formation of elastic fibers, cell-matrix adhesion, regulation of cell growth, modulation of matrix proteases and integrin-dependent regulation of ROS (reactive oxygen species) in the ECM.<sup>113,209-213</sup> F5 also contains six calcium-binding epidermal growth factor like motifs (cbEGF-like) that ensures protein stability and assists in protein-protein interaction.

Fibulin-5 plays a key role during elastogenesis in the ECM. Elastogenesis involves polymerization of tropoelastin monomers into elastic fibers through a sequential step. This includes coacervation of tropoelastin, proper assembly, crosslinking of monomeric tropoelastin and final polymerization into elastic fibers. F5 also assist in the deposition of deaminating enzyme, LoxL1 (Lysyl oxidase like-1) and its activation by pro-peptide cleavage in the ECM. Activated LoxL1 then crosslinks tropoelastin monomers by lysyl-deamination following

# **CHAPTER 5**

**Fibulin-5; an extracellular scaffold protein in the development of PEX.**

- ❖ Knockout cell preparation through CRISPR-Cas9 genome editing
- ❖ Analysing of chromatin interactions through chromosome-conformation capture assays

## **6.6 Future prospective**

- ❖ Further studies are needed to find more regulatory SNPs within the clusterin gene in association with PEX.
- ❖ Detailed role of genes, *PTK2B* and *EPHX2* in the progression of PEX warrants further research.
- ❖ Functional role of Fibulin-5 associated polymorphisms with PEX needs to be studied further.

#### **6.4 Key findings from the study**

- Genetic polymorphisms, rs3087554 and rs2279590 within clusterin gene are risk factors for PEX in Indian population.
- *CLU* expression was significantly upregulated in the PEXG individuals than in control and PEXS individuals.
- Common variant, rs2279590 is a functional polymorphism and creates a binding site for transcription factor, heat shock factor 1 (HSF1).
- Binding of HSF1 diminishes the regulatory effect of rs2279590 enhancer element and decreases *CLU* gene expression.
- HSF1, a heat shock factor is significantly upregulated in anterior eye tissues of PEXS subjects compared to that of control but not in PEXG individuals.
- Locus containing rs2279590 acts as a wide spread enhancer element and regulates two distal genes, *PTK2B* and *EPHX2*.
- Noncoding variants, rs7149187 and rs929608 within Fibulin-5 gene are found to be novel risk factors in the pathogenesis of pseudoexfoliation.
- Fibulin-5 expression was found to be significantly downregulated in the lens capsules of PEXS subjects than in those of control individuals.

#### **6.5 Methods standardized during the course of this project in the laboratory**

- ❖ Standardization of capillary sequencing using Sanger's method
- ❖ RNA extraction, cDNA synthesis and Quantitative real-time PCR for checking target gene expression
- ❖ Protein extraction, quantitation and western blotting for protein assays
- ❖ Competent cell preparation and cloning
- ❖ Molecular DNA binding assays (EMSA, ChIP and Luciferase assays)

developing PEX.<sup>15,17,109</sup> This further supports a probable role of F5 in PEX individuals. Further, studies need to be done to understand the molecular mechanism by which F5 plays a role in the deposition of fibrillar aggregates in PEX subjects.

### **6.3 Conclusion:**

Our work has shown a genetic association of noncoding polymorphisms, rs3087554 and rs2279590 in clusterin (*CLU*) gene as risk factors in the pathogenesis of pseudoexfoliation in Indian population. Additionally, we found a significantly increased expression of *CLU* gene in the lens capsule of PEXG cases in comparison to control but not in PEXS subjects. Further, one of the intronic polymorphisms, rs2279590 is shown to be a functional regulatory polymorphism and regulates clusterin gene expression. Protective allele “A” at rs2279590 creates a binding site for a transcription factor, heat shock factor 1 (HSF1). Binding of HSF1 to rs2279590 abrogates the enhancer effect of the locus and decreases the *CLU* gene expression and thereby decreases the cytotoxicity of accumulated CLU. In addition, enhancer element surrounding rs2279590 also has a wide spread enhancer effect and regulates the expression of two distal genes, *PTK2B* and *EPHX2*, which have been previously reported to be candidate genes for pathogenesis of Alzheimer’s disease.

We also have found a novel association between common genetic variants in Fibulin-5 gene as risk factors in the pathogenesis of pseudoexfoliation. Further, in lens capsules of PEXS subjects, F5 expression was found to be downregulated compared to that of in control subjects but not in case of PEXG. This implicates that an impaired maintenance of ECM proteins due to decreased F5 expression may lead to formation of fibrillar aggregates in PEX affected individuals.

elastinopathies.<sup>221,225,226</sup> Similarly, intronic non-coding polymorphisms within F5 gene also have been associated with disorders like age related macular degeneration, cutis laxa (CL) and pelvic organ prolapse (POP).<sup>216,232</sup>

Current work has found novel genetic association between noncoding intronic SNPs, rs7149187 and rs929608 residing in the 1<sup>st</sup> exon and 10<sup>th</sup> intron, respectively within F5 gene as risk factors in the pathogenesis of PEX. Since, F5 acts as a scaffold protein in the ECM,<sup>113</sup> genetic association of polymorphisms in F5 gene with PEX indicates a perturbation in the extracellular matrix formation in affected tissues. However, we did not find any coding variation in PEX affected individuals. Although, the associated variations are in non-coding region they may act as functional regulatory SNPs and may alter F5 gene expression in PEX individuals. Further studies are needed to find the role of these SNPs in PEX progression.

### **6.2.2 Downregulated F5 expression may lead to impaired maintenance of ECM**

Dysregulated expression and/or abnormal accumulation of F5 is seen in individuals with pathogenic conditions like CL, POP and abdominal aorta aneurysm.<sup>108,215-218</sup> Similarly, we have found a decreased level of F5 in the lens capsule of PEXS subjects compared to that of control. Choi *et al.* also have shown that interaction with F5 is necessary for LoxL1 activation, an interacting partner necessary for deposition of elastin fibrils.<sup>214</sup> Downregulated expression of F5 in the extracellular matrix can thus lead to improper activation of LoxL1 and abnormal deposition of extracellular proteins comprising of elastin and fibrillin-1 including LoxL1 during the progression of these elastinopathic diseases. Further, accumulation of disrupted F5 increases with age and this may decrease the elastogenic activity of F5. Also, Want *et al.* have reported that 3D culture of tenon fibroblasts from PEX donors showed an aberrant deposition of Fibulin-5 *in vitro*.<sup>228</sup> Additionally, individuals with other elastinopathy diseases like POP and abdominal aortic aneurysm where F5 is a candidate gene, have shown to be at high risk of

rs2279590 regulates *CLU* expression through interacting with *CLU* promoter. Such an enhancer mediated regulation over *CLU* expression increases both secretory (s*CLU*) and nuclear (n*CLU*) form of *CLU*. s*CLU* can lead to cytotoxicity by incorporating itself within the PEX aggregates when substrate is in large molar excess in a failed attempt to prevent aggregation; leading to large insoluble aggregates.<sup>173</sup> While s*CLU* gets secreted out of the cell, n*CLU* tends to localize within the nucleus and activates the expression of a group of cytotoxic genes which ultimately lead to death of the cell.<sup>238</sup> n*CLU* is produced in the cell during chronic stress and initiates caspase-3 dependent apoptosis,<sup>186</sup> a feature seen in degeneration of optic nerve head cells (ONH) in advanced cases of PEXG affected individuals. Stress such as proteotoxic stress leads to induction of n*CLU* in the neurons and can lead to apoptosis. Thus, an increase in the expression of both secretory and nuclear *CLU* can be detrimental to the neuronal cells. However, binding of HSF1 to the protective allele “A” at rs2279590 abrogates the enhancer effect and hence decreases the cytotoxicity of overexpressed s*CLU* and n*CLU*.

## **6.2 Fibulin-5 as a novel candidate in development of PEX**

Fibulin-5 (F5) is another potential candidate which poses as a risk factor in the pathogenesis of PEX. Extracellular functions such as activation of LoxL1, proper orientation and deposition of elastin fibrils and being a key protein in maintaining scaffold structure in the ECM for microfibrils supports the hypothesis that it may play a role in PEX aggregate formation.<sup>113,209-</sup>

214

### **6.2.1 Genetic association of polymorphisms in F5 gene with PEX**

Coding variations within exons of F5 gene have been shown in individuals with various pathogenic conditions. Earlier studies have found pathogenic coding variants that leads to amino-acid substitutions and disrupted secretion of F5 to the extracellular space which leads to increased protein aggregation in individuals suffering from various types of

### 6.1.2 Dysregulated expression of CLU can be pathogenic for PEX progression

Clusterin plays an indispensable role in maintaining extracellular proteins. It prevents the aggregation of abnormal protein in the ECM and also carries out basal cellular functions such as lipid transport, cell matrix formation and cell membrane remodeling.<sup>163-165</sup> Dysregulation in *CLU* gene expression has been implicated in various pathogenic conditions. *CLU* expression is shown to be dysregulated in various cancerous tissue samples and thus is used as a diagnostic marker.<sup>167,168</sup> Upregulation in *CLU* protein has been shown in different types of malignancies such as hepatocellular carcinoma,<sup>234</sup> renal cell carcinoma,<sup>235</sup> colorectal cancers<sup>236</sup> and breast cancer.<sup>237</sup> In these pathogenic conditions level, of *CLU* accumulation is correlated with the aggressiveness of tumors. Similar to that of cancer tissues, *CLU* expression is also found to be elevated in brain tissues from individuals affected by Alzheimer's disease. Giri *et al.* have shown that individuals affected by AD have shown a faster decline of brain function with increased *CLU* protein than unaffected individuals.<sup>184</sup> Further, knock out of clusterin in an Alzheimer's mice model (PDAPP mice) lead to decrease in fibrillar plaque formation and neuritic dystrophy.<sup>183</sup> Yerbury *et al.* have shown that it's the Clusterin:substrate ratio in the extracellular space that decides the fate of the *CLU* to be cytotoxic or cytoprotective. When *CLU* is at a higher concentration in comparison to its substrate, it deposits along with the extracellular deposits in a failed attempt to clear the fibrillar aggregates.<sup>173</sup>

Our work has shown an increased accumulation of *CLU* protein in the aqueous humour of PEXG subjects in comparison to that of control and PEXS individuals. Clusterin over-accumulation may lead to deposition of *CLU* protein on the surface of lens capsule along with PEX aggregates, as shown through immunohistochemistry as suggested by Yerbury *et al.* and increases the cytotoxicity.<sup>173</sup> Further, risk genotype "GG" at rs2279590 regulates *CLU* expression by 2-fold compared to that of individuals with genotype "AA". We also found through chromosome conformation capture that enhancer element containing allele "G" at

## 6. Discussion:

### 6.1 Clusterin in the pathogenesis of pseudoexfoliation

Clusterin (*CLU*) or Apolipoprotein-J (*APOJ*) residing in chromosome 8 (p21.1) plays a crucial role in deciding the cell's fate.<sup>155,156,233</sup> Ubiquitous expression of *CLU* suggests its prominent non-redundant role in tissues.<sup>155,158-161</sup> Previously, *CLU* has been associated with various disorders<sup>125,126,162</sup> including PEX.<sup>62</sup> Our work involved a detailed functional analysis of *CLU* genetic variants as well as its expression in PEX affected and non-affected tissues.

#### 6.1.1 Genetic variants in clusterin as a risk factor for PEX

Association of genetic polymorphisms within *CLU* gene has been a risk factor for a variety of disorders. Through GWAS studies, Lambert *et al.* have shown non-coding variants such as rs9331896, rs2279590, rs11136000 and rs7982 within *CLU* gene as risk factor in PEX pathogenesis.<sup>125,191</sup> Similarly, Daimon *et al.* have shown association of *CLU* variants with type-2 diabetes mellitus patients and suggested that it is primarily through an increase in insulin resistance primarily and secondarily through an impairment of insulin secretion secondarily.<sup>126</sup>

Previously, Krumbeigel *et al.* carried out a case-control study in German population and reported a genetic association between the SNP, rs2279590 located in the 7<sup>th</sup> intronic region of clusterin gene and PEX.<sup>62</sup> However, they couldn't find an association of the SNP, rs3087554 residing in the 3' untranslated region with PEX. Later, Burdon *et al.* have shown an association of SNP, rs3087554 with PEX in an Australian cohort.<sup>124</sup> Our study has shown that both variants of clusterin gene *i.e* rs3087554 and rs2279590 are risk factors for PEX pathogenesis in Indian population. Allele "A" at rs3087554 is found to be the risk allele similar to that of in Australian population.<sup>124</sup> While allele "G" at rs2279590 is found to be the risk allele opposite to that of found in German cohort.<sup>62</sup> Reversal allelic association at rs2279590 suggests a moderate contribution towards PEX pathogenesis.

# **Chapter 6**

## **Discussion**

236. Mourra, N., Couvelard, A., Tiret, E., Olschwang, S. & Flejou, J.F. Clusterin is highly expressed in pancreatic endocrine tumours but not in solid pseudopapillary tumours. *Histopathology* **50**, 331-7 (2007).
237. Kevans, D. *et al.* High clusterin expression correlates with a poor outcome in stage II colorectal cancers. *Cancer Epidemiol Biomarkers Prev* **18**, 393-9 (2009).

212. Lee, Y.H., Albig, A.R., Regner, M., Schiemann, B.J. & Schiemann, W.P. Fibulin-5 initiates epithelial-mesenchymal transition (EMT) and enhances EMT induced by TGF-beta in mammary epithelial cells via a MMP-dependent mechanism. *Carcinogenesis* **29**, 2243-51 (2008).
213. Schluterman, M.K. *et al.* Loss of fibulin-5 binding to beta1 integrins inhibits tumor growth by increasing the level of ROS. *Dis Model Mech* **3**, 333-42 (2010).
214. Choi, J. *et al.* Analysis of dermal elastic fibers in the absence of fibulin-5 reveals potential roles for fibulin-5 in elastic fiber assembly. *Matrix Biol* **28**, 211-20 (2009).
215. Claus, S. *et al.* A p.C217R mutation in fibulin-5 from cutis laxa patients is associated with incomplete extracellular matrix formation in a skin equivalent model. *J Invest Dermatol* **128**, 1442-50 (2008).
216. Elahi, E. *et al.* Homozygous missense mutation in fibulin-5 in an Iranian autosomal recessive cutis laxa pedigree and associated haplotype. *J Invest Dermatol* **126**, 1506-9 (2006).
217. Cheng, S. *et al.* Adult-onset demyelinating neuropathy associated with FBLN5 gene mutation. *Clin Neuropathol* **36**, 171-177 (2017).
218. Stone, E.M. *et al.* Missense variations in the fibulin 5 gene and age-related macular degeneration. *N Engl J Med* **351**, 346-53 (2004).
219. Loeys, B. *et al.* Homozygosity for a missense mutation in fibulin-5 (FBLN5) results in a severe form of cutis laxa. *Hum Mol Genet* **11**, 2113-8 (2002).
220. Markova, D. *et al.* Genetic heterogeneity of cutis laxa: a heterozygous tandem duplication within the fibulin-5 (FBLN5) gene. *Am J Hum Genet* **72**, 998-1004 (2003).
221. Hu, Q. *et al.* Fibulin-5 mutations: mechanisms of impaired elastic fiber formation in recessive cutis laxa. *Hum Mol Genet* **15**, 3379-86 (2006).
222. Megarbane, H. *et al.* An autosomal-recessive form of cutis laxa is due to homozygous elastin mutations, and the phenotype may be modified by a heterozygous fibulin 5 polymorphism. *J Invest Dermatol* **129**, 1650-5 (2009).
223. Auer-Grumbach, M. *et al.* Fibulin-5 mutations link inherited neuropathies, age-related macular degeneration and hyperelastic skin. *Brain* **134**, 1839-52 (2011).
224. Zhou, Y., Ling, O. & Bo, L. Expression and significance of lysyl oxidase-like 1 and fibulin-5 in the cardinal ligament tissue of patients with pelvic floor dysfunction. *J Biomed Res* **27**, 23-8 (2013).
225. Lotery, A.J. *et al.* Reduced secretion of fibulin 5 in age-related macular degeneration and cutis laxa. *Hum Mutat* **27**, 568-74 (2006).
226. Jones, R.P. *et al.* Structural effects of fibulin 5 missense mutations associated with age-related macular degeneration and cutis laxa. *Invest Ophthalmol Vis Sci* **51**, 2356-62 (2010).
227. Schiemann, W.P., Blobel, G.C., Kalume, D.E., Pandey, A. & Lodish, H.F. Context-specific effects of fibulin-5 (DANCE/EVEC) on cell proliferation, motility, and invasion. Fibulin-5 is induced by transforming growth factor-beta and affects protein kinase cascades. *J Biol Chem* **277**, 27367-77 (2002).
228. Want, A. *et al.* Autophagy and Mitochondrial Dysfunction in Tenon Fibroblasts from Exfoliation Glaucoma Patients. *PLoS One* **11**, e0157404 (2016).
229. Hirai, M. *et al.* Fibulin-5/DANCE has an elastogenic organizer activity that is abrogated by proteolytic cleavage in vivo. *J Cell Biol* **176**, 1061-71 (2007).
230. Callewaert, B. *et al.* Comprehensive clinical and molecular analysis of 12 families with type 1 recessive cutis laxa. *Hum Mutat* **34**, 111-21 (2013).
231. Safka Brozkova, D. *et al.* Czech family confirms the link between FBLN5 and Charcot-Marie-Tooth type 1 neuropathy. *Brain* **136**, e232 (2013).
232. Kaur, I., Rathi, S. & Chakrabarti, S. Variations in TIMP3 are associated with age-related macular degeneration. *Proc Natl Acad Sci U S A* **107**, E112-3 (2010).
233. Murphy, M.P. & LeVine, H., 3rd. Alzheimer's disease and the amyloid-beta peptide. *J Alzheimers Dis* **19**, 311-23 (2010).
234. Xie, D. *et al.* Up-regulated expression of cytoplasmic clusterin in human ovarian carcinoma. *Cancer* **103**, 277-83 (2005).
235. Kang, Y.K., Hong, S.W., Lee, H. & Kim, W.H. Overexpression of clusterin in human hepatocellular carcinoma. *Hum Pathol* **35**, 1340-6 (2004).

188. Ortner, V., Ludwig, A., Riegel, E., Dunzinger, S. & Czerny, T. An artificial HSE promoter for efficient and selective detection of heat shock pathway activity. *Cell Stress Chaperones* **20**, 277-88 (2015).
189. Dourlen, P. *et al.* Functional screening of Alzheimer risk loci identifies PTK2B as an in vivo modulator and early marker of Tau pathology. *Mol Psychiatry* **22**, 874-883 (2017).
190. Szymanski, M., Wang, R., Bassett, S.S. & Avramopoulos, D. Alzheimer's risk variants in the clusterin gene are associated with alternative splicing. *Transl Psychiatry* **1**(2011).
191. Lambert, J.C. *et al.* Meta-analysis of 74,046 individuals identifies 11 new susceptibility loci for Alzheimer's disease. *Nat Genet* **45**, 1452-8 (2013).
192. Zhou, Y. *et al.* Intracellular clusterin interacts with brain isoforms of the bridging integrator 1 and with the microtubule-associated protein Tau in Alzheimer's disease. *PLoS One* **9**, e103187 (2014).
193. Wang, X. *et al.* The systemic amyloid precursor transthyretin (TTR) behaves as a neuronal stress protein regulated by HSF1 in SH-SY5Y human neuroblastoma cells and APP23 Alzheimer's disease model mice. *J Neurosci* **34**, 7253-65 (2014).
194. Anckar, J. & Sistonen, L. Regulation of HSF1 function in the heat stress response: implications in aging and disease. *Annu Rev Biochem* **80**, 1089-115 (2011).
195. Fujimoto, M. *et al.* Active HSF1 significantly suppresses polyglutamine aggregate formation in cellular and mouse models. *J Biol Chem* **280**, 34908-16 (2005).
196. Lechler, M.C. *et al.* Reduced Insulin/IGF-1 Signaling Restores the Dynamic Properties of Key Stress Granule Proteins during Aging. *Cell Rep* **18**, 454-467 (2017).
197. Jiang, Y.Q. *et al.* Increased heat shock transcription factor 1 in the cerebellum reverses the deficiency of Purkinje cells in Alzheimer's disease. *Brain Res* **1519**, 105-11 (2013).
198. Gouras, G.K. mTOR: at the crossroads of aging, chaperones, and Alzheimer's disease. *J Neurochem* **124**, 747-8 (2013).
199. Goetzl, E.J. *et al.* Low neural exosomal levels of cellular survival factors in Alzheimer's disease. *Ann Clin Transl Neurol* **2**, 769-73 (2015).
200. Li, Y.Q. *et al.* Common variant in PTK2B is associated with late-onset Alzheimer's disease: A replication study and meta-analyses. *Neurosci Lett* **621**, 83-87 (2016).
201. Rosenthal, S.L. & Kamboh, M.I. Late-Onset Alzheimer's Disease Genes and the Potentially Implicated Pathways. *Curr Genet Med Rep* **2**, 85-101 (2014).
202. Chapuis, J. *et al.* Genome-wide, high-content siRNA screening identifies the Alzheimer's genetic risk factor FERMT2 as a major modulator of APP metabolism. *Acta Neuropathol* **133**, 955-966 (2017).
203. Nelson, J.W. *et al.* Role of soluble epoxide hydrolase in age-related vascular cognitive decline. *Prostaglandins Other Lipid Mediat* **113-115**, 30-7 (2014).
204. Kohler, C., Dinekov, M. & Gotz, J. Active glycogen synthase kinase-3 and tau pathology-related tyrosine phosphorylation in pR5 human tau transgenic mice. *Neurobiol Aging* **34**, 1369-79 (2013).
205. Chan, G. *et al.* CD33 modulates TREM2: convergence of Alzheimer loci. *Nat Neurosci* **18**, 1556-8 (2015).
206. Koerner, I.P. *et al.* Polymorphisms in the human soluble epoxide hydrolase gene EPHX2 linked to neuronal survival after ischemic injury. *J Neurosci* **27**, 4642-9 (2007).
207. Nakamura, T. *et al.* DANCE, a novel secreted RGD protein expressed in developing, atherosclerotic, and balloon-injured arteries. *J Biol Chem* **274**, 22476-83 (1999).
208. Yanagisawa, H., Schluterman, M.K. & Brekken, R.A. Fibulin-5, an integrin-binding matricellular protein: its function in development and disease. *J Cell Commun Signal* **3**, 337-47 (2009).
209. Budatha, M. *et al.* Extracellular matrix proteases contribute to progression of pelvic organ prolapse in mice and humans. *J Clin Invest* **121**, 2048-59 (2011).
210. Chen, X. *et al.* Fibulin-5 inhibits Wnt/beta-catenin signaling in lung cancer. *Oncotarget* **6**, 15022-34 (2015).
211. Chin, K. *et al.* Pelvic Organ Support in Animals with Partial Loss of Fibulin-5 in the Vaginal Wall. *PLoS One* **11**, e0152793 (2016).

163. Matsuda, A. *et al.* Clusterin, an abundant serum factor, is a possible negative regulator of MT6-MMP/MMP-25 produced by neutrophils. *J Biol Chem* **278**, 36350-7 (2003).
164. Seiberg, M. & Marthinuss, J. Clusterin expression within skin correlates with hair growth. *Dev Dyn* **202**, 294-301 (1995).
165. Thomas-Salgar, S. & Millis, A.J. Clusterin expression in differentiating smooth muscle cells. *J Biol Chem* **269**, 17879-85 (1994).
166. Yang, C.R. *et al.* Nuclear clusterin/XIP8, an x-ray-induced Ku70-binding protein that signals cell death. *Proc Natl Acad Sci U S A* **97**, 5907-12 (2000).
167. Trougakos, I.P., So, A., Jansen, B., Gleave, M.E. & Gonos, E.S. Silencing expression of the clusterin/apolipoprotein j gene in human cancer cells using small interfering RNA induces spontaneous apoptosis, reduced growth ability, and cell sensitization to genotoxic and oxidative stress. *Cancer Res* **64**, 1834-42 (2004).
168. Shannan, B. *et al.* Challenge and promise: roles for clusterin in pathogenesis, progression and therapy of cancer. *Cell Death Differ* **13**, 12-9 (2006).
169. Yang, C.R. *et al.* Isolation of Ku70-binding proteins (KUBs). *Nucleic Acids Res* **27**, 2165-74 (1999).
170. Tschopp, J., Chonn, A., Hertig, S. & French, L.E. Clusterin, the human apolipoprotein and complement inhibitor, binds to complement C7, C8 beta, and the b domain of C9. *J Immunol* **151**, 2159-65 (1993).
171. Jenne, D.E. *et al.* Clusterin (complement lysis inhibitor) forms a high density lipoprotein complex with apolipoprotein A-I in human plasma. *J Biol Chem* **266**, 11030-6 (1991).
172. Li, X. *et al.* Clusterin in Alzheimer's disease: a player in the biological behavior of amyloid-beta. *Neurosci Bull* **30**, 162-8 (2014).
173. Yerbury, J.J. *et al.* The extracellular chaperone clusterin influences amyloid formation and toxicity by interacting with prefibrillar structures. *FASEB J* **21**, 2312-22 (2007).
174. Leskov, K.S., Klokov, D.Y., Li, J., Kinsella, T.J. & Boothman, D.A. Synthesis and functional analyses of nuclear clusterin, a cell death protein. *J Biol Chem* **278**, 11590-600 (2003).
175. Giannakopoulos, P. *et al.* Possible neuroprotective role of clusterin in Alzheimer's disease: a quantitative immunocytochemical study. *Acta Neuropathol* **95**, 387-94 (1998).
176. Killick, R. *et al.* Clusterin regulates beta-amyloid toxicity via Dickkopf-1-driven induction of the wnt-PCP-JNK pathway. *Mol Psychiatry* **19**, 88-98 (2014).
177. Creasey, R. *et al.* Detecting protein aggregates on untreated human tissue samples by atomic force microscopy recognition imaging. *Biophys J* **99**, 1660-7 (2010).
178. Sharma, S. *et al.* Identification of LOXL1 protein and Apolipoprotein E as components of surgically isolated pseudoexfoliation material by direct mass spectrometry. *Exp Eye Res* **89**, 479-85 (2009).
179. Arvind, H. *et al.* Pseudoexfoliation in South India. *Br J Ophthalmol* **87**, 1321-3 (2003).
180. Jones, S.E., Meerabux, J.M., Yeats, D.A. & Neal, M.J. Analysis of differentially expressed genes in retinitis pigmentosa retinas. Altered expression of clusterin mRNA. *FEBS Lett* **300**, 279-82 (1992).
181. Schrijvers, E.M., Koudstaal, P.J., Hofman, A. & Breteler, M.M. Plasma clusterin and the risk of Alzheimer disease. *JAMA* **305**, 1322-6 (2011).
182. Byun, K. *et al.* Clusterin/ApoJ enhances central leptin signaling through Lrp2-mediated endocytosis. *EMBO Rep* **15**, 801-8 (2014).
183. DeMattos, R.B. *et al.* Clusterin promotes amyloid plaque formation and is critical for neuritic toxicity in a mouse model of Alzheimer's disease. *Proc Natl Acad Sci U S A* **99**, 10843-8 (2002).
184. Giri, M., Zhang, M. & Lu, Y. Genes associated with Alzheimer's disease: an overview and current status. *Clin Interv Aging* **11**, 665-81 (2016).
185. Karch, C.M. *et al.* Expression of novel Alzheimer's disease risk genes in control and Alzheimer's disease brains. *PLoS One* **7**, e50976 (2012).
186. Caccamo, A.E. *et al.* Cell detachment and apoptosis induction of immortalized human prostate epithelial cells are associated with early accumulation of a 45 kDa nuclear isoform of clusterin. *Biochem J* **382**, 157-68 (2004).
187. Hagege, H. *et al.* Quantitative analysis of chromosome conformation capture assays (3C-qPCR). *Nat Protoc* **2**, 1722-33 (2007).

141. Yagci, R., Ersoz, I., Erdurmus, M., Gurel, A. & Duman, S. Protein carbonyl levels in the aqueous humour and serum of patients with pseudoexfoliation syndrome. *Eye (Lond)* **22**, 128-31 (2008).
142. Yilmaz, A., Ayaz, L. & Tamer, L. Selenium and pseudoexfoliation syndrome. *Am J Ophthalmol* **151**, 272-6 e1 (2011).
143. Strzalka-Mrozik, B. *et al.* Quantitative analysis of SOD2, ALDH1A1 and MGST1 messenger ribonucleic acid in anterior lens epithelium of patients with pseudoexfoliation syndrome. *Mol Vis* **19**, 1341-9 (2013).
144. Lesiewska-Junk, H., Malukiewicz, G., Olszewska-Slonina, D., Wozniak, A. & Jung, S. Erythrocytes' oxidative stress markers in patients with pseudoexfoliation syndrome. *Acta Ophthalmol* **91**, e648-9 (2013).
145. Lesiewska, H., Malukiewicz, G., Linkowska, K. & Grzybowski, T. Analysis of SOD1 polymorphisms in Polish population with pseudoexfoliation syndrome. *Acta Ophthalmol* **93**, e322-3 (2015).
146. Abu-Amero, K.K., Morales, J., Mohamed, G.H., Osman, M.N. & Bosley, T.M. Glutathione S-transferase M1 and T1 polymorphisms in Arab glaucoma patients. *Mol Vis* **14**, 425-30 (2008).
147. Tanito, M., Kaidzu, S., Takai, Y. & Ohira, A. Status of systemic oxidative stresses in patients with primary open-angle glaucoma and pseudoexfoliation syndrome. *PLoS One* **7**, e49680 (2012).
148. Dursun, F. *et al.* Total oxidative stress, paraoxonase and arylesterase levels at patients with pseudoexfoliation syndrome and pseudoexfoliative glaucoma. *Int J Ophthalmol* **8**, 985-90 (2015).
149. Sarenac Vulovic, T.S., Pavlovic, S.M., Jakovljevic, V., Janicijevic, K.B. & Zdravkovic, N.S. Nitric oxide and tumour necrosis factor alpha in the process of pseudoexfoliation glaucoma. *Int J Ophthalmol* **9**, 1138-42 (2016).
150. Gartaganis, S.P., Patsoukis, N.E., Nikolopoulos, D.K. & Georgiou, C.D. Evidence for oxidative stress in lens epithelial cells in pseudoexfoliation syndrome. *Eye (Lond)* **21**, 1406-11 (2007).
151. Harnisch, J.P., Barrach, H.J., Hassell, J.R. & Sinha, P.K. Identification of a basement membrane proteoglycan in exfoliation material. *Albrecht Von Graefes Arch Klin Exp Ophthalmol* **215**, 273-8 (1981).
152. Konstas, A.G. & Williamson, T.H. Co-existence of exfoliation syndrome, previous iris surgery, and heterochromia. *Acta Ophthalmol (Copenh)* **71**, 850-2 (1993).
153. Lee, R.K. The molecular pathophysiology of pseudoexfoliation glaucoma. *Curr Opin Ophthalmol* **19**, 95-101 (2008).
154. Schlotzer-Schrehardt, U. Pseudoexfoliation syndrome: the puzzle continues. *J Ophthalmic Vis Res* **7**, 187-9 (2012).
155. de Silva, H.V., Harmony, J.A., Stuart, W.D., Gil, C.M. & Robbins, J. Apolipoprotein J: structure and tissue distribution. *Biochemistry* **29**, 5380-9 (1990).
156. Murphy, B.F., Kirszbaum, L., Walker, I.D. & d'Apice, A.J. SP-40,40, a newly identified normal human serum protein found in the SC5b-9 complex of complement and in the immune deposits in glomerulonephritis. *J Clin Invest* **81**, 1858-64 (1988).
157. Purrello, M. *et al.* The gene for SP-40,40, human homolog of rat sulfated glycoprotein 2, rat clusterin, and rat testosterone-repressed prostate message 2, maps to chromosome 8. *Genomics* **10**, 151-6 (1991).
158. Nishida, K., Kawasaki, S., Adachi, W. & Kinoshita, S. Apolipoprotein J expression in human ocular surface epithelium. *Invest Ophthalmol Vis Sci* **37**, 2285-92 (1996).
159. Nishida, K. *et al.* A gene expression profile of human corneal epithelium and the isolation of human keratin 12 cDNA. *Invest Ophthalmol Vis Sci* **37**, 1800-9 (1996).
160. Jomary, C., Neal, M.J. & Jones, S.E. Comparison of clusterin gene expression in normal and dystrophic human retinas. *Brain Res Mol Brain Res* **20**, 279-84 (1993).
161. Reeder, D.J., Stuart, W.D., Witte, D.P., Brown, T.L. & Harmony, J.A. Local synthesis of apolipoprotein J in the eye. *Exp Eye Res* **60**, 495-504 (1995).
162. Al-Maghrabi, J.A. *et al.* Clusterin immunoexpression is associated with early stage endometrial carcinomas. *Acta Histochem* **118**, 430-4 (2016).

116. Li, J. *et al.* Genetic Evidence for Possible Involvement of the Calcium Channel Gene CACNA1A in Autism Pathogenesis in Chinese Han Population. *PLoS One* **10**, e0142887 (2015).
117. Tomlinson, S.E. *et al.* In vivo impact of presynaptic calcium channel dysfunction on motor axons in episodic ataxia type 2. *Brain* **139**, 380-91 (2016).
118. Tantsis, E.M. *et al.* Eye movement disorders are an early manifestation of CACNA1A mutations in children. *Dev Med Child Neurol* **58**, 639-44 (2016).
119. Reinhardt, D.P., Ono, R.N. & Sakai, L.Y. Calcium stabilizes fibrillin-1 against proteolytic degradation. *J Biol Chem* **272**, 1231-6 (1997).
120. Poliak, S. *et al.* Caspr2, a new member of the neurexin superfamily, is localized at the juxtaparanodes of myelinated axons and associates with K<sup>+</sup> channels. *Neuron* **24**, 1037-47 (1999).
121. Horresh, I. *et al.* Multiple molecular interactions determine the clustering of Caspr2 and Kv1 channels in myelinated axons. *J Neurosci* **28**, 14213-22 (2008).
122. Friedman, J.I. *et al.* CNTNAP2 gene dosage variation is associated with schizophrenia and epilepsy. *Mol Psychiatry* **13**, 261-6 (2008).
123. Alarcon, M. *et al.* Linkage, association, and gene-expression analyses identify CNTNAP2 as an autism-susceptibility gene. *Am J Hum Genet* **82**, 150-9 (2008).
124. Burdon, K.P. *et al.* Genetic analysis of the clusterin gene in pseudoexfoliation syndrome. *Mol Vis* **14**, 1727-36 (2008).
125. Lambert, J.C. *et al.* Genome-wide association study identifies variants at CLU and CR1 associated with Alzheimer's disease. *Nat Genet* **41**, 1094-9 (2009).
126. Daimon, M. *et al.* Association of the clusterin gene polymorphisms with type 2 diabetes mellitus. *Metabolism* **60**, 815-22 (2011).
127. Jiang, Y., Goldberg, I.D. & Shi, Y.E. Complex roles of tissue inhibitors of metalloproteinases in cancer. *Oncogene* **21**, 2245-52 (2002).
128. Mohammed, F.F., Smookler, D.S. & Khokha, R. Metalloproteinases, inflammation, and rheumatoid arthritis. *Ann Rheum Dis* **62 Suppl 2**, ii43-7 (2003).
129. Zenkel, M. *et al.* Proinflammatory cytokines are involved in the initiation of the abnormal matrix process in pseudoexfoliation syndrome/glaucoma. *Am J Pathol* **176**, 2868-79 (2010).
130. Yildirim, Z., Yildirim, F., Ucgun, N.I. & Sepici-Dincel, A. The role of the cytokines in the pathogenesis of pseudoexfoliation syndrome. *Int J Ophthalmol* **6**, 50-3 (2013).
131. Khalef, N. *et al.* Levels of cytokines in the aqueous humor of eyes with primary open angle glaucoma, pseudoexfoliation glaucoma and cataract. *Electron Physician* **9**, 3833-3837 (2017).
132. Lesiewska, H., Malukiewicz, G., Olszewska-Slonina, D. & Wozniak, A. Lysosomal enzymes activity in patients with pseudoexfoliation syndrome. *Acta Ophthalmol* **93**, e170-1 (2015).
133. Schlotzer-Schrehardt, U. Genetics and genomics of pseudoexfoliation syndrome/glaucoma. *Middle East Afr J Ophthalmol* **18**, 30-6 (2011).
134. Turkyilmaz, K. *et al.* Serum YKL-40 levels as a novel marker of inflammation and endothelial dysfunction in patients with pseudoexfoliation syndrome. *Eye (Lond)* **27**, 854-9 (2013).
135. Wallace, D.M. *et al.* Anti-connective tissue growth factor antibody treatment reduces extracellular matrix production in trabecular meshwork and lamina cribrosa cells. *Invest Ophthalmol Vis Sci* **54**, 7836-48 (2013).
136. Browne, J.G. *et al.* Connective tissue growth factor is increased in pseudoexfoliation glaucoma. *Invest Ophthalmol Vis Sci* **52**, 3660-6 (2011).
137. Bleich, S. *et al.* Elevated homocysteine levels in aqueous humor of patients with pseudoexfoliation glaucoma. *Am J Ophthalmol* **138**, 162-4 (2004).
138. Nilforoushan, N. *et al.* Lack of association between the C677T single nucleotide polymorphism of the MTHFR gene and glaucoma in Iranian patients. *Acta Med Iran* **50**, 208-12 (2012).
139. Khan, M.I. *et al.* Association of tumor necrosis factor alpha gene polymorphism G-308A with pseudoexfoliative glaucoma in the Pakistani population. *Mol Vis* **15**, 2861-7 (2009).
140. Sorkhabi, R., Ghorbanihaghjo, A., Ahoor, M., Nahaei, M. & Rashtchizadeh, N. High-sensitivity C-reactive Protein and Tumor Necrosis Factor Alpha in Pseudoexfoliation Syndrome. *Oman Med J* **28**, 16-9 (2013).

92. Park, D.Y., Won, H.H., Cho, H.K. & Kee, C. Evaluation of lysyl oxidase-like 1 gene polymorphisms in pseudoexfoliation syndrome in a Korean population. *Mol Vis* **19**, 448-53 (2013).
93. Guadarrama-Vallejo, D., Miranda-Duarte, A. & Zenteno, J.C. The T allele of lysyl oxidase-like 1 rs41435250 is a novel risk factor for pseudoexfoliation syndrome and pseudoexfoliation glaucoma independently and through intragenic epistatic interaction. *Mol Vis* **19**, 1937-44 (2013).
94. Micheal, S. *et al.* Role of Lysyl oxidase-like 1 gene polymorphisms in Pakistani patients with pseudoexfoliative glaucoma. *Mol Vis* **18**, 1040-4 (2012).
95. Malukiewicz, G. *et al.* Analysis of LOXL1 single nucleotide polymorphisms in Polish population with pseudoexfoliation syndrome. *Acta Ophthalmol* **89**, e64-6 (2011).
96. Abu-Amero, K.K. *et al.* Analysis of LOXL1 polymorphisms in a Saudi Arabian population with pseudoexfoliation glaucoma. *Mol Vis* **16**, 2805-10 (2010).
97. Challa, P. *et al.* Analysis of LOXL1 polymorphisms in a United States population with pseudoexfoliation glaucoma. *Mol Vis* **14**, 146-9 (2008).
98. Fan, B.J. *et al.* DNA sequence variants in the LOXL1 gene are associated with pseudoexfoliation glaucoma in a U.S. clinic-based population with broad ethnic diversity. *BMC Med Genet* **9**, 5 (2008).
99. Pasutto, F. *et al.* Pseudoexfoliation syndrome-associated genetic variants affect transcription factor binding and alternative splicing of LOXL1. *Nat Commun* **8**, 15466 (2017).
100. Hayashi, H., Gotoh, N., Ueda, Y., Nakanishi, H. & Yoshimura, N. Lysyl oxidase-like 1 polymorphisms and exfoliation syndrome in the Japanese population. *Am J Ophthalmol* **145**, 582-585 (2008).
101. Chen, L. *et al.* Evaluation of LOXL1 polymorphisms in exfoliation syndrome in a Chinese population. *Mol Vis* **15**, 2349-57 (2009).
102. Williams, S.E. *et al.* Major LOXL1 risk allele is reversed in exfoliation glaucoma in a black South African population. *Mol Vis* **16**, 705-12 (2010).
103. Challa, P. Genetics of pseudoexfoliation syndrome. *Curr Opin Ophthalmol* **20**, 88-91 (2009).
104. Whigham, B.T. & Allingham, R.R. Review: The role of LOXL1 in exfoliation syndrome/glaucoma. *Saudi J Ophthalmol* **25**, 347-52 (2011).
105. Sharma, S. *et al.* Biological effect of LOXL1 coding variants associated with pseudoexfoliation syndrome. *Exp Eye Res* **146**, 212-23 (2016).
106. Aung, T. *et al.* Genetic association study of exfoliation syndrome identifies a protective rare variant at LOXL1 and five new susceptibility loci. *Nat Genet* **49**, 993-1004 (2017).
107. Fan, B.J. *et al.* LOXL1 promoter haplotypes are associated with exfoliation syndrome in a U.S. Caucasian population. *Invest Ophthalmol Vis Sci* **52**, 2372-8 (2011).
108. Jung, H.J. *et al.* Changes in expression of fibulin-5 and lysyl oxidase-like 1 associated with pelvic organ prolapse. *Eur J Obstet Gynecol Reprod Biol* **145**, 117-22 (2009).
109. Wirostko, B.M. *et al.* Risk for Exfoliation Syndrome in Women With Pelvic Organ Prolapse : A Utah Project on Exfoliation Syndrome (UPEXS) Study. *JAMA Ophthalmol* **134**, 1255-1262 (2016).
110. Remus, E.W. *et al.* The role of lysyl oxidase family members in the stabilization of abdominal aortic aneurysms. *Am J Physiol Heart Circ Physiol* **303**, H1067-75 (2012).
111. Gonzalez-Santamaria, J. *et al.* Matrix cross-linking lysyl oxidases are induced in response to myocardial infarction and promote cardiac dysfunction. *Cardiovasc Res* **109**, 67-78 (2016).
112. Mitchell, P., Wang, J.J. & Smith, W. Association of pseudoexfoliation syndrome with increased vascular risk. *Am J Ophthalmol* **124**, 685-7 (1997).
113. Liu, X. *et al.* Elastic fiber homeostasis requires lysyl oxidase-like 1 protein. *Nat Genet* **36**, 178-82 (2004).
114. Yu, H.G. *et al.* Increased choroidal neovascularization following laser induction in mice lacking lysyl oxidase-like 1. *Invest Ophthalmol Vis Sci* **49**, 2599-605 (2008).
115. Kaja, S. *et al.* Severe and progressive neurotransmitter release aberrations in familial hemiplegic migraine type 1 Cacna1a S218L knock-in mice. *J Neurophysiol* **104**, 1445-55 (2010).

- humor and serum of patients with pseudoexfoliation syndrome. *Clin Ophthalmol* **8**, 305-9 (2014).
71. Zenkel, M. *et al.* Differential gene expression in pseudoexfoliation syndrome. *Invest Ophthalmol Vis Sci* **46**, 3742-52 (2005).
  72. Ho, S.L. *et al.* Elevated aqueous humour tissue inhibitor of matrix metalloproteinase-1 and connective tissue growth factor in pseudoexfoliation syndrome. *Br J Ophthalmol* **89**, 169-73 (2005).
  73. Schlotzer-Schrehardt, U., Kortje, K.H. & Erb, C. Energy-filtering transmission electron microscopy (EFTEM) in the elemental analysis of pseudoexfoliative material. *Curr Eye Res* **22**, 154-62 (2001).
  74. Jelodari-Mamaghani, S. *et al.* Contribution of the latent transforming growth factor-beta binding protein 2 gene to etiology of primary open angle glaucoma and pseudoexfoliation syndrome. *Mol Vis* **19**, 333-47 (2013).
  75. Stein, J.D. *et al.* Geographic and climatic factors associated with exfoliation syndrome. *Arch Ophthalmol* **129**, 1053-60 (2011).
  76. Damji, K.F. *et al.* Is pseudoexfoliation syndrome inherited? A review of genetic and nongenetic factors and a new observation. *Ophthalmic Genet* **19**, 175-85 (1998).
  77. Kang, J.H., Wiggs, J.L. & Pasquale, L.R. Relation between time spent outdoors and exfoliation glaucoma or exfoliation glaucoma suspect. *Am J Ophthalmol* **158**, 605-14 e1 (2014).
  78. Pasquale, L.R. *et al.* Solar exposure and residential geographic history in relation to exfoliation syndrome in the United States and Israel. *JAMA Ophthalmol* **132**, 1439-45 (2014).
  79. Kang, J.H., Loomis, S.J., Wiggs, J.L., Willett, W.C. & Pasquale, L.R. A prospective study of folate, vitamin B(6), and vitamin B(1)(2) intake in relation to exfoliation glaucoma or suspected exfoliation glaucoma. *JAMA Ophthalmol* **132**, 549-59 (2014).
  80. Turkcu, F.M., Koz, O.G., Yarangumeli, A., Oner, V. & Kural, G. Plasma homocysteine, folic acid, and vitamin B(1)(2) levels in patients with pseudoexfoliation syndrome, pseudoexfoliation glaucoma, and normotensive glaucoma. *Medicina (Kaunas)* **49**, 214-8 (2013).
  81. Pasquale, L.R., Wiggs, J.L., Willett, W.C. & Kang, J.H. The Relationship between caffeine and coffee consumption and exfoliation glaucoma or glaucoma suspect: a prospective study in two cohorts. *Invest Ophthalmol Vis Sci* **53**, 6427-33 (2012).
  82. Yang, H. *et al.* Caffeine suppresses metastasis in a transgenic mouse model: a prototype molecule for prophylaxis of metastasis. *Clin Exp Metastasis* **21**, 719-35 (2004).
  83. Ringvold, A. Epidemiology of the pseudo-exfoliation syndrome. *Acta Ophthalmol Scand* **77**, 371-5 (1999).
  84. Ringvold, A. Light and electron microscopy of the anterior iris surface in eyes with and without pseudo-exfoliation syndrome. *Albrecht Von Graefes Arch Klin Exp Ophthalmol* **188**, 131-7 (1973).
  85. Kuchle, M. & Naumann, G.O. Occurrence of pseudoexfoliation following penetrating keratoplasty for keratoconus. *Br J Ophthalmol* **76**, 98-100 (1992).
  86. Konstas, A.G. *et al.* Exfoliation syndrome in a 17-year-old girl. *Arch Ophthalmol* **115**, 1063-7 (1997).
  87. Horven, I. & Hutchinson, B.T. Exfoliation syndrome. Case reports of 31 and 35-year-old patients. *Acta Ophthalmol (Copenh)* **45**, 294-8 (1967).
  88. Hewitt, A.W. *et al.* Ancestral LOXL1 variants are associated with pseudoexfoliation in Caucasian Australians but with markedly lower penetrance than in Nordic people. *Hum Mol Genet* **17**, 710-6 (2008).
  89. Lee, K.Y. *et al.* Association of LOXL1 polymorphisms with pseudoexfoliation in the Chinese. *Mol Vis* **15**, 1120-6 (2009).
  90. Ozaki, M. *et al.* Association of LOXL1 gene polymorphisms with pseudoexfoliation in the Japanese. *Invest Ophthalmol Vis Sci* **49**, 3976-80 (2008).
  91. Ramprasad, V.L. *et al.* Association of non-synonymous single nucleotide polymorphisms in the LOXL1 gene with pseudoexfoliation syndrome in India. *Mol Vis* **14**, 318-22 (2008).

48. Kozobolis, V.P., Papatzanaki, M., Vlachonikolis, I.G., Pallikaris, I.G. & Tsambarlakis, I.G. Epidemiology of pseudoexfoliation in the island of Crete (Greece). *Acta Ophthalmol Scand* **75**, 726-9 (1997).
49. Kozart, D.M. & Yanoff, M. Intraocular pressure status in 100 consecutive patients with exfoliation syndrome. *Ophthalmology* **89**, 214-8 (1982).
50. Thomas, R., Nirmalan, P.K. & Krishnaiah, S. Pseudoexfoliation in southern India: the Andhra Pradesh Eye Disease Study. *Invest Ophthalmol Vis Sci* **46**, 1170-6 (2005).
51. Jonas, J.B. *et al.* Pseudoexfoliation: normative data and associations. The Central India Eye and Medical Study. *PLoS One* **8**, e76770 (2013).
52. Ovodenko, B. *et al.* Proteomic analysis of exfoliation deposits. *Invest Ophthalmol Vis Sci* **48**, 1447-57 (2007).
53. Li, Z.Y., Streeten, B.W. & Wallace, R.N. Association of elastin with pseudoexfoliative material: an immunoelectron microscopic study. *Curr Eye Res* **7**, 1163-72 (1988).
54. Schlotzer-Schrehardt, U., Dorfler, S. & Naumann, G.O. Immunohistochemical localization of basement membrane components in pseudoexfoliation material of the lens capsule. *Curr Eye Res* **11**, 343-55 (1992).
55. Ritch, R., Schlotzer-Schrehardt, U. & Konstas, A.G. Why is glaucoma associated with exfoliation syndrome? *Prog Retin Eye Res* **22**, 253-75 (2003).
56. Fitzsimmons, T.D., Fagerholm, P. & Wallin, O. Hyaluronan in the exfoliation syndrome. *Acta Ophthalmol Scand* **75**, 257-60 (1997).
57. Schlotzer-Schrehardt, U. & Naumann, G.O. Ocular and systemic pseudoexfoliation syndrome. *Am J Ophthalmol* **141**, 921-937 (2006).
58. Streeten, B.W., Li, Z.Y., Wallace, R.N., Eagle, R.C., Jr. & Keshgegian, A.A. Pseudoexfoliative fibrilopathy in visceral organs of a patient with pseudoexfoliation syndrome. *Arch Ophthalmol* **110**, 1757-62 (1992).
59. Gonzalez-Iglesias, H. *et al.* Comparative proteomic study in serum of patients with primary open-angle glaucoma and pseudoexfoliation glaucoma. *J Proteomics* **98**, 65-78 (2014).
60. Hardenborg, E. *et al.* Protein content in aqueous humor from patients with pseudoexfoliation (PEX) investigated by capillary LC MALDI-TOF/TOF MS. *Proteomics Clin Appl* **3**, 299-306 (2009).
61. Aung, T. *et al.* A common variant mapping to CACNA1A is associated with susceptibility to exfoliation syndrome. *Nat Genet* **47**, 387-92 (2015).
62. Krumbiegel, M. *et al.* Exploring functional candidate genes for genetic association in german patients with pseudoexfoliation syndrome and pseudoexfoliation glaucoma. *Invest Ophthalmol Vis Sci* **50**, 2796-801 (2009).
63. Padhy, B. *et al.* Role of an extracellular chaperone, Clusterin in the pathogenesis of Pseudoexfoliation Syndrome and Pseudoexfoliation Glaucoma. *Exp Eye Res* **127**, 69-76 (2014).
64. Zenkel, M., Kruse, F.E., Junemann, A.G., Naumann, G.O. & Schlotzer-Schrehardt, U. Clusterin deficiency in eyes with pseudoexfoliation syndrome may be implicated in the aggregation and deposition of pseudoexfoliative material. *Invest Ophthalmol Vis Sci* **47**, 1982-90 (2006).
65. Krumbiegel, M. *et al.* Genome-wide association study with DNA pooling identifies variants at CNTNAP2 associated with pseudoexfoliation syndrome. *Eur J Hum Genet* **19**, 186-93 (2011).
66. Schlotzer-Schrehardt, U. *et al.* LOXL1 deficiency in the lamina cribrosa as candidate susceptibility factor for a pseudoexfoliation-specific risk of glaucoma. *Ophthalmology* **119**, 1832-43 (2012).
67. Thorleifsson, G. *et al.* Common sequence variants in the LOXL1 gene confer susceptibility to exfoliation glaucoma. *Science* **317**, 1397-400 (2007).
68. Khan, T.T. *et al.* LOXL1 expression in lens capsule tissue specimens from individuals with pseudoexfoliation syndrome and glaucoma. *Mol Vis* **16**, 2236-41 (2010).
69. Fountoulakis, N. *et al.* Tissue inhibitor of metalloproteinase 4 in aqueous humor of patients with primary open angle glaucoma, pseudoexfoliation syndrome and pseudoexfoliative glaucoma and its role in proteolysis imbalance. *BMC Ophthalmol* **13**, 69 (2013).
70. Kara, S., Yildirim, N., Ozer, A., Colak, O. & Sahin, A. Matrix metalloproteinase-2, tissue inhibitor of matrix metalloproteinase-2, and transforming growth factor beta 1 in the aqueous

23. Atalar, P.T. *et al.* Impaired systemic endothelial function in patients with pseudoexfoliation syndrome. *Int Heart J* **47**, 77-84 (2006).
24. Citirik, M., Acaroglu, G., Batman, C., Yildiran, L. & Zilelioglu, O. A possible link between the pseudoexfoliation syndrome and coronary artery disease. *Eye (Lond)* **21**, 11-5 (2007).
25. Turacli, M.E. *et al.* Sensorineural hearing loss in pseudoexfoliation. *Can J Ophthalmol* **42**, 56-9 (2007).
26. Samarai, V., Samarei, R., Haghighi, N. & Jalili, E. Sensory-neural hearing loss in pseudoexfoliation syndrome. *Int J Ophthalmol* **5**, 393-6 (2012).
27. Shrum, K.R., Hattenhauer, M.G. & Hodge, D. Cardiovascular and cerebrovascular mortality associated with ocular pseudoexfoliation. *Am J Ophthalmol* **129**, 83-6 (2000).
28. Speckauskas, M., Tamosiunas, A. & Jasinskas, V. Association of ocular pseudoexfoliation syndrome with ischaemic heart disease, arterial hypertension and diabetes mellitus. *Acta Ophthalmol* **90**, e470-5 (2012).
29. Emiroglu, M.Y. *et al.* Is pseudoexfoliation syndrome associated with coronary artery disease? *N Am J Med Sci* **2**, 487-90 (2010).
30. Slettedal, J.K., Sandvik, L. & Ringvold, A. Ocular pseudoexfoliation syndrome and life span. *EBioMedicine* **2**, 765-9 (2015).
31. Andrikopoulos, G.K., Alexopoulos, D.K. & Gartaganis, S.P. Pseudoexfoliation syndrome and cardiovascular diseases. *World J Cardiol* **6**, 847-54 (2014).
32. Janciauskiene, S. & Krakau, T. Alzheimer's peptide: a possible link between glaucoma, exfoliation syndrome and Alzheimer's disease. *Acta Ophthalmol Scand* **79**, 328-9 (2001).
33. Linner, E. *et al.* The exfoliation syndrome in cognitive impairment of cerebrovascular or Alzheimer's type. *Acta Ophthalmol Scand* **79**, 283-5 (2001).
34. Akarsu, C. & Unal, B. Cerebral haemodynamics in patients with pseudoexfoliation glaucoma. *Eye (Lond)* **19**, 1297-300 (2005).
35. May, C.A. Specific densified regions in the postlaminar human glaucomatous optic nerve. *Open Ophthalmol J* **9**, 20-4 (2015).
36. Ekstrom, C. & Kilander, L. Pseudoexfoliation and Alzheimer's disease: a population-based 30-year follow-up study. *Acta Ophthalmol* **92**, 355-8 (2014).
37. Anastasopoulos, E. *et al.* Association of LOXL1 polymorphisms with pseudoexfoliation, glaucoma, intraocular pressure, and systemic diseases in a Greek population. The Thessaloniki eye study. *Invest Ophthalmol Vis Sci* **55**, 4238-43 (2014).
38. Arnarsson, A.M. Epidemiology of exfoliation syndrome in the Reykjavik Eye Study. *Acta Ophthalmol* **87 Thesis** **3**, 1-17 (2009).
39. Bartholomew, R.S. Incidence of pseudoexfoliation in South African Negroes and Scots. *Trans Ophthalmol Soc U K* **99**, 299-301 (1979).
40. Forsius, H. Exfoliation syndrome in various ethnic populations. *Acta Ophthalmol Suppl* **184**, 71-85 (1988).
41. Aasved, H. Study of relatives of persons with fibrilloglucosar (pseudoexfoliation of the lens capsule). *Acta Ophthalmol (Copenh)* **53**, 879-86 (1975).
42. Aasved, H. Mass screening for fibrilloglucosar, so-called senile exfoliation or pseudoexfoliation of the anterior lens capsule. *Acta Ophthalmol (Copenh)* **49**, 334-43 (1971).
43. Crittendon, J.J. & Shields, M.B. Exfoliation syndrome in the southeastern United States. II. Characteristics of patient population and clinical course. *Acta Ophthalmol Suppl* **184**, 103-6 (1988).
44. Aasved, H. The geographical distribution of fibrilloglucosar, so-called senile exfoliation or pseudoexfoliation of the anterior lens capsule. *Acta Ophthalmol (Copenh)* **47**, 792-810 (1969).
45. Jeng, S.M. *et al.* The risk of glaucoma in pseudoexfoliation syndrome. *J Glaucoma* **16**, 117-21 (2007).
46. Henry, J.C. *et al.* Long-term follow-up of pseudoexfoliation and the development of elevated intraocular pressure. *Ophthalmology* **94**, 545-52 (1987).
47. Hirvela, H., Luukinen, H. & Laatikainen, L. Prevalence and risk factors of lens opacities in the elderly in Finland. A population-based study. *Ophthalmology* **102**, 108-17 (1995).

## References:

1. Schlotzer-Schrehardt, U. & Naumann, G.O. Trabecular meshwork in pseudoexfoliation syndrome with and without open-angle glaucoma. A morphometric, ultrastructural study. *Invest Ophthalmol Vis Sci* **36**, 1750-64 (1995).
2. Rao, A. & Padhy, D. Pattern of pseudoexfoliation deposits on the lens and their clinical correlation--clinical study and review of literature. *PLoS One* **9**, e113329 (2014).
3. Pena, J.D. *et al.* Elastosis of the lamina cribrosa in glaucomatous optic neuropathy. *Exp Eye Res* **67**, 517-24 (1998).
4. Ritch, R. & Schlotzer-Schrehardt, U. Exfoliation syndrome. *Surv Ophthalmol* **45**, 265-315 (2001).
5. Karagiannis, D. *et al.* Central retinal vein occlusion and pseudoexfoliation syndrome. *Clin Interv Aging* **10**, 879-83 (2015).
6. Kozobolis, V.P. *et al.* Correlation between age-related macular degeneration and pseudoexfoliation syndrome in the population of Crete (Greece). *Arch Ophthalmol* **117**, 664-9 (1999).
7. Gunes, A., Yigit, M., Tok, L. & Tok, O. Evaluation of anterior segment parameters in patients with pseudoexfoliation syndrome using Scheimpflug imaging. *Arq Bras Oftalmol* **79**, 177-9 (2016).
8. Oltulu, R. *et al.* Characteristics of the cornea in patients with pseudoexfoliation syndrome. *Arq Bras Oftalmol* **78**, 348-51 (2015).
9. Tomaszewski, B.T., Zalewska, R. & Mariak, Z. Evaluation of the endothelial cell density and the central corneal thickness in pseudoexfoliation syndrome and pseudoexfoliation glaucoma. *J Ophthalmol* **2014**, 123683 (2014).
10. Honjo, M. *et al.* Retinal Thickness and the Structure/Function Relationship in the Eyes of Older Adults with Glaucoma. *PLoS One* **10**, e0141293 (2015).
11. Dursun, A. *et al.* Evaluation of Choroidal Thickness in Patients with Pseudoexfoliation Syndrome and Pseudoexfoliation Glaucoma. *J Ophthalmol* **2016**, 3545180 (2016).
12. Moghimi, S. *et al.* Evaluation of Lamina Cribrosa and Choroid in Nonglaucomatous Patients With Pseudoexfoliation Syndrome Using Spectral-Domain Optical Coherence Tomography. *Invest Ophthalmol Vis Sci* **57**, 1293-300 (2016).
13. Braunsman, C. *et al.* Evaluation of lamina cribrosa and peripapillary sclera stiffness in pseudoexfoliation and normal eyes by atomic force microscopy. *Invest Ophthalmol Vis Sci* **53**, 2960-7 (2012).
14. Amari, F. *et al.* Lectin electron microscopic histochemistry of the pseudoexfoliative material in the skin. *Invest Ophthalmol Vis Sci* **35**, 3962-6 (1994).
15. Gonen, K.A., Gonen, T. & Gumus, B. Renal artery stenosis and abdominal aorta aneurysm in patients with pseudoexfoliation syndrome. *Eye (Lond)* **27**, 735-41 (2013).
16. Akdemir, M.O., Sayin, M.R., Armut, M., Akpınar, I. & Ugurbas, S.H. Pseudoexfoliation syndrome and coronary artery ectasia. *Eye (Lond)* **28**, 594-9 (2014).
17. Schumacher, S., Schlotzer-Schrehardt, U., Martus, P., Lang, W. & Naumann, G.O. Pseudoexfoliation syndrome and aneurysms of the abdominal aorta. *Lancet* **357**, 359-60 (2001).
18. Praveen, M.R. *et al.* Pseudoexfoliation as a risk factor for peripheral vascular disease: a case-control study. *Eye (Lond)* **25**, 174-9 (2011).
19. Alpaslan, M., Karalezli, A., Borazan, M., Koktekir, B.E. & Muderrisoglu, I.H. Decreased aortic root elasticity-as a novel systemic manifestation of the pseudoexfoliation syndrome: an observational study. *Anadolu Kardiyol Derg* **12**, 483-7 (2012).
20. Singham, N.V., Zahari, M., Peyman, M., Prepageran, N. & Subrayan, V. Association between Ocular Pseudoexfoliation and Sensorineural Hearing Loss. *J Ophthalmol* **2014**, 825936 (2014).
21. Gokce, S.E. & Gokce, M.I. Relationship between pseudoexfoliation syndrome and erectile dysfunction: a possible cause of endothelial dysfunction for development of erectile dysfunction. *Int Braz J Urol* **41**, 547-51 (2015).
22. Temporale, H. *et al.* Evaluating the Hearing of Patients with Pseudoexfoliation Syndrome. *Adv Clin Exp Med* **25**, 1215-1221 (2016).

# **Chapter 7**

## **References**